AD-A154 292 MUTUAL COUPLING ANALYSIS FOR CONFORMAL MICROSTRIP ANTENNAS(U) OHIO STATE UNIV COLUMBUS ELECTROSCIENCE LAB B W KWAN ET AL. DEC 84 712692-4 N00014-78-C-0049 1/3

UNCLASSIFIED F/G 9/5 NL

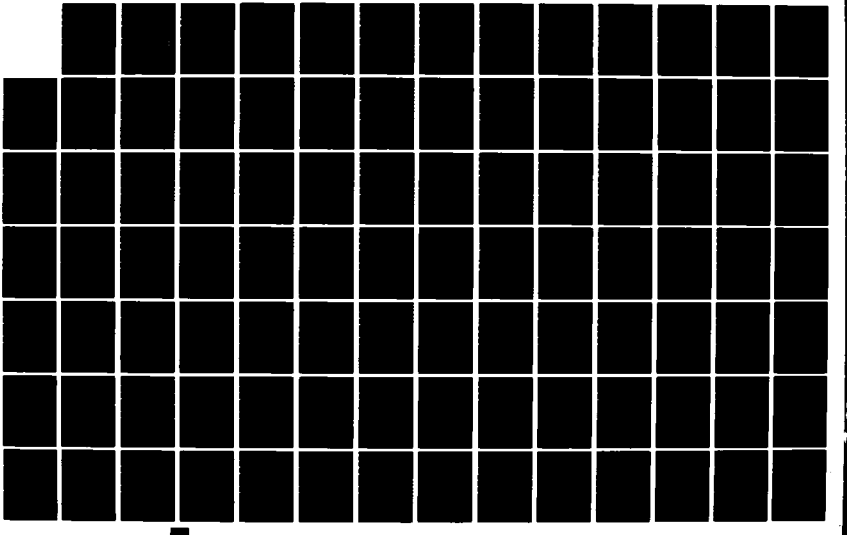

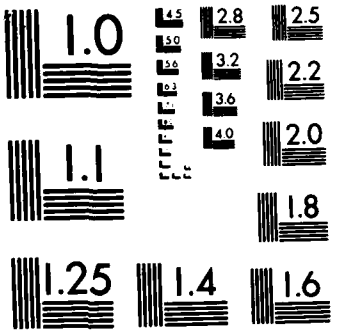

(6)

OSU

The Ohio State University

MUTUAL COUPLING ANALYSIS FOR CONFORMAL MICROSTRIP ANTENNAS

B.W. Kwan and E.H. Newman

The Ohio State University

ElectroScience Laboratory

Department of Electrical Engineering
Columbus, Ohio 43212

Technical Report 712692-4

Contract No. N00014-78-C-0049

December 1984

Department of the Navy
Office of Naval Research
800 North Quincy Street
Arlington, Virginia 22217

NOTICES

When Government drawings, specifications, or other data are used for any purpose other than in connection with a definitely related Government procurement operation, the United States Government thereby incurs no responsibility nor any obligation whatsoever, and the fact that the Government may have formulated, furnished, or in any way supplied the said drawings, specifications, or other data, is not to be regarded by implication or otherwise as in any manner licensing the holder or any other person or corporation, or conveying any rights or permission to manufacture, use, or sell any patented invention that may in any way be related thereto.

50272-101

REPORT DOCUMENTATION PAGE	1. REPORT NO.	2. AD-A154 292	3. Recipient's Accession No.

4. Title and Subtitle
MUTUAL COUPLING ANALYSIS FOR CONFORMAL MICROSTRIP ANTENNAS

5. Report Date
December 1984

6.

7. Author(s)
B.W. Kwan and E.H. Newman

8. Performing Organization Rept. No.
712692-4

9. Performing Organization Name and Address
The Ohio State University ElectroScience Laboratory
Department of Electrical Engineering
1320 Kinnear Road
Columbus, Ohio 43221

10. Project/Task/Work Unit No.

11. Contract(C) or Grant(G) No
(C) N00014-78-C-0049
(G)

12. Sponsoring Organization Name and Address
Department of the Navy
Office of Naval Research
800 North Quincy Street
Arlington, Virginia 22217

13. Type of Report & Period Covered
Technical

14.

15. Supplementary Notes

16. Abstract (Limit: 200 words)

Integral equations based upon appropriate Green's functions are employed to rigorously treat the mutual coupling of microstrip patches on 1) an infinite grounded dielectric slab, and 2) a dielectric coated circular cylinder. A moment method solution for the first problem using the dielectric slab Green's function is presented. Calculated values of the mutual impedance are found to be in good agreement with measurements. The second problem is restricted to the calculation of the elements of the impedance and voltage matrices which are needed to carry out the solution by the moment method. These elements are derived using the Green's dyadic for the coated cylinder. It is found that the self impedance of a dipole mode at the surface of a coated cylinder converges to that of the infinite slab case as the radius of the cylinder increases. Two examples of the mutual coupling between two dipole modes are considered and numerical results are presented for cylinders of different size. In addition, alternative representations suitable for asymptotic evaluation are derived from the eigenfunction solution obtained by the Green's dyadic. A two-dimensional example is presented to illustrate the usefulness of asymptotic solutions when the dielectric coated cylinder is large in terms of a wavelength.

17. Document Analysis a. Descriptors

Microstrip Antennas, Green's Function, Eigenfunction Expansion
Mutual Coupling, Cylinder
Conformal Arrays, Moment Method

b. Identifiers/Open-Ended Terms

c. COSATI Field/Group

18. Availability Statement

DISTRIBUTION STATEMENT A
Approved for public release;
Distribution Unlimited

19. Security Class (This Report)	21. No. of Pages
UNCLASSIFIED	267
20. Security Class (This Page)	**22. Price**
UNCLASSIFIED	

(See ANSI-Z39.18) See Instructions on Reverse

OPTIONAL FORM 272 (4-77)
(Formerly NTIS-35)
Department of Commerce

TABLE OF CONTENTS

APPENDICES

LIST OF TABLES

LIST OF FIGURES

CHAPTER I

INTRODUCTION AND PRELIMINARY

A. BRIEF REVIEW

A microstrip device basically consists of a sandwich of two parallel conducting layers separted by a single thin dielectric substrate. The lower conductor functions as a ground plane, and the upper conductor may be a simple resonant patch of regular shape, a resonant dipole, or a monolithically printed array of patches or dipoles and the associated feed network. The concept of microstrip antennas was first proposed in this country a by Deschamps [1] and in France by Gutton and Baissinot [2]. However, the main interest in the microstrip antenna concept did not emerge unitl the early 1970's. It was probably the need for conformal missile and spacecraft antennas that provided this impetus together with the advance of printed circuit technology based on the good selection of microstrip substrates that were becoming available. The first practical antennas were developed in the early 1970's by Howell [3] and Munson [4]. Since then, extensive research

and development of microstrip antennas have led to diversified applications and to the establishment of the topic as a separate entity within the broad field of microwave antennas. The state of the art, in both theory and experiment, is summarized in the books by Bahl and Bhartia [5], and James, et al. [6]. In particular, a recent special issue of IEEE Transactions on Antennas and Propagation [7] was devoted to microstrip antennas and arrays. In this special issue, Carver and Mink [8] presented a comprehensive survey of the state of microstrip antenna element technology; while Mailloux, et al. [9] discussed microstrip array design techniques.

In its simplest configuration a microstrip antenna consists of a thin metallic radiating patch bonded to a thin grounded dielectric substrate (Figure 1.1). The patch conductor typically has some regular shape, for example, rectangular, circular or elliptical. The feed is often a coaxial probe or a microstrip transmission line. Microstrip antennas exhibit all the properties inherent to microstrip devices: a) they are light weight, small size and low profile planar configurations which can be made conformal; b) they are inexpensive to build and ideally suited for large scale production by printed circuit techniques; c) they are compatible with modular designs (solid state devices such as oscillators, amplifiers, phase shifters, etc., can be added directly to the antenna substrate board); d) their feed lines and matching networks can be fabricated simultaneously with the antenna structure so that discontinuities due to connectors can be eliminated. All these

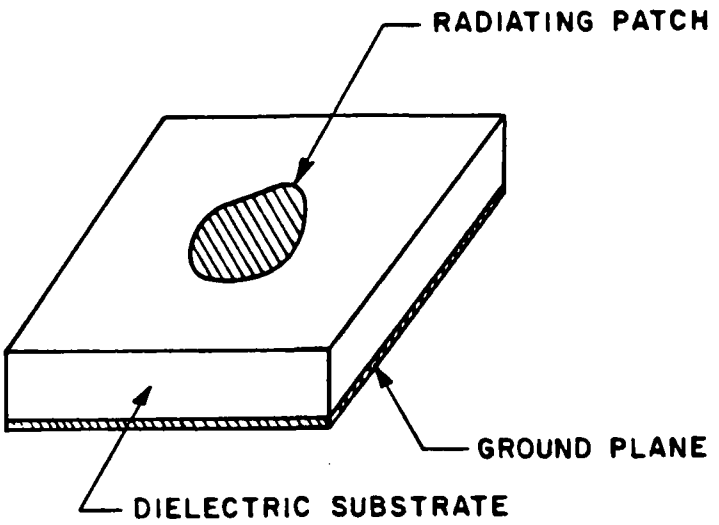

Figure 1.1. Microstrip antenna configuration.

advantages compensate, at least in part, a number of drawbacks: a) simple microstrip antennas have narrow bandwidths; b) their gain is low; c) they have a small power handling capability; d) their dielectric losses reduce the radiation efficiency; e) unwanted surface waves may cause spurious radiation at the edges of the microstrip patch.

Most of the work in printed antenna theory and technology during the last decade was for antennas operating in the UHF to microwave frequency bands (300 MHz to 10 GHz). There are two somewhat successful methods in calculating input impedance and radiation. One is the transmission line model proposed by Derneryd [10], and the other is the cavity model used by Lo, et al. [11]. However, both methods fail

to rigorously account for the surface waves on the antenna substrate and for the mutual coupling between antenna elements. More recently, a moment method solution to the microstrip strip antenna problem was proposed by Newman and Tulyathan [12]. In [12], an integral equation was formulated with the aid of image theory which accounted for the presence of the ground plane; the field within the dielectric slab was treated by an equivalent current. This method gives good results for the input impedance, but requires an extremely accurate evaluation of the elements of the impedance matrix.

The above studies all deal with planar substrates. From a practical viewpoint it is also important to consider microstrip antennas and arrays on curved surfaces, especially on portions of cylinders, cones or spheres. Microstrip dipoles have indeed been considered for cylindrical substrates and some preliminary results have been published by Alexopoulos, et al. [13], who utilized the dyadic Green's function to give the electric field produced by an electric dipole tangent to the outer surface of the coating layer. Their results were restricted to the far field and to the surface field. At about the same time, Fonseca and Attilio [30] reported results on the radiation patterns of microstrip wraparound antennas using a theory based upon the dyadic Green's function for a dielectric coated cylinder. In both papers, the Green's dyadic was constructed using the principle of scattering superposition. The free space Green's dyadic employed was quoted from

Tai [19] who used a different method from the one adopted in this work for constructing the free space Green's dyadic. However, the above papers did not specifically address the mutual coupling problem.

B. STATEMENT OF PROBLEM

It is likely that there will be increasing interest in millimeter wave systems and applications, such as imaging array antennas and aircraft-to-satellite communications. Also of interest is the development of complete monolithic systems which combine antenna elements or arrays on the same substrate as the integrated RF/IF front-end detector and amplifier circuits. In these applications, substrates are often thicker and have higher dielectric constants than at lower frequencies. Consequently the electrical performance of these antennas will be severely degraded due to surface waves or mutual coupling. It is then evident that the analysis of mutual coupling between microstrips is important in the design of antenna arrays, especially if tight pattern control or low sidelobes are required.

This work considers the mutual coupling of two types of conformal microstrip antennas:

1. microstrip patches on a dielectric slab (dielectric slab problem);
2. microstrip patches on a dielectric coated cylinder (dielectric coated cylinder problem).

C. OVERVIEW OF APPROACH

1. Integral Equation Formulation

The present approach is based on the Green's function method which yields the total electric field $\bar{E}$ produced by the electric surface currents $\bar{J}_s$ on the microstrip antenna elements (patches) as

$$\bar{E} = \bar{E}^i + \int_S \bar{\bar{G}} \cdot \bar{J}_s \, ds \tag{1.1}$$

where $\bar{E}^i$ is the incident field excited by an impressed curent source $\bar{J}_i$; $\bar{\bar{G}}$ is an appropriate dyadic Green's function which accounts for the grounded substrate; and S is the surface of the microstrip patches.

Introducing the boundary condition on the microstrip patches

$$\hat{n} \times \bar{E} = 0 \qquad \text{on } S \tag{1.2}$$

yields an electric field integral equation for $\bar{J}_s$; here $\hat{n}$ is the unit vector normal to the surface of the microstrip patches.

2. Moment Method Solution

The integral Equation (1.2) is solved using the Galerkin form of the moment method where both the basis and testing functions are taken as a surface patch dipole mode. Thus the unknown current $\bar{J}_s$ is expanded in a set of N basis functions or modes

$$\bar{J}_s = \sum_{n=1}^{N} I_n \bar{J}_n \quad , \tag{1.3}$$

where $\bar{J}_n$ is the n^{th} mode and I_n is its unknown amplitude. Use of the same set of functions as testing function leads to a system of linear algebraic equations to be solved for the unknown I_n

$$[Z][I] = [V] \quad , \tag{1.4}$$

where [Z] is known as the impedance matrix with elements

$$Z_{mn} = - \int_{S_n} \bar{E}_m \cdot \bar{J}_n \, ds \quad , \tag{1.5}$$

[V] is the voltage vector whose elements are given by

$$V_m = \int_{V_i} \bar{E}_m \cdot \bar{J}_i \, dv \quad , \tag{1.6}$$

and I_n are the elements of the current vector [I]. In Equations (1.5) and (1.6), $\bar{E}_m$ is the electric field due to the mode current $\bar{J}_m$ in the presence of the dielectric substrate and ground plane; $\bar{J}_i$ is the impressed (source) current; and S_n, V_i denote the surface, volume where currents $\bar{J}_n$, $\bar{J}_i$ exist, respectively. The expressions in (1.5) and (1.6) were obtained using the reciprocity principle.

3. Feed Modeling

Referring to Figure 1.2(a), a coaxial feed with terminal current I_i can be modeled by

$$\bar{J}_i = \hat{z} I_i \delta(x-x_o)\delta(y-y_o) \tag{1.7}$$

to represent a $\hat{z}$-directed current source at the probe position (x_o,y_o). To account for the probe self inductance, jX_p (for $e^{j\omega t}$ time dependence) can be added to the input impedance, where [8]

$$X_p = \frac{Z_o}{\sqrt{\varepsilon_r}} \tan(\sqrt{\varepsilon_r}\, k_o t) \quad , \tag{1.8}$$

with $Z_o = \sqrt{\mu_o/\varepsilon_o}$, $k_o = \omega\sqrt{\mu_o\varepsilon_o}$, μ_o and ε_o are the constitutive parameters of free space (air); and t is the thickness of the dielectric layer with dielectric constant ε_r.

In Figure 1.2(b), a microstrip line feed with terminal current I_i also can be modeled by using Equation (1.7) to represent an equivalent $\hat{z}$-directed current source at the point (x_o,y_o) where the feed line joins the microstrip patch. Such a model furnishes good results for the narrow feed lines that are in common use. Alexopoulos and Rana [14] pointed out that the voltage term (1.6) should be modified by the factor $\sqrt{W_e/t}$ to account for edge effects of the microstrip line of width W, where W_e is the effective width given by [8]

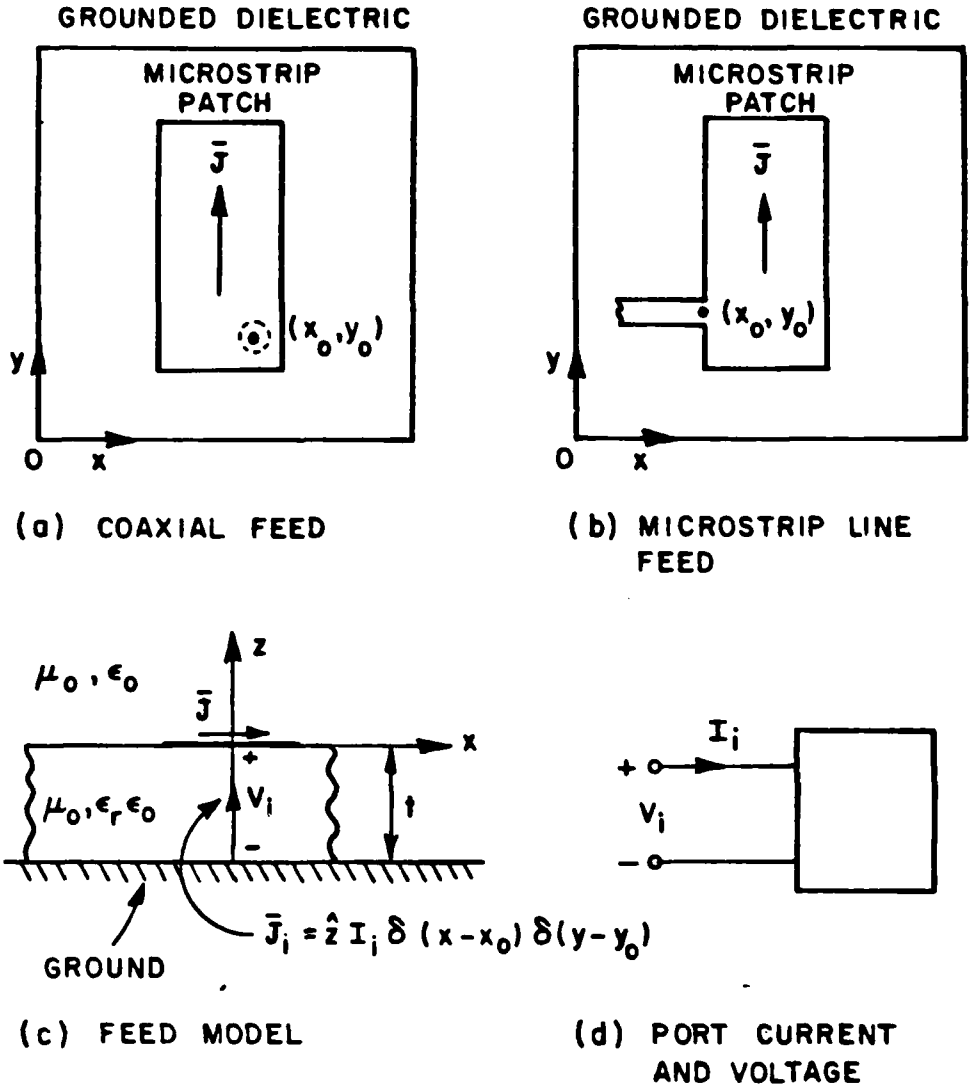

Figure 1.2. Microstrip antenna feed modeling.

$$W_e = W + 0.412 \left[\frac{\varepsilon_e + 0.3}{\varepsilon_e - 0.258}\right] \left[\frac{W + 0.262t}{W + 0.813t}\right] t \quad . \tag{1.9}$$

In Equation (1.9), the effective dielectric constant

$$\varepsilon_e = \frac{\varepsilon_r + 1}{2} + \frac{\varepsilon_r - 1}{2} \left[1 + \frac{10t}{W}\right]^{-1/2} \quad . \tag{1.10}$$

The feed model (Figure 1.2(c)) can be thought of as a port with terminal current I_i and voltage V_i as shown in Figure 1.2(d). V_i is the voltage due to surface current on the patch excited by the impressed $\bar{J}_i$.

4. Port Impedances

An M-element microstrip array can be modeled as an M-port whose currents and voltages (defined in Figure 1.3) are related in matrix form as

$$[Z^p]\ [I^p] = [V^p] \quad . \tag{1.11}$$

One should differentiate between these port quantities (indicated by the superscript p) and those associated with the moment method solution defined in Equations (1.4) -(1.6). The moment method quantities depend on the choice of the basis functions. The port quantities are the ones of interest for determining input impedance and mutual coupling. The relation between these quantities is now described.

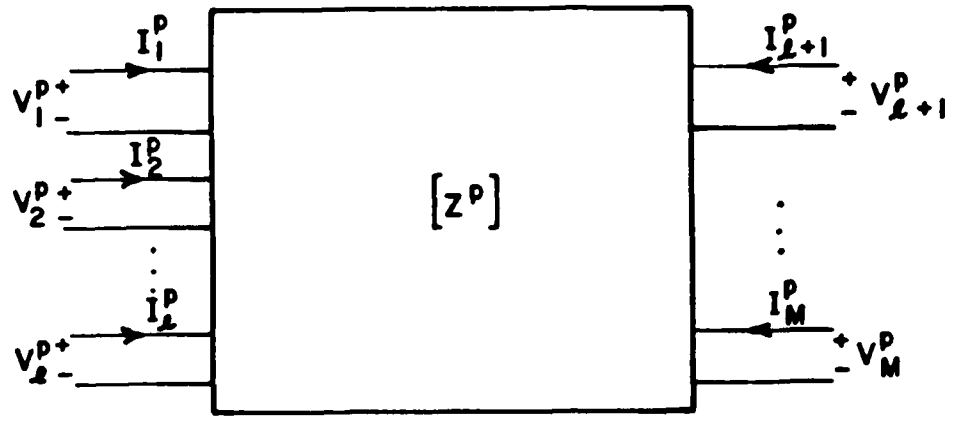

Figure 1.3. Voltages and currents of an M-port.

The input impedance at port m is given by

$$Z_{mm}^p = \frac{-\int_{V_m} \bar{E}^m \cdot \bar{J}_i^m \, dv}{[I_m^p]^2} \quad , \tag{1.12}$$

where $\bar{J}_i^m$ is the impressed source current at port m and $\bar{E}^m$ is the total electric field due to the N expansion modes $\bar{J}_\ell$, $\ell=1,2,\ldots,N$, excited by $\bar{J}_i^m$ with the other ports open circuited. $\bar{E}^m$ can be expanded in terms of $\bar{E}_\ell$ which represent the electric fields due to expansion modes $\bar{J}_\ell$ as follows

$$\bar{E}^m = \sum_{\ell=1}^{N} I_\ell^m \bar{E}_\ell \quad . \tag{1.13}$$

Substituting Equation (1.13) into (1.12) and applying (1.6) yields

$$Z_{mm}^p = \sum_{\ell=1}^{N} I_\ell^m V_\ell^m / \left[I_m^p\right]^2 = \frac{V_m^p(m)}{I_m^p} \quad , \tag{1.14}$$

where I_ℓ^m are the expansion mode current amplitudes found from Equation (1.4); V_ℓ^m are the voltages induced at port m due to $\bar{E}_\ell$; and $V_m^p(m)$ denotes the total voltage at port m due to $\bar{E}^m$.

The mutual impedance between port m and port n can be written as

$$Z_{mn}^p = \frac{-\int_{V_n} \bar{E}^m \cdot \bar{J}_i^n \, dv}{I_m^p \, I_n^p} \quad , \tag{1.15}$$

where $\bar{E}^m$ is the total electric field due to N expansion modes, $\bar{J}_\ell$, ℓ=1,2,...,N, excited by $\bar{J}_i^m$ with port n open circuited. Using Equations (1.6) and (1.13) in (1.15) produces

$$Z_{mn}^p = - \frac{\sum_{\ell=1}^{N} I_\ell^m V_\ell^n}{I_m^p \, I_n^p} = \frac{V_n^p(m)}{I_m^p} \quad , \tag{1.16}$$

where V_ℓ^n are the voltages induced at port n due to $\bar{E}_\ell$ when $\bar{J}_i^n$ is set to zero (open circuited); and $V_n^p(m)$ is the total voltage at port n due to $\bar{E}^m$. Via reciprocity,

$$Z_{mn}^p = Z_{nm}^p \quad , \text{ for all } m,n \quad . \tag{1.17}$$

It is common that the mutual coupling is measured in terms of scattering parameters S_{mn}. From the circuit theory for waveguiding systems, one finds that the scattering matrix [S] is given by

$$[S] = ([Z^p] + [U])^{-1} ([Z^p] - [U]) \quad , \tag{1.18}$$

where [U] denotes the unity matrix.

From the above discussion it is seen that the port impedances are functions of the impedance matrix [Z]. Therefore, in order to analyze the mutual coupling between microstrip antennas, it is essential to have full knowledge of the self and mutual impedances between expansion modes (i.e., the elements of [Z]). In this work, the major effort will be focused on the computation of these parameters.

D. ORGANIZATION

A general solution to the dielectric slab problem is presented in Chapter II. Numerical results for specific examples are obtained and compared with measurements. Expressions for the far zone radiation fields are derived and details of the calculations are discussed.

In Chapter III, the structure of free space dyadic Green's function is characterized in terms of solenoidal and irrotational components. A complete eigenfunction expansion for the free space dyadic Green's function is obtained. This expansion is used in determining the dyadic Green's function for a dielectric coated cylinder. Certain orthogonality properties of the cylindrical vector wave functions [15] are established in this chapter.

The dielectric coated cylinder problem is treated in Chapter IV. Fields due to current sources at the dielectric-air interface can be obtained in two ways. One approach relies on the technique used in Chapter II. The other is based on the dyadic Green's function determined in Chapter III. Use of these fields yields the impedance matrix [Z]. The method of steepest descent is employed to derive an expression for the far field of the currents on a patch.

The impedance expressions obtained in Chapter IV are basically eigenfunction solutions which converge slowly as the radius of cylinder increases. In Chapter V, the Poisson summation formula is introduced to convert the Green's dyadic function to an alternative representation which is more rapidly converging. To illustrate this approach, a two dimensional coupling problem is considered.

Concluding remarks are presented in Chapter VI, and various analytical details are given in the appendices.

CHAPTER II

MICROSTRIP PATCHES ON A GROUNDED PLANAR DIELECTRIC SLAB

A. INTRODUCTION

This chapter deals with mutual coupling between microstrip patches printed on a grounded dielectric slab. For the calculation of impedance matrix and voltage vector elements, the electric field due to an expansion patch mode is needed. A general solution to the field equations pertaining to the microstrip patch on a grounded dielectric slab is presented in Section B. The surface current on the patch is introduced only through the boundary conditions; this simplifies the calculation, which is performed in the Fourier transform domain. The solution is essentially of the Green's function type even though the Green's function is not constructed explicitly. It is exact in the sense that both the dielectric slab and the ground plane are taken into account rigorously. Thus surface waves and coupling to adjacent antenna elements can be accurately determined. An efficient evaluation of the Green's function is also discussed. A moment method solution for mutual

coupling between rectangular microstrip antenna elements is treated in Section C. In Section D, numerical results of mutual coupling for two antenna geometries are presented. These results are compared with measurements. Finally, in Section E a general expression for the far field of a patch mode using the method of stationary phase is derived. An $e^{j\omega t}$ time dependence is assumed and suppressed throughout this chapter.

B. THEORY AND GENERAL SOLUTION

The geometry under consideration is shown in Figure 2.1. The grounded dielectric slab is infinite in extent in the x,y directions with uniform thickness t. A microstrip patch is printed on the slab at the dielectric-air interface with current density $\bar{J}_s$. Since both regions 1 and 2 are source free, an arbitrary field that satisfies Maxwell's equations can be constructed from two scalar functions [16]: ψ_{mi} which generates a TM field and ψ_{ei} which generates a TE field, where i = 1 for the region inside the dielectric, and i = 2 for the region outside the dielectric. Both scalar functions ψ_{mi} and ψ_{ei} satisfy the scalar wave equation:

$$(\nabla^2 + k_i^2) \begin{vmatrix} \psi_{mi}(\bar{r}) \\ \psi_{ei}(\bar{r}) \end{vmatrix} = 0 \quad , \tag{2.1}$$

$$\text{where } k_i^2 = \begin{cases} \epsilon_r k_o^2 & \text{in region 1} \quad (i = 1) \\ k_o^2 & \text{in region 2} \quad (i = 2) \end{cases} ,$$

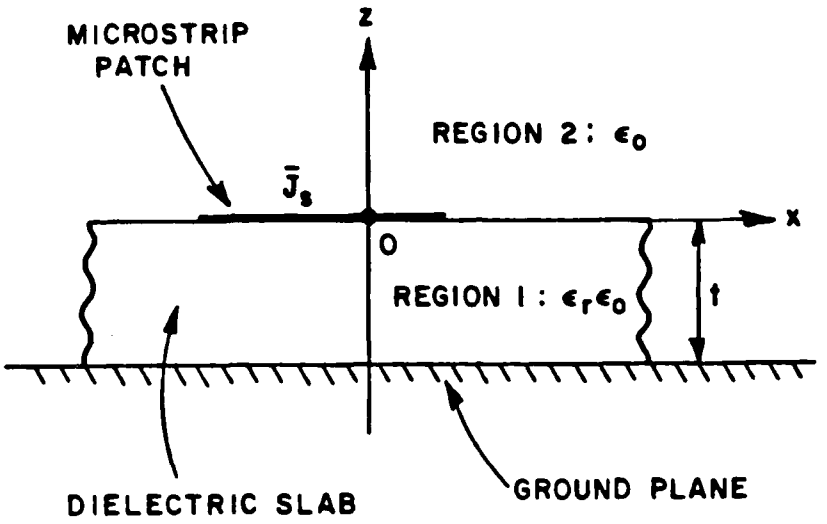

Figure 2.1. Geometry of a microstrip patch printed on a grounded dielectric slab.

k_o is the free space propagation constant, and ϵ_r is the relative dielectric constant in region 1.

Upon multiplying ψ_{mi} and ψ_{ei} by the unit vector $\hat{z}$, one can construct the fields as [16]

$$\bar{E}_i(\bar{r}) = -\nabla x(\hat{z}\psi_{ei}(\bar{r})) + \frac{1}{j\omega\epsilon_i}\nabla \times \nabla \times (\hat{z}\psi_{mi}(\bar{r})) \quad , \tag{2.2}$$

$$\bar{H}_i(\bar{r}) = \nabla x(\hat{z}\psi_{mi}(\bar{r})) + \frac{1}{j\omega\mu_o}\nabla \times \nabla \times (\hat{z}\psi_{ei}(\bar{r})) \quad , \tag{2.3}$$

where $\varepsilon_1 = \varepsilon_r\varepsilon_o$ and $\varepsilon_2 = \varepsilon_o$. The explicit form of the field components can be found in Appendix A.

Since the structure is infinite in the x-y plane, the four scalar wave functions can be represented in terms of their 2-D Fourier transforms (or 2-D plane wave expansions) as follows:

in region 1

$$\begin{bmatrix} \psi_{m1}(\bar{r}) \\ \psi_{e1}(\bar{r}) \end{bmatrix} = \frac{1}{4\pi^2} \int\int_{-\infty}^{\infty} \begin{bmatrix} \tilde{\psi}_{m1}(k_x,k_y)\cos k_{z1}(z+t) \\ \tilde{\psi}_{e1}(k_x,k_y)\sin k_{z1}(z+t) \end{bmatrix} e^{-j(k_x x+k_y y)}\, dk_x dk_y \ , \tag{2.4}$$

in region 2

$$\begin{bmatrix} \psi_{m2}(\bar{r}) \\ \psi_{e2}(\bar{r}) \end{bmatrix} = \frac{1}{4\pi^2} \int\int_{-\infty}^{\infty} \begin{bmatrix} \tilde{\psi}_{m1}(k_x,k_y) \\ \tilde{\psi}_{e1}(k_x,k_y) \end{bmatrix} e^{-j\bar{k}\cdot\bar{r}}\, dk_x dk_y \ , \tag{2.5}$$

where

$$\begin{aligned} k_{z1} &= \sqrt{\varepsilon_r k_o^2 - k_x^2 - k_y^2} \quad , \ \mathrm{Re}\, k_{z1} > 0 \ , \ \mathrm{Im}\, k_{z1} < 0 \ , \\ k_{z2} &= \sqrt{k_o^2 - k_x^2 - k_y^2} \quad , \ \mathrm{Re}\, k_{z2} > 0 \ , \ \mathrm{Im}\, k_{z2} < 0 \ , \\ \bar{k} &= \hat{x}k_x + \hat{y}k_y + \hat{z}k_{z2} \quad , \end{aligned} \tag{2.6}$$

and

$$\bar{r} = \hat{x}x + \hat{y}y + \hat{z}z \quad .$$

It should be pointed out that using Equations (2.4,5) in (2.2,3) will automatically satisfy:

a. the boundary condition at the conducting ground plane:

$$\hat{z} \times \bar{E}_1 = 0 \quad \text{at } z = -t \quad ; \tag{2.7}$$

b. the radiation condition as $r = |\bar{r}| \to \infty$; and

c. the criterion for the integrals in (2.5) to converge as $z \to \infty$.

To specify the fields uniquely, the boundary conditions at the dielectric-air interface must be satisfied:

$$\hat{z} \times (\bar{E}_2 - \bar{E}_1) = 0 \quad \text{at} \quad z = 0 \quad , \tag{2.8}$$

and

$$\hat{z} \times (\bar{H}_2 - \bar{H}_1) = \bar{J}_s \quad \text{at } z = 0 \quad . \tag{2.9}$$

Without loss of generality, the current density is assumed to be Fourier transformable and to have both x and y components. Hence, $\bar{J}_s$ can be written as

$$\begin{aligned} \bar{J}_s(x,y) &= \hat{x}J_{sx}(x,y) + \hat{y}J_{sy}(x,y) \\ &= \frac{1}{4\pi^2} \int_{-\infty}^{\infty}\int \{\hat{x}\tilde{J}_{sx}(k_x,k_y) + \hat{y}\tilde{J}_{sy}(k_x,k_y)\} e^{-j(k_x x + k_y y)} dk_x dk_y \quad . \end{aligned} \tag{2.10}$$

Use of Equations (2.8) and (2.9) will determine completely the spectral functions $\tilde{\psi}_{mi}, \tilde{\psi}_{ei} (i=1,2)$. The algebraic details are carried out in Appendix A. Only the field components are listed below:

region 1 ($-\infty < x,y < \infty$, $-t < z < 0$)

$$E_{x1}(\bar{r}) = \frac{j}{4\pi^2} \int_{-\infty}^{\infty} \int \left[k_y \tilde{\psi}_{e1} - \frac{jk_x k_{z1}}{\omega\varepsilon_o\varepsilon_r} \tilde{\psi}_{m1} \right] e^{-j(k_x x + k_y y)} \sin k_{z1}(z+t) dk_x dk_y \quad , \tag{2.11}$$

$$E_{y1}(\bar{r}) = \frac{-j}{4\pi^2} \int_{-\infty}^{\infty} \int \left[k_x \tilde{\psi}_{e1} + \frac{jk_y k_{z1}}{\omega\varepsilon_o\varepsilon_r} \tilde{\psi}_{m1} \right] e^{-j(k_x x + k_y y)} \sin k_{z1}(z+t) dk_x dk_y \quad , \tag{2.12}$$

$$E_{z1}(\bar{r}) = \frac{-j}{4\pi^2} \int_{-\infty}^{\infty} \int \frac{(k_x^2 + k_y^2)}{\omega\varepsilon_o\varepsilon_r} \tilde{\psi}_{m1} e^{-j(k_x x + k_y y)} \cos k_{z1}(z+t) dk_x dk_y \quad , \tag{2.13}$$

$$H_{x1}(\bar{r}) = \frac{j}{4\pi^2} \iint_{-\infty}^{\infty} \left[\frac{jk_x k_{z1}}{\omega\mu_o} \tilde{\psi}_{e1} - k_y \tilde{\psi}_{m1} \right] e^{-j(k_x x + k_y y)} \cos k_{z1}(z+t)\, dk_x dk_y \quad , \tag{2.14}$$

$$H_{y1}(\bar{r}) = \frac{j}{4\pi^2} \iint_{-\infty}^{\infty} \left[\frac{jk_y k_{z1}}{\omega\mu_o} \tilde{\psi}_{e1} + k_x \tilde{\psi}_{m1} \right] e^{-j(k_x x + k_y y)} \cos k_{z1}(z+t)\, dk_x dk_y \quad , \tag{2.15}$$

and

$$H_{z1}(\bar{r}) = \frac{-j}{4\pi^2} \iint_{-\infty}^{\infty} \frac{(k_x^2 + k_y^2)}{\omega\mu_o} \tilde{\psi}_{e1}\, e^{-j(k_x x + k_y y)} \sin k_{z1}(z+t)\, dk_x dk_y \quad ; \tag{2.16}$$

region 2 ($-\infty < x,y < \infty$, $0 \leq z < \infty$)

$$E_{x2}(\bar{r}) = \frac{j}{4\pi^2} \iint_{-\infty}^{\infty} \left[k_y \tilde{\psi}_{e2} + \frac{k_x k_{z2}}{\omega\varepsilon_o} \tilde{\psi}_{m2} \right] e^{-j(k_x x + k_y y + k_{z2} z)}\, dk_x dk_y \quad , \tag{2.17}$$

$$E_{y2}(\bar{r}) = \frac{-j}{4\pi^2} \int\int_{-\infty}^{\infty} \left[k_x \tilde{\psi}_{e2} - \frac{k_y k_{z2}}{\omega\varepsilon_o} \tilde{\psi}_{m2} \right] e^{-j(k_x x + k_y y + k_{z2} z)} dk_x dk_y \,, \tag{2.18}$$

$$E_{z2}(\bar{r}) = \frac{-j}{4\pi^2} \int\int_{-\infty}^{\infty} \frac{(k_x^2 + k_y^2)}{\omega\varepsilon_o} \tilde{\psi}_{e2} e^{-j(k_x x + k_y y + k_{z2} z)} dk_x dk_y \,, \tag{2.19}$$

$$H_{x2}(\bar{r}) = \frac{j}{4\pi^2} \int\int_{-\infty}^{\infty} \left[\frac{k_x k_{z2}}{\omega\mu_o} \tilde{\psi}_{e2} - k_y \tilde{\psi}_{m2} \right] e^{-j(k_x x + k_y y + k_{z2} z)} dk_x dk_y \,, \tag{2.20}$$

$$H_{y2}(\bar{r}) = \frac{j}{4\pi^2} \int\int_{-\infty}^{\infty} \left[\frac{k_y k_{z2}}{\omega\mu_o} \tilde{\psi}_{e2} + k_x \tilde{\psi}_{m2} \right] e^{-j(k_x x + k_y y + k_{z2} z)} dk_x dk_y \,, \tag{2.21}$$

and

$$H_{z2}(\bar{r}) = \frac{-j}{4\pi^2} \int\int_{-\infty}^{\infty} \frac{(k_x^2 + k_y^2)}{\omega\mu_o} \tilde{\psi}_{e2} e^{-j(k_x x + k_y y + k_{z2} z)} dk_x dk_y \,, \tag{2.22}$$

where

$$\tilde{\psi}_{e1} = \frac{\omega\mu_o}{(k_x^2+k_y^2)D_e} [k_x\tilde{J}_{sy} - k_y\tilde{J}_{sx}] \quad , \tag{2.23}$$

$$\tilde{\psi}_{e2} = \frac{\omega\mu_o \sin k_{z1}t}{(k_x^2+k_y^2)D_e} [k_x\tilde{J}_{sy} - k_y\tilde{J}_{sx}] \quad , \tag{2.24}$$

$$\tilde{\psi}_{m1} = - \frac{j\epsilon_r k_{z2}}{(k_x^2+k_y^2)D_m} [k_x\tilde{J}_{sx} + k_y\tilde{J}_{sy}] \quad , \tag{2.25}$$

$$\tilde{\psi}_{m2} = - \frac{k_{z1}\sin k_{z1}t}{(k_x^2+k_y^2)D_m} [k_x\tilde{J}_{sx} + k_y\tilde{J}_{sy}] \quad , \tag{2.26}$$

$$D_e = k_{z1}\cos k_{z1}t + jk_{z2}\sin k_{z1}t \quad , \tag{2.27}$$

and

$$D_m = \epsilon_r k_{z2}\cos k_{z1}t + jk_{z1}\sin k_{z1}t \quad . \tag{2.28}$$

It should be pointed out that there are two dyadic Green's functions $\bar{\bar{G}}^1$ and $\bar{\bar{G}}^2$, associated with the grounded dielectric slab. $\bar{\bar{G}}^1$ corresponds to the case where the field points are inside the substrate (region 1), and $\bar{\bar{G}}^2$ corresponds to the case where the field points are

outside the substrate (region 2). Only six components of each dyadic Green's function are considered since the surface current on a microstrip patch has no z-component. These components can be identified from Equations (2.11) through (2.13), and (2.17) through (2.19) as follows:

$$G^i_{\alpha\beta}(\bar{r},\bar{r}') = \frac{j}{\omega\mu_o} \int\int_{-\infty}^{\infty} g^i_{\alpha\beta}(\bar{r},k_x,k_y)\, e^{j\bar{k}\cdot\bar{r}'}\, dk_x dk_y \quad , \tag{2.29}$$

where

$i = i,2$

$\bar{k} = \hat{x}k_x + \hat{y}k_y$

$\bar{r}' = \hat{x}x' + \hat{y}y'$

$\bar{r} = \hat{x}x + \hat{y}y + \hat{z}z$

$\alpha = x,y,z$

$\beta = x,y$

and $g^i_{\alpha\beta}$ are obtained from the electric field components which typically have the following form:

$$E_{\alpha i}(\bar{r}) = \int\int_{-\infty}^{\infty} [g^i_{\alpha x}(\bar{r},k_x,k_y)\tilde{J}_{sx}(k_x,k_y) + g^i_{\alpha y}(\bar{r},k_x,k_y)\tilde{J}_{sy}(k_x,k_y)]dk_x dk_y. \tag{2.30}$$

It follows from Equation (2.30) that the calculations of either electric fields or mutual impedances will invariably involve the numerical evaluation of an integral of the form:

$$I = \int_{-\infty}^{\infty}\int \frac{F(k_x,k_y)}{D_e D_m}\, dk_x dk_y \quad , \tag{2.31}$$

which, however, can be facilitated by changing to polar coordinates k,ϕ where

$$k_x = k\cos\phi \quad , \tag{2.32}$$

$$k_y = k\sin\phi \quad . \tag{2.33}$$

Thus,

$$I = \int_{C_k} k\,dk \int_0^{2\pi} \frac{F(k,\phi)}{D_e D_m}\, d\phi \quad . \tag{2.34}$$

The contour C_k for the k integration is shown in Figure 2.2. The branch cuts for the branch points $k = \pm k_o$ are defined by the analytic properties that

a) $\text{Im } k_{z2} = \text{Im } \sqrt{k_o^2 - k^2} < 0$ on the entire top Riemann sheet;

b) $\text{Re } k_{z2} > 0$ in the first and third quadrants; and

c) $\text{Re } k_{z2} < 0$ in the second and fourth quadrants.

However, $k = \pm \sqrt{\epsilon_r}\, k_o$ are not branch points since the integrand is a single-valued function of $k_{z1} = \sqrt{\epsilon_r k_o^2 - k^2}$. The branch cuts are also shown in Figure 2.2.

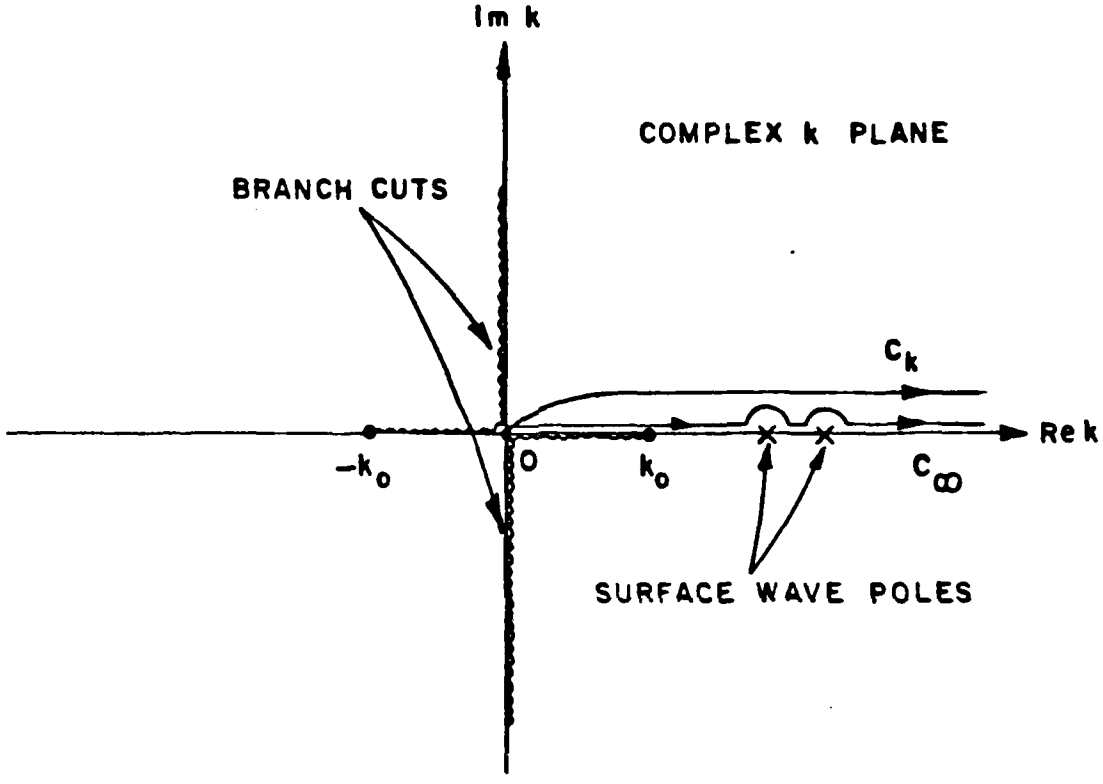

Figure 2.2. Proper contours of integration and branch cuts in the complex k plane.

The denominator in the integrand of Equation (2.24) defines the surface wave modes. These modes are determined by the roots of

$$D_e = 0 \quad \text{(for the TE waves)} \quad , \tag{2.35}$$

$$D_m = 0 \quad \text{(for the TM waves)} \quad . \tag{2.36}$$

Substituting $a = k_o t\sqrt{\varepsilon_r - 1}$ and $\sigma = t\sqrt{\varepsilon_r k_o^2 - k^2}$ into Equations (2.35) and (2.36) and rearranging terms yields, respectively,

$$\sqrt{a^2 - \sigma^2} + \sigma\cot\sigma = 0 \quad , \tag{2.37}$$

$$-\varepsilon_r\sqrt{a^2 - \sigma^2} + \sigma\tan\sigma = 0 \quad . \tag{2.38}$$

It can be demonstrated that if ε_r is real and $\varepsilon_r \neq 1$, the roots of Equations (2.37) and (2.38) are real and located inside the segemnt $k_o < k < \sqrt{\varepsilon_r}k_o$. If N_e, N_m represents the number of roots for the TE, TM case, respectively, then it can be shown that

$$N_e = \begin{cases} 0 & , \text{ for } a < \pi/2 \\ n & , \text{ for } (n-1/2)\pi < a < (n+1/2)\pi, \quad n = 1,2,3,.... \end{cases} ,$$

and

$$N_m = n+1 \quad , \text{ for } n\pi < a < (n+1)\pi, \; n = 0,1,2,.... \quad .$$

It is noted that the dominant TM mode has a zero cutoff frequency. For lossy dielectric (Im $\varepsilon_r \neq 0$), the roots just move off the real k-axis with the form $k = k_r - jk_i$, $k_i > 0$. The exact root locations can be determined by using the Newton-Rhapson procedure.

For efficient numerical evaluation of the integral in Equation (2.34), the new contour C_∞ is adopted by deforming C_k (as shown in Figure 2.2). The integration along C_∞ is performed by computing the Cauchy value of the integrals around the surface wave poles. Assuming the surface wave poles constitute an ordered set as $\{p_\ell, \ell=1,2,\ldots,n\}$, Equation (2.34) can be written as

$$\Gamma = \lim_{\delta \to 0^+} \left[\int_0^{p_1-\delta} + \int_{p_1+\delta}^{p_2-\delta} + \cdots + \int_{p_{n-1}+\delta}^{p_n-\delta} + \int_{p_n+\delta}^{\infty} \right] k\,dk \int_0^{2\pi} \frac{F(k,\phi)}{D_e D_m}\, d\phi$$

$$- j\pi \sum_{\ell=1}^{n} \int_0^{2\pi} d\phi \; \text{Residue} \left[\frac{F(k,\phi)}{D_e D_m} \right]_{k=p_\ell} . \qquad (2.39)$$

In the case of lossy dielectric, the integrations from $p_\ell - \delta$ to $p_\ell + \delta$, $\ell=1,2,3,\ldots,n$, can be evaluated analytically without indenting the contour C_∞. This is done by using two terms of a Taylor series expansion of $D_e D_m$ about p_ℓ, and by taking the value of the numerator $F(k,\phi)$ at $k=p_\ell$ throughout the interval.

In actual numerical evaluation of (2.39), $\delta \sim 0.001/k_0$, and the infinite integral is terminated at $k \sim 150\ k_0$.

C. MUTUAL COUPLING ANALYSIS

In this section, the moment method solution for coupled microstrip antennas is described. Without loss of generality, an array of M arbitrarily oriented rectangular microstrip antenna patches on a grounded dielectric slab is considered. When patch q is excited by a vertical filament of constant current density $\bar{J}_i^q$ (a rough approximation to a coaxial or microstrip line feed), an incident field $\bar{E}_i^q$ is radiated. Let the sum of the surface currents induced on each of the patches by $\bar{J}_i^q$ be denoted as $\bar{J}_s^q$; this $\bar{J}_s^q$ radiates to produce the scattered field $\bar{E}_s^q$. On the surface of the patches, the total tangential electric field vanishes so that

$$\int_S \bar{J}_T \cdot (\bar{E}_i^q + \bar{E}_s^q) ds = 0 \quad , \tag{2.41}$$

where $\bar{J}_T$ is an arbitrary non-zero test current (usually called the test mode) located on the surface S of the microstrip patches (where $\bar{J}_s^q$ exists). Denoting the electric field due to $\bar{J}_T$ by $\bar{E}_T$, and applying the reciprocity theorem to the pair of fields ($\bar{E}_s^q$; $\bar{E}_T$) and sources ($\bar{J}_s^q$; $\bar{J}_T$) yields

$$\int_S \bar{J}_T \cdot \bar{E}_s^q \, ds = \int_S \bar{E}_T \cdot \bar{J}_s^q \, ds \quad .$$

Applying the reciprocity theorem once again to the pair of fields ($\bar{E}_i^q$; $\bar{E}_T$) and sources ($\bar{J}_i^q$; $\bar{J}_T$) yields

$$\int_S \bar{J}_T \cdot \bar{E}_i^q \, ds = \int_V \bar{E}_T \cdot \bar{J}_i^q \, dv \quad .$$

It then follows from the above reciprocity relations and Equation (2.41) that

$$- \int_S \bar{E}_T \cdot \bar{J}_s^q \, ds = \int_V \bar{E}_T \cdot \bar{J}_i^q \, dv \quad . \tag{2.42}$$

The next step in the moment method solution is to expand $\bar{J}_s^q$ in terms of known basis functions from a finite ordered set

$$\Xi = \{\bar{J}_n^\alpha = \hat{x} J_{nx}^\alpha + \hat{y} J_{ny}^\alpha : n = 1,\ldots,N_\alpha, \alpha = 1,2,\ldots,M, \; N_1 + N_2 + \ldots + N_M = N\}.$$

Thus

$$\bar{J}_s^q = \sum_{\alpha=1}^{M} \sum_{n=1}^{N_\alpha} I_n^\alpha(q) \, \bar{J}_n^\alpha \quad , \tag{2.43}$$

where $\bar{J}_n^\alpha$, known as an expansion dipole mode, is the current density of mode n on patch α, and $I_n^\alpha(q)$ is its unknown current amplitude. In the Galerkin scheme $\bar{J}_T$ is chosen to be an element $\bar{J}_m^\beta \varepsilon \Xi$ which excites the electric field $\bar{E}_m^\beta$. Hence, inserting Equation (2.43) into (2.42) for all m and β yields

$$\sum_{\alpha=1}^{M} \sum_{n=1}^{N_\alpha} I_n^\alpha(q) z_{mn}^{\beta\alpha} = v_m^\beta(q) \quad , \tag{2.44}$$

where $m = 1,2,\ldots,N_\beta$, $\beta = 1,2,\ldots,M$, $\sum_\beta N_\beta = N$, and

$$z_{mn}^{\beta\alpha} = - \int_S \bar{E}_m^\beta(\bar{r}_{mn}^{\beta\alpha} + \bar{r}_n^\alpha) \cdot \bar{J}_n^\alpha(\bar{r}_n^\alpha) ds \quad , \tag{2.45}$$

$$v_m^\beta(q) = \int_V \bar{E}_m^\beta(\bar{r}_m^\beta) \cdot \bar{J}_i^q(\bar{r}_m^\beta) dv \quad , \tag{2.46}$$

where

$\bar{r}_{mn}^{\beta\alpha} = (x_{mn}^{\beta\alpha}, y_{mn}^{\beta\alpha}, 0)$ is the displacement vector from the center of mode m on patch β to the center of mode n on patch α, and

$\bar{r}_m^{\beta} = (x_m^{\beta}, y_m^{\beta}, z)$ is the postion vector referenced to the center of mode m on patch β.

In Equation (2.46), the excitation J_i^q at port q is modeled as $\bar{J}_i^q(\bar{r}_m^{\beta}) = \hat{z} I_i^q \delta(x - x_{mf}^{\beta q}) \delta(y - y_{mf}^{\beta q})$, $-\infty < x,y < \infty$, $-t \leq z \leq 0$, where $(x_{mf}^{\beta q}, y_{mf}^{\beta q}, 0)$ is the displacement vector from the center of mode m on patch β to the feed location on patch q.

The geometry of modes m and n pertaining to the evaluation of $z_{mn}^{\beta\alpha}$ and $v_m^{\beta}(q)$ is depicted in Figure 2.3. In terms of matrix notations, (2.44) can be written as

$$[Z][I(q)] = [V(q)] \quad , \tag{2.47}$$

where

$$[Z] = \begin{bmatrix} & & \\ & & \\ & & \\ \hline & & \\ & \begin{matrix} z_{11}^{\beta\alpha} & \cdots & z_{1N_\alpha}^{\beta\alpha} \\ \vdots & & \vdots \\ z_{N_\beta 1}^{\beta\alpha} & \cdots & z_{N_\beta N_\alpha}^{\beta\alpha} \end{matrix} & \\ & & \\ \hline & & \\ & & \\ & & \end{bmatrix} \begin{matrix} \\ \\ \\ \\ \beta^{th} \text{ row block} \\ \\ \\ \\ \\ \end{matrix} \tag{2.48}$$

α^{th} column block

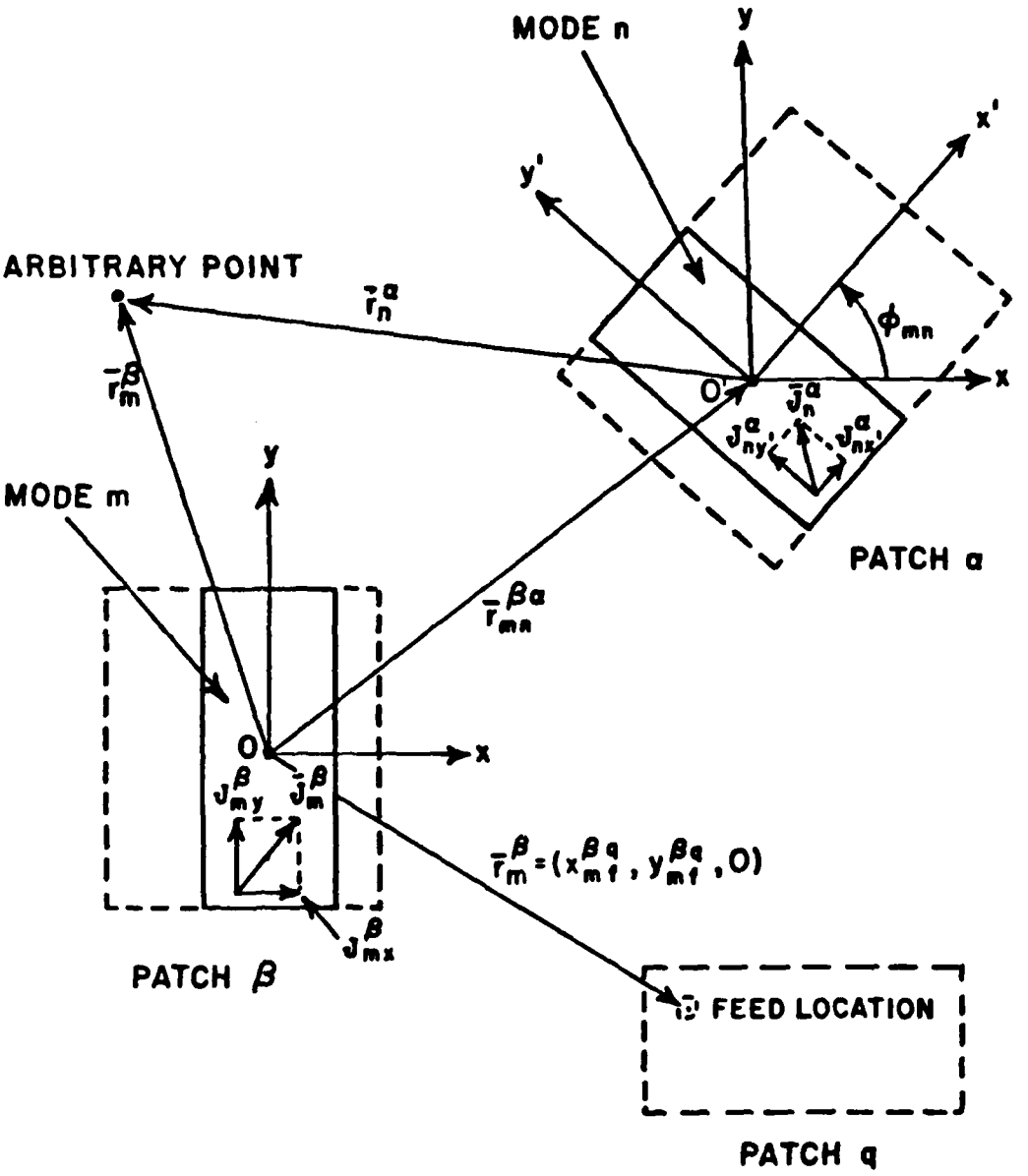

Figure 2.3. Geometry of patches and expansion dipole modes for the evaluation of $z_{mn}^{\beta\alpha}$ and $v_m^\beta(q)$.

$$[I(q)] = [I_1^1(q)\ldots I_{N_1}^1(q)\,|\ldots|\,I_1^\alpha(q)\ldots I_{N_\alpha}^\alpha(q)\,|\ldots|\,I_1^M(q)\ldots I_{N_M}^M(q)]^T, \tag{2.49}$$

$$[V(q)] = [v_1^1(q)\ldots v_{N_1}^1(q)\,|\ldots|\,v_1^\alpha(q)\ldots v_{N_\alpha}^\alpha(q)\,|\ldots|\,v_1^M(q)\ldots v_{N_M}^M(q)]^T. \tag{2.50}$$

In Equations (2.49) and (2.50), T denotes taking the transpose of the row vector. Thus, the current amplitudes [I(q)] can be solved algebraically by matrix inversion:

$$[I(q)] = [Z]^{-1}[V(q)] \quad . \tag{2.51}$$

As indicated in Equation (2.51), the current amplitudes will depend on the feed location on patch q.

According to Equation (1.14), the input impedance at port q is given by

$$z_{qq}^p = - \frac{\sum_{\alpha=1}^{M} \sum_{n=1}^{N_\alpha} I_n^\alpha(q) v_n^\alpha(q)}{(I_i^q)^2} \quad . \tag{2.52}$$

Similarly, it follows from Equation (1.16) that the mutual impedance between port q and port r is given by

$$z_{qr}^p = - \frac{\sum_{\alpha=1}^{M} \sum_{n=1}^{N_\alpha} I_n^\alpha(q) v_n^\alpha(r)}{I_i^q \; I_i^r} \quad . \tag{2.53}$$

In Equations (2.52) and (2.53), it is understood that I_i^q and I_i^r are the terminal currents at port q and port r, respectively; the $I_n^\alpha(q)$ are obtained from (2.51); $v_n^\alpha(q)$ and $v_n^\alpha(r)$ are the voltages at port q and port r, respectively, due to mode n on patch α excited by source $\bar{J}_i^q$ when all other ports are open circuited.

To compute the moment method solution for mutual coupling between microstrip patch antennas, one needs to evaluate Equations (2.45) and (2.46). As presented in Appendix B, the exact expressions for $z_{mn}^{\beta\alpha}$ and $v_m^\beta(q)$ are given by

$$z_{mn}^{\beta\alpha} = -\frac{j}{4\pi^2}\int_{-\infty}^{\infty}\int \Bigg[\Bigg[(k_y\tilde{\psi}_{e2}^\beta + \frac{k_x k_{z2}}{\omega\varepsilon_o}\tilde{\psi}_{m2}^\beta)\cos\phi_{mn} - (k_x\tilde{\psi}_{e2}^\beta - \frac{k_x k_{z2}}{\omega\varepsilon_o}\tilde{\psi}_{m2}^\beta)\sin\phi_{mn}\Bigg]\tilde{J}_{nx'}^\alpha - \Bigg[(k_y\tilde{\psi}_{e2}^\beta + \frac{k_x k_{z2}}{\omega\varepsilon_o}\tilde{\psi}_{m2}^\beta)\sin\phi_{mn} + (k_x\tilde{\psi}_{e2}^\beta - \frac{k_y k_{z2}}{\omega\varepsilon_o}\tilde{\psi}_{m2}^\beta)\cos\phi_{mn}\Bigg]\tilde{J}_{ny'}^\alpha\Bigg] \cdot e^{-j(k_x x_{mn}^{\beta\alpha} + k_y y_{mn}^{\beta\alpha})}\, dk_x dk_y \quad , \tag{2.54}$$

$$v_m^\beta(q) = -\frac{jI_i^q}{4\pi^2}\int_{-\infty}^{\infty}\int \frac{(k_x^2+k_y^2)}{\omega\varepsilon_o\varepsilon_r k_{z1}}\tilde{\psi}_{m1}^\beta e^{-j(k_x x_{mf}^{\beta q} + k_y y_{mf}^{\beta q})}\sin k_{z1}t\, dk_x dk_y \quad , \tag{2.55}$$

where

$$\tilde{\psi}^{\beta}_{m1} = -\frac{j\varepsilon_r k_{z2}}{(k_x^2+k_y^2)D_m}\,(k_x\tilde{J}^{\beta}_{mx} + k_y\tilde{J}^{\beta}_{my}) \quad , \tag{2.56}$$

$$\tilde{\psi}^{\beta}_{e2} = \frac{\omega\mu_o \sin k_{z1}t}{(k_x^2+k_y^2)D_e}\,(k_x\tilde{J}^{\beta}_{my} - k_y\tilde{J}^{\beta}_{mx}) \quad , \tag{2.57}$$

$$\tilde{\psi}^{\beta}_{m2} = -\frac{k_{z1}\sin k_{z1}t}{(k_x^2+k_y^2)D_m}\,(k_x\tilde{J}^{\beta}_{mx} + k_y\tilde{J}^{\beta}_{my}) \quad , \tag{2.58}$$

$$\tilde{J}^{\beta}_{mx} = \int_{-y^{\beta}_m}^{y^{\beta}_m}\int_{-x^{\beta}_m}^{x^{\beta}_m} J^{\beta}_{mx}(x,y)e^{j(k_x x+k_y y)}\,dxdy \quad , \tag{2.59}$$

$$\tilde{J}^{\beta}_{my} = \int_{-y^{\beta}_m}^{y^{\beta}_m}\int_{-x^{\beta}_m}^{x^{\beta}_m} J^{\beta}_{my}(x,y)e^{j(k_x x+k_y y)}\,dxdy \quad , \tag{2.60}$$

$$\tilde{J}^{\alpha}_{nx'} = \int_{-y^{\alpha}_n}^{y^{\alpha}_n}\int_{-x^{\alpha}_n}^{x^{\alpha}_n} J^{\alpha}_{nx'}(x',y')\, e^{-j[x'(k_x\cos\phi_{mn}+k_y\sin\phi_{mn}) + y'(-k_x\sin\phi_{mn}+k_y\cos\phi_{mn})]}\,dx'dy' \quad , \tag{2.61}$$

$$\tilde{J}^{\alpha}_{ny'} = \int_{-y^{\alpha}_n}^{y^{\alpha}_n} \int_{-x^{\alpha}_n}^{x^{\alpha}_n} J^{\alpha}_{ny'}(x',y') \, e^{-j[x'(k_x\cos\phi_{mn}+k_y\sin\phi_{mn}) + y'(-k_x\sin\phi_{mn}+k_y\cos\phi_{mn})]} dx'dy' \quad , \tag{2.62}$$

ϕ_{mn} is the angle between the x-axis of mode m and the x'-axis of mode n (see Figure 2.3); $2x^{\beta}_m$ and $2y^{\beta}_m$ are the widths of mode m on patch β in the x and y directions, respectively, and likewise, $2x^{\alpha}_n$, $2y^{\alpha}_n$ are the widths of mode n on patch α in the x',y' directions.

D. NUMERICAL EXAMPLES

Calculation of mutual coupling (s_{12} parameter) between two identical coax-fed rectangular microstrip antennas is presented in this section. Two antenna geometries (E-plane and H-plane coupling) are considered. In both examples, the expansion set is chosen to be

$$\Xi = \{\bar{J}^{\alpha}_n = \hat{x}J^{\alpha}_{nx}: \quad n=1, \ \alpha=1,2, \ N_1=N_2=1 \} \quad , \tag{2.63}$$

where

$$J^{\alpha}_{1x}(x,y) = \begin{cases} \dfrac{\sin\kappa(x^{\alpha}_1-|x|)}{2y^{\alpha}_1\sin\kappa x^{\alpha}_1} & , \ |x| \leq x^{\alpha}_1, \ |y| \leq y^{\alpha}_1, \ \alpha=1,2 \\ 0 & , \text{otherwise} \end{cases} \quad . \tag{2.64}$$

In Equation (2.64), the coordinates x, y are referenced to the center of the expansion dipole mode of length $2x^{\alpha}_1$ (along the direction of the current) and width $2y^{\alpha}_1$. Furthermore,

$$\kappa = \omega\sqrt{\mu_o \varepsilon_{eq}} \quad , \tag{2.65}$$

$$\varepsilon_{eq} = \varepsilon_o \left[\frac{\varepsilon_r + 1}{2} + \frac{\varepsilon_r - 1}{2} \left(1 + \frac{10t}{2y_1^\alpha}\right)^{-1/2} \right] \quad . \tag{2.66}$$

The choice of dipole mode currents $\bar{J}_1^\alpha$ and constant κ is suggested by [17]. It should be remarked that a current expansion mode in the set Ξ is employed to approximate the even (dominant) current mode (Figure 2.4(a)) on a isolated microstrip patch at its first resonance. As indicated in Equation (2.64), such an expansion mode is uniform in the y-direction and piecewise sinusoidal in the x-direction. It is understood, nevertheless, that at least one odd (attachment) mode (Figure 2.4(b)) also exists simultaneously at resonance to account for the discontinuity in current due to the feed. Summing the even and odd modes will reasonably represent the true current distribution on the patch (Figure 2.4(c)). For the sake of simplicity, however, only the even dominant mode is considered in the calculations with the understanding that at resonance only the even mode will dominate and closely resemble the true current distribution.

Since $x_1^1 = x_1^2$, $y_1^1 = y_1^2$ (identical patches), and $J_{1y}^1 = J_{1y'}^2 = 0$, Equations (2.54) and (2.55) reduce to, respectively,

$$z_{11}^{\beta\alpha} = -\frac{j}{4\pi^2} \iint_{-\infty}^{\infty} \left[(k_y \tilde{\psi}_{e2}^\beta + \frac{k_x k_{z2}}{\omega\varepsilon_o} \tilde{\psi}_{m2}^\beta)\cos\phi_{11} - (k_x \tilde{\psi}_{e2}^\beta - \frac{k_x k_{z2}}{\omega\varepsilon_o} \tilde{\psi}_{m2}^\beta)\sin\phi_{11} \right] \cdot \tilde{J}_{1x'}^\alpha \, e^{-j(k_x x_{11}^{\beta\alpha} + k_y y_{11}^{\beta\alpha})} dk_x dk_y \quad , \quad \alpha,\beta=1,2 \quad , \tag{2.67}$$

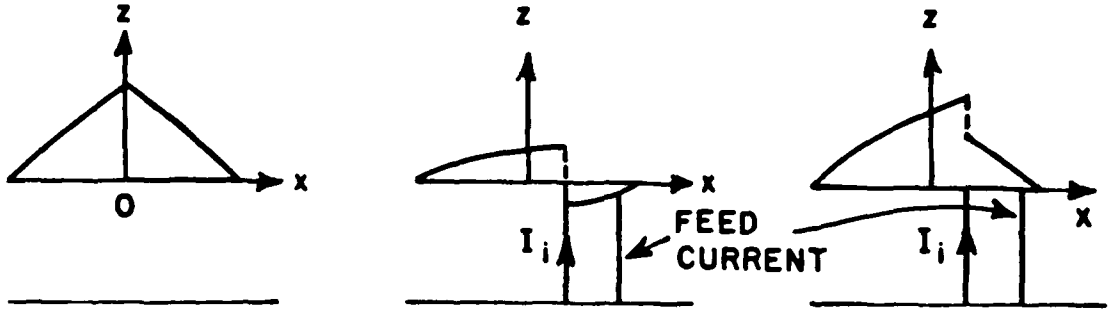

(a) EVEN (DOMINANT) MODE (b) ODD (ATTACHMENT) MODE (c) TRUE CURRENT

Figure 2.4. Current distribution on an isolated microstrip patch at resonance.

$$v_1^{\beta}(\alpha) = \frac{-I_i^{\alpha}}{4\pi^2\omega\varepsilon_o} \iint_{-\infty}^{\infty} \frac{k_x k_{z2} \tilde{J}_{1x}^{\beta}}{k_{z1} D_m} e^{-j(k_x x_{1f}^{\beta\alpha} + k_y y_{1f}^{\beta\alpha})} \sin k_{z1} t \, dk_x dk_y, \quad \alpha,\beta=1,2 \quad , \tag{2.68}$$

where

$$\tilde{\psi}_{e2}^{\beta} = - \frac{\omega\mu_o \sin k_{z1} t}{(k_x^2+k_y^2) D_e} k_y \tilde{J}_{1x}^{\beta} \quad , \tag{2.69}$$

$$\tilde{\psi}_{m2}^{\beta} = - \frac{k_{z1} \sin k_{z1} t}{(k_x^2+k_y^2) D_m} k_x \tilde{J}_{1x}^{\beta} \tag{2.70}$$

$$\begin{aligned} \tilde{J}_{1x}^{\beta} &= \int_{-y_1^1}^{y_1^1} \int_{-x_1^1}^{x_1^1} J_{1x}^{\beta}(x,y) \, e^{j(k_x x + k_y y)} \, dxdy \\ &= \frac{2\kappa(\cos k_x x_1^1 - \cos \kappa x_1^1)}{\sin \kappa x_1^1 (\kappa^2 - k_x^2)} \cdot \frac{\sin k_y y_1^1}{k_y y_1^1} \quad , \beta=1,2 \end{aligned} \tag{2.71}$$

$$\tilde{J}^{\alpha}_{1x'} = \int_{-y_1^2}^{y_1^2} \int_{-x_1^2}^{x_1^2} J^{\alpha}_{1x}(x,y)$$

$$e^{-j[x(k_x\cos\phi_{11}+k_y\sin\phi_{11}) + y(-k_x\sin\phi_{11}+k_y\cos_{11})]}dxdy$$

$$\alpha=1,2 \quad , \tag{2.72}$$

$$(x^{\beta\alpha}_{1f}, y^{\beta\alpha}_{1f}) = (x^{\beta\alpha}_{11}, y^{\beta\alpha}_{11}) + (x^{\alpha\alpha}_{1f}, y^{\alpha\alpha}_{1f}) \quad , \alpha,\beta=1,2 \quad . \tag{2.73}$$

It should be noted that $(x^{\alpha\alpha}_{1f}, y^{\alpha\alpha}_{1f})$ is determined from Equation (2.68) by enforcing the condition that $v^{\alpha}_1(\alpha)/I^{\alpha}_i$ is a real quantity. This corresponds to the condition that the isolated microstrip antenna is at resonance.

Example 1: E-plane coupling

The antenna geometry is shown in Figure 2.5. In this special case,

$x^1_1 = x^2_1 = 3.275$ cm

$y^1_1 = y^2_1 = 5.285$ cm

$x^{11}_{1f} = x^{22}_{1f} = -1.115$ cm

$y^{11}_{1f} = y^{22}_{1f} = 0$ cm

$\phi_{11} = 0$

$y^{\beta\alpha}_{11} = 0 \quad , \beta,\alpha=1,2$

frequency = 1417 MHz

$t = 0.1575$ cm, and

$\varepsilon_r = 2.5$.

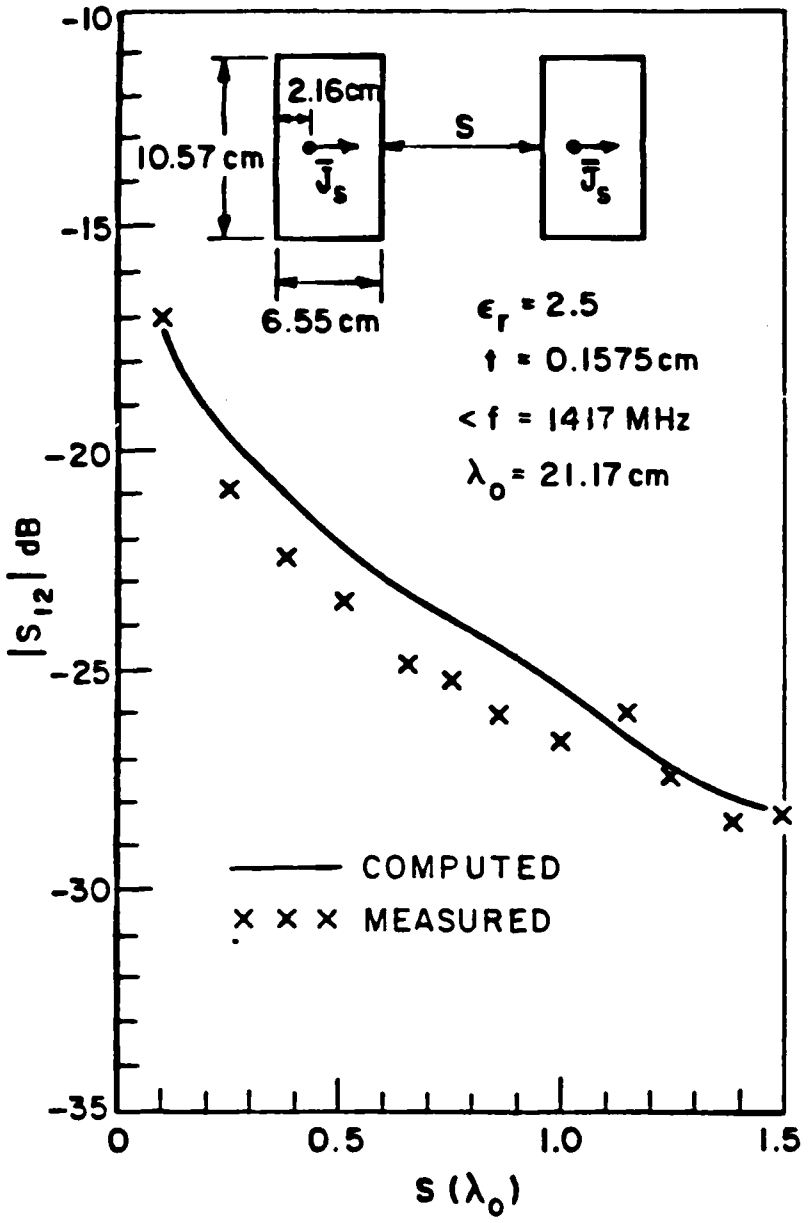

Figure 2.5. E-plane coupling for identical microstrips.

It can be deduced from Equation (2.72) that $\tilde{J}^{\alpha}_{1x'} = \tilde{J}^{\alpha}_{1x}$, $\alpha=1,2$. Also, (2.73) implies that $y^{\beta\alpha}_{1f} = 0$, $\alpha,\beta=1,2$. Thus Equations (2.67) and (2.68) reduce to

$$z^{\beta\alpha}_{11} = \frac{j\eta_o}{4\pi^2 k_o} \int\int_{-\infty}^{\infty} Q_{xx}(k_x,k_y)\tilde{J}^{\beta}_{1x}\tilde{J}^{\alpha}_{1x}\, e^{-jk_x x^{\beta\alpha}_{11}}\, dk_x dk_y, \quad \alpha,\beta=1,2 \quad , \tag{2.74}$$

$$v^{\beta}_{1}(\alpha) = -\frac{I^{\alpha}_{i}\eta_o}{4\pi^2 k_o} \int\int_{-\infty}^{\infty} \frac{k_x k_{z2}}{k_{z1}\eta_m} \sin k_{z1} t\, \tilde{J}^{\beta}_{1x}\, e^{-jk_x x^{\beta\alpha}_{1f}}\, dk_x dk_y, \quad \alpha,\beta=1,2 \quad , \tag{2.75}$$

where

$$Q_{xx}(k_x,k_y) = \frac{\sin k_{z1} t}{D_m D_e} \{k_{z2}(\varepsilon_r k_o^2 - k_x^2)\cos k_{z1} t + jk_{z1}(k_o^2 - k_x^2)\sin k_{z1} t\} \quad , \tag{2.76}$$

$$\eta_o = \sqrt{\frac{\mu_o}{\varepsilon_o}} \quad . \tag{2.77}$$

As mentioned earlier, the infinite k_x, k_y integrations can b facilitated by converting to polar coordinates k and σ defined by

$$k = \sqrt{k_x^2 + k_y^2} \quad , \tag{2.78}$$

$$\sigma = \tan^{-1}(k_y/k_x) \quad . \tag{2.79}$$

Also, the even and odd properties of the integrands can be used to reduce the domain of the σ integration from $[0,2\pi]$ to $[0,\pi/2]$. Equations (2.74) and (2.75) can then be written as

$$z_{11}^{\beta\alpha} = \frac{j\eta_o}{\pi^2 k_o} \int_0^{\infty} \int_0^{\pi/2} Q_{xx}(k,\sigma)\tilde{J}_{1x}^{\beta}\tilde{J}_{1x}^{\alpha} \cos k_x x_{11}^{\beta\alpha}\, k\,d\sigma\,dk \quad , \alpha,\beta=1,2 \tag{2.80}$$

$$v_1^{\beta}(\alpha) = \frac{jI_i^{\alpha}\eta_o}{\pi^2 k_o} \int_0^{\infty} \int_0^{\pi/2} \frac{k_x k_{z2}}{k_{z1} D_m} \sin k_{z1} t \, \sin k_x x_{1f}^{\beta\alpha} \tilde{J}_{1x}^{\beta}\, k\,d\sigma\,dk \quad ,\alpha,\beta=1,2 \; . \tag{2.81}$$

Equations (2.80) and (2.81) are the final forms used for computing the impedance matrix and voltage vector elements.

Example 2: H-plane coupling

Figure 2.6 shows an antenna configuration for studying the H-plane coupling. In this case,

$$x_1^1 = x_1^2 = 3.275 \text{ cm}$$

$$y_1^1 = y_1^2 = 5.285 \text{ cm}$$

$$x_{1f}^{11} = x_{1f}^{22} = -1.115 \text{ cm}$$

$$y_{1f}^{11} = y_{1f}^{22} = 0 \text{ cm}$$

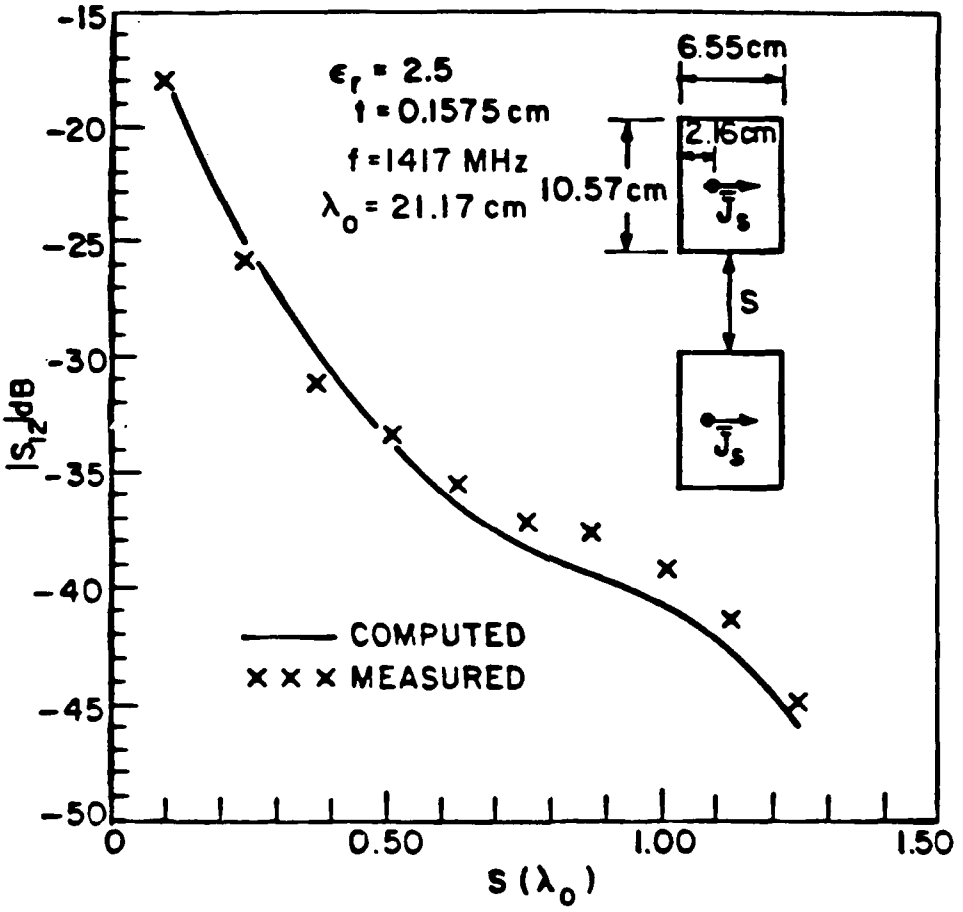

Figure 2.6. H-plane coupling for identical microstrips.

$\phi_{11} = 0$

$x_{11}^{\beta\alpha} = 0$, $\alpha,\beta=1,2$

frequency = 1417 MHz

t = 0.1575 cm, and

$\varepsilon_r = 2.5$.

As noted in Example 1, $\tilde{J}_{1x'}^{\alpha} = \tilde{J}_{1x}^{\alpha}$, $\alpha=1,2$. Moreover, it follows from Equation (2.73) that $(x_{1f}^{\beta\alpha}, y_{1f}^{\beta\alpha}) = (x_{1f}^{\alpha\alpha}, y_{11}^{\beta\alpha})$, $\alpha,\beta=1,2$. Then Equations (2.67) and (2.68) can be simplified to

$$z_{11}^{\beta\alpha} = \frac{j\eta_o}{4\pi^2 k_o} \iint_{-\infty}^{\infty} Q_{xx}(k_x,k_y)\tilde{J}_{1x}^{\beta}\tilde{J}_{1x}^{\alpha} e^{-jk_y y_{11}^{\beta\alpha}} dk_x dk_y, \quad \alpha,\beta=1,2 \quad , \tag{2.82}$$

$$v_1^{\beta}(\alpha) = -\frac{I_i^{\alpha}\eta_o}{4\pi^2 k_o} \iint_{-\infty}^{\infty} \frac{k_x k_{z2}}{k_{z1} D_m} \tilde{J}_{1x}^{\beta} e^{-j(k_x x_{1f}^{\alpha\alpha} + k_y y_{11}^{\beta\alpha})} \sin k_{z1} t \, dk_x dk_y \quad \alpha,\beta=1,2 \quad . \tag{2.83}$$

Introducing polar coordinates k and σ in Equations (2.82) and (2.83) to obtain

$$z_{11}^{\beta\alpha} = \frac{j\eta_o}{\pi^2 k_o} \int_0^{\infty} \int_0^{\pi/2} Q_{xx}(k,\sigma)\tilde{J}_{1x}^{\beta}\tilde{J}_{1x}^{\alpha} \cos k_y y_{11}^{\beta\alpha}\, k\,d\sigma\,dk \quad , \alpha,\beta=1,2 \ , \tag{2.84}$$

$$v_1^{\beta}(\alpha) = \frac{jI_i^{\alpha}\eta_o}{\pi^2 k_o} \int_0^{\infty} \int_0^{\pi/2} \frac{k_x k_{z2}}{k_{z1} D_m} \tilde{J}_{1x}^{\beta} \sin k_{z1} t \, \sin k_x x_{1f}^{\alpha\alpha} \cos k_y y_{11}^{\beta\alpha}\, k\,d\sigma\,dk \ , \quad \alpha,\beta=1,2 \ . \tag{2.85}$$

From Figures 2.5 and 2.6, one can observe that the E-plane coupling is larger than the H-plane coupling. This is due to a stronger surface wave which is excited for the E-plane configuration. In general, the magnitude of the scattering parameter s_{12} is seen to have good agreement with measurements by Jedlicka, et al. [18]. For the data, the isolated microstrips were resonant with 50-Ω resistance. This occured at 1417 MHz for the computations, and at 1410 MHz for the measurements. It is noted that the percentage tolerance on the substrate permittivity and patch size are of the same order of magnitude as the antenna bandwidth (typically a few percent). Such an error causes a shift in resonant frequency, but it is found that the change in the calculated terminal impedance is negligible.

E. FAR ZONE RADIATION FIELD

The radiation field refers to the electric field in region 2 when the field point is significantly removed from the source. From Equations (2.17) to (2.19), it can be shown that the electric field may be expressed by the 2-D Fourier transform as follows:

$$\bar{E}_2(\bar{r}) = \frac{1}{4\pi^2} \iint_{-\infty}^{\infty} \tilde{\bar{E}}_2(k_x,k_y)\, e^{-j\bar{k}\cdot\bar{r}}\, dk_x dk_y \quad , \tag{2.86}$$

where

$$\bar{k} = \hat{x}k_x + \hat{y}k_y + \hat{z}k_{z2}, \quad k_{z2} = \sqrt{k_o^2 - k_x^2 - k_y^2} \quad , \quad \text{Re } k_{z2} > 0, \ \text{Im } k_{z2} < 0,$$

$$\bar{r} = \hat{x}x + \hat{y}y + \hat{z}z \quad , \ -\infty < x,y < \infty \ , \ 0 \leq z < \infty \quad \text{(region 2)},$$

$$\tilde{\bar{E}}_2(k_x,k_y) = \hat{x}\tilde{E}_{x2}(k_x,k_y) + \hat{y}\tilde{E}_{y2}(k_x,k_y) + \hat{z}\tilde{E}_{z2}(k_x,k_y),$$

$$\tilde{E}_{x2} = g_{xx}^2(k_x,k_y)\tilde{J}_{sx} + g_{xy}^2(k_x,k_y)\tilde{J}_{sy} \quad ,$$

$$\tilde{E}_{y2} = g_{yx}^2(k_x,k_y)\tilde{J}_{sx} + g_{yy}^2(k_x,k_y)\tilde{J}_{sy} \quad ,$$

$$\tilde{E}_{z2} = g_{zx}^2(k_x,k_y)\tilde{J}_{sx} + g_{zy}^2(k_x,k_y)\tilde{J}_{sy} \quad ,$$

$$g^2_{xx}(k_x,k_y) = -\frac{jn_o \sin k_{z1} t}{k_o D_e D_m}$$

$$[(\varepsilon_r k_o^2 - k_x^2) k_{z2} \cos k_{z1} t + j(k_o^2 - k_x^2) k_{z1} \sin k_{z1} t] \quad ,$$

$$g^2_{xy}(k_x,k_y) = \frac{jn_o k_x k_y \sin k_{z1} t}{k_o D_e D_m} \left[k_{z2} \cos k_{z1} t + j k_{z1} \sin k_{z1} t \right] \quad ,$$

$$g^2_{yy}(k_x,k_y) = -\frac{jn_o \sin k_{z1} t}{k_o D_e D_m}$$

$$[(\varepsilon_r k_o^2 - k_y^2) k_{z2} \cos k_{z1} t + j(k_o^2 - k_y^2) k_{z1} \sin k_{z1} t] \quad ,$$

$$g^2_{yx}(k_x,k_y) = g^2_{xy}(k_x,k_y) \quad ,$$

$$g^2_{zx}(k_x,k_y) = \frac{jn_o^2 \, k_y \sin k_{z1} t}{D_e} \quad ,$$

$$g_{zy}^2(k_x,k_y) = \frac{-j\eta_o^2 k_x \sin k_{z1} t}{D_e} \quad ,$$

$$D_e = k_{z1}\cos k_{z1} t + jk_{z2}\sin k_{z1} t \quad ,$$

$$D_e = \varepsilon_r k_{z2}\cos k_{z1} t + jk_{z1}\sin k_{z1} t \quad .$$

Since $\nabla \cdot \bar{E}_2(\bar{r}) = 0$ in region 2, the divergence of Equation (2.86) gives

$$\nabla \cdot \tilde{\bar{E}}_2 e^{-j\bar{k}\cdot\bar{r}} = \tilde{\bar{E}}_2 \cdot \nabla e^{-j\bar{k}\cdot\bar{r}} = -j\bar{k} \cdot \tilde{\bar{E}}_2 e^{-j\bar{k}\cdot\bar{r}} = 0 \quad . \tag{2.87}$$

Thus only two components of $\tilde{\bar{E}}_2$ are independent. Then $\tilde{\bar{E}}_2$ can be expressed by

$$\tilde{\bar{E}}_2 = \hat{x}\tilde{E}_{x2} + \hat{y}\tilde{E}_{y2} - \hat{z}\frac{1}{k_{z2}}(k_x\tilde{E}_{x2} + k_y\tilde{E}_{y2}) \quad . \tag{2.88}$$

As shown in Appendix C, the integral in Equation (2.86) can be evaluated asymptotically by the method of stationary phase as $r \to \infty$. Using Equation (2.88) and (C.15) in (2.86) yields the far zone radiation field as follows:

$$\bar{E}(\bar{r}) \sim j \frac{e^{-jk_o r}}{2\pi r} k_o \cos\theta \left[\hat{x}\tilde{E}_{x2}(k_x,k_y) + \hat{y}\tilde{E}_{y2}(k_x,k_y)\right.$$

$$\left. - \hat{z} \frac{1}{k_{z2}} (k_x \tilde{E}_{x2}(k_x,k_y) + k_y \tilde{E}_{y2}(k_x,k_y))\right] \Big|_{(k_x,k_y) = (k_{xo},k_{yo})},$$

$$r \to \infty \quad , \tag{2.89}$$

where $(k_{xo},k_{yo}) = (k_o \sin\theta\cos\phi,\ k_o \sin\theta\sin\phi)$ is the stationary phase point, $k_{z2} = k_o \cos\theta$, and θ and ϕ are the usual angle variables in spherical coordinates.

In terms of spherical components, Equation (2.89) becomes

$$\bar{E}(\bar{r}) \sim jk_o \frac{e^{-jk_o r}}{2\pi r} \{\hat{\phi}[\cos\phi\ \tilde{E}_{y2}(k_{xo},k_{yo}) - \sin\phi\ \tilde{E}_{x2}(k_{xo},k_{yo})]\cos\theta$$

$$+ \hat{\theta}[\cos\phi\ \tilde{E}_{x2}(k_{xo},k_{yo}) + \sin\phi\ \tilde{E}_{y2}(k_{xo},k_{yo})]\} \quad . \tag{2.90}$$

Once the current density $\bar{J}_s$ on the microstrip antenna is determined, the radiation field can be obtained from Equation (2.90).

CHAPTER III

DYADIC GREEN'S FUNCTIONS

A. INTRODUCTION

For many electromagnetic problems, the eigenfunction expansion method provides the most useful solution to the (electric or magnetic) field; the boundary conditions of the problem are readily incorporated into the solution. For waveguides and cavities, in particular, the eigenfunction expansion method is usually the preferable way to solve problems involving current sources and wave scattering. The whole procedure for finding the eigenfunction expansion of the electric field can be organized in a systematic way by introducing the electric dyadic Green's function or simply Green's dyadic ($\bar{\bar{G}}_e$) which is discussed in this chapter.

The eigenfunction expansion of $\bar{\bar{G}}_e$ had been a subject of misconception and controversy in the past. The difficulty centered about the completeness of the expansion. Initially, Tai developed expansions for the dyadic Green's functions in his book [19] which

included only the $\bar{M}$ and $\bar{N}$ functions which are the solenoidal (transverse) Hansen vector wave functions. After the publication of his book, Tai noted that his expansions were incomplete in the source region and discovered the need for the irrotational (longitudinal) Hansen vector wave function $\bar{L}$. In his subsequent amendments [20,21], Tai indicated how the complete expansions of the dyadic Green's functions could be obtained via the method of $\bar{\bar{G}}_m$, where $\bar{\bar{G}}_m$ is the magnetic dyadic Green's function with zero divergence and may be constructed in terms of only the solenoidal eigenfunctions. $\bar{\bar{G}}_e$ is then obtained from $\nabla \times \bar{\bar{G}}_m$, together with a dyadic delta function term at the source point. Thus, he avoided having to deal with the $\bar{L}$ functions explicitly. About the same time, Collin [22] discovered independently the lack of completeness for the E and H modes in the same waveguide problem considered by Tai. Later, Rahmat-Samii [23] modified Tai's method of $\bar{\bar{G}}_m$ via the use of symbolic functions (distributions). More recently, Collin [24] successfully unified the various results on the dyadic Green's functions as presented by different authors. Various representations for the Green's dyadic were presented and their inter-relationships pointed out. Most recently, Pathak [25] described a relatively simple method for constructing a complete expansion of $\bar{\bar{G}}_e$ in a compact and useful form which contains only the solenoidal type eigenfunctions plus an explicit dyadic delta function term that accounts for completeness at the source point.

A main feature of this chapter is on the eigenfunction expansion of $\bar{\bar{G}}_e$ in free space. The present approach follows that of [25] in obtaining the source conditions that govern the Green's dyadic in free space. It then conjectures that the free space Green's dyadic can be expressed as the sum of a solenoidal component and an irrotational component which is allowed to be a symbolic function. The solenoidal component, as usual, is expanded in terms of the $\bar{M}$ and $\bar{N}$ functions; and the irrotational component is deduced from the differential equation governing $\bar{\bar{G}}_e$. Of course, the irrotational component turns out to be in the form of a dyadic delta function as in [20,21] and [25]. Making use of the free space Green's dyadic and the principle of scattering superposition, the dyadic Green's function for an infinite dielectric coated conducting cylinder can be determined without additional analytical difficulty.

The remainder of this chapter is organized as follows. Section B reviews some basic relations governing the electric field ($\bar{E}$), the magnetic field ($\bar{H}$), $\bar{\bar{G}}_e$ and $\bar{\bar{G}}_m$. Only $\bar{E}$ and $\bar{\bar{G}}_e$, however, will be used in the chapters that follow. The free space Green's dyadic is characterized and expanded in Section C which also establishes the orthogonality of the $\bar{M}$ and $\bar{N}$ functions in cylindrical coordinates. In Section D, the Green's dyadic for a dielectric coated cylinder is constructed. Finally, Section E expands the Green's dyadic into component form from which the electric field is easily identified when the source is known.

In the remaining portion of this report, all time-harmonic quantities are assumed to have an $e^{-j\omega t}$ time dependence which will be suppressed throughout.

B. SOME BASIC RELATIONS GOVERNING $\bar{E}$, $\bar{H}$, $\bar{\bar{G}}_e$ AND $\bar{\bar{G}}_m$

The electromagnetic fields $\bar{E}$ and $\bar{H}$ excited by the electric current source $\bar{J}$ in a region V of linear, isotropic and time-invariant medium satisfy the Maxwell's equations:

$$j\omega\mu\bar{H}(\bar{r}) = \nabla \times \bar{E}(\bar{r}) \quad , \tag{3.1}$$

$$k^2\bar{E}(\bar{r}) = j\omega\mu(\nabla \times \bar{H}(\bar{r}) - \bar{J}(\bar{r})) \quad , \tag{3.2}$$

$$\nabla \cdot \bar{H}(\bar{r}) = 0 \quad , \tag{3.3}$$

and

$$\nabla \cdot \bar{E}(\bar{r}) = \frac{\rho(\bar{r})}{\varepsilon} = -\nabla \cdot \left(\frac{j\omega\mu}{k^2}\bar{J}(\bar{r})\right) \quad , \tag{3.4}$$

where $\bar{r} \in V$, μ and ε denote the constitutive parameters of region V; $k^2 = \omega^2\mu\varepsilon$; and ρ is the charge density associated with $\bar{J}$. One can verify from Equations (3.1) and (3.2) that $\bar{E}$ and $\bar{H}$ satisfy the following differential equations, respectively:

$$\nabla \times \nabla \times \bar{E}(\bar{r}) - k^2 \bar{E}(\bar{r}) = j\omega\mu \bar{J}(\bar{r}) \quad , \tag{3.5}$$

and

$$\nabla \times \nabla \times \bar{H}(\bar{r}) - k^2 \bar{H}(\bar{r}) = \nabla \times \bar{J}(\bar{r}) \quad . \tag{3.6}$$

The electric Green's dyadic $\bar{\bar{G}}_e$ for region V is defined as the solution of the vector wave equation:

$$\nabla \times \nabla \times \bar{\bar{G}}_e(\bar{r},\bar{r}') - k^2 \bar{\bar{G}}_e(\bar{r},\bar{r}') = \bar{\bar{I}}\delta(\bar{r}-\bar{r}') \quad , \tag{3.7}$$

and the boundary conditions pertaining to V, where $\bar{r},\bar{r}' \in V$ denote, respectively, the field observation and the point source locations; $\bar{\bar{I}}$ is the unit dyad; and $\delta(\bar{r}-\bar{r}')$ is the Dirac delta function. It can be proved that, for region V, there exists another dyadic function known as the magnetic Green's dyadic, denoted by $\bar{\bar{G}}_m$, which satisfies the differential equation:

$$\nabla \times \nabla \times \bar{\bar{G}}_m(\bar{r},\bar{r}') - k^2 \bar{\bar{G}}_m(\bar{r},\bar{r}') = \nabla \times \bar{\bar{I}}\delta(\bar{r}-\bar{r}') \tag{3.8}$$

together with the associated boundary conditions, and is related to $\bar{\bar{G}}_e$ as

$$\bar{\bar{G}}_m(\bar{r},\bar{r}') = \nabla \times \bar{\bar{G}}_e(\bar{r},\bar{r}') \quad . \tag{3.9}$$

From Equations (3.7) and (3.9) it can be readily verified that

$$k^2\bar{\bar{G}}_e(\bar{r},\bar{r}') = \nabla \times \bar{\bar{G}}_m(\bar{r},\bar{r}') - \bar{\bar{I}}\delta(\bar{r}-\bar{r}') \quad . \tag{3.10}$$

It is also clear from (3.9) and (3.10) that

$$\nabla \cdot \bar{\bar{G}}_m(\bar{r},\bar{r}') = 0 \tag{3.11}$$

and

$$\nabla \cdot \bar{\bar{G}}_e(\bar{r},\bar{r}') = -\nabla \cdot [\bar{\bar{I}}\delta(\bar{r}-\bar{r}')/k^2] = -\nabla\delta(\bar{r}-\bar{r}')/k^2 \quad . \tag{3.12}$$

Comparing Equations (3.1) - (3.4) with (3.9) - (3.12), it is seen that $\bar{\bar{G}}_e$, $\bar{\bar{G}}_m/j\omega\mu$ and $\bar{\bar{I}}\delta(\bar{r}-\bar{r}')/j\omega\mu$ represent the dyadic analogs of $\bar{E}$, $\bar{H}$ and $\bar{J}$, respectively. It may be noted that relations (3.9) and (3.10) must be modified should $\bar{r}$ and $\bar{r}'$ be located in different regions each with distinct permeability. This will be discussed further in Section D.

It is of interest to consider that $\bar{E}$ and $\bar{\bar{G}}_e$ are solutions in region V to the differential Equations (3.5) and (3.7), respectively, pertaining to the geometry depicted in Figure 3.1. Thus $\bar{E}$ and $\bar{\bar{G}}_e$ must satisfy the following boundary conditions:

on the perfect conducting surface S,

$$\hat{n} \times \bar{E}(\bar{r}) \Big|_S = 0 \quad , \tag{3.13}$$

$$\hat{n} \times \bar{\bar{G}}_e(\bar{r},\bar{r}') \Big|_S = 0 \quad ; \tag{3.14}$$

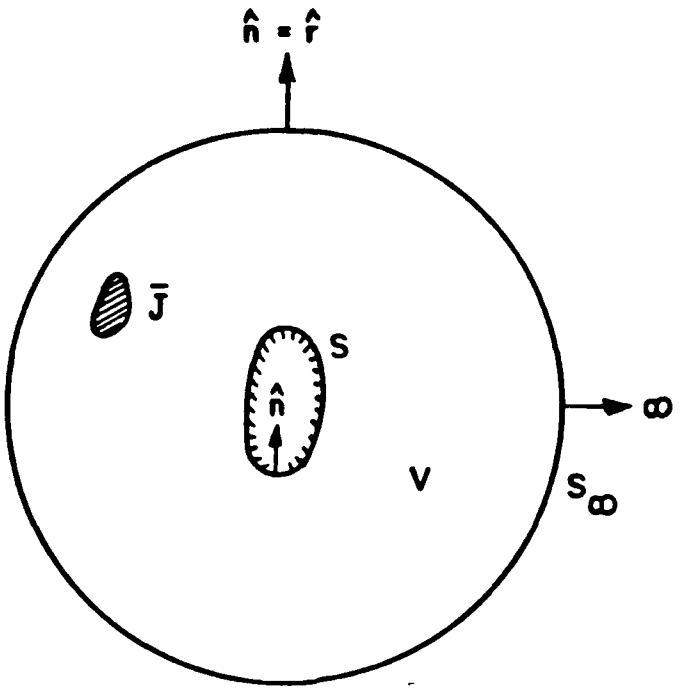

Figure 3.1. Region V, bounded by a perfect conducting surface S and a surface S_∞ at infinity, contains an electric source $\bar{J}$. V can be inhomogeneous.

on the surface S_∞ at infinity,

$$\lim_{r\to\infty} r \left[\nabla \times \bar{E}(\bar{r}) - jk\hat{r} \times \bar{E}(\bar{r}) \right] = 0 \quad , \tag{3.15}$$

$$\lim_{r\to\infty} r \left[\nabla \times \bar{\bar{G}}_e(\bar{r},\bar{r}') - jk\hat{r} \times \bar{\bar{G}}_e(\bar{r},\bar{r}') \right] = 0 \quad . \tag{3.16}$$

The latter set of conditions is commonly known as the radiation condition. The region V, bounded by surfaces S and S_∞, contains the source $\bar{J}$ and can be inhomogeneous. Next employing the Green's theorem for the pair $\bar{E}$ and $\bar{\bar{G}}_e$ over V, and enforcing the appropriate boundary conditions on $\bar{E}$ and $\bar{\bar{G}}_e$ yield

$$\bar{E}(\bar{r}) = j\omega\mu \int_V \bar{\bar{G}}_e(\bar{r},\bar{r}") \cdot \bar{J}(\bar{r}")dv", \quad \bar{r},\bar{r}" \in V \quad . \tag{3.17}$$

From (3.1) and (3.9), it can be verified that

$$\bar{H}(\bar{r}) = \int_V \bar{\bar{G}}_{m(}\bar{r},\bar{r}") \cdot \bar{J}(\bar{r}")dv", \quad \bar{r},\bar{r}" \in V \quad . \tag{3.18}$$

In particular, if $\bar{J}(\bar{r}")$ is an arbitrarily oriented electric point source of strength $\bar{p}_e$ located at $\bar{r}"=\bar{r}'$, i.e.,

$$\bar{J}(\bar{r}") = \bar{p}_e \delta(\bar{r}"-\bar{r}') \quad , \tag{3.19}$$

then (3.17) and (3.18) will reduce to

$$\bar{E}(\bar{r}) = j\omega\mu \, \bar{\bar{G}}_e(\bar{r},\bar{r}') \cdot \bar{p}_e \tag{3.20}$$

and

$$\bar{H}(\bar{r}) = \bar{\bar{G}}_m(\bar{r},\bar{r}') \cdot \bar{p}_e \quad . \tag{3.21}$$

C. EIGENFUNCTION EXPANSION OF THE FREE SPACE GREEN'S DYADIC

The analysis of mutual coupling between microstrip patch antennas involves only the electric field and electric current. It is sufficient to consider the electric Green's dyadic ($\bar{\bar{G}}_e(\bar{r},\bar{r}')$) because, as observed in the previous section, $\bar{\bar{G}}_e(\bar{r},\bar{r}')$ is directly related to the electric field due to an electric current point source. The mangetic Green's dyadic $\bar{\bar{G}}_m(\bar{r},\bar{r}')$), if needed, can be obtained by taking the curl of $\bar{\bar{G}}_e(\bar{r},\bar{r}')$.

This section is devoted to the eigenfunction expansion of the free space Greeen's dyadic which will be denoted by $\bar{\bar{G}}_0(\bar{r},\bar{r}')$. Without loss of generality, it is assumed that the electromagnetic problem under consideration can be formulated in a general orthogonal curvilinear coordinate system (u_1, u_2, u_3) with corresponding metric parameters, h_1, h_2, h_3, and associated unit vectors $\hat{u}_1, \hat{u}_2, \hat{u}_3$ (Figure 3.2). This requires that the scalar wave equation is separable in this system.

For the sake of being specific, it is assumed that coordinate u_1 satisfies the following two criteria:

C.1. Any set $S = \{(u_1,u_2,u_3): u_1 = \rho_0, \rho_0 \text{ fixed}, u_2,u_3 \text{ arbitrary}\}$ forms a closed surface, i.e., surface S partitions the space into two distinct regions, $V^+ = \{(u_1,u_2,u_3): u_1>\rho_0, u_2,u_3 \text{ arbitrary}\}$ and $V^- = \{(u_1,u_2,u_3): u_1<\rho_0, u_2,u_3 \text{ arbitrary}\}$.

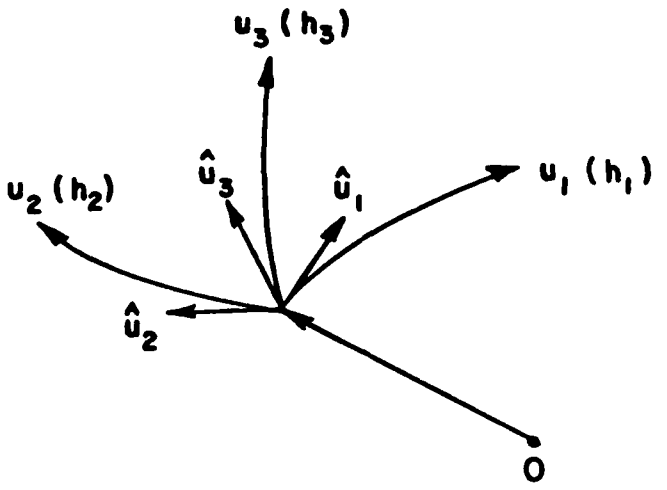

Figure 3.2. A general orthogonal curvilinear system with coordinates u_1, u_2, u_3 and their corresponding unit vectors $\hat{u}_1$, $\hat{u}_2$, $\hat{u}_3$ and metric parameters h_1, h_2, h_3.

C.2. The u_1-propagating solutions of the scalar wave equation can be obtained so that the construction of the u_1-propagating vector solenoidal eigenmodes or wave functions, denoted by $\bar{M}_q$ and $\bar{N}_q$, is possible.

It should be remarked that at any point on S, the outward unit vector normal to S coincides with $\hat{u}_1$. Also, the shorthand notation q stands for a particular combination of various mode characteristics such as evenness, oddness and order.

It is of significance to consider an arbitarily oriented point source $\bar{J}$ of strength $\bar{p}_e$, located at $\bar{r}' = (u_1', u_2', u_3')$, radiating in free space Vo. According to criterion C.1, V_o is partitioned into two distinct regions (Figure 3.3):

$$V^+ = \{\bar{r} = (u_1,u_2,u_3): u_1 > u_1', \; u_2,u_3 \text{ arbitrary}\} \quad ,$$

and

$$V^- = \{\bar{r} = (u_1,u_2,u_3): u_1 < u_1', \; u_2,u_3 \text{ arbitrary}\} \quad .$$

The interface between V^+ and V^- forms a closed surface defined by

$$S = \{\bar{r} = (u_1,u_2,u_3): \; u_1 = u_1', \; u_2,u_3 \text{ arbitrary}\} \quad ,$$

which contains the source represented by

$$\bar{J}(\bar{r}) = \bar{p}_e \delta(\bar{r}-\bar{r}') = \bar{p}_e \frac{\delta(u_1-u_1')\delta(u_2-u_2')\delta(u_3-u_3')}{h_1h_2h_3} \quad . \tag{3.22}$$

From (3.12) it is clear that

$$\nabla \cdot \bar{\bar{G}}_o(\bar{r},\bar{r}') = \begin{cases} -\nabla\delta(\bar{r}-\bar{r}')/k_o^2 & , \; \bar{r} \in S \\ 0 & , \; \bar{r} \in V^+ \text{ or } \bar{r} \in V^- \end{cases} \tag{3.23}$$

where $k_o^2 = \omega^2\mu_o\epsilon_o$, and μ_o, ϵ_o are the constitutive parameters of free space V_o. Equation (3.23) simply says that $\bar{\bar{G}}_o(\bar{r},\bar{r}')$ is solenoidal in both V^+ and V^-, but irrotational on S. Thus one can conjecture that

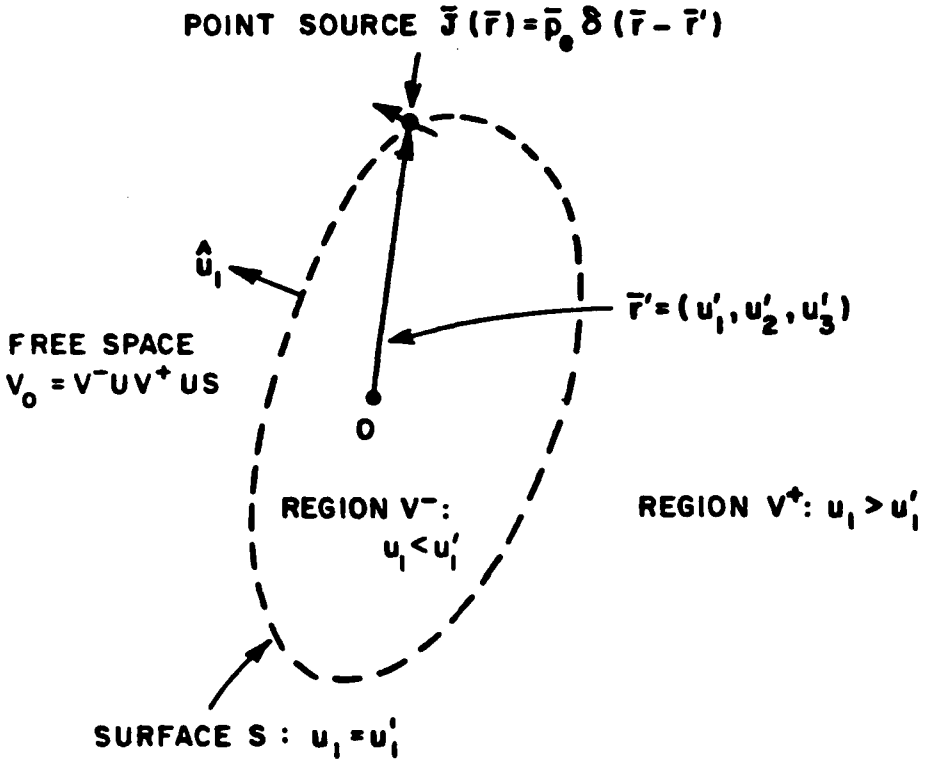

Figure 3.3. Free space V_0 is partitioned into regions V^+ and V^- with closed surface S as interface which contains the point source $\bar{J}$ at $\bar{r}' = (u_1, u_2, u_3)$.

$$\bar{\bar{G}}_0(\bar{r},\bar{r}') = U(u_1-u_1')\bar{\bar{g}}_0^{+}(\bar{r},\bar{r}') + U(u_1'-u_1)\bar{\bar{g}}_0^{-}(\bar{r},\bar{r}') - \bar{\bar{\psi}}(r,r')\frac{\delta(u_1-u_1')}{h_1} , \tag{3.24}$$

where

$$\bar{\bar{g}}_0^{+}(\bar{r},\bar{r}') \triangleq \bar{\bar{G}}_0(\bar{r},\bar{r}') \quad \text{for } \bar{r} \in V^{+} , \tag{3.25}$$

$$\bar{\bar{g}}_0^{-}(\bar{r},\bar{r}') \triangleq \bar{\bar{G}}_0(\bar{r},\bar{r}') \quad \text{for } \bar{r} \in V^{-} , \tag{3.26}$$

$$U(\xi) = \begin{cases} 1 & , \xi > 0 \\ 0 & , \xi < 0 \end{cases} \quad \text{(unit step function)} ,$$

and $\bar{\bar{\psi}}(\bar{r},\bar{r}')$ is a dyadic symbolic function (distribution) which is used as if it was an ordinary function with the understanding that it will produce valid results under the integral sign (in the present case, the volume integral over a subset of V_0).

It should be recognized that, by definitions, $\bar{\bar{g}}_0^{+}$ and $\bar{\bar{g}}_0^{-}$ are solenoidal (divergenceless) in V^{+} and V^{-}, respectively, while $\bar{\bar{\psi}}$ is irrotational on S. Mathematically these mean

$$\nabla \cdot \bar{g}_0^{\pm}(\bar{r},\bar{r}') = 0 \quad \text{for } \bar{r} \in V^{\pm} , \tag{3.27}$$

and

$$\nabla \cdot \bar{\bar{\psi}}(\bar{r},\bar{r}') \neq 0 \quad \text{for } \bar{r} \in S . \tag{3.28}$$

It may be mentioned that (3.28) implies $\nabla\cdot\bar{\bar{\psi}}$ is non-zero in the sense of distributions. In addition, $\bar{\bar{g}}_0^{\pm}$ satisfies the homogeneous vector wave equation:

$$\nabla x \nabla x \bar{\bar{g}}_0^{\pm}(\bar{r},\bar{r}') - k_0^2 \bar{\bar{g}}_0^{\pm}(\bar{r},\bar{r}') = 0 \qquad \bar{r} \in V^{\pm} \quad , \tag{3.29}$$

and the radiation condition:

$$\lim_{r\to\infty} r[\nabla x \bar{\bar{g}}_0^{\pm}(\bar{r},\bar{r}') - jk_0 \hat{r} x \bar{\bar{g}}_0^{\pm}(\bar{r},\bar{r}')] = 0 \quad . \tag{3.30}$$

Now from (3.20) and (3.21), it is seen that the electromagnetic fields apart from the surface S can be defined as

$$\bar{E}^{\pm}(\bar{r}) = j\omega\mu_0 \bar{\bar{g}}_0^{\pm}(\bar{r},\bar{r}') \cdot \bar{p}_e \qquad , \bar{r} \in V^{\pm} \quad , \tag{3.31}$$

$$\bar{H}^{\pm}(\bar{r}) = \nabla \times \bar{\bar{g}}_0^{\pm}(\bar{r},\bar{r}') \cdot \bar{p}_e \qquad , \bar{r} \in V^{\pm} \quad . \tag{3.32}$$

Since the tangential electric field is continuous at S, it requires that

$$\hat{u}_1 \times [\bar{E}^{+}(\bar{r}) - \bar{E}^{-}(\bar{r})] \frac{\delta(u_1-u_1')}{h_1} = 0$$

or

$$\hat{u}_1 \times [\bar{\bar{g}}_0^{+}(\bar{r},\bar{r}') - \bar{\bar{g}}_0^{-}(\bar{r},\bar{r}')] \frac{\delta(u_1-u_1')}{h_1} = 0 \quad . \tag{3.33}$$

Equation (3.33) is obtained by using (3.31) and the fact that $\bar{\bar{p}}_e$ is arbitrary. Likewise, by enforcing the boundary condition on the magnetic field at the interface S one gets

$$\hat{u}_1 \times [\bar{H}^+(\bar{r}) - \bar{H}^-(\bar{r})] \frac{\delta(u_1-u_1')}{h_1} = \bar{\bar{I}}_t \cdot \bar{J}(\bar{r}) = \bar{\bar{I}}_t \cdot \bar{p}_e \delta(\bar{r}-\bar{r}') \quad , \tag{3.34}$$

where $\bar{\bar{I}}_t$ denotes the transverse part of the unit dyad with respect to the propagation direction $\hat{u}_1$, and is defined by

$$\bar{\bar{I}} = \bar{\bar{I}}_t + \hat{u}_1\hat{u}_1 \; ; \; \bar{\bar{I}}_t = \hat{u}_2\hat{u}_2 + \hat{u}_3\hat{u}_3 \quad . \tag{3.35}$$

Employing (3.32) in (3.34) and the fact that $\bar{p}_e$ is arbitrary lead to

$$\hat{u}_1 \times [\nabla \times \bar{\bar{g}}_0^+(\bar{r},\bar{r}') - \nabla \times \bar{\bar{g}}_0^-(\bar{r},\bar{r}')] \frac{\delta(u_1-u_1')}{h_1} = \bar{\bar{I}}_t \delta(\bar{r}-\bar{r}') \; . \tag{3.36}$$

Equations (3.33) and (3.36) constitute the boundary conditions on $\bar{\bar{G}}_0(\bar{r},\bar{r}')$ at the surface S.

Next the irrotational component $\bar{\bar{\psi}}$ will be determined by enforcing $\bar{\bar{G}}_0(\bar{r},\bar{r}')$ to satisfy the inhomogeneous vector wave equation described in (3.11) (with k^2 replaced by k_0^2). Taking the curl of $\bar{\bar{G}}_0$ in (3.24) gives

$$\begin{aligned} \nabla \times \bar{\bar{G}}_0(\bar{r},\bar{r}') &= U(u_1-u_1')\nabla \times \bar{\bar{g}}_0^+(\bar{r},\bar{r}') + U(u_1'-u_1)\nabla \times \bar{\bar{g}}_0^-(\bar{r},\bar{r}') \\ &+ \hat{u}_1 \times [\bar{\bar{g}}_0^+(\bar{r},\bar{r}') - \bar{\bar{g}}_0^-(\bar{r},\bar{r}')] \frac{\delta(u_1-u_1')}{h_1} - \nabla \times \left[\bar{\bar{\psi}}(\bar{r},\bar{r}') \frac{\delta(u_1-u_1')}{h_1} \right] . \end{aligned} \tag{3.37}$$

The third term on the R.H.S. of (3.37) vanishes because of (3.33) and it is permissible to choose $\bar{\bar{\psi}}$ such that

$$\nabla \times \left[\bar{\bar{\psi}}(\bar{r},\bar{r}') \frac{\delta(u_1-u_1')}{h_1} \right] = 0 \qquad , \bar{r} \in S \quad , \tag{3.38}$$

since up to this point $\bar{\bar{\psi}}$ is still arbitrary other than the requirement that $\nabla \cdot \bar{\bar{\psi}} \neq 0$ on S. It may be noted that $\bar{\bar{\psi}}(\bar{r},\bar{r}') \frac{\delta(u_1-u_1')}{h_1}$ is a symbolic function, hence (3.38) means its curl vanishes on S in the sense of distributions. Consequently, one will find (3.37) reduces to

$$\nabla \times \bar{\bar{G}}_0(\bar{r},\bar{r}') = U(u_1-u_1')\nabla \times \bar{\bar{g}}_0^{+}(\bar{r},\bar{r}') + U(u_1'-u_1)\nabla \times \bar{\bar{g}}_0^{-}(\bar{r},\bar{r}') \; . \tag{3.39}$$

Taking curl of both sides of (3.39) yields

$$\nabla x \nabla x \bar{\bar{G}}_0(\bar{r},\bar{r}') = U(u_1-u_1')\nabla x \nabla x \bar{\bar{g}}_0^{+}(\bar{r},\bar{r}') + U(u_1'-u_1)\nabla x \nabla x \bar{\bar{g}}_0^{-}(\bar{r},\bar{r}')$$

$$+ \hat{u}_1 x [\nabla x \bar{\bar{g}}_0^{+}(\bar{r},\bar{r}') - \nabla x \bar{\bar{g}}_0^{-}(\bar{r},\bar{r}')] \frac{\delta(u_1-u_1')}{h_1} \; . \tag{3.40}$$

From (3.29) and (3.36) it can be verified that (3.40) will become

$$\nabla x \nabla x \bar{\bar{G}}_0(\bar{r},\bar{r}') = k_0^2 [U(u_1-u_1')\bar{\bar{g}}_0^{+}(\bar{r},\bar{r}') + U(u_1'-u_1)\bar{\bar{g}}_0^{-}(\bar{r},\bar{r}') - \frac{\hat{u}_1\hat{u}_1}{k_0^2}\delta(\bar{r}-\bar{r}')]$$

$$+ \bar{\bar{I}}\delta(\bar{r}-\bar{r}') \; . \tag{3.41}$$

Comparing (3.24) and (3.41) suggests that choosing

$$\overline{\overline{\psi}}(\bar{r},\bar{r}') = \frac{\delta(u_2-u_2')\delta(u_3-u_3')}{k_o^2\, h_2 h_3}\, \hat{u}_1\hat{u}_1 \tag{3.42}$$

will make

$$\overline{\overline{G}}_o(\bar{r},\bar{r}') = U(u_1-u_1')\overline{\overline{g}}_o^{+}(\bar{r},\bar{r}') + U(u_1'-u_1)\overline{\overline{g}}_o^{-}(\bar{r},\bar{r}') - \frac{\hat{u}_1\hat{u}_1}{k_o^2}\,\delta(\bar{r}-\bar{r}') \tag{3.43}$$

a valid representation of the free space Green's dyadic provided conditions (3.23), (3.28) and (3.38) are satisfied. To verify these conditions one may integrate $\nabla\cdot\overline{\overline{\psi}}$ over region V-US and then apply the Gauss' theorem:

$$\int_{V-US} \nabla\cdot\overline{\overline{\psi}}(\bar{r},\bar{r}')dv = \int_S \overline{\overline{\psi}}(\bar{r},\bar{r}')\cdot\hat{u}_1 h_2h_3du_2du_3 = \frac{\hat{u}_1}{k_o^2} \quad . \tag{3.44}$$

Equation (3.44) indicates that $\nabla\cdot\overline{\overline{\psi}}(r,r')$ does not vanish on S.

Likewise, integrating $\nabla \times [\overline{\overline{\psi}}(r,r')\,\frac{\delta(u_1-u_1')}{h_1}]$ over region V-US and applying Stokes' theorem show

$$\int_{V-US} \nabla \times [\overline{\overline{\psi}}(r,r')\frac{\delta(u_1-u_1')}{h_1}]dv = \int_S \hat{u}_1 \times [\overline{\overline{\psi}}(r,r')\frac{\delta(u_1-u_1')}{h_1}]h_2h_3du_2du_3$$

$$= \int_S \hat{u}_1 \times [\frac{\hat{u}_1\hat{u}_1}{k_o^2}\,\delta(\bar{r}-\bar{r}')]\, h_2h_3du_2du_3 = 0 \quad . \tag{3.45}$$

Equation (3.45) implies that $\nabla \times [\bar{\bar{\psi}} \frac{\delta(u_1-u_1')}{h_1}]$ indeed vanishes on S. Thus the validity of the representation of $\bar{\bar{G}}_0$ by (3.43) has been established. Moreover, this representation proves to be most useful and compact for the eigenfunction expansion of $\bar{\bar{G}}_0$ which is considered next.

Anticipating the $\bar{\bar{G}}_0$ will be needed in the construction of the Green's dyadic for a dielectric-coated circular cylinder, one would look for the eigenfunction expansion of $\bar{\bar{G}}_0$ in cylindrical coordinates (ρ,ϕ,z) which are natural for cylindrical structures. To do so, one of the coordinates ρ, ϕ, z must be designated as the "u_1 coordinate" that satisfies the criteria C.1 and C.2 stated earlier.

It is relatively easy to verify that

1. the set

   $S = \{\bar{r}=(\rho,\phi,z):\rho=\rho',\ \rho' \text{ fixed},\ 0<\phi<2\pi,\ -\infty<z<\infty\}$ forms an infinite circular closed surface that divides the entire (free) space into two distinct regions denoted by

   $V^+ = \{\bar{r} = (\rho,\phi,z):\ \rho>\rho',\ 0<\phi<2\pi,\ -\infty<z<\infty\}$ and

   $V^- = \{\bar{r} = (\rho,\phi,z):\ \rho<\rho',\ 0<\phi<2\pi,\ -\infty<z<\infty\}$;

2. the "ρ-propagating" solenoidal vector eigenmodes or wave functions which satisfy the homogeneous vector wave equation are found be [15,19]

$$\bar{M}^{\pm}_{e_{o}m\lambda'}(h',\bar{r}) = \left[\mp \hat{\rho}\,\frac{m}{\rho}\,Z^{\pm}_{m}(\lambda'\rho)\begin{Bmatrix}\sin\\ \cos\end{Bmatrix}m\phi\} - \hat{\phi}\,\frac{\partial}{\partial\rho}\,Z^{\pm}_{m}(\lambda'\rho)\begin{Bmatrix}\cos\\ \sin\end{Bmatrix}m\phi\}\right]e^{jh'z} \tag{3.46}$$

$$\bar{N}^{\pm}_{e_{o}m\lambda'}(h',\bar{r}) = \frac{1}{k_o}\,\nabla \times \bar{M}^{\pm}_{e_{o}m\lambda'}(h',\bar{r})$$

$$= \left[\hat{\rho}\,\frac{jh'}{k_o}\,\frac{\partial}{\partial\rho}\,Z^{\pm}_{m}(\lambda'\rho)\begin{Bmatrix}\cos\\ \sin\end{Bmatrix}m\phi\} \mp \hat{\phi}\,\frac{jh'm}{k_o\rho}\,Z^{\pm}_{m}(\lambda'\rho)\begin{Bmatrix}\sin\\ \cos\end{Bmatrix}m\phi\}\right.$$

$$\left. + \hat{z}\lambda'^{2}Z^{\pm}_{m}(\lambda'\rho)\begin{Bmatrix}\cos\\ \sin\end{Bmatrix}m\phi\}\right]e^{jh'z} \quad , \tag{3.47}$$

where

$$m = 0,1,2,\ldots;\ -\infty<h'<\infty;\quad \lambda' = \sqrt{k_o^2 - h'^2}\ \text{ with } \mathrm{Im}\lambda' > 0 \quad ,$$

$$Z^{\pm}_{m}(\lambda'\rho) = \begin{cases} H^{(1)}_{m}(\lambda'\rho), \text{ an } m^{th} \text{ order Hankel function of the first kind} \\ J_{m}(\lambda'\rho) \quad , \text{ an } m^{th} \text{ order Bessel function;} \end{cases}$$

and e,o refers to even, odd mode, respectively.

Evidently, it is permissible to assign

$$(u_1,u_2,u_3) = (\rho,\phi,z) \quad ,$$

and, correspondingly, the metric parameters are given by

$$(h_1,h_2,h_3) = (1,\rho,1) \quad .$$

To be more specific, it is assumed that an arbitrary electric point source of strength $\bar{p}_e$ is located at $\bar{r}' = (\rho',\phi',z') \in S$, and the observation point is at $\bar{r} = (\rho,\phi,z) \in V^+$ or V^-. Then, according to Equation (3.43), $\bar{\bar{G}}_o$ has the specific form below:

$$\bar{\bar{G}}_o(\bar{r},\bar{r}') = U(\rho-\rho')\bar{\bar{g}}_o^{+}(\bar{r},\bar{r}') + U(\rho'-\rho)\bar{\bar{g}}_o^{-}(\bar{r},\bar{r}') - \frac{\hat{\rho}\hat{\rho}}{k_o^2}\,\delta(\bar{r}-\bar{r}') \quad . \tag{3.48}$$

It follows that the resulting electric field is given by

$$\bar{E}^{\pm}(\bar{r}) = j\omega\mu_o \bar{\bar{g}}_o^{\pm}(\bar{r},\bar{r}') \cdot \bar{p}_e \ , \quad \bar{r} \in V^{\pm} \quad . \tag{3.49}$$

Since $\bar{E}^{\pm}(\bar{r})$ or $\bar{\bar{g}}_o^{\pm}(\bar{r},\bar{r}')\cdot\bar{p}_e$ is solenoidal for $\bar{r} \in V^{\pm}$, they can be expanded in terms of the solenoidal eigenmodes as follows:

$$\bar{\bar{g}}_o^{\pm}(\bar{r},\bar{r}')\cdot\bar{p}_e = \int_{-\infty}^{\infty} dh' \sum_{m=0}^{\infty} \begin{bmatrix} \bar{\Gamma}_q(h',\bar{r}') \\ \bar{C}_q(h',\bar{r}') \end{bmatrix} \bar{M}_{q\lambda'}^{\pm}(h',\bar{r}) + \begin{bmatrix} \bar{T}_q(h',\bar{r}') \\ \bar{D}_q(h',\bar{r}') \end{bmatrix} \bar{N}_{q\lambda'}^{\pm}(h',\bar{r}) \tag{3.50}$$

where Γ_q, T_q, C_q and D_q denote the expansion coefficients; q is a shorhand notation for $^{e}_{o}m$ and

$$C_q(h',r')\bar{M}^{\pm}_{q\lambda'}(h',\bar{r}) = C_{\substack{e\\o}m}(h',\bar{r}')M^{\pm}_{\substack{e\\o}m\lambda'}(h',\bar{r})$$

$$\triangleq \begin{cases} C_{em}(h',\bar{r}')\bar{M}^{\pm}_{em}(h',\bar{r}) + C_{om}(h',\bar{r}')\bar{M}^{\pm}_{om\lambda'}(h',\bar{r}) & , m>0 \\ C_{em}(h',\bar{r}')\bar{M}^{\pm}_{em\lambda'}(h',\bar{r}) & , m=0 \end{cases} . \qquad (3.51)$$

It may be noted that (3.51) will also hold if $\bar{M}^{\pm}_{q\lambda'}(h',\bar{r})$ is replaced by $\bar{N}^{\pm}_{q\lambda'}(h',\bar{r})$ since both $\bar{M}^{\pm}_{om\lambda'}(h',\bar{r})$ and $\bar{N}^{\pm}_{om\lambda'}(h',\bar{r})$ are zero for m=0.

The determination of the expansion coefficients in (3.50) requires a set of orthogonal properties of the vector wave functions which are stated in the form of lemmas below. The proofs of these lemmas can be found in Appendix D.

Lemma 1.

$$\int_{-\infty}^{\infty} dh' \int_{-\infty}^{\infty} dz \int_0^{2\pi} \rho d\phi \, [A_{\substack{e\\o}n}\, \hat{\rho} \times \nabla \times \bar{M}^{S_n}_{\substack{e\\o}n\lambda}(h,\bar{r})] \cdot [\Gamma_{\substack{e\\o}m}\, \bar{M}^{S_m}_{\substack{e\\o}m\lambda'}(h',\bar{r})]$$

$$= \frac{4\pi^2}{\varepsilon_n} A_{\substack{e\\o}n}\, \Gamma_{\substack{e\\o}m}\, \rho\lambda^2\, Z_n^{S_n}(\lambda\rho)\, \frac{\partial}{\partial\rho} Z_m^{S_m}(\lambda\rho)\, \delta_{mn} .$$

Lemma 2.

$$\int_{-\infty}^{\infty} dh' \int_{-\infty}^{\infty} dz \int_0^{2\pi} \rho d\phi \, [A_{\substack{e\\o}n}\, \hat{\rho} \times \nabla \times \bar{N}^{S_n}_{\substack{e\\o}n\lambda}(h,\bar{r})] \cdot [\Gamma_{\substack{e\\o}m}\, \bar{N}^{S_m}_{\substack{e\\o}m\lambda'}(h',\bar{r})]$$

$$= -\frac{4\pi^2}{\varepsilon_n} A_{\substack{e\\o}n}\, \Gamma_{\substack{e\\o}m}\, \rho\lambda^2\, \frac{\partial}{\partial\rho} Z_n^{S_n}(\lambda\rho) Z_m^{S_m}(\lambda\rho)\, \delta_{mn} .$$

Lemma 3.

$$\int_{-\infty}^{\infty} dh' \int_{-\infty}^{\infty} dz \int_{0}^{2\pi} \rho d\phi \left[A_{\substack{e_n \\ o}} \hat{\rho} \times \nabla \times \bar{M}^{\bar{S}_n}_{\substack{e_{n\lambda} \\ o}}(h,\bar{r}) \right] \cdot \left[\Gamma_{\substack{e_m \\ o}} \bar{N}^{\bar{S}_m}_{\substack{e_{m\lambda'} \\ o}}(h',\bar{r}) \right] = 0 \quad .$$

Lemma 4.

$$\int_{-\infty}^{\infty} dh' \int_{-\infty}^{\infty} dz \int_{0}^{2\pi} \rho d\phi \left[A_{\substack{e_n \\ o}} \hat{\rho} \times \nabla \times \bar{N}^{\bar{S}_n}_{\substack{e_{n\lambda} \\ o}}(h,\bar{r}) \right] \cdot \left[\Gamma_{\substack{e_m \\ o}} \bar{M}^{\bar{S}_m}_{\substack{e_{m\lambda'} \\ o}}(h',\bar{r}) \right] = 0 \quad .$$

In these Lemmas, the shorthand notation $A_{\substack{e_n \\ o}} \Gamma_{\substack{e_m \\ o}}$ has the same meaning defined by (3.51); ε_n is 1 for n=0 and 2 for n>1; δ_{mn} is the Kronecker delta function which is 1 when m=n and 0 otherwise; and S_n stands for "+" or "-" sign, n=0,1,2,... .

It is worth pointing out that the orthogonal properties of the cylindrical vector wave functions have been established in a mixed domain of (ϕ,z,h) which is partly spatial and partly spectral. This implies that these functions are orthogonal on any closed surface at which the ρ coordinate is constant. It is the very feature that makes the eigenfunction expansion process simple and elegant. It should be mentioned that different forms of orthogonal properties of these vector wave functions have previously been investigated by Stratton [15] who used a mixed domain of (ρ,ϕ,λ); and by Tai [19] who used the entire spatial domain of (ρ,ϕ,z). Since coordinate ρ is involved, both [15] and [19] spent extra effort in dealing with the orthogonal properties of the cylinder functions.

To see how the expansion coefficients ($C_{o}^{e}{}_{n}$, $D_{o}^{e}{}_{n}$, $\Gamma_{o}^{e}{}_{n}$ and $T_{o}^{e}{}_{n}$) are determined, it is helpful to consider a region V containing the point source $\bar{J}(\bar{r}) = \bar{p}_e \delta(\bar{r}-\bar{r}')$ and bounded by a surface in V^+ denoted by

$$S^+ = \{\bar{r} = (\rho^+,\phi,z):\ \rho^+>\rho' ,\ 0<\phi<2\pi,\ -\infty<z<\infty\} \quad ,$$

and another surface in V^- denoted by

$$S^- = \{\bar{r} = (\rho^-,\phi,z):\ \rho^-<\rho' ,\ 0<\phi<2\pi,\ -\infty<z<\infty\} \quad .$$

The geometry is shown in Figure 3.4. Now Green's theorem (vector version) is applied to the pair $(\bar{M}_{o}^{e}{}_{n\lambda}^{+}(h,\bar{r}),\ \bar{\bar{G}}_o(\bar{r},\bar{r}')\cdot\bar{p}_e)$ over region V:

$$\int_V [\bar{M}_{o}^{e}{}_{n\lambda}^{+}(h,\bar{r})\cdot\nabla x\nabla x(\bar{\bar{G}}_o(\bar{r},\bar{r}')\cdot\bar{p}_e) - \nabla x\nabla x\bar{M}_{o}^{e}{}_{n\lambda}^{+}(h,\bar{r})\cdot(\bar{\bar{G}}_o(\bar{r},\bar{r}')\cdot\bar{p}_e)]dv$$

$$= \int_{S^+US^-} [(\bar{\bar{G}}_o(\bar{r},\bar{r}')\cdot\bar{p}_e)x\nabla x\bar{M}_{o}^{e}{}_{n\lambda}^{+}(h,\bar{r}) - \bar{M}_{o}^{e}{}_{n\lambda}^{+}(h,\bar{r})x\nabla x(\bar{\bar{G}}_o(\bar{r},\bar{r}')\cdot\bar{p}_e)]\cdot\hat{n}ds \quad . \tag{3.52}$$

Since $\bar{\bar{G}}_o(\bar{r},\bar{r}')$ and $\bar{M}_{o}^{e}{}_{n\lambda}^{+}(h,\bar{r})$ are solutions of (3.11) and (3.29), respectively, the L.H.S. of (3.52) can be reduced significantly as follows:

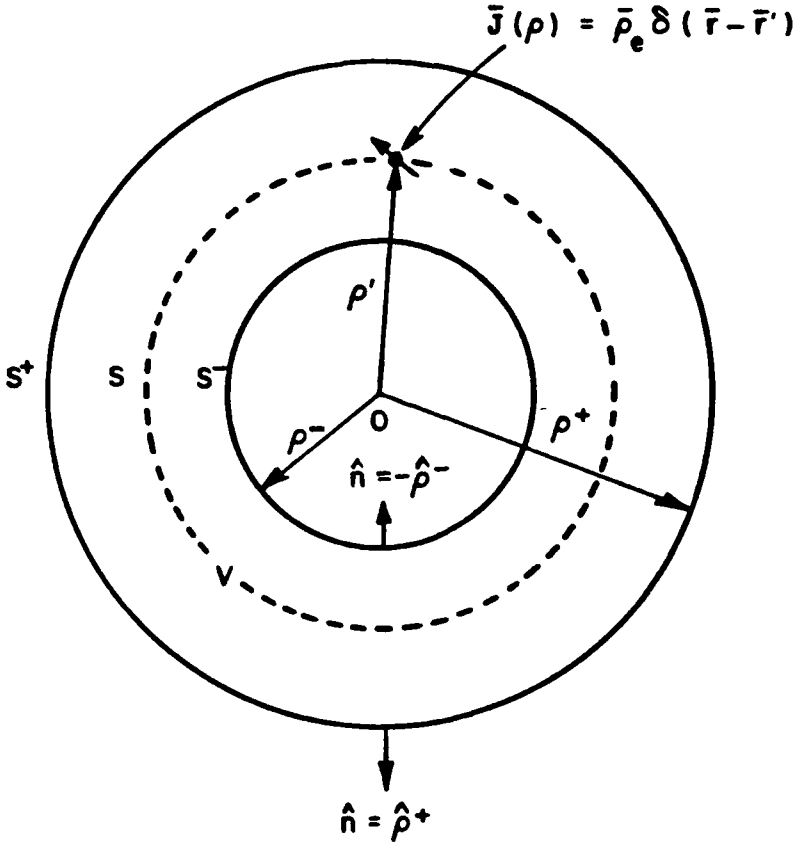

Figure 3.4. Configuration for determining $C_{e_{on}}$, $D_{e_{on}}$, $\Gamma_{e_{on}}$ and $T_{e_{on}}$ - region V is bounded by surfaces S^+ at $\rho=\rho^+$ and S^- at $\rho=\rho^-$, and source $\bar{J}$ is located on surface S at $\rho=\rho'(\rho^+>\rho'>\rho^-)$.

$$\text{L.H.S.} = \int_V [\bar{M}^{+}_{e_{o}n\lambda}(h,\bar{r})\cdot(\bar{p}_e\delta(\bar{r}-\bar{r}')+k_o^2\bar{\bar{G}}_o(\bar{r},\bar{r}')\cdot\bar{p}_e)$$

$$- k_o^2\bar{M}^{+}_{e_{o}n\lambda}(h,\bar{r})\cdot(\bar{\bar{G}}_o(\bar{r},\bar{r}')\cdot\bar{p}_e)]dv$$

$$= \int_V \bar{M}^{+}_{e_{o}n\lambda}(h,\bar{r})\cdot\bar{p}_e\delta(\bar{r}-\bar{r}')dv = \bar{M}^{+}_{e_{o}n\lambda}(h,\bar{r}')\cdot\bar{p}_e \quad . \qquad (3.53)$$

From (3.48) and the fact that $\hat{n}=\hat{\rho}^{+}$ at S^{+} and $\hat{n}=-\hat{\rho}^{-}$ at S^{-}, it is clear that

$$\text{R.H.S.} = \int_{S^+} [(\bar{\bar{g}}^{+}_o(\bar{r},\bar{r}')\cdot\bar{p}_e)\times\nabla\times\bar{M}^{+}_{e_{o}n\lambda}(h,\bar{r})$$

$$- \bar{M}^{+}_{e_{o}n\lambda}(h,\bar{r})\times\nabla\times(\bar{\bar{g}}^{+}_o(\bar{r},\bar{r}')\cdot\bar{p}_e)]\cdot\hat{\rho}^{+}ds$$

$$+ \int_{S^-} [(\bar{\bar{g}}^{-}_o(\bar{r},\bar{r}')\cdot\bar{p}_e)\times\nabla\times\bar{M}^{+}_{e_{o}n\lambda}(h,\bar{r})$$

$$- \bar{M}^{+}_{e_{o}n\lambda}(h,\bar{r})\times\nabla\times(\bar{\bar{g}}^{-}_o(\bar{r},\bar{r}')\cdot\bar{p}_e)]\cdot(-\hat{\rho}^{-})ds \quad . \qquad (3.54)$$

Employing the expanded form of $(\bar{\bar{g}}^{\pm}_o\cdot\bar{p}_e)$ in (3.50), the two surface integrals of (3.54) can be manipulated as follows:

$$\int_{S^+} [\ ]\cdot\hat{\rho}^+ ds$$

$$= \int_{-\infty}^{\infty} dz \int_0^{2\pi} \rho^+ d\phi \int_{-\infty}^{\infty} dh' \sum_{m=0}^{\infty} \Bigg[\Big[\Gamma_{0}^{e_m}(h',\bar{r}') \bar{M}_{0}^{+e_m\lambda'}(h',\bar{r})$$

$$+ T_{0}^{e_m}(h',\bar{r}') \bar{N}_{0}^{+e_m\lambda'}(h',\bar{r}) \Big] x \nabla x M_{0}^{+e_m\lambda}(h,r)\cdot\hat{\rho}^+$$

$$- \bar{M}_{0}^{+e_n\lambda}(h,\bar{r}) x \nabla x \Big[\Gamma_{0}^{e_m}(h',\bar{r}') \bar{M}_{0}^{+e_m\lambda'}(h',\bar{r}) + T_{0}^{e_m}(h',\bar{r}') \bar{N}_{0}^{+e_m\lambda'}(h',\bar{r}) \Big]\cdot\hat{\rho}^+ \Bigg]$$

$$= - \sum_{m=0}^{\infty} \int_{-\infty}^{\infty} dh' \int_{-\infty}^{\infty} dz \int_0^{2\pi} \rho^+ d\phi \Bigg[\hat{\rho}^+ x \nabla x \bar{M}_{0}^{+e_n\lambda}(h,\bar{r})$$

$$\cdot \Big[\Gamma_{0}^{e_m}(h',\bar{r}') \bar{M}_{0}^{+e_m\lambda'}(h',\bar{r}) + T_{0}^{e_m}(h',\bar{r}') \bar{N}_{0}^{+e_m\lambda'}(h',\bar{r}) \Big]$$

$$- \hat{\rho}^+ x \Big[\Gamma_{0}^{e_m}(h',\bar{r}') \nabla x \bar{M}_{0}^{+e_m\lambda'}(h',\bar{r}) + T_{0}^{e_m}(h',\bar{r}') \nabla x \bar{N}_{0}^{+e_m\lambda'}(h',\bar{r}) \Big]$$

$$\cdot \bar{M}_{0}^{+e_n\lambda}(h,\bar{r}) \Bigg] \ .$$

Using Lemmas 1, 3 and 4 one obtains

$$\int_{S^+} [\ ]\cdot\hat{\rho}^+ ds = - \sum_{m=0}^{\infty} \Bigg[\frac{4\pi^2}{\varepsilon_n} \Gamma_{0}^{e_m} \rho^+ \lambda^2 H_n^{(1)}(\lambda\rho^+) \frac{\partial}{\partial\rho^+} H_m^{(1)}(\lambda\rho^+) \delta_{mn}$$

$$- \frac{4\pi^2}{\varepsilon_m} \Gamma_{0}^{e_m} \rho^+ \lambda^2 H_m^{(1)}(\lambda\rho^+) \frac{\partial}{\partial\rho^+} H_n^{(1)}(\lambda\rho^+) \delta_{mn} \Bigg] = 0 \qquad (3.55)$$

$$\int_{S^-} [\ ]\cdot(-\hat{\rho}^-)ds$$

$$= \int_{-\infty}^{\infty} dz \int_0^{2\pi} \rho^- d\phi \int_{-\infty}^{\infty} dh' \sum_{m=0}^{\infty} \Big|_- \Big[C_{0e_m}(h',\bar{r}')\bar{M}^-_{0e_m\lambda'}(h',\bar{r})$$

$$+ D_{0e_m}(h',\bar{r}')\bar{N}^-_{0e_m\lambda'}(h',\bar{r})\Big] x\nabla x\bar{M}^+_{0e_m\lambda}(h,\bar{r})\cdot(-\hat{\rho}^-)$$

$$- \bar{M}^+_{0e_n\lambda}(h,\bar{r}) x\nabla x\Big[C_{0e_m}(h',\bar{r}')\bar{M}^-_{0e_m\lambda'}(h',\bar{r}) + D_{0e_m}(h',\bar{r}')\bar{N}^-_{0e_m\lambda'}(h',\bar{r})\Big]\cdot(-\hat{\rho}^-)\Big|_-$$

$$= \sum_{m=0}^{\infty} \int_{-\infty}^{\infty} dh' \int_{-\infty}^{\infty} dz \int_0^{2\pi} \rho^- d\phi \Big|_- \hat{\rho}^- x\nabla x\bar{M}^+_{0e_n\lambda}(h,\bar{r})$$

$$\cdot \Big[C_{0e_m}(h',\bar{r}')\bar{M}^-_{0e_m\lambda'}(h',\bar{r}) + D_{0e_m}(h',\bar{r}')\bar{N}^-_{0e_m\lambda'}(h',\bar{r})\Big]$$

$$- \hat{\rho}^- x\nabla x\Big[C_{0e_m}(h',\bar{r}')\bar{M}^-_{0e_m\lambda'}(h',\bar{r}) + D_{0e_m}(h',\bar{r}')\bar{N}^-_{0e_m\lambda'}(h',\bar{r})\Big]$$

$$\cdot \bar{M}^+_{0e_n\lambda}(h,\bar{r})\Big|_- \quad .$$

Again, making use of Lemmas 1, 3 and 4,

$$\int_{S^+} [\ ]\cdot(-\hat{\rho}^-)ds = \sum_{m=0}^{\infty} \Big|_- \frac{4\pi^2}{\varepsilon_n} C_{0e_m}(-h,\bar{r}')\rho^-\lambda^2 H_n^{(1)}(\lambda\rho^-)\frac{\partial}{\partial\rho^-} J_m(\lambda\rho^-)\delta_{mn}$$

$$- \frac{4\pi^2}{\varepsilon_m} C_{0e_m}(-h,\bar{r}')\rho^-\lambda^2 J_m(\lambda\rho^-)\frac{\partial}{\partial\rho^-} H_n^{(1)}(\lambda\rho^-)\delta_{mn}\Big|_-$$

$$= \frac{4\pi^2}{\varepsilon_n} C_{0e_n}(-h,\bar{r}')\rho^-\lambda^2\cdot\lambda\left[H_n^{(1)}(\lambda\rho^-)J_n'(\lambda\rho^-) - J_n(\lambda\rho^-)H_n^{(1)'}(\lambda\rho^-)\right] \quad .$$

The Wronskian

$$W[H_n^{(1)}(z),J_n(z)] = H_n^{(1)}(z)J_n'(z) - H_n^{(1)'}(z)J_n(z) = -\frac{j2}{\pi z} \quad .$$

Hence,

$$\int_{S^-} [\ ] \cdot (-\hat{\rho}^-)ds = \frac{-j8\pi}{\varepsilon_n} \lambda^2 \, C_{o}^{e_n}(-h,\bar{r}') \quad . \tag{3.56}$$

It is obvious from (3.55) and (3.56) that

$$R.H.S. = \int_{S^+} [\ ] \cdot \hat{\rho}^+ ds + \int_{S^-} [\ ] \cdot (-\hat{\rho}^-)ds = \frac{-j8\pi}{\varepsilon_n} \lambda^2 \, C_{o}^{e_n}(-h,\bar{r}') \quad .$$

Equating L.H.S. and R.H.S. gives

$$\bar{M}_{o}^{e_n\lambda +}(h,\bar{r}') \cdot \bar{p}_e = \frac{-j8\pi\lambda^2}{\varepsilon_n} \, C_{o}^{e_n}(-h,\bar{r}') \quad .$$

Reversing the sign of h and solving for $C_{o}^{e_n}$ gives

$$C_{o}^{e_n}(h,\bar{r}') = \frac{j\varepsilon_n}{8\pi\lambda^2} \bar{M}_{o}^{e_n\lambda +}(-h,\bar{r}') \cdot \bar{p}_e \quad . \tag{3.57}$$

If one applies Green's theorem to the following pairs:

$(\bar{N}_{o}^{e_n\lambda +}(h,\bar{r}), \bar{\bar{G}}_o(\bar{r},\bar{r}') \cdot \bar{p}_e)$, $(\bar{M}_{o}^{e_n\lambda -}(h,\bar{r}), \bar{\bar{G}}_o(\bar{r},\bar{r}') \cdot \bar{p}_e)$, $(\bar{N}_{o}^{e_n\lambda -}(h,\bar{r}), \bar{\bar{G}}_o(\bar{r},\bar{r}') \cdot \bar{p}_e)$, and follows the preceeding steps closely, then one obtains

$$D^{e_n}_{o}(h,\bar{r}') = \frac{j\varepsilon_n}{8\pi\lambda^2}\,\bar{N}^{+}_{e_{n\lambda}}(-h,\bar{r}')\cdot\bar{p}_e \quad , \tag{3.58}$$

$$\Gamma^{e_n}_{o}(h,\bar{r}') = \frac{j\varepsilon_n}{8\pi\lambda^2}\,\bar{\bar{M}}_{e_{n\lambda}}(-h,\bar{r}')\cdot\bar{p}_e \quad , \tag{3.59}$$

and

$$T^{e_n}_{o}(h,\bar{r}') = \frac{j\varepsilon_n}{8\pi\lambda^2}\,\bar{\bar{N}}_{e_{n\lambda}}(-h,\bar{r}')\cdot\bar{p}_e \quad , \tag{3.60}$$

respectively.

Substituting (3.57) - (3.60) into (3.50) results in the complete eigenfunction expansions of the solenoidal components of $\bar{\bar{G}}_o$ given below:

$$\bar{\bar{g}}^{\pm}_{o}(\bar{r},\bar{r}') = \frac{j}{8\pi}\int_{-\infty}^{\infty} dh \sum_{n=o}^{\infty}\frac{\varepsilon_n}{\lambda^2}\left[\bar{M}^{\pm}_{e_{n\lambda}}(h,\bar{r})\bar{M}^{\mp}_{e_{n\lambda}}(-h,\bar{r}') + \bar{N}^{\pm}_{e_{n\lambda}}(h,\bar{r})\bar{N}^{\mp}_{e_{n\lambda}}(-h,\bar{r}')\right]. \tag{3.61}$$

Hence, the formal eigenfunction expansion of $\bar{\bar{G}}_o$ has been completed. It is, however, of interest to mention that Tai [19] has shown that

$$\bar{\bar{G}}_o(\bar{r},\bar{r}') = (\bar{\bar{I}} + \frac{1}{k_o^2}\nabla\nabla)g_o(\bar{r},\bar{r}') \quad , \text{ for all } \bar{r},\bar{r}' \in V_o \quad , \tag{3.62}$$

where

$$g_0(\bar{r},\bar{r}') = \frac{e^{jk_0|\bar{r}-\bar{r}'|}}{4\pi|\bar{r}-\bar{r}'|} \quad . \tag{3.63}$$

Since, for $\bar{r}\neq\bar{r}'$, $\bar{\bar{G}}_0(\bar{r},\bar{r}')$ is identically equal to either $\bar{\bar{g}}_0^{+}(\bar{r},\bar{r}')$ or $\bar{\bar{g}}_0^{-}(\bar{r},\bar{r}')$ (depending on the location of $\bar{r}$), it is straightforward to conclude from Equations (3.61) and (3.62) that

$$\frac{j}{8\pi}\int_{-\infty}^{\infty} dh \sum_{n=0}^{\infty} \frac{\varepsilon_n}{\lambda^2} \left[\bar{M}_{0e_{n\lambda}}^{\pm}(h,\bar{r})\bar{M}_{0e_{n\lambda}}^{\mp}(-h,\bar{r}') + \bar{N}_{0e_{n\lambda}}^{\pm}(h,\bar{r})\bar{N}_{0e_{n\lambda}}^{\mp}(-h,\bar{r}') \right]$$

$$= \left(\bar{\bar{I}} + \frac{1}{k_0^2}\nabla\nabla\right) g_0(\bar{r},\bar{r}') \quad , \quad \bar{r} \neq \bar{r}' \quad . \tag{3.64}$$

D. GREEN'S DYADIC FOR A DIELECTRIC COATED CONDUCTING CYLINDER

The geometry of a dielectric coated cylinder is illustrated in Figure 3.5. It consists of an infinitely long, perfectly conducting circular cylinder of radius a coated by a uniform dielectric layer of thickness t = b-a, permittivity $\varepsilon_1 = \varepsilon_r\varepsilon_0$ and permeability $\mu_1 = \mu_0$. ε_r is in general complex to account for lossy dielectric. The z-axis of the cylindrical coordinate system (ρ,ϕ,z) coincides with the axis of the cylinder.

In order to determine the electric Green's dyadic for this geometry, it is convenient to divide the entire space surrounding the conducting cylinder, denoted by V, into two distinct regions defined below:

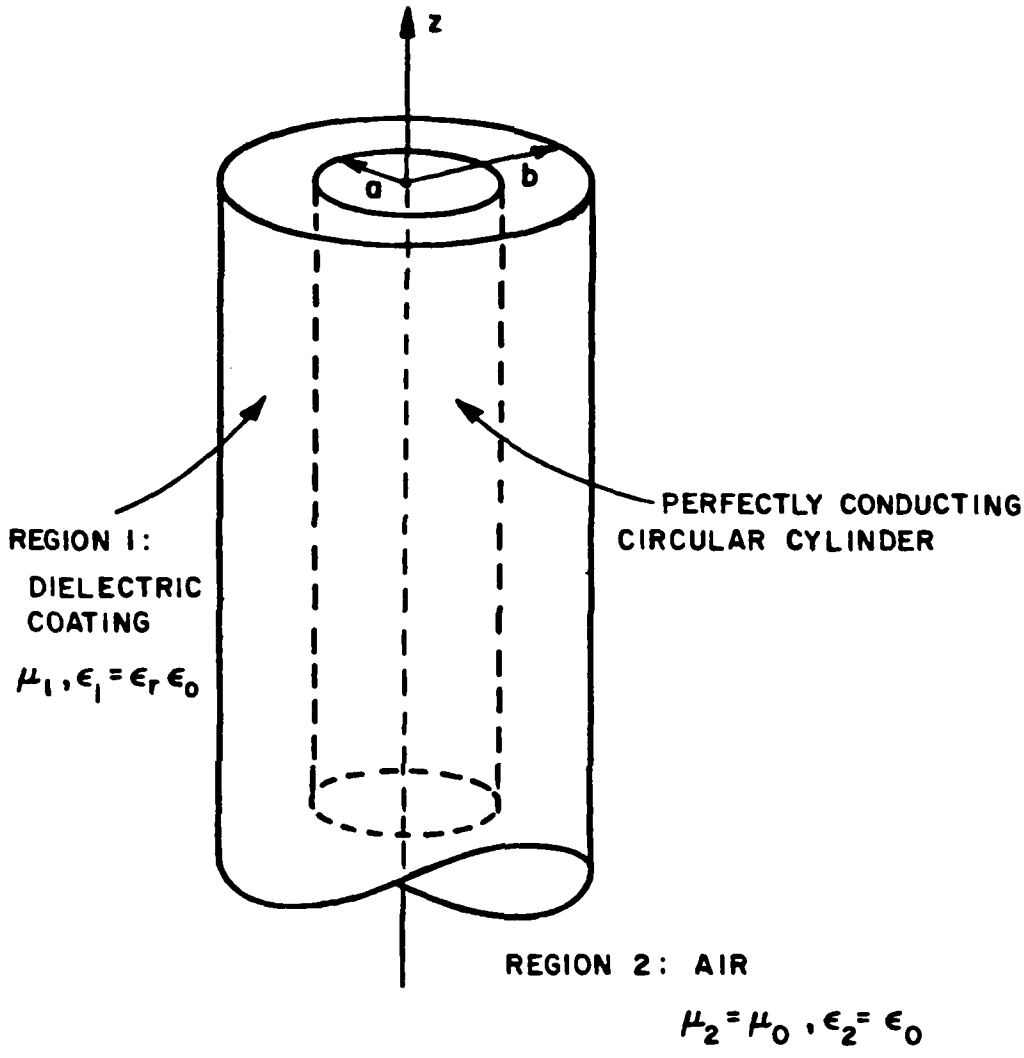

Figure 3.5. Geometry of a dielectric coated cylinder.

$$V_1 = \{\bar{r} = (\rho,\phi,z): a<\rho<b,\ 0<\phi<2\pi,\ -\infty<z<\infty\} \quad , \tag{3.65}$$

and

$$V_2 = \{\bar{r} = (\rho,\phi,z): b<\rho<\infty,\ 0<\phi<2\pi,\ -\infty<z<\infty\} \quad . \tag{3.66}$$

As a consequence, V_1 is the dielectric layer, while V_2 is the air region surrounding the coated cylinder, and $V = V_1 U V_2$.

In analyzing conformal microstrip antennas, it is sufficient to consider the electric current source that is located in region V_2 only. Consequently the electric Green's dyadic $\bar{\bar{G}}_e$ for region V will consist of two components, denoted by $\bar{\bar{G}}_{e1}$ and $\bar{\bar{G}}_{e2}$, such that

$$\bar{\bar{G}}_e(\bar{r},\bar{r}') = U(\rho-b)\bar{\bar{G}}_{e2}(\bar{r},\bar{r}') + U(b-\rho)\bar{\bar{G}}_{e1}(\bar{r},\bar{r}') \tag{3.67}$$

where $\bar{\bar{G}}_{e1}$ and $\bar{\bar{G}}_{e2}$ satisfy the following vector wave equations:

$$\nabla x \nabla x \bar{\bar{G}}_{e1}(\bar{r},\bar{r}') - k_1^2 \bar{\bar{G}}_{e1}(\bar{r},\bar{r}') = 0 \quad , \ \bar{r} \in V_1,\ \bar{r}' \in V_2 \quad , \tag{3.68}$$

$$\nabla x \nabla x \bar{\bar{G}}_{e2}(\bar{r},\bar{r}') - k_2^2 \bar{\bar{G}}_{e2}(\bar{r},\bar{r}') = \bar{\bar{I}}\delta(\bar{r}-\bar{r}') \quad , \ \bar{r},\bar{r}' \in V_2 \quad , \tag{3.69}$$

$k_1^2 = \omega^2\mu_1\varepsilon_1$ and $k_2^2 = \omega^2\mu_2\varepsilon_2 = \omega^2\mu_o\varepsilon_o = k_o^2$. In general terms, $\bar{\bar{G}}_{e1}(\bar{\bar{G}}_{e2})$ can be thought as the electric field in $V_1(V_2)$ due to a point source in V_2. Correspondingly, there exists two mangetic Green's dyadics, denoted by $\bar{\bar{G}}_{m1}$ and $\bar{\bar{G}}_{m2}$, such that

$$\nabla x \nabla x \overline{\overline{G}}_{m1}(\bar{r},\bar{r}') - k_1^2 \overline{\overline{G}}_{m1}(\bar{r},\bar{r}') = 0 \quad , \quad \bar{r} \in V_1, \quad \bar{r}' \in V_2 \quad , \tag{3.70}$$

$$\nabla x \nabla x \overline{\overline{G}}_{m2}(\bar{r},\bar{r}') - k_2^2 \overline{\overline{G}}_{m2}(\bar{r},\bar{r}') = \nabla x \overline{\overline{I}} \delta(\bar{r}-\bar{r}') \quad , \quad \bar{r},\bar{r}' \in V_2 \, , \tag{3.71}$$

and they are related to their electric counterparts as

$$\overline{\overline{G}}_{m1}(\bar{r},\bar{r}') = \frac{\mu_2}{\mu_1} \nabla x \overline{\overline{G}}_{e1}(\bar{r},\bar{r}') \quad , \bar{r} \in V_1, \bar{r}' \in V_2 \quad , \tag{3.72}$$

$$\overline{\overline{G}}_{m2}(\bar{r},\bar{r}') = \nabla x \overline{\overline{G}}_{e2}(\bar{r},\bar{r}') \quad , \bar{r},\bar{r}' \in V_2 \quad . \tag{3.73}$$

Equation (3.73) follows directly from (3.9), while (3.72) is established in Appendix E which also shows that

$$\bar{E}_1(\bar{r}) = j\omega\mu_2 \int_{V_2} \overline{\overline{G}}_{e1}(\bar{r},\bar{r}') \cdot \bar{J}(\bar{r}')dv' \quad , \bar{r} \in V_1 \tag{3.74}$$

$$\bar{H}_1(\bar{r}) = \int_{V_2} \overline{\overline{G}}_{m1}(\bar{r},\bar{r}') \cdot \bar{J}(\bar{r}')dv' \quad , \bar{r} \in V_1 \tag{3.75}$$

where $\bar{E}_1$ and $\bar{H}_1$ refer to the electric and magnetic fields in V_1 due to source $\bar{J}$ in V_2. And, of course, it follows from (3.17) and (3.18) that

$$\bar{E}_2(\bar{r}) = j\omega\mu_2 \int_{V_2} \overline{\overline{G}}_{e2}(\bar{r},\bar{r}') \cdot \bar{J}(\bar{r}')dv' \quad , \bar{r} \in V_2 \tag{3.76}$$

$$\bar{H}_2(\bar{r}) = \int_{V_2} \bar{\bar{G}}_{m2}(\bar{r},\bar{r}') \cdot \bar{J}(\bar{r}')dv' \quad , \quad \bar{r} \in V_2 \quad , \tag{3.77}$$

where $\bar{E}_2$ and $\bar{H}_2$ represent the electric and magnetic fields in V_2. It may be noted that the magnetic Green's dyadic for region V can also be cast into a form similar to (3.67) as follows:

$$\begin{aligned}\bar{\bar{G}}_m(\bar{r},\bar{r}') &= U(\rho-b)\bar{\bar{G}}_{m2}(\bar{r},\bar{r}') + U(b-\rho)\bar{\bar{G}}_{m1}(\bar{r},\bar{r}') \\ &= U(\rho-b)\nabla x\bar{\bar{G}}_{e2}(\bar{r},\bar{r}') + U(b-\rho)\frac{\mu_2}{\mu_1}\nabla x\bar{\bar{G}}_{e1}(\bar{r},\bar{r}') \quad , \bar{r}' \in V_2 \ . \end{aligned} \tag{3.78}$$

However, $\bar{\bar{G}}_m$ will not be involved in the following analysis, and it is being introduced for the sake of completeness.

To specify $\bar{\bar{G}}_e$ uniquely for region V, it requires $\bar{\bar{G}}_{e1}$ and $\bar{\bar{G}}_{e2}$ to satisfy the boundary conditions pertaining to V. These conditions can be readily derived by considering the corresponding boundary conditions imposed upon the electromagnetic fields in V. First it is observed that the tangential electric field vanishes at the conducting surface of the cylinder, namely,

$$\hat{\rho} \times \bar{E}_1(\bar{r}) \Big|_{\rho=a} = 0 \quad . \tag{3.79}$$

Secondly, at the interface between regions V_1 and V_2, the tangential electric and magnetic fields are continuous, i.e.

$$\hat{\rho} \times [\bar{E}_2(\bar{r}) - \bar{E}_1(\bar{r})]_{\rho=b} = 0 \quad , \tag{3.80}$$

$$\hat{\rho} \times [\bar{H}_2(\bar{r}) - \bar{H}_1(\bar{r})]_{\rho=b} = 0 \quad . \tag{3.81}$$

Next substituting the integral representations of the electric and magnetic fields defined by (3.74) -(3.77) into (3.79) -(3.81) one obtains in the following set of boundary conditions on the dyadic fields:

$$\hat{\rho} \times \bar{\bar{G}}_{e1}(\bar{r},\bar{r}')\Big|_{\rho=a} = 0 \quad , \tag{3.82}$$

$$\hat{\rho} \times [\bar{\bar{G}}_{e2}(\bar{r},\bar{r}') - \bar{\bar{G}}_{e1}(\bar{r},\bar{r}')]_{\rho=b} = 0 \tag{3.83}$$

$$\hat{\rho} \times [\nabla \times \bar{\bar{G}}_{e2}(\bar{r},\bar{r}') - \frac{\mu_2}{\mu_1} \nabla \times \bar{\bar{G}}_{e1}(\bar{r},\bar{r}')]_{\rho=b} = 0 \quad . \tag{3.84}$$

In addition, $\bar{\bar{G}}_{e2}$ must also satisfy the radiation condition:

$$\lim_{r\to\infty} r\,[\nabla \times \bar{\bar{G}}_{e2}(\bar{r},\bar{r}') - jk_2 \hat{r} \times \bar{\bar{G}}_{e2}(\bar{r},\bar{r}')] = 0 \quad . \tag{3.85}$$

The simplest way of finding $\bar{\bar{G}}_{e2}$ is to apply the principle of scattering superposition. Thus one will consider

$$\bar{\bar{G}}_{e2}(\bar{r},\bar{r}') = \bar{\bar{G}}_0(\bar{r},\bar{r}') + \bar{\bar{G}}_{s2}(\bar{r},\bar{r}') \quad , \bar{r},\bar{r}' \in V_2 \quad . \tag{3.86}$$

In Equation (3.86), $\bar{\bar{G}}_o$ is the free space Green's dyadic found in Section C; and is expressed explicitly below for convenience:

$$\bar{\bar{G}}_o(\bar{r},\bar{r}') = U(\rho-\rho')\bar{\bar{g}}_o^{+}(\bar{r},\bar{r}') + U(\rho'-\rho)\bar{\bar{g}}_o^{-}(\bar{r},\bar{r}') - \frac{\hat{\rho}\hat{\rho}}{k_2^2}\delta(\bar{r}-\bar{r}')$$

$$= U(\rho-\rho')\left[-\frac{j}{8\pi}\int_{-\infty}^{\infty} dh \sum_{n=0}^{\infty} \frac{\varepsilon_n}{\lambda^2}\left[\bar{M}_{o_{e_n\lambda}}^{+}(h,\bar{r})\bar{M}_{o_{e_n\lambda}}^{-}(-h,\bar{r}') + \bar{N}_{o_{e_n\lambda}}^{+}(h,\bar{r})\bar{N}_{o_{e_n\lambda}}^{-}(-h,\bar{r}')\right]\right]$$

$$+ U(\rho'-\rho)\left[-\frac{j}{8\pi}\int_{-\infty}^{\infty} dh \sum_{n=0}^{\infty} \frac{\varepsilon_n}{\lambda^2}\left[\bar{M}_{o_{e_n\lambda}}^{-}(h,\bar{r})\bar{M}_{o_{e_n\lambda}}^{+}(-h,\bar{r}') + \bar{N}_{o_{e_n\lambda}}^{-}(h,\bar{r})\bar{N}_{o_{e_n\lambda}}^{+}(-h,\bar{r}')\right]\right] - \frac{\hat{\rho}\hat{\rho}}{k_2^2}\delta(\bar{r}-\bar{r}') \quad , \; \bar{r},\bar{r}' \in V_2, \tag{3.87}$$

and $\bar{\bar{G}}_{s2}$ satisfies the homogeneous vector wave equation and therefore must have the form

$$\bar{\bar{G}}_{s2}(\bar{r},\bar{r}') = \frac{j}{8\pi}\int_{-\infty}^{\infty} dh \sum_{n=0}^{\infty} \frac{\varepsilon_n}{\lambda^2}\left[\left[A_{e_{o_n}}\bar{M}_{o_{e_n\lambda}}^{+}(h,\bar{r}) + B_{o_{e_n}}\bar{N}_{e_{o_n\lambda}}^{+}(h,\bar{r})\right]\bar{M}_{o_{e_n\lambda}}^{+}(-h,\bar{r}') + \left[C_{e_{o_n}}\bar{N}_{o_{e_n\lambda}}^{+}(h,\bar{r}) + D_{o_{e_n}}\bar{M}_{e_{o_n\lambda}}^{+}(h,\bar{r})\right]\bar{N}_{o_{e_n\lambda}}^{+}(-h,\bar{r}')\right]$$

$$\bar{r},\bar{r}' \in V_2 \quad . \tag{3.88}$$

AD-A154 292 MUTUAL COUPLING ANALYSIS FOR CONFORMAL MICROSTRIP ANTENNAS(U) OHIO STATE UNIV COLUMBUS ELECTROSCIENCE LAB B W KWAN ET AL. DEC 84 712692-4 N00014-78-C-0049 2/3

UNCLASSIFIED F/G 9/5 NL

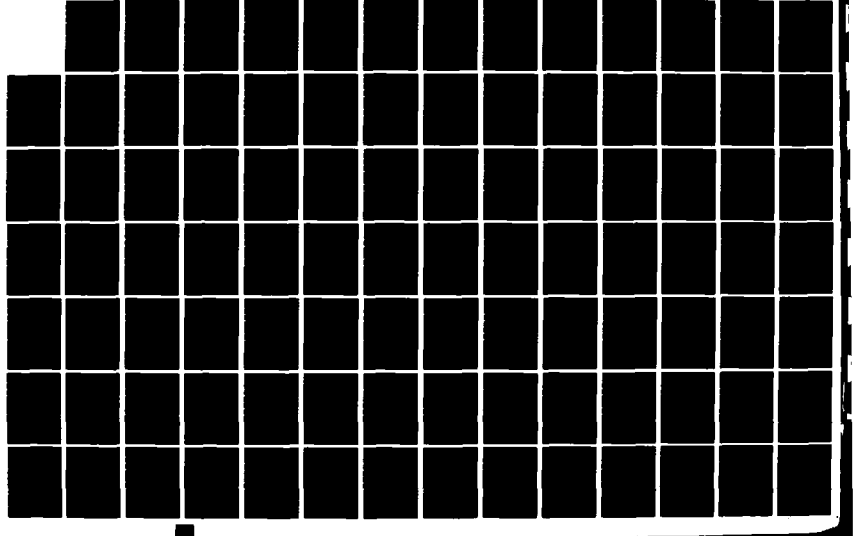

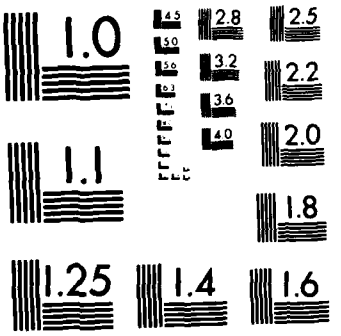

It is clear that the sum of $\bar{\bar{G}}_o$ and $\bar{\bar{G}}_{s2}$ will automatically satisfy (3.69) that governs $\bar{\bar{G}}_{e2}$. Loosely speaking, $\bar{\bar{G}}_o$ may be interpreted as the incident or direct field, and $\bar{\bar{G}}_{s2}$ as the scattered field. As for the form of $\bar{\bar{G}}_{s2}$, the choice of $\bar{M}^{+}_{e_o n\lambda}(h,\bar{r})$ and $\bar{N}^{+}_{e_o n\lambda}(h,\bar{r})$ as the anterior elements is dictated by the radiation condition (3.85), and the choice of $\bar{M}^{+}_{e_o n\lambda}(-h,\bar{r}')$ and $\bar{N}^{+}_{e_o n\lambda}(-h,\bar{r}')$ as the posterior elements is guided by the expression for $\bar{\bar{g}}_o^-$ because various boundary conditions such as (3.83) and (3.84) can be satisfied only if the posterior elements of $\bar{\bar{g}}_o^-$ and $\bar{\bar{G}}_{s2}$ are the same.

Once the form of $\bar{\bar{G}}_{s2}$ is determined, it is relatively easy to formulate the expansion for $\bar{\bar{G}}_{e1}$ given below:

$$\bar{\bar{G}}_{e1}(\bar{r},\bar{r}') = \frac{j}{8\pi} \int_{-\infty}^{\infty} dh \sum_{n=0}^{\infty} \frac{\varepsilon_n}{\lambda^2} \Bigg\{ \Big[\alpha_{{}_{e_o}n} \bar{M}^{+}_{e_o n\mu}(h,\bar{r}) + \beta_{{}_{o_e}n} \bar{N}^{+}_{o_e n\mu}(h,\bar{r}) + \gamma_{{}_{e_o}n} \bar{M}^{-}_{e_o n\mu}(h,\bar{r}) + \tau_{{}_{o_e}n} \bar{N}^{-}_{o_e n\mu}(h,\bar{r}) \Big]$$

$$\bar{M}^{+}_{e_o n\lambda}(-h,\bar{r}') + \Big[a_{{}_{e_o}n} \bar{N}^{+}_{e_o n\mu}(h,\bar{r}) + b_{{}_{o_e}n} \bar{M}^{+}_{o_e n\mu}(h,\bar{r}) + d_{{}_{e_o}n} \bar{N}^{-}_{e_o n\mu}(h,\bar{r}) + f_{{}_{o_e}n} \bar{M}^{-}_{o_e n\mu}(h,\bar{r}) \Big] \bar{N}^{+}_{e_o n\lambda}(-h,\bar{r}') \Bigg\} ,$$

$$\bar{r} \in V_1 , \ \bar{r}' \in V_2 \quad . \qquad (3.89)$$

In the case of $\bar{\bar{G}}_{e1}$, the posterior elements $\bar{M}^{+}_{o e_n \lambda}(-h,\bar{r}')$ and $\bar{N}^{+}_{o e_n \lambda}(-h,\bar{r}')$ must be chosen to match those of $\bar{\bar{G}}_{e2}$ such that the boundary conditions at the interface (ρ=b) can be satisfied, and the anterior elements $\bar{M}^{\pm}_{o e_n \mu}(h,\bar{r})$ and $\bar{N}^{\pm}_{o e_n \mu}(h,\bar{r})$ are chosen because they are the solenoidal eigenmodes and will constitute the bouncing waves inside the dielectric (region V_1).

It is important to note that the parameters λ and μ which appear in (3.87) - (3.89) are defined as follows:

$$\lambda = \sqrt{k_2^2 - h^2} \quad , \text{Im } \lambda > 0 \quad , \text{Re } \lambda \geq 0 \quad , \tag{3.90}$$

$$\mu = \sqrt{k_1^2 - h^2} \quad , \text{Im } \mu > 0 \quad , \text{Re } \mu > 0 \quad . \tag{3.91}$$

There are totally 24 unknown coefficients in the expansions of $\bar{\bar{G}}_{e1}$ and $\bar{\bar{G}}_{e2}$. Not too surprisingly, however, there are exactly 24 linear equations that govern these coefficients after expanding the boundary conditions (3.82) - (3.84). This 24 x 24 system of simultaneous linear equations can be solved analytically. The algebraic details are presented in Apendix F and only the final results are listed here:

$$A_{o e_n} = A_n \tag{3.92}$$

$$B_{o e_n} = \pm B_n \tag{3.93}$$

$$C_{e_{o_n}} = C_n \tag{3.94}$$

$$D_{e_{o_n}} = B_{e_{o_n}} = \pm B_n \tag{3.95}$$

$$\tau_{e_{o_n}} = \pm \tau_n \tag{3.96}$$

$$\alpha_{e_{o_n}} = q_n \gamma_n \tag{3.97}$$

$$\gamma_{e_{o_n}} = \gamma_n \tag{3.98}$$

$$\beta_{e_{o_n}} = \pm p_n \tau_n \tag{3.99}$$

$$d_{e_{o_n}} = d_n \tag{3.100}$$

$$a_{e_{o_n}} = p_n d_n \tag{3.101}$$

$$f_{e_{o_n}} = \pm f_n \tag{3.102}$$

$$b_{e_{o_n}} = \pm q_n f_n \tag{3.103}$$

where

$$\tau_n = \frac{2hn}{\pi k_1 b^2} \left(\frac{\mu_2}{\mu_1}\right) \left(1 - \frac{\mu^2}{\lambda^2}\right) \frac{T_n}{H_n(\lambda b) Y_n} \tag{3.104}$$

$$\gamma_n = \frac{j2}{\pi b} \left[\frac{-\left(\frac{\mu_2}{\mu_1}\right) \mu P_n + (k_2/k_1)^2 \frac{\mu^2}{\lambda} r_n S_n}{H_n(\lambda b) Y_n} \right]$$

$$d_n = \frac{j2}{\pi b}\left(\frac{k_2}{k_1}\right)\left[\frac{-\mu Q_n + \left(\frac{\mu_2}{\mu_1}\right)\frac{\mu^2}{\lambda} r_n T_n}{H_n(\lambda b) Y_n}\right] \tag{3.106}$$

$$f_n = \frac{2hn}{\pi b^2}\left(\frac{k_2}{k_1^2}\right)\left(1 - \frac{\mu^2}{\lambda^2}\right)\frac{S_n}{H_n(\lambda b) Y_n} \tag{3.107}$$

$$A_n = -\frac{J_n(\lambda b)}{H_n(\lambda b)} + \left(\frac{\mu_2}{\mu_1}\right)\frac{\mu^2}{\lambda^2}\frac{T_n}{H_n(\lambda b)}\ Y_n \tag{3.108}$$

$$B_n = \left(\frac{k_2}{k_1}\right)\frac{\mu^2}{\lambda^2}\frac{S_n}{H_n(\lambda b)}\ \tau_n \tag{3.109}$$

$$C_n = -\frac{J_n(\lambda b)}{H_n(\lambda b)} + \left(\frac{k_2}{k_1}\right)\frac{\mu^2}{\lambda^2}\frac{S_n}{H_n(\lambda b)}\ d_n \tag{3.110}$$

$$S_n = J_n(\mu b) + p_n H_n(\mu b) \tag{3.111}$$

$$P_n = J_n'(\mu b) + p_n H_n'(\mu b) \tag{3.112}$$

$$T_n = J_n(\mu b) + q_n H_n(\mu b) \tag{3.113}$$

$$Q_n = J_n'(\mu b) + q_n H_n'(\mu b) \tag{3.114}$$

$$Y_n = \left[-\mu Q_n + \left(\frac{\mu_2}{\mu_1}\right) \frac{\mu^2}{\lambda} r_n T_n\right] \left[-\left(\frac{\mu_2}{\mu_1}\right) \mu P_n + \left(\frac{k_2}{k_2}\right)^2 \frac{\mu^2}{\lambda} r_n S_n\right]$$

$$- \left(\frac{hn}{k_1 b}\right)^2 \left(\frac{\mu_2}{\mu_1}\right) \left(1 - \frac{\mu^2}{\lambda^2}\right)^2 S_n T_n \qquad (3.115)$$

$$p_n = - \frac{J_n(\mu a)}{H_n(\mu a)} \qquad (3.116)$$

$$q_n = - \frac{J_n'(\mu a)}{H_n'(\mu a)} \qquad (3.117)$$

$$r_n = \frac{H_n'(\lambda b)}{H_n(\lambda b)} \qquad (3.118)$$

$$H_n(\xi) \triangleq H_n^{(1)}(\xi) \text{ , and } \quad H_n'(\xi) \triangleq \frac{d}{d\xi} H_n^{(1)}(\xi) \quad . \qquad (3.119)$$

Making use of (3.92) - (3.103) in (3.88) and (3.89) leads to the following simplified versions of $\bar{\bar{G}}_{s2}$ and $\bar{\bar{G}}_{e1}$, respectively:

$$\bar{\bar{G}}_{s2}(\bar{r},\bar{r}') = \frac{j}{8\pi} \int_{-\infty}^{\infty} \frac{dh}{\lambda^2} \sum_{n=0}^{\infty} \epsilon_n \Bigg[\left[A_n \bar{M}_{e_o n\lambda}^{+}(h,\bar{r}) \mp B_n \bar{N}_{o_e n\lambda}^{+}(h,\bar{r})\right]$$

$$\bar{M}_{e_o n\lambda}^{+}(-h,\bar{r}') + \left[C_n \bar{N}_{e_o n\lambda}^{+}(h,\bar{r}) \mp B_n \bar{M}_{o_e n\lambda}^{+}(h,\bar{r})\right] \bar{N}_{e_o n\lambda}^{+}(-h,\bar{r}') \Bigg] \quad ,$$

(3.120)

and

$$\bar{\bar{G}}_{e1}(\bar{r},\bar{r}') = \frac{j}{8\pi} \int_{-\infty}^{\infty} \frac{dh}{\lambda^2} \sum_{n=0}^{\infty} \varepsilon_n \left[\left[\gamma_n \left(\bar{\bar{M}}^{--}_{oenu}(h,\bar{r}) + q_n \bar{\bar{M}}^{-+}_{oenu}(h,\bar{r}) \right) \right. \right.$$

$$\left. \mp \tau_n \left(\bar{\bar{N}}^{--}_{eonu}(h,\bar{r}) + p_n \bar{\bar{N}}^{-+}_{eonu}(h,\bar{r}) \right) \right]$$

$$\bar{\bar{M}}^{+}_{oen\lambda}(-h,\bar{r}') + \left[d_n \left(\bar{\bar{N}}^{--}_{eonu}(h,\bar{r}) + p_n \bar{\bar{N}}^{-+}_{eonu}(h,\bar{r}) \right) \right.$$

$$\left. \left. \mp f_n \left(\bar{\bar{M}}^{--}_{eonu}(h,\bar{r}) + q_n \bar{\bar{M}}^{-+}_{eonu}(h,\bar{r}) \right) \right] \bar{\bar{N}}^{+}_{oen\lambda}(-h,\bar{r}') \right] . \tag{3.121}$$

This completes the construction of the dyadic Green's function for the dielectric coated cylinder.

E. EXPANDING THE GREEN'S DYADICS

One may have already observed that dyadic functions are notationally so compact that they greatly simplify many formal manipulations. Ironically it is this very compactness feature that tends to conceal information. Often enough deeper insight can only be gained after the dyadic functions have been expanded. Anticipating that the Green's dyadic for the coated cylinder will be used in the analysis in the chapters that follow, it may be worthwhile to expand $\bar{\bar{G}}_e$ into component form such that the electric field can be easily read off once excitation is known.

Various components of $\bar{\bar{G}}_e$ in regions V_1 and V_2 are presented in the following.

Region V_2 (air): $b<\rho,\rho'<\infty$, $0<\phi,\phi'<2\pi$, $-\infty<z,z'<\infty$

It follows from Equations (3.67), (3.86) and (3.87) that

$$\bar{\bar{G}}_e(\bar{r},\bar{r}') = \bar{\bar{G}}_{e2}(\bar{r},\bar{r}') = \bar{\bar{G}}_0(\bar{r},\bar{r}') + \bar{\bar{G}}_{s2}(\bar{r},\bar{r}')$$

$$= U(\rho-\rho')\bar{\bar{g}}_0^{+-}(\bar{r},\bar{r}') + U(\rho'-\rho)\bar{\bar{g}}_0^{-+}(\bar{r},\bar{r}') - \frac{\hat{\rho}\hat{\rho}}{k_2^2}\delta(\bar{r}-\bar{r}') + \bar{\bar{G}}_{s2}(\bar{r},\bar{r}'). \tag{3.122}$$

Making use of (3.46) and (3.47) in (3.87) yields

$$\bar{\bar{g}}_0^{\pm}(\bar{r},\bar{r}') =$$

$$\frac{j}{8\pi}\int_{-\infty}^{\infty} dh \sum_{n=0}^{\infty} \frac{\epsilon_n}{\lambda^2} \left[\hat{\rho}\hat{\rho}' \left[\frac{n^2}{\rho\rho'} Z_n^{\pm}(\lambda\rho)Z_n^{\mp}(\lambda\rho') + \left(\frac{h\lambda}{k_2}\right)^2 Z_n^{\pm'}(\lambda\rho)Z_n^{\mp'}(\lambda\rho') \right] \right.$$

$$\cdot \cos n(\phi-\phi') + \hat{\rho}\hat{\phi}' \left[\frac{n\lambda}{\rho} Z_n^{\pm}(\lambda\rho)Z_n^{\mp'}(\lambda\rho') + \frac{n\lambda h^2}{k_2^2\rho'} Z_n^{\pm'}(\lambda\rho)Z_n^{\mp}(\lambda\rho') \right] \sin n(\phi-\phi')$$

$$+ \hat{\rho}\hat{z} \left[\frac{jh\lambda^3}{k_2^2} Z_n^{\pm'}(\lambda\rho)Z_n^{\mp}(\lambda\rho') \right] \cos n(\phi-\phi') - \hat{\phi}\hat{\rho}' \left[\frac{n\lambda}{\rho'} Z_n^{\pm'}(\lambda\rho)Z_n^{\mp}(\lambda\rho') \right.$$

$$\left. + \frac{n\lambda h^2}{k_2^2\rho} Z_n^{\pm}(\lambda\rho)Z_n^{\mp'}(\lambda\rho') \right] \sin n(\phi-\phi') + \hat{\phi}\hat{\phi}' \left[\lambda^2 Z_n^{\pm'}(\lambda\rho)Z_n^{\mp'}(\lambda\rho') \right.$$

$$\left. + \left(\frac{nh}{k_2}\right)^2 \frac{1}{\rho\rho'} Z_n^{\pm}(\lambda\rho)Z_n^{\mp}(\lambda\rho') \right] \cos n(\phi-\phi') - \hat{\phi}\hat{z} \left[\frac{jn\lambda^2 h}{k_2^2\rho} Z_n^{\pm}(\lambda\rho)Z_n^{\mp}(\lambda\rho') \right] \sin n(\phi-\phi')$$

$$- \hat{z}\hat{\rho}' \left[\frac{jh\lambda^3}{k_2^2} Z_n^{\pm}(\lambda\rho)Z_n^{\mp'}(\lambda\rho') \right] \cos n(\phi-\phi') - \hat{z}\hat{\phi}' \left[\frac{jnh\lambda^2}{k_2^2\rho'} Z_n^{\pm}(\lambda\rho)Z_n^{\mp}(\lambda\rho') \right] \sin n(\phi-\phi')$$

$$\left. + \hat{z}\hat{z} \left[\frac{\lambda^4}{k_2^2} Z_n^{\pm}(\lambda\rho)Z_n^{\mp}(\lambda\rho') \right] \cos n(\phi-\phi') \right] e^{jh(z-z')} , \tag{1.123}$$

where,

$$Z_n^+(\xi) = H_n^{(1)}(\xi);\ Z_n^-(\xi) = J_n(\xi) \text{ and } Z_n^{\pm\prime}(\xi) = \frac{d}{d\xi} Z_n^{\pm}(\xi) .$$

It is of interest to point out that formally carrying out the operation $(\bar{\bar{I}} + \frac{1}{k_2^2} \nabla\nabla)\, g_0(\bar{r},\bar{r}')$ in (3.64) will lead to the closed forms of $\bar{\bar{g}}_0^{\pm}$ given below:

$$\begin{aligned}
\bar{\bar{g}}_0^{\pm}(r,r') = \frac{1}{4\pi k_2^2} \Bigg[& \hat{\rho}\hat{\rho}' \left[\left(k_2^2 \frac{e^{jk_2R}}{R} + P \frac{e^{jk_2R}}{R^3}\right) \cos(\phi-\phi') \right. \\
& \left. + Q(\rho-\rho'\cos(\phi-\phi')) \cdot (\rho\cos(\phi-\phi')-\rho') \frac{e^{jk_2R}}{R^3} \right] \\
& + \hat{\rho}\hat{\phi}' \left[k_2^2 \frac{e^{jk_2R}}{R} + [P+\rho(\rho-\rho'\cos(\phi-\phi'))Q] \cdot \frac{e^{jk_2R}}{R^3} \right] \sin(\phi-\phi') \\
& + \hat{\rho}\hat{z} \left[(z-z')(\rho-\rho'\cos(\phi-\phi'))Q \frac{e^{jk_2R}}{R^3} \right] \\
& - \hat{\phi}\hat{\rho}' \left[k_2^2 \frac{e^{jk_2R}}{R} + [P+\rho'(\rho'-\rho\cos(\phi-\phi'))Q] \cdot \frac{e^{jk_2R}}{R^3} \right] \sin(\phi-\phi') \\
& + \hat{\phi}\hat{\phi}' \left[\left(k_2^2 \frac{e^{jk_2R}}{R} + P \frac{e^{jk_2R}}{R^3}\right) \cos(\phi-\phi') + \rho\rho' Q \sin^2(\phi-\phi') \frac{e^{jk_2R}}{R^3} \right] \\
& + \hat{\phi}\hat{z} \left[\rho'(z-z')\sin(\phi-\phi') Q \frac{e^{jk_2R}}{R^3} \right] + \hat{z}\hat{\rho}' \left[(z-z')(\rho\cos(\phi-\phi')-\rho') Q \frac{e^{jk_2R}}{R^3} \right] \\
& + \hat{z}\hat{\phi}' \left[\rho(z-z')\sin(\phi-\phi') Q \frac{e^{jk_2R}}{R^3} \right] + \hat{z}\hat{z} \left[k_2^2 \frac{e^{jk_2R}}{R} + (P+(z-z')^2 Q) \frac{e^{jk_2R}}{R^3} \right] \Bigg]
\end{aligned} \tag{3.124}$$

where

$$R = |\bar{r}-\bar{r}'| = [\rho^2 + \rho'^2 - 2\rho\rho'\cos(\phi-\phi') + (z-z')^2]^{1/2} ,$$

$$P = jk_2R-1 ,$$

$$Q = - k_2^2 - \frac{j3k_2}{R} + \frac{3}{R^2} .$$

Next substituting (3.46) and (3.47) into (3.120) gives

$$\overline{\overline{G}}_{s2}(\bar{r},\bar{r}') = \frac{j}{8\pi} \int_{-\infty}^{\infty} dh \sum_{n=0}^{\infty} \varepsilon_n \Bigg\{ \hat{\rho}\hat{\rho}' \Big[A_n\Big[\frac{n^2}{\lambda^2\rho\rho'} H_n(\lambda\rho)H_n(\lambda\rho')\Big]$$

$$+ B_n \frac{jnh}{\lambda k_2}\Big[\frac{1}{\rho'} H_n'(\lambda\rho)H_n(\lambda\rho') + \frac{1}{\rho} H_n(\lambda\rho)H_n'(\lambda\rho')\Big]$$

$$+ C_n\Big[\Big(\frac{h}{k_2}\Big)^2 H_n'(\lambda\rho)H_n'(\lambda\rho')\Big]\Big]\cos n(\phi-\phi')$$

$$+ \hat{\rho}\hat{\phi}' \Big[A_n\Big[\frac{n}{\lambda\rho} H_n(\lambda\rho)H_n(\lambda\rho')\Big] + B_n \frac{jh}{k_2}\Big[H_n(\lambda\rho)H_n'(\lambda\rho')$$

$$+ \frac{n^2}{\lambda^2\rho\rho'} H_n(\lambda\rho)H_n(\lambda\rho')\Big] + C_n\Big[\frac{nh^2}{k_2^2\lambda\rho'} H_n'(\lambda\rho)H_n(\lambda\rho')\Big]\Big]\sin n(\phi-\phi')$$

$$+ \hat{\rho}\hat{z} \Big[C_n\Big[\frac{jh\lambda}{k_2^2} H_n'(\lambda\rho)H_n(\lambda\rho')\Big] - B_n\Big[\frac{n}{k_2\rho} H_n(\lambda\rho)H_n(\lambda\rho')\Big]\Big]\cos n(\phi-\phi')$$

$$- \hat{\phi}\hat{\rho}' \Big[A_n\Big[\frac{n}{\lambda\rho'} H_n'(\lambda\rho)H_n(\lambda\rho')\Big] + B_n \frac{jh}{k_2}\Big[\frac{n^2}{\lambda^2\rho\rho'} H_n(\lambda\rho)H_n(\lambda\rho')$$

$$+ H_n'(\lambda\rho)H_n'(\lambda\rho')\Big] + C_n\Big[\frac{nh^2}{k_2^2\lambda\rho} H_n(\lambda\rho)H_n'(\lambda\rho')\Big]\Big]\sin n(\phi-\phi')$$

$$+ \hat{\phi}\hat{\phi}' \Big[A_n[H_n'(\lambda\rho)H_n'(\lambda\rho')] + B_n \frac{jnh}{k_2\lambda}\Big[\frac{1}{\rho} H_n(\lambda\rho)H_n'(\lambda\rho') +$$

$$+\frac{1}{\rho'}H_n'(\lambda\rho)H_n(\lambda\rho')\Big] + C_n\Big[\Big(\frac{nh}{k_2\lambda}\Big)^2\frac{1}{\rho\rho'}H_n(\lambda\rho)H_n(\lambda\rho')\Big]\Big]\cos n(\phi-\phi')$$

$$-\hat{\phi}\hat{z}\Big[C_n\Big[\frac{jnh}{k_2^2\rho}H_n(\lambda\rho)H_n(\lambda\rho')\Big] - B_n\Big[\frac{\lambda}{k_2}H_n'(\lambda\rho)H_n(\lambda\rho')\Big]\Big]\sin n(\phi-\phi')$$

$$+\hat{z}\hat{\rho}'\Big[B_n\Big[\Big(\frac{n}{k_2\rho'}\Big)H_n(\lambda\rho)H_n(\lambda\rho')\Big] - C_n\Big[\frac{jh\lambda}{k_2^2}H_n(\lambda\rho)H_n'(\lambda\rho')\Big]\Big]\cos n(\phi-\phi')$$

$$+\hat{z}\hat{\phi}'\Big[B_n\Big[\frac{\lambda}{k_2}H_n(\lambda\rho)H_n'(\lambda\rho')\Big] - C_n\Big[\frac{jnh}{k_2^2\rho'}H_n(\lambda\rho)H_n(\lambda\rho')\Big]\Big]\sin n(\phi-\phi')$$

$$+\hat{z}\hat{z}\Big[C_n\Big[\Big(\frac{\lambda}{k_2}\Big)^2H_n(\lambda\rho)H_n(\lambda\rho')\Big]\cdot\cos n(\phi-\phi')\Big]e^{jh(z-z')} \quad . \tag{3.125}$$

where

$$H_n(\xi) = H_n^{(1)}(\xi) \quad \text{and} \quad H_n'(\xi) = \frac{d}{d\xi}H_n^{(1)}(\xi) \quad .$$

Region V_1 (dielectric): $a<\rho<b$, $b<\rho'<\infty$, $0<\phi,\phi'<2\pi$, $-\infty<z,z'<\infty$

It is clear from Equation (3.67) that

$$\bar{\bar{G}}_e(\bar{r},\bar{r}) = \bar{\bar{G}}_{e1}(\bar{r},\bar{r}') \quad .$$

Using Equations (3.46) and (3.47) in (3.121) yields

$$\bar{\bar{G}}_{el}(\bar{r},\bar{r}') = \frac{j}{8\pi}\int_{-\infty}^{\infty} dh \sum_{n=0}^{\infty}\varepsilon_n \Bigg\{ \hat{\rho}\hat{\rho}' \Bigg[\gamma_n \left[\frac{n^2}{\lambda^2\rho\rho'} H_n(\lambda\rho')\right][J_n(\mu\rho)+q_n H_n(\mu\rho)]$$

$$+ \tau_n \left[\frac{jnh\mu}{k_1\lambda^2\rho'} H_n(\lambda\rho')\right]\left[J_n'(\mu\rho)+p_n H_n'(\mu\rho)\right]$$

$$+ d_n\left[\frac{h^2\mu}{k_1k_2\lambda} H_n'(\lambda\rho')\right][J_n'(\mu\rho)+p_n H_n'(\mu\rho)] + f_n\left[\frac{jnh}{k_2\lambda\rho} H_n'(\lambda\rho')\right]$$

$$\cdot [J_n(\mu\rho)+q_n H_n(\mu\rho)]\Bigg]\cos n(\phi-\phi') + \hat{\rho}\hat{\phi}'\Bigg[\gamma_n\left[\frac{n}{\lambda\rho} H_n'(\lambda\rho')\right][J_n(\mu\rho)+q_n H_n(\mu\rho)]$$

$$+ \tau_n\left[\frac{jh\mu}{k_1\lambda} H_n'(\lambda\rho')\right]\left[J_n'(\mu\rho)+p_n H_n'(\mu\rho)\right] + d_n\left[\frac{nh^2\mu}{k\,k_1\lambda^2\rho'} H_n(\lambda\rho')\right]$$

$$\cdot [J_n'(\mu\rho)+p_n H_n'(\mu\rho)] + f_n\left[\frac{jn^2h}{k_2\lambda^2\rho\rho'} H_n(\lambda\rho')\right][J_n(\mu\rho)+q_n H_n(\mu\rho)]\Bigg]\sin n(\phi-\phi')$$

$$+ \hat{\rho}\hat{z}\Bigg[d_n\left[\frac{jh\mu}{k_1k_2} H_n(\lambda\rho')\right][J_n'(\mu\rho)+p_n H_n'(\mu\rho)] - f_n\left[\frac{n}{k_2\rho} H_n(\lambda\rho')\right]$$

$$\cdot [J_n(\mu\rho)+q_n H_n(\mu\rho)]\Bigg]\cos n(\phi-\phi') - \hat{\phi}\hat{\rho}'\Bigg[\gamma_n\left[\frac{n\mu}{\lambda^2\rho'} H_n(\lambda\rho')\right]$$

$$\cdot [J_n'(\mu\rho)+q_n H_n'(\mu\rho)] + \tau_n\left[\frac{jhn^2}{k_1\lambda^2\rho\rho'} H_n(\lambda\rho')\right][J_n(\mu\rho)+p_n H_n(\mu\rho)]$$

$$+ d_n\left[\frac{nh^2}{k_1k_2\lambda\rho} H_n'(\lambda\rho')\right][J_n(\mu\rho)+p_n H_n(\mu\rho)] + f_n\left[\frac{jh\mu}{k_2\lambda} H_n'(\lambda\rho')\right]$$

$$\cdot [J_n'(\mu\rho)+q_n H_n'(\mu\rho)]\Bigg]\sin n(\phi-\phi') + \hat{\phi}\hat{\phi}'\Bigg[\gamma_n\left[\frac{\mu}{\lambda} H_n'(\lambda\rho')\right][J_n'(\mu\rho)+q_n H_n'(\mu\rho)]$$

$$+ \tau_n\left[\frac{jnh}{k_1\lambda\rho} H_n'(\lambda\rho')\right][J_n(\mu\rho)+p_n H_n(\mu\rho)] + d_n\left[\frac{n^2h^2}{k_1k_2\lambda^2\rho\rho'} H_n(\lambda\rho')\right] \cdot$$

$$\cdot [J_n(\mu\rho)+p_nH_n(\mu\rho)] + f_n \left[\frac{jnh\mu}{k_2\lambda^2\rho'} H_n(\lambda\rho')\right][J_n'(\mu\rho)+q_nH_n'(\mu\rho)]\Big]\cosn(\phi-\phi')$$

$$- \hat{\phi}\hat{z} \Big[d_n\left[\frac{jnh}{k_1k_2\rho} H_n(\lambda\rho')\right][J_n(\mu\rho)+p_nH_n(\mu\rho)] - f_n \left[\frac{\mu}{k_2} H_n'(\lambda\rho')\right]$$

$$\cdot [J_n'(\mu\rho)+q_nH_n'(\mu\rho)]\Big]\sinn(\phi-\phi') + \hat{z}\hat{\rho}' \Big[\tau_n \left[\frac{n\mu^2}{k_1\lambda^2\rho'} H_n(\lambda\rho')\right]$$

$$\cdot [J_n(\mu\rho)+p_nH_n(\mu\rho)] - d_n \left[\frac{jh\mu^2}{k_1k_2\lambda} H_n'(\lambda\rho')\right][J_n(\mu\rho)+p_nH_n(\mu\rho)]\Big]\cosn(\phi-\phi')$$

$$+ \hat{z}\hat{\phi}' \Big[\tau_n \left[\frac{\mu^2}{k_1\lambda} H_n'(\lambda\rho'][J_n(\mu\rho)+p_nH_n(\mu\rho)] - d_n \left[\frac{jn\, h\mu^2}{k_1k_2\lambda^2\rho'} H_n(\lambda\rho')\right]$$

$$\cdot [J_n(\mu\rho)+p_nH_n(\mu\rho)]\Big]\sinn(\phi-\phi') + \hat{z}\hat{z} \Big[d_n\left[\frac{\mu^2}{k_1k_2} H_n(\lambda\rho')\right]$$

$$\cdot [J_n(\mu\rho)+p_nH_n(\mu\rho)]\Big]\cosn(\phi-\phi') \Big] e^{jh(z-z')} \quad , \qquad (3.126)$$

where

$$H_n(\xi) = H_n^{(1)}(\xi) \text{ and } H_n'(\xi) = \frac{d}{d\xi} H_n^{(1)}(\xi).$$

Thus, the dyadic Green's function for the coated cylinder has been expanded into a form from which the electric field components can be readily identified once the current density is specified.

CHAPTER IV

PATCH DIPOLES ON A DIELECTRIC COATED CYLINDER

A. INTRODUCTION

The main goal of this chapter is to obtain expressions which will enable one to compute either directly or indirectly the self and mutual impedances between expansion dipole modes, and to evaluate the elements of the voltage vector for the case of a dielectric coated cylinder. These impedance and voltage elements are crucial to implementing the method of moments to analyze the coupling between microstrip antennas. The single most important quantity in these computations is the electric field excited by an expansion dipole mode at the air-dielectric interface associated with the dielectric coated conducting cylinder. This is due to the fact that an appropriate combination of expansion modes is used in the moment method solution to model or approximate the true current on a printed antenna patch.

Extensive use is made of the electric Green's dyadic constructed in Chapter III to obtain expressions for the electric field or its components. To ensure continuity and consistency relevant symbols

or notations will retain their original meanings defined in Chapter III, unless stated otherwise. For convenience, some pertinent notations are summarized below.

V refers to the space surrounding the circular conducting cylinder of radius a. It consists of two distinct regions V_1 and V_2 such that $V = V_1 \cup V_2$, where

$$V_1 = \{\bar{r} = (\rho,\phi,z): \ a<\rho<b = t+a \ , \ 0<\phi<2\pi \ , \ -\infty<z<\infty\}$$

represents the uniform layer of dielectric coating of thickness t, and

$$V_2 = \{\bar{r} = (\rho,\phi,z): \ b<\rho<\infty \ , \ 0<\phi<2\pi \ , \ -\infty<z<\infty\}$$

stands for the (free) space or air surrounding the coated cylinder. The constitutive parameters for V_1 and V_2 are, respectively, (μ_1,ε_1) and (μ_2,ε_2) with corresponding propagation constants $k_1=\omega\sqrt{\mu_1\varepsilon_1}$ and $k_2=\omega\sqrt{\mu_2\varepsilon_2}$. The Green's dyadic for V is denoted by $\bar{\bar{G}}_e(\bar{r},\bar{r}')$, where $\bar{r} \in V$ designates the field point and $\bar{r}' \in V_2$ refers to the source point which is restricted to V_2. The Green's dyadic can be conveniently represented as

$$\bar{\bar{G}}_e(\bar{r},\bar{r}') = U(b-\rho)\bar{\bar{G}}_{e1}(\bar{r},\bar{r}') + U(\rho-b)\bar{\bar{G}}_{e2}(\bar{r},\bar{r}') \ , \ \bar{r} \in V, \ \bar{r}' \in V_2 \ , \tag{4.1}$$

with $\bar{\bar{G}}_{e1}$ (Equation (3.126)) being the Green's dyadic for V_1, and $\bar{\bar{G}}_{e2}$ (Equation (3.122)) being the Green's dyadic for V_2. Likewise, the electric field is written as

$$\bar{E}(\bar{r}) = U(b-\rho)\bar{E}_1(\bar{r}) + U(\rho-b)\bar{E}_2(\bar{r}) \ , \quad \bar{r} \in V \tag{4.2}$$

where $\bar{E}_1(\bar{r}) = \hat{\rho}E_{1\rho}(\bar{r}) + \hat{\phi}E_{1\phi}(\bar{r}) + \hat{z}E_{1z}(\bar{r})$ is the electric field in V_1 given by

$$\bar{E}_1(\bar{r}) = j\omega\mu_2 \int_{V_2} \bar{\bar{G}}_{e1}(\bar{r},\bar{r}') \cdot \bar{J}(\bar{r}')dv' \quad , \ \bar{r} \in V_1 \ , \tag{4.3}$$

and $\bar{E}_2(\bar{r}) = \hat{\rho}E_{2\rho}(\bar{r}) + \hat{\phi}E_{2\phi}(\bar{r}) + \hat{z}E_{2z}(\bar{r})$ is the electric field in V_2 given by

$$\bar{E}_2(\bar{r}) = j\omega\mu_2 \int_{V_2} \bar{\bar{G}}_{e2}(\bar{r},\bar{r}') \cdot \bar{J}(\bar{r}')dv' \quad , \ \bar{r} \in V_2 \ . \tag{4.4}$$

$\bar{J}$ denotes the electric current source immersed in V_2. The corresponding magnetic field $\bar{H}$ takes the form

$$\bar{H}(\bar{r}) = U(b-\rho)\bar{H}_1(\bar{r}) + U(\rho-b)\bar{H}_2(\bar{r}), \quad \bar{r} \in V \ , \tag{4.5}$$

with $\bar{H}_1(\bar{r}) = 1/(j\omega\mu_1)\ \nabla x\bar{E}_1(\bar{r})$, $\bar{r} \in V_1$, and $\bar{H}_2(\bar{r}) = 1/(j\omega\mu_2)\ \nabla x\bar{E}_2(\bar{r})$, $\bar{r} \in V_2$. Finally, all the expansion coefficients associated with the Green's dyadics are defined by Equation (3.92) through Equation (3.119) which in general cannot be readily expressed because of their formidable complexity.

It should be mentioned that there is an attractive alternative to the Green's function approach for calculating fields due to the surface current source located right at the air-dielectric interface of the dielectric coated cylinder. Such an approach is discussed in Section B. It is analogous to the planar dielectric slab case treated in Chapter II. Section C utilizes the Green's dyadic to obtain the electric field in regions V_1 and V_2. The excitation is taken to be the current of an expansion dipole mode placed at the interface. A general expression for the mutual impedance between two arbitrary expansion modes is derived. The computation of these mutual impedances is an extremely important step in the moment method solution to the problem of analyzing the coupling between microstrip antennas. In Section D, examples of coupling between two expansion dipole modes, both with z-polarized currents, are studied. It reveals certain interesting but important numerical aspects of the Green's function solution. In the last section, an expression useful for far field calculation is derived via the method of steepest descent.

B. A SPECIALIZED METHOD OF SOLUTION

This section presents a method particularly suited for analyzing patch antennas printed on a dielectric coated conducting circular cylinder. This method is conceptually simple and is analogous to the approach described earlier in Chapter II for the planar dielectric slab case. Thus the presentation will be brief. The inclusion of this

method is due to the fact that it does provide an attractive alternative to the Green's function method on which the analysis in later sections is based. In the present method, the electric surface current on the printed conductor that is situated right at the air-dielectric interface is introduced only through the boundary conditions. The solution is rigorous since the effects of the dielectric coating and the cylindrical conductor are both accounted for. It inclu' the radiation field and surface waves. Only formal expressions for the total fields (electric and magnetic) are derived here.

Being a surface current, the microstrip patch current is introduced through the boundary conditions. As a result Maxwell's equations have to be solved for homogeneous source-free regions V_1 and V_2. An arbitrary field in V_i, i=1,2, can be constructed from two scalar functions: ψ_{ei} which generates a TE field and ψ_{mi} which generates a TM field. Both ψ_{ei} and ψ_{mi} satisfy the scalar wave equation:

$$(\nabla^2 + k_i^2) \begin{Bmatrix} \psi_{ei} \\ \psi_{mi} \end{Bmatrix} = 0 \quad , \tag{4.6}$$

where $k_i^2 = \omega^2 \mu_i \varepsilon_i$, i=1,2.

The electric and magnetic fields can be constructed as follows [16]:

$$\begin{aligned} \bar{E}_i(\bar{r}) &= \hat{\rho} E_{i\rho}(\bar{r}) + \hat{\phi} E_{i\phi}(\bar{r}) + \hat{z} E_{iz}(\bar{r}) \\ &= -\nabla \times (\hat{z} \psi_{ei}(\bar{r})) - \frac{1}{j\omega\varepsilon_i} \nabla \times \nabla \times (\hat{z} \psi_{mi}(\bar{r})) \quad , \end{aligned} \tag{4.7}$$

$$\bar{H}_i(\bar{r}) = \hat{\rho}H_{i\rho}(\bar{r}) + \hat{\phi}H_{i\phi}(\bar{r}) + \hat{z}H_{iz}(\bar{r})$$

$$= \nabla x(\hat{z}\psi_{mi}(\bar{r})) - \frac{1}{j\omega\mu_i} \nabla x\nabla x(\hat{z}\psi_{ei}(\bar{r})) \quad . \tag{4.8}$$

The explicit forms of the field components are given below for convenience:

$$E_{i\rho}(\bar{r}) = -\frac{1}{\rho}\frac{\partial}{\partial\phi}\psi_{ei} - \frac{1}{j\omega\varepsilon_i}\frac{\partial^2}{\partial\rho\partial z}\psi_{mi} \quad , \tag{4.9}$$

$$E_{i\phi}(\bar{r}) = \frac{\partial}{\partial\rho}\psi_{ei} - \frac{1}{j\omega\varepsilon_i}\frac{1}{\rho}\frac{\partial^2}{\partial\phi\partial z}\psi_{mi} \quad , \tag{4.10}$$

$$E_{iz}(\bar{r}) = -\frac{1}{j\omega\varepsilon_i}\left(\frac{\partial^2}{\partial z^2} + k_i^2\right)\psi_{mi} \quad , \tag{4.11}$$

$$H_{i\rho}(\bar{r}) = \frac{1}{\rho}\frac{\partial}{\partial\phi}\psi_{mi} - \frac{1}{j\omega\mu_i}\frac{\partial^2}{\partial\rho\partial z}\psi_{ei} \quad , \tag{4.12}$$

$$H_{i\phi}(\bar{r}) = -\frac{\partial}{\partial\rho}\psi_{mi} - \frac{1}{j\omega\mu_i\rho}\frac{\partial^2}{\partial\phi\partial z}\psi_{ei} \quad , \tag{4.13}$$

$$H_{iz}(\bar{r}) = -\frac{1}{j\omega\mu_i}\left(\frac{\partial^2}{\partial z^2} + k_i^2\right)\psi_{ei} \quad . \tag{4.14}$$

In order to specify the fields uniquely, the wave Equation (4.6) must be solved together with the following boundary conditions:

on the surface of the conducting cylinder,

$$\hat{\rho} \times \bar{E}_1(\bar{r})\Big|_{\rho=a} = 0 \quad ; \tag{4.15}$$

on the air-dielectric interface,

$$\hat{\rho} \times [\bar{E}_2(\bar{r}) - \bar{E}_1(\bar{r})]_{\rho=b} = 0 \quad , \tag{4.16}$$

$$\hat{\rho} \times [\bar{H}_2(\bar{r}) - \bar{H}_1(\bar{r})]_{\rho=b} = \bar{J}_s(\bar{r}) \quad , \tag{4.17}$$

where

$$\bar{J}_s(\bar{r}) = \hat{\phi} J_{s\phi}(\bar{r}) + \hat{z} J_{sz}(\bar{r}) \tag{4.18}$$

is the surface current density on the interface at $\rho=b$. Of course, the solution must be chosen so that the radiation condition is satisfied as $|\bar{r}| \to \infty$, $\bar{r} \in V_2$.

Due to the cylindrical symmetry of the structure under consideration, the scalar functions, ψ_{ei} and ψ_{mi}, can be expressed as a Fourier series - Fourier integral:

$$\begin{bmatrix} \psi_{ei}(\bar{r}) \\ \psi_{mi}(\bar{r}) \end{bmatrix} = \frac{1}{2\pi} \sum_{n=-\infty}^{\infty} \int_{-\infty}^{\infty} \begin{bmatrix} \tilde{\psi}_{ei}(\rho,n,h) \\ \tilde{\psi}_{mi}(\rho,n,h) \end{bmatrix} e^{jn\phi} e^{jhz} \, dh \quad , \tag{4.19}$$

where

$$\begin{bmatrix} \tilde{\psi}_{ei}(\rho,n,h) \\ \tilde{\psi}_{mi}(\rho,n,h) \end{bmatrix} = \frac{1}{2\pi} \int_0^{2\pi} \int_{-\infty}^{\infty} \begin{bmatrix} \psi_{ei}(\bar{r}) \\ \psi_{mi}(\bar{r}) \end{bmatrix} e^{-jn\phi} e^{-jhz} \, dz \, d\phi \quad . \tag{4.20}$$

Similarly, $\bar{J}_s(\bar{r})$ can be formally represented as

$$\bar{J}_s(\bar{r}) = \frac{1}{2\pi} \sum_{n=-\infty}^{\infty} \{\hat{\phi}\tilde{J}_{s\phi}(\rho,n,h) + \hat{z}\tilde{J}_{sz}(\rho,n,h)\} e^{jn\phi} e^{jhz} \, dh \quad , \tag{4.21}$$

with

$$\begin{bmatrix} \tilde{J}_{s\phi}(\rho,n,h) \\ \tilde{J}_{sz}(\rho,n,h) \end{bmatrix} = \frac{1}{2\pi} \int_0^{2\pi} \int_{-\infty}^{\infty} \begin{bmatrix} J_{s\phi}(\bar{r}) \\ J_{sz}(\bar{r}) \end{bmatrix} e^{-jn\phi} e^{-jhz} \, dz \, d\phi \quad . \tag{4.22}$$

Substituting (4.19) into the wave Equation (4.16) leads to the Besssel's equation of order n:

$$\left[\rho \frac{d}{d\rho} \left(\rho \frac{d}{d\rho}\right) + \left((k_{\rho i}\rho)^2 - n^2\right)\right] \begin{bmatrix} \tilde{\psi}_{ei}(\rho,n,h) \\ \tilde{\psi}_{mi}(\rho,n,h) \end{bmatrix} = 0 \quad , \; i=1,2 \quad , \tag{4.23}$$

where $k_{\rho i} = \sqrt{k_i^2 - h^2}$. The solution for region V_1 can be written as

$$\begin{bmatrix} \tilde{\psi}_{e1}(\rho,n,h) \\ \tilde{\psi}_{m1}(\rho,n,h) \end{bmatrix} = \begin{bmatrix} A_e(n,h) \\ A_m(n,h) \end{bmatrix} H_n^{(1)}(k_{\rho_1}\rho) + \begin{bmatrix} B_e(n,h) \\ B_m(n,h) \end{bmatrix} H_n^{(2)}(k_{\rho_1}\rho) \quad , \tag{4.24}$$

where $H_n^{(1)}(\xi)$ and $H_n^{(2)}(\xi)$ are the Hankel functions of the first and second kind which represent, respectively, the outgoing and ingoing waves in V_1. As for region V_2, the solution takes the following form:

$$\begin{bmatrix} \tilde{\psi}_{e2}(\rho,n,h) \\ \tilde{\psi}_{m2}(\rho,n,h) \end{bmatrix} = \begin{bmatrix} \Gamma_e(n,h) \\ \Gamma_m(n,h) \end{bmatrix} H_n^{(1)}(k_{\rho_2}\rho) \quad , \tag{4.25}$$

since there are only outgoing waves in V_2.

Making use of (4.24), (4.25) and (4.19) in (4.9) to (4.14) one can express the field components more explicitly. In particular, the transverse field components with respect to the ρ-direction can be rewritten as follows:

<u>in region V_1</u> $(a<\rho<b,\ 0<\phi<2\pi,\ -\infty<z<\infty)$,

$$E_{1\phi}(\bar{r}) = \frac{1}{2\pi} \sum_{n=-\infty}^{\infty} \int_{-\infty}^{\infty} dh \{k_{\rho_1}[A_e H_n^{(1)'}(k_{\rho_1}\rho) + B_e H_n^{(2)'}(k_{\rho_1}\rho)] + \frac{nh}{j\omega\epsilon_1\rho}$$

$$\cdot [A_m H_n^{(1)}(k_{\rho_1}\rho) + B_m H_n^{(2)}(k_{\rho_1}\rho)]\} e^{jn\phi} e^{jhz} \quad , \tag{4.26}$$

$$E_{1z}(\bar{r}) = \frac{1}{2\pi} \sum_{n=-\infty}^{\infty} \int_{-\infty}^{\infty} dh$$

$$\cdot \{-\frac{k_{\rho_1}^2}{j\omega\varepsilon_1} [A_m H_n^{(1)}(k_{\rho_1}\rho) + B_m H_n^{(2)}(k_{\rho_1}\rho)]\} e^{jn\phi} e^{jhz} \quad , \qquad (4.27)$$

$$H_{1\phi}(\bar{r}) = \frac{1}{2\pi} \sum_{n=-\infty}^{\infty} \int_{-\infty}^{\infty} dh\{-k_{\rho_1}[A_m H_n^{(1)'}(k_{\rho_1}\rho) + B_m H_n^{(2)'}(k_{\rho_1}\rho)] + \frac{nh}{j\omega\mu_1\rho}$$

$$\cdot [A_e H_n^{(1)}(k_{\rho_1}\rho) + B_e H_n^{(2)}(k_{\rho_1}\rho)]\} e^{jn\phi} e^{jhz} \quad , \qquad (4.28)$$

$$H_{1z}(\bar{r}) = \frac{1}{2\pi} \sum_{n=-\infty}^{\infty} \int_{-\infty}^{\infty} dh$$

$$\cdot \{-\frac{k_{\rho_1}^2}{j\omega\mu_1} [A_e H_n^{(1)}(k_{\rho_1}\rho) + B_e H_n^{(2)}(k_{\rho_1}\rho)]\} e^{jn\phi} e^{jhz} \quad ; \qquad (4.29)$$

<u>in region V_2</u> ($b<\rho<\infty$, $0<\phi<2\pi$, $-\infty<z<\infty$),

$$E_{2\phi}(\bar{r}) = \frac{1}{2\pi} \sum_{n=-\infty}^{\infty} \int_{-\infty}^{\infty} dh\{[k_{\rho_2} \Gamma_e H_n^{(1)'}(k_{\rho_2}\rho)]$$

$$+ \frac{nh}{j\omega\varepsilon_2\rho} [\Gamma_m H_n^{(1)}(k_{\rho_2}\rho)]\} e^{jn\phi} e^{jhz} \quad , \qquad (4.30)$$

$$E_{2z}(\bar{r}) = \frac{1}{2\pi} \sum_{n=-\infty}^{\infty} \int_{-\infty}^{\infty} dh$$

$$\cdot \left\{ - \frac{k_{\rho_2}^2}{j\omega\varepsilon_2} \Gamma_m H_n^{(1)}(k_{\rho_2}\rho) \right\} e^{jn\phi} e^{jhz} \quad , \tag{4.31}$$

$$H_{2\phi}(\bar{r}) = \frac{1}{2\pi} \sum_{n=-\infty}^{\infty} \int_{-\infty}^{\infty} dh \left\{ - \left[k_{\rho_2} \Gamma_m H_n^{(1)'}(k_{\rho_2}\rho) \right] \right.$$

$$\left. + \left[\frac{nh}{j\omega\mu_2\rho} \Gamma_e H_n^{(1)}(k_{\rho_2}\rho) \right] \right\} e^{jn\phi} e^{jhz} \quad , \tag{4.32}$$

$$H_{2z}(\bar{r}) = \frac{1}{2\pi} \sum_{n=-\infty}^{\infty} \int_{-\infty}^{\infty} dh$$

$$\cdot \left\{ - \frac{k_{\rho_2}^2}{j\omega\mu_2} \Gamma_e H_n^{(1)}(k_{\rho_2}\rho) \right\} e^{jn\phi} e^{jhz} \quad , \tag{4.33}$$

where $H_n^{(i)'}(\xi) = \frac{d}{d\xi} H_n^{(i)}(\xi)$, i=1,2.

The unknown coefficients can be found from the boundary conditions. The solution procedure is rather straightforward, hence the algebraic details will be omitted. Only the key steps and final results are presented here. From boundary condition (4.15), it is evident that

$$B_e = -\alpha_e A_e \quad , \quad \alpha_e = \frac{H_n^{(1)'}(k_{\rho_1} a)}{H_n^{(2)'}(k_{\rho_1} a)} \quad , \tag{4.34}$$

$$B_m = -\alpha_m A_m \quad , \quad \alpha_m = \frac{H_n^{(1)}(k_{\rho_1} a)}{H_n^{(2)}(k_{\rho_1} a)} \quad . \tag{4.35}$$

Next it follows from boundary condition (4.16) that

$$A_e k_{\rho_1}[H_n^{(1)'}(k_{\rho_1} b) - \alpha_e H_n^{(2)'}(k_{\rho_1} b)]$$

$$+ \frac{nh}{j\omega\varepsilon_1 b} A_m[H_n^{(1)}(k_{\rho_1} b) - \alpha_m H_n^{(2)}(k_{\rho_1} b)]$$

$$= \Gamma_e k_{\rho_2} H_n^{(1)'}(k_{\rho_2} b) + \frac{nh}{j\omega\varepsilon_2 b} \Gamma_m H_n^{(1)}(k_{\rho_2} b) \quad , \tag{4.36}$$

and

$$- \frac{k_{\rho_1}^2}{j\omega\varepsilon_1} A_m[H_n^{(1)}(k_{\rho_1} b) - \alpha_m H_n^{(2)}(k_{\rho_1} b)] = - \frac{k_{\rho_2}^2}{j\omega\varepsilon_2} \Gamma_m H_n^{(1)}(k_{\rho_2} b) \quad . \tag{4.37}$$

Finally, boundary condition (4.17) implies

$$\left[\frac{nh}{j\omega\mu_2 b} H_n^{(1)}(k_{\rho 2}b)\Gamma_e - k_{\rho 2}H_n^{(1)'}(k_{\rho 2}b)\Gamma_m\right]$$

$$+ A_m k_{\rho 1}[H_n^{(1)'}(k_{\rho 1}b) - \alpha_m H_n^{(2)'}(k_{\rho 1}b)]$$

$$- \frac{nh}{j\omega\mu_1 b} A_e[H_n^{(1)}(k_{\rho 1}b) - \alpha_e H_n^{(2)}(k_{\rho 1}b)] = \tilde{J}_{sz}(\rho,n,h) \quad , \tag{4.38}$$

and

$$\left[\frac{k_{\rho 2}^2}{j\omega\mu_2} H_n^{(1)}(k_{\rho 2}b)\Gamma_e\right] + \left\{-\frac{k_{\rho 1}^2}{j\omega\mu_1} A_e[H_n^{(1)}(k_{\rho 1}b) - \alpha_e H_n^{(2)}(k_{\rho 1}b)]\right\}$$

$$= \tilde{J}_{s\phi}(\rho,n,h) \quad . \tag{4.39}$$

Solving (4.36) - (4.39) for A_e, A_m, Γ_e, Γ_m simultaneously yields

$$A_m = \beta_m \Gamma_m \tag{4.40}$$

$$A_e = \gamma_e \Gamma_e + \gamma_m \Gamma_m \tag{4.41}$$

$$Q_{\phi e}\Gamma_e + Q_{\phi m}\Gamma_m = \tilde{J}_{s\phi} \tag{4.42}$$

$$Q_{ze}\Gamma_e + Q_{zm}\Gamma_m = \tilde{J}_{sz} \tag{4.43}$$

or

$$\Gamma_e = \frac{1}{Q_d} \left[Q_{zm} \tilde{J}_{s\phi} - Q_{\phi m} \tilde{J}_{sz} \right] \tag{4.44}$$

$$\Gamma_m = \frac{1}{Q_d} \left[-Q_{ze} \tilde{J}_{s\phi} + Q_{\phi e} \tilde{J}_{sz} \right] \tag{4.45}$$

where

$$\beta_m = \left(\frac{\varepsilon_1}{\varepsilon_2}\right) \left(\frac{k_{\rho 2}}{k_{\rho 1}}\right)^2 \frac{H_n^{(1)}(k_{\rho 2} b)}{D_m} \tag{4.46}$$

$$D_g = H_n^{(1)}(k_{\rho 1} b) - \alpha_g H_n^{(2)}(k_{\rho 1} b) \quad , \; g=e,m \tag{4.47}$$

$$D_g' = k_{\rho 1} \left[H_n^{(1)'}(k_{\rho 1} b) - \alpha_g H_n^{(2)'}(k_{\rho 1} b) \right] \quad , \; g=e,m \tag{4.48}$$

$$\gamma_e = \frac{k_{\rho 2} H_n^{(1)'}(k_{\rho 2} b)}{D_e'} \tag{4.49}$$

$$\gamma_m = \frac{nh}{j\omega\varepsilon_2 b} \frac{(k_1^2 - k_2^2)}{k_{\rho 1}^2} \frac{H_n^{(1)}(k_{\rho 2} b)}{D_e'} \tag{4.50}$$

$$Q_{\phi e} = -\frac{1}{j\omega} \left[\frac{k_{\rho 1}^2}{\mu_1} D_e \gamma_e - \frac{k_{\rho 2}^2}{\mu_2} H_n^{(1)}(k_{\rho 2} b) \right] \tag{4.51}$$

$$Q_{\phi m} = -\frac{k_{\rho 1}^2}{j\omega\mu_1} D_e \gamma_m \tag{4.52}$$

$$Q_{ze} = \frac{nh}{j\omega b}\left[\frac{H_n^{(1)}(k_{\rho_2}b)}{\mu_2} - \frac{D_e\gamma_e}{\mu_1}\right] \tag{4.53}$$

$$Q_{zm} = \beta_m D_m' - k_{\rho_2}H_n^{(1)'}(k_{\rho_2}b) - \frac{nh}{j\omega\mu_1}D_e\gamma_m \tag{4.54}$$

and

$$Q_d = Q_{\phi e}Q_{zm} - Q_{\phi m}Q_{ze} \quad . \tag{4.55}$$

Thus all the coefficients have been completely determined. These in turn uniquely specify the scalar functions ψ_{ei} and ψ_{mi}, i=1,2, from which the electric and magnetic fields in both regions V_1 and V_2 are readily obtained via Equations (4.9) to (4.14). One may have already observed that this solution is very appealing for analyzing problems that involve printed dipoles or patch antennas provided the surface current density has a closed form transform in the sense of (4.22). For general volumetric electric sources, the present solution scheme will certainly fail. In such event, the Green's function approach can be used although finding the Green's function itself often presents the most difficulty; however, once the Green's function is found its formal use in the solution is straightforward.

C. MUTUAL COUPLING BETWEEN EXPANSION DIPOLE MODES

In this section, the field evaluation is based on the Green's dyadic $\bar{\bar{G}}_e$ for the dielectric coated cylinder constructed in Chapter III. $\bar{\bar{G}}_e$ essentially describes a linear relation between the electric field and an elementary current source as indicated by (3.20). Hence the total electric field $\bar{E}$ produced by a distributed current source $\bar{J}$ is obtained through an integration (summation) process described by (4.3) or (4.4).

In the analysis of mutual coupling between conformal microstrip antennas on the dielectric coated cylinder formulated by the moment method, the chosen set of expansion dipole modes plays a very important role. The efficiency as well as accuracy of the analysis depend intimately on how closely an individual mode resembles the actual current distribution on a microstrip patch, and on the transformability of a mode in the Fourier sense (i.e., the sense of Fourier series and Fourier integral). Furthermore, one's ability to accurately evaluate the field due to a mode will also affect the quality of analysis in a grand manner. The electric field obtained via the Green's dyadic will be an exact solution since the dyadic function accounts for the conducting cylindrical ground and its dielectric coating rigorously.

A microstrip antenna on the dielectric coated cylinder consists of a printed conductor that conforms with the coated cylinder. The printed conductor is typically very thin so that the current flowing on it can

be regarded as a surface current. Hence it is appropriate to choose a set of expansion dipole modes as described below:

$$\Xi = \{\bar{J}_\ell(r):\ \ell = 1,2,\ldots,\ L < \infty\} \quad ,$$

where

$$\bar{J}_\ell(\bar{r}) = \begin{cases} \hat{\phi}J_{\ell\phi}(\bar{r}) + \hat{z}J_{\ell z}(\bar{r}) & , \bar{r} \in S_\ell \\ 0 & , \bar{r} \notin S_\ell \end{cases} \quad , \tag{4.56}$$

$$S_\ell = \{\bar{r}=(\rho,\phi,z):\ \rho=b^+\ ,\ \phi_{\ell c}-\phi_\ell<\phi<\phi_{\ell c}+\phi_\ell\ ,\ z_{\ell c}-z_\ell<z<z_{\ell c}+z_\ell\}\ V_2 \ .$$

The symbol b^+ denotes a real number which is infinitesimally greater than b. This essentially says the basis set Ξ consists of L (finite) expansion dipole modes. A typical mode $\bar{J}_\ell$ represents a surface current density which vanishes outside a rectangular surface patch S_ℓ on the air-dielectric interface with widths $2b\phi_\ell$ in the ϕ-direction, $2z_\ell$ in the z-direction, and centered at $(b^+,\ \phi_{\ell c},\ z_{\ell c})$. One may note that it is not necessary to think of S_ℓ as being a conducting surface patch. The reason for requiring S_ℓ to be located at $\rho=b^+$ instead of $\rho=b$ is consistent with the use of the Green's dyadic and also is closer to the actual structure being modeled.

Denoting the electric field in V due to mode $\bar{J}_\ell$, $\ell=1,2,\ldots,L$, by

$$\bar{E}^\ell_i(\bar{r}) = \hat{\rho}E^\ell_{i\rho}(\bar{r}) + \hat{\phi}E^\ell_{i\phi}(\bar{r}) + \hat{z}E^\ell_{iz}(\bar{r}) \ , \quad \bar{r} \in V_i \quad , \quad i=1,2 \quad , \tag{4.57}$$

and employing (4.3) and (3.126), one will find

$$E^{\ell}_{1\rho}(\bar{r}) = -\frac{\omega\mu_2}{8\pi} \int_{S_\ell} ds' \int_{-\infty}^{\infty} dh \sum_{n=0}^{\infty} \varepsilon_n \{(\frac{n}{\lambda\rho}\,[J_n(\mu\rho) + q_n H_n(\mu\rho)]$$

$$\cdot\,[\gamma_n H_n'(\lambda b) + \frac{jnh}{k_2\lambda b}\, f_n H_n(\lambda b)] + \frac{h\mu}{k_1\lambda}\,[J_n'(\mu\rho)+p_n H_n'(\mu\rho)]$$

$$\cdot\,[j\tau_n H_n'(\lambda b) + \frac{nh}{k_2\lambda b}\, d_n H_n(\lambda b)])\sin n(\phi-\phi')J_{\ell\phi}(\bar{r}')$$

$$+\,(\frac{jh\mu}{k_1 k_2}\,[J_n'(\mu\rho)+p_n H_n'(\mu\rho)]d_n H_n(\lambda b)$$

$$-\frac{n}{k_2\rho}\,[J_n(\mu\rho) + q_n H_n(\mu\rho)]f_n H_n(\lambda b))\cos n(\phi-\phi')J_{\ell z}(\bar{r}')\}e^{jh(z-z')}\,, \tag{4.58}$$

$$E^{\ell}_{1\phi}(\bar{r}) = -\frac{\omega\mu_2}{8\pi} \int_{S_\ell} ds' \int_{-\infty}^{\infty} dh \sum_{n=0}^{\infty} \varepsilon_n \{(\frac{\mu}{\lambda}\,[J_n'(\mu\rho) + q_n H_n'(\mu\rho)]$$

$$\cdot\,[\gamma_n H_n'(\lambda b) + \frac{jnh}{k_2\lambda b}\, f_n H_n(\lambda b)] + \frac{nh}{k_1\lambda\rho}\,[J_n(\mu\rho)+p_n H_n(\mu\rho)]$$

$$\cdot\,[j\tau_n H_n'(\lambda b) + \frac{nh}{k_2\lambda b}\, d_n H_n(\lambda b)])\cos n(\phi-\phi')J_{\ell\phi}(\bar{r}')$$

$$-\,(\frac{jnh}{k_1 k_2\rho}\,[J_n(\mu\rho)+p_n H_n(\mu\rho)]d_n H_n(\lambda b)$$

$$-\frac{\mu}{k_2}\,[J_n'(\mu\rho) + q_n H_n'(\mu\rho)]f_n H_n(\lambda b))\sin n(\phi-\phi')J_{\ell z}(\bar{r}')\}e^{jh(z-z')}\,, \tag{4.59}$$

$$E^{\ell}_{1z}(\bar{r}) = -\frac{\omega\mu_2}{8\pi}\int_{S_\ell} ds' \int_{-\infty}^{\infty} dh \sum_{n=0}^{\infty} \epsilon_n \{(\frac{\mu^2}{k_1\lambda}[J_n(\mu\rho) + p_n H_n(\mu\rho)]$$

$$\cdot [\tau_n H_n'(\lambda b) - \frac{jnh}{k_2\lambda b} d_n H_n(\lambda b)])\sin n(\phi-\phi') J_{\ell\phi}(\bar{r}')$$

$$+ (\frac{\mu^2}{k_1 k_2}[J_n(\mu\rho)+p_n H_n(\mu\rho)]d_n H_n(\lambda b))\cos n(\phi-\phi') J_{\ell z}(\bar{r}')\} e^{jh(z-z')}, \tag{4.60}$$

and similarly, using an appropriate form of $\bar{\bar{G}}_{e2}$ in (4.4) yields

$$E^{\ell}_{2\rho}(\bar{r}) = -\frac{\omega\mu_2}{8\pi}\int_{S_\ell} ds' \int_{-\infty}^{\infty} dh \sum_{n=0}^{\infty} \epsilon_n \{(\frac{n}{\lambda\rho} H_n(\lambda\rho)[J_n'(\lambda b)$$

$$+ (A_n + \frac{jnh}{k_2\lambda b} B_n) H_n(\lambda b)] + \frac{h}{k_2} H_n'(\lambda\rho)[\frac{nh}{k_2\lambda b} J_n(\lambda b)$$

$$+ (jB_n H_n'(\lambda b) + \frac{nh}{k_2\lambda b} C_n H_n(\lambda b))])\sin n(\phi-\phi') J_{\ell\phi}(\bar{r}')$$

$$+ (\frac{jh\lambda}{k_2^2} H_n'(\lambda\rho)[J_n(\lambda b)+C_n H_n(\lambda b)]$$

$$- \frac{n}{k_2\rho} B_n H_n(\lambda\rho) H_n(\lambda b))\cos n(\phi-\phi') J_{\ell z}(\bar{r}')\} e^{jh(z-z')}, \tag{4.61}$$

$$E^{\ell}_{2\phi}(\bar{r}) = -\frac{\omega\mu_2}{8\pi}\int_{S_\ell} ds' \int_{-\infty}^{\infty} dh \sum_{n=0}^{\infty} \epsilon_n \{(H_n'(\lambda\rho)[J_n'(\lambda b)$$

$$+ (A_n H_n'(\lambda b) + \frac{jnh}{k_2\lambda b} B_n H_n(\lambda b))] + (\frac{nh}{k_2\lambda\rho} H_n(\lambda\rho)\ [\frac{nh}{k_2\lambda b} J_n(\lambda b)$$

$$+ (jB_n H_n'(\lambda b) + \frac{nh}{k_2\lambda b} C_n H_n(\lambda b))])\cos n(\phi-\phi') J_{\ell\phi}(\bar{r}')$$

$$- (\frac{jnh}{k_2^2\rho} H_n(\lambda\rho)[J_n(\lambda b)+C_n H_n(\lambda b)]$$

$$- \frac{\lambda}{k_2} B_n H_n'(\lambda\rho) H_n(\lambda b))\sin n(\phi-\phi') J_{\ell z}(\bar{r}')\} e^{jh(z-z')} \quad , \tag{4.62}$$

and

$$E^{\ell}_{2z}(\bar{r}) = -\frac{\omega\mu_2}{8\pi}\int_{S_\ell} ds' \int_{-\infty}^{\infty} dh \sum_{n=0}^{\infty} \epsilon_n \{(-\frac{jnh}{k_2^2 b} H_n(\lambda\rho)[J_n(\lambda b)+C_n H_n(\lambda b)]$$

$$+ \frac{\lambda}{k_2} B_n H_n(\lambda\rho) H_n'(\lambda b))\sin n(\phi-\phi') J_{\ell\phi}(\bar{r}')$$

$$+ (\frac{\lambda^2}{k_2^2} H_n(\lambda\rho)[J_n(\lambda b)+C_n H_n(\lambda b)])\cos n(\phi-\phi') J_{\ell z}(\bar{r}')\} e^{jh(z-z')} \quad . \tag{4.63}$$

It should be remarked that the expressions for $E^{\ell}_{2\rho}$, $E^{\ell}_{2\phi}$ and E^{ℓ}_{2z} are derived with the understanding that $b^+<\rho<\infty$. Furthermore, in carrying out the calculation of the electric fields using the Green's function according to Equations (4.3) and (4.4), the $\bar{J}_v(\bar{r}')dv'$ term has been replaced by the $\bar{J}_s(\bar{r}')ds'$ term, where $\bar{J}_v$ and $\bar{J}_s$ denote the volumetric and the surface current densities, respectively. This is necessary because the expansion modes in Ξ are surface currents. Clearly,

$$\bar{\bar{G}}_{e2}(\bar{r},\bar{r}') = \bar{\bar{G}}_{o}(\bar{r},\bar{r}') + \bar{\bar{G}}_{s2}(\bar{r},\bar{r}') = \bar{\bar{g}}_{o}^{+}(\bar{r},\bar{r}') + \bar{\bar{G}}_{s2}(\bar{r},\bar{r}') \quad , \tag{4.64}$$

where $\bar{\bar{g}}_{o}^{+}$ and $\bar{\bar{G}}_{s2}$ are expressed by Equations (3.123) and (3.125), respectively.

The fundamental definition of mutual impedance between expansion modes $\bar{J}_{\ell}$ and $\bar{J}_{m}$ is given by

$$z_{\ell m} = -\int_{S_m} \bar{E}_{2}^{\ell}(\bar{r}) \cdot \bar{J}_{m}(\bar{r})ds \quad , \quad \ell, m=1,2,\ldots,L, \tag{4.65}$$

where the limiting process $\rho \to b^{+}$ is implied. It follows from (4.56) and (4.57) that $z_{\ell m}$ can be rewritten as

$$z_{\ell m} = -\int_{S_m} [E_{2\phi}^{\ell}(\bar{r})J_{m\phi}(\bar{r}) + E_{2z}^{\ell}(\bar{r})J_{mz}(\bar{r})]ds \quad . \tag{4.66}$$

Letting $b^{+} \to b$ and defining

$$\begin{bmatrix} \tilde{J}^{s}_{\alpha\beta}(\ell,m;n,h) \\ \tilde{J}^{c}_{\alpha\beta}(\ell,m;n,h) \end{bmatrix} = \int_{S_m} ds \int_{S_\ell} ds' J_{\ell\alpha}(\bar{r}')J_{m\beta}(\bar{r}) \begin{bmatrix} \sin n(\phi-\phi') \\ \cos n(\phi-\phi') \end{bmatrix} e^{jh(z-z')}$$

$$= \int_{z_{mc}-z_m}^{z_{mc}+z_m} dz \int_{\phi_{mc}-\phi_m}^{\phi_{mc}+\phi_m} bd\phi \begin{bmatrix} \int_{z_{\ell c}-z_\ell}^{z_{\ell c}+z_\ell} dz' \int_{\phi_{\ell c}-\phi_\ell}^{\phi_{\ell c}+\phi_\ell} bd\phi' J_{\ell\alpha}(b,\phi',z')J_{m\beta}(b,\phi,z) \end{bmatrix}$$

$$\cdot \begin{bmatrix} \sin n(\phi-\phi') \\ \cos n(\phi-\phi') \end{bmatrix} e^{jh(z-z')} \quad , \tag{4.67}$$

where $\alpha = \phi,z$ and $\beta = \phi,z$, one will arrive at a general expression for $z_{\ell m}$ by substituting (4.62) and (4.63) into (4.66) as follows:

$$z_{\ell m} = + \frac{\omega\mu_2}{8\pi} \int_{-\infty}^{\infty} dh \sum_{n=0}^{\infty} \epsilon_n \{(H_n'(\lambda b)[J_n'(\lambda b) + A_n H_n'(\lambda b) + \frac{jnh}{k_2\lambda b} B_n H_n(\lambda b)] + \frac{nh}{k_2\lambda b} H_n(\lambda b) [\frac{nh}{k_2\lambda b} (J_n(\lambda b) + C_n H_n(\lambda b)) + jB_n H_n'(\lambda b)]) \tilde{J}^c_{\phi\phi}(\ell,m;n,h)$$

$$- (\frac{jnh}{k_2^2 b} H_n(\lambda b)[J_n(\lambda b)+C_n H_n(\lambda b)] - \frac{\lambda}{k_2} B_n H_n'(\lambda b) H_n(\lambda b)) \tilde{J}^s_{z\phi}(\ell,m;n,h)$$

$$+ (- \frac{jnh}{k_2^2 b} H_n(\lambda b)[J_n(\lambda b)+C_n H_n(\lambda b)] + \frac{\lambda}{k_2} B_n H_n(\lambda b) H_n'(\lambda b)) \tilde{J}^s_{\phi z}(\ell,m;n,h)$$

$$+ (\frac{\lambda^2}{k_2^2} H_n(\lambda b)[J_n(\lambda b)+C_n H_n(\lambda b)]) \tilde{J}^c_{zz}(\ell,m;n,h)\} \quad , \ell,m=1,2,\ldots L. \tag{4.68}$$

From (4.68) one can readily obtain the mutual impedance between two ϕ-polarized modes, two z-polarized modes, or two modes each with different polarization.

The remaining quantities to be calculated in order to set up the moment method solution are the elements of the voltage vector which, in the present case, are defined as follows:

$$V_\ell = \int_{V_1} \bar{E}_1^{\ell}(\bar{r}) \cdot \bar{J}_i(\bar{r}) dv \quad , \ell=1,2,\ldots,L \ , \tag{4.69}$$

where $\bar{J}_i$ denotes the excitation current source. Assuming the constant current filament model described in Chapter I for the planar slab case still holds for both the coaxial feed and the microstrip line feed, each of which joins a microstrip patch at (b,ϕ_s,z_s) with terminal current I_i, one can immediately write

$$\bar{J}_i(\bar{r}) = \hat{\rho} I_i \frac{\delta(\phi-\phi_s)\delta(z-z_s)}{\rho} \quad , \bar{r} \in V_1 \quad . \tag{4.70}$$

Making use of (4.58) and (4.70) in (4.69) will lead to

$$\begin{aligned} V_\ell = - \frac{\omega\mu_2 I_i}{8\pi} \int_{-\infty}^{\infty} dh \sum_{n=0}^{\infty} \varepsilon_n \{ & (\frac{1}{\lambda} [\gamma_n H_n'(\lambda b) + \frac{jnh}{k_2 \lambda b} f_n H_n(\lambda b)] \\ & \cdot [I(q_n,n-1) - I'(q_n,n)] + \frac{h}{k_1 \lambda} [j\tau_n H_n'(\lambda b) \\ & + \frac{nh}{k_2 \lambda b} d_n H_n(\lambda b)] I'(p_n,n)) \tilde{J}_\phi^s(\ell;\phi_s,n,h) + (\frac{jh}{k_1 k_2} d_n H_n(\lambda b) I'(p_n,n) \\ & - \frac{1}{k_2} f_n H_n(\lambda b)[I(q_n,n-1) - I'(q_n,n)]) \tilde{J}_z^c(\ell;\phi_s,n,h) \} e^{jhz_s} \quad , \ell=1,2,\ldots,L, \end{aligned} \tag{4.71}$$

where

$$\begin{aligned} \begin{bmatrix} I'(p_n,n) \\ I'(q_n,n) \end{bmatrix} &= \int_a^b \mu [J_n'(\mu\rho) + \begin{bmatrix} p_n \\ q_n \end{bmatrix} H_n'(\mu\rho)] \, d\rho \\ &= [J_n(\mu\rho) + \begin{bmatrix} p_n \\ q_n \end{bmatrix} H_n(\mu\rho)]_a^b \quad , \end{aligned} \tag{4.72}$$

$$\begin{bmatrix} I(p_n,n) \\ I(q_n,n) \end{bmatrix} = \int_a^b \mu \left[J_n(\mu\rho) + \begin{bmatrix} p_n \\ q_n \end{bmatrix} H_n(\mu\rho) \right] d\rho \quad , \tag{4.73}$$

and

$$\begin{bmatrix} \tilde{J}^c_\alpha(\ell;\phi,n,h) \\ \tilde{J}^s_\alpha(\ell;\phi,n,h) \end{bmatrix} = \int_{S_\ell} ds' J_{\ell\alpha}(b,\phi',z') \begin{bmatrix} \cos n(\phi-\phi') \\ \sin n(\phi-\phi') \end{bmatrix} e^{-jhz'}$$

$$= \int_{z_{\ell c}-z_\ell}^{z_{\ell c}+z_\ell} dz' \int_{\phi_{\ell c}-\phi_\ell}^{\phi_{\ell c}+\phi_\ell} b d\phi' J_{\ell\alpha}(b,\phi',z') \begin{bmatrix} \cos n(\phi-\phi') \\ \sin n(\phi-\phi') \end{bmatrix} e^{-jhz'} \tag{4.74}$$

with $\alpha = \phi,z$. In Equation (4.71), the integral $I(q_n,n-1)$ does not have a closed form and hence must be evaluated by numerical means. However, in the case of thin coating, where $t \ll a$, $I(q_n,n-1)$ can be approximated as

$$I(q_n,n-1) \approx \mu(b-a)[J_{n-1}(\mu a) + q_n H_{n-1}(\mu a)] + \frac{\mu^2(b-a)^2}{2} [J'_{n-1}(\mu a) + q_n H'_{n-1}(\mu a)] \quad , \tag{4.75}$$

which is obtained by integrating the two leading terms of the Taylor series of the integrand.

D. NUMERICAL EXAMPLES

The mutual coupling between two expansion dipole modes is studied in this section. Figure 4.1 shows two expansion dipole modes on the surface of the dielectric coated cylinder. Mode 1, centered at (b,0,0), has width $2w_1=2b\phi_1$ and length $2h_1=2z_1$; mode 2, centered at (b,ϕ_{2c},z_{2c}), has width $2w_2=2b\phi_2$ and length $2h_2=2z_2$. Both modes have only z-polarized currents. Past experience with the planar dielectric slab problem in Chapter II suggests that a reasonable choice of expansion modes (basis functions) is a set of piecewise sinusoids. Hence the currents of modes 1 and 2 are defined as

$$\bar{J}_\ell(\bar{r}) = \hat{z}J_{\ell z}(\bar{r}) = \begin{cases} \hat{z}\,\dfrac{\sin[\kappa_\ell(z_\ell-|z-z_{\ell c}|)]}{2b\phi_\ell\sin(\kappa_\ell z_\ell)} & , \bar{r}\in S_\ell \\ 0 & , \text{elsewhere} \end{cases} , \tag{4.76}$$

where $S_\ell=\{\bar{r}=(b,\phi,z):|\phi-\phi_{\ell c}|<\phi_\ell\ ,\ |z-z_{\ell c}|<z_\ell\}$, $\ell=1,2$, and (referring to Equations (2.65) and (2.66))

$$\kappa_\ell = \omega\sqrt{\mu_2\tilde{\varepsilon}_\ell} \quad , \tag{4.77}$$

with

$$\tilde{\varepsilon}_\ell = \varepsilon_2\left[\frac{\varepsilon_r+1}{2} + \left(\frac{\varepsilon_r-1}{2}\right)\left(1+\frac{10t}{2b\phi_\ell}\right)^{-1/2}\right] . \tag{4.78}$$

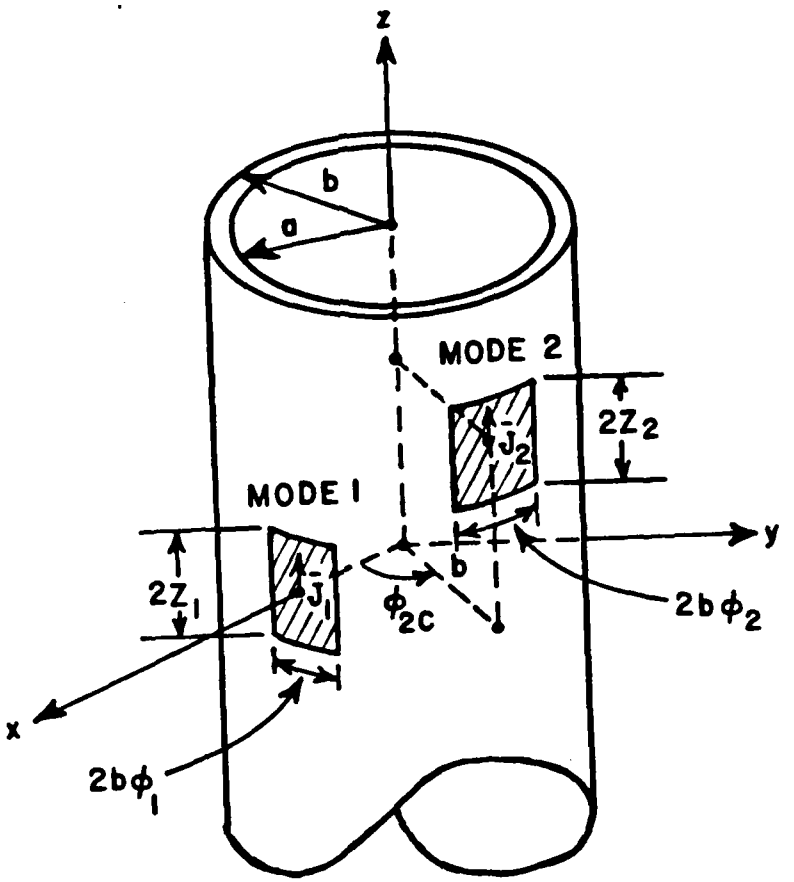

Figure 4.1. Two z-polarized dipole modes on the surface of a dielectric coated cylinder.

It then follows from Equation (4.67) that, for $\ell=1$, $m=2$,

$$\tilde{J}^{c}_{\phi\phi}(1,2;n,h) = \tilde{J}^{s}_{z\phi}(1,2;n,h) = \tilde{J}^{s}_{\phi z}(1,2;n,h) = 0 \quad , \tag{4.79}$$

and

$$\tilde{J}^{c}_{zz}(1,2;n,h) =$$

$$\int_{z_{2c}-z_2}^{z_{2c}+z_2} dz \int_{\phi_{2c}-\phi_2}^{\phi_{2c}+\phi_2} bd\phi \int_{-z_1}^{z_1} dz' \int_{-\phi_1}^{\phi_1} bd\phi' J_{1z}(b,\phi',z') J_{2z}(b,\phi,z)$$

$$\cdot \cos n(\phi-\phi') e^{jh(z-z')}$$

$$= \frac{4\kappa_1\kappa_2}{\phi_1\phi_2 \sin(\kappa_1 z_1)\sin(\kappa_2 z_2)} \frac{\sin(n\phi_1)}{n} \frac{\sin(n\phi_2)}{n} \cos(n\phi_{2c}) \tilde{Z}_1(h) \tilde{Z}_2(h)$$

$$\cdot e^{jhz_{2c}} \quad , \tag{4.80}$$

where

$$\tilde{Z}_\ell(h) = \frac{\cos(hz_\ell) - \cos(\kappa_\ell z_\ell)}{(\kappa_\ell^2 - h^2)} \quad , \ \ell=1,2 \quad . \tag{4.81}$$

Substituting (4.79) and (4.80) into (4.68), with $\ell=1$, $m=2$, and recognizing that the integrand, excluding $e^{jhz_{2c}}$, is an even function of h yield

$$Z_{12} = A_{12} \int_0^\infty dh \sum_{n=0}^{\infty} \varepsilon_n W(n,h) \frac{\sin(n\phi_1)}{n} \frac{\sin(n\phi_2)}{n}$$

$$\cdot \cos(n\phi_{2c}) \cos(hz_{2c}) \tilde{Z}_1(h)\tilde{Z}_2(h) \quad , \tag{4.82}$$

where

$$A_{12} = \frac{\omega\mu_2 \kappa_1\kappa_2}{\pi k_2^2 \phi_1 \phi_2 \sin(\kappa_1 z_1)\sin(\kappa_2 z_2)} \quad , \tag{4.83}$$

$$W(n,h) = \lambda^2 H_n(\lambda b)[J_n(\lambda b) + C_n H_n(\lambda b)] \quad . \tag{4.84}$$

Recalling the definition of C_n in (3.110), one can rewrite W(n,h) as

$$W(n,h) = \left(\frac{j2}{\pi b}\right) \left(\frac{k_2}{k_1}\right)^2 \mu^2 \frac{1}{[X_2(n,h) - X_3(n,h)/X_1(n,h)]} \quad , \tag{4.85}$$

where

$$X_1(n,h) = -\mu \frac{Q_n}{T_n} + \left(\frac{\mu_2}{\mu_1}\right) \frac{\mu^2}{\lambda} r_n \quad , \tag{4.86}$$

$$X_2(n,h) = -\left(\frac{\mu_2}{\mu_1}\right) \mu \frac{P_n}{S_n} + \left(\frac{k_2}{k_1}\right)^2 \frac{\mu^2}{\lambda} r_n \quad , \tag{4.87}$$

$$X_3(n,h) = \left(\frac{\mu_2}{\mu_1}\right)\left(\frac{nh}{k_1 b}\right)^2 \left[1 - \left(\frac{\mu}{\lambda}\right)^2\right]^2 \quad , \tag{4.88}$$

$$\Gamma_n = \frac{H_n'(\lambda b)}{H_n(\lambda b)} \quad , \tag{4.89}$$

$$P_n = J_n'(\mu b) - \frac{J_n(\mu a)}{H_n(\mu a)} H_n'(\mu b) \quad , \tag{4.90}$$

$$Q_n = J_n'(\mu b) - \frac{J_n'(\mu a)}{H_n'(\mu a)} H_n'(\mu b) \quad , \tag{4.91}$$

$$S_n = J_n(\mu b) - \frac{J_n(\mu a)}{H_n(\mu a)} H_n(\mu b) \quad , \tag{4.92}$$

$$T_n = J_n(\mu b) - \frac{J_n'(\mu a)}{H_n'(\mu a)} H_n(\mu b) \quad , \tag{4.93}$$

and

$$\lambda = \sqrt{k_2^2 - h^2} \quad , \quad \mu = \sqrt{k_1^2 - h^2} \quad , \text{ with } \mathrm{Re}\begin{vmatrix} \lambda \\ \mu \end{vmatrix} > 0, \ \mathrm{Im}\begin{vmatrix} \lambda \\ \mu \end{vmatrix} > 0 \quad . \tag{4.94}$$

It may be assumed that $\mu_1 = \mu_2$ without much to the loss of generality. In the evaluation of z_{12} in (4.82), there are several critical points that need special attention, namely:

a. It is computationally more efficient to perform summation over n before integration over the h variable. This is due to the fact that the sequence of cylinder functions

$$\{J_n(\xi), J_n'(\xi), H_n(\xi), H_n'(\xi)\}_0^N$$

can be generated efficiently for $\xi = \mu a$, μb, and λb. N is the maximum index number which, as indicated in Appendix I, is dictated by the

dynamic range of the computer being used to compute the sequence. The number of terms summed in the series of (4.82) can be determined by considering the well-known series:

$$S = \sum_{n=1}^{\infty} \frac{1}{n^2} = \frac{\pi^2}{6} \quad . \tag{4.95}$$

Supposing $\delta>0$ is an error threshold, there will exist an integer N_{max} such that

$$S - \sum_{n=1}^{N_{max}} \frac{1}{n^2} < \delta \quad . \tag{4.96}$$

It is clear that using N_{max} as the terminating index value for the series in (4.82) will also satisfy the same error criterion in the sense of (4.96) since the the tail end of the series is dominated by $\sum_{N_{max}}^{\infty} 1/n^2$ In general, N is no greater than N_{max}. The evaluation of W(n,h), for $0\leq n\leq N$, is straight-forward provided the sequence

$$\{J_n(\xi), J_n'(\xi), H_n(\xi), H_n'(\xi)\}_0^N$$

has been calculated. The calculation of this sequence of cylinder functions is discussed in Appendix I which also deals with the case as $Im\xi\to\infty$.

As for $N<n\leq N_{max}$, the evaluation of W(n,h) requires two separate treatments:

1. When $|\xi-n|>n^{1/3}$, the Debye's asymptotic approximations of $J_n(\xi)$, $J_n'(\xi)$, $H_n(\xi)$, and $H_n'(\xi)$ are valid and can be used to reduce the burden to computing W(n,h). More specifically, one can write

$$H_n^{(\frac{1}{2})}(\xi) \sim e^{\pm\phi_n(\xi)}\, g_n^{(\frac{1}{2})}(\xi) \quad , \tag{4.97}$$

where

$$\phi_n(\xi) = n(\tanh\gamma - \gamma) - j\frac{\pi}{4} \quad , \tag{4.98}$$

$$g_n^{(\frac{1}{2})}(\xi) = \sqrt{\frac{1}{\frac{-j\pi}{2}\, n \tanh\gamma}} \left[1 \pm \frac{.5A_1}{\frac{n}{2}\tanh\gamma} + \frac{.75A_2}{\left(\frac{n}{2}\tanh\gamma\right)^2} + \cdots \right] , \tag{4.99}$$

$$A_1 = \frac{1}{8} - \frac{5}{24}\coth^2\gamma \quad , \tag{4.100}$$

$$A_2 = \frac{3}{128} - \frac{77}{576}\coth^2\gamma + \frac{385}{3456}\coth^4\gamma \quad , \tag{4.101}$$

and

$$\cosh\gamma = \frac{n}{\xi} \quad . \tag{4.102}$$

Directly differentiating $H_n^{(\frac{1}{2})}(\xi)$ with respect to ξ yields

$$H_n^{(\frac{1}{2})'}(\xi) = \frac{d}{d\xi} H_n^{(\frac{1}{2})}(\xi) = e^{\pm\phi_n(\xi)} \left[g_n^{(\frac{1}{2})'}(\xi) \pm \phi_n'(\xi)\, g_n^{(\frac{1}{2})}(\xi) \right] , \tag{4.103}$$

where

$$\phi_n'(\xi) = \frac{d}{d\xi}\,\phi_n(\xi) = \sinh\gamma \quad , \tag{4.104}$$

and

$$g_n^{(2)'}(\xi) = \frac{d}{d\xi}\,g_n^{(2)}(\xi)$$

$$= \frac{1}{2\xi\sinh^2\gamma\sqrt{-\frac{j\pi}{2}\,n\tanh\gamma}}\left[\left[1 \pm \frac{.5A_1}{\frac{n}{2}\tanh\gamma} + \frac{.75A_2}{\left(\frac{n}{2}\tanh\gamma\right)^2}\right]\right.$$

$$+ \left[\pm\frac{1}{4n}\left(\coth\gamma - 5\coth^3\gamma\right) + \frac{3}{8n^2}\left(\frac{3}{4}\coth^2\gamma - \frac{77}{9}\coth^4\gamma\right.\right.$$

$$\left.\left.\left.+ \frac{385}{36}\coth^6\gamma\right)\right]\right] \quad . \tag{4.105}$$

The asymptotic approximations of $J_n(\xi)$ and $J_n'(\xi)$ are naturally derived from the relation that $J_n(\xi) = \frac{1}{2}[H_n^{(1)}(\xi) + H_n^{(2)}(\xi)]$.

2. When $|\xi-n|<n^{1/3}$, the so-called transition region, the asymptotic approxmations of $J_n(\xi)$, $H_n(\xi)$ and their corresponding derivatives take on different forms which are described in [26] and will not be repeated here. It may be noted that in this region, both n and ξ are sufficiently large. Again employing these approximations to compute W(n,h) will significantly improve the efficiency.

As a consequence, it is convinced that the mutual impedance between mode 1 and mode 2 is reasonably approximated by

$$z_{12} \simeq A_{12} \int_0^{\infty} dh \sum_{n=0}^{N_{max}} \epsilon_n W(n,h) \frac{\sin(n\phi_1)}{n} \frac{\sin(n\phi_2)}{n}$$

$$\cdot \cos(n\phi_{2c}) \cos(hz_{2c}) \cdot \tilde{Z}_1(h)\tilde{Z}_2(h) \quad . \qquad (4.106)$$

b. Appendix G suggests that condition (4.94) will restrict the contour of integration to the fourth quadrant in the complex h-plane. In Figure 4.2, the broken lines denote the appropriate branch cuts starting from the branch point $h=k_2(-k_2)$ going to $h=0$ on the real axis and then to $h=j\infty(-j\infty)$. Quite significantly, Appendix H indicates that both P_n/S_n and Q_n/T_n are odd functions of μ. Hence, it follows from (4.85)-(4.87) that $W(n,h)$ is an even function of μ. Thus no branch cut is required for the square root function μ, i.e., k_1 is not a branch point.

c. There is at least one pole for each n on or above the real h-axis (depending on lossless or lossy dielectric) between $h=k_2$ and $h=\mathrm{Re}k_1$. The original integral for z_{12} in (4.106) can be computed along the contour Γ which runs along the real h-axis and overpasses the the poles with infinitesimal half circles as shown in Figure 4.2. Such contour requires the knowledge of the pole for each n, $0 \leq n \leq N_{max}$. To avoid the numerical burden of locating these singular points, it is computationally more suitable, and justifiable by Cauchy's theory as

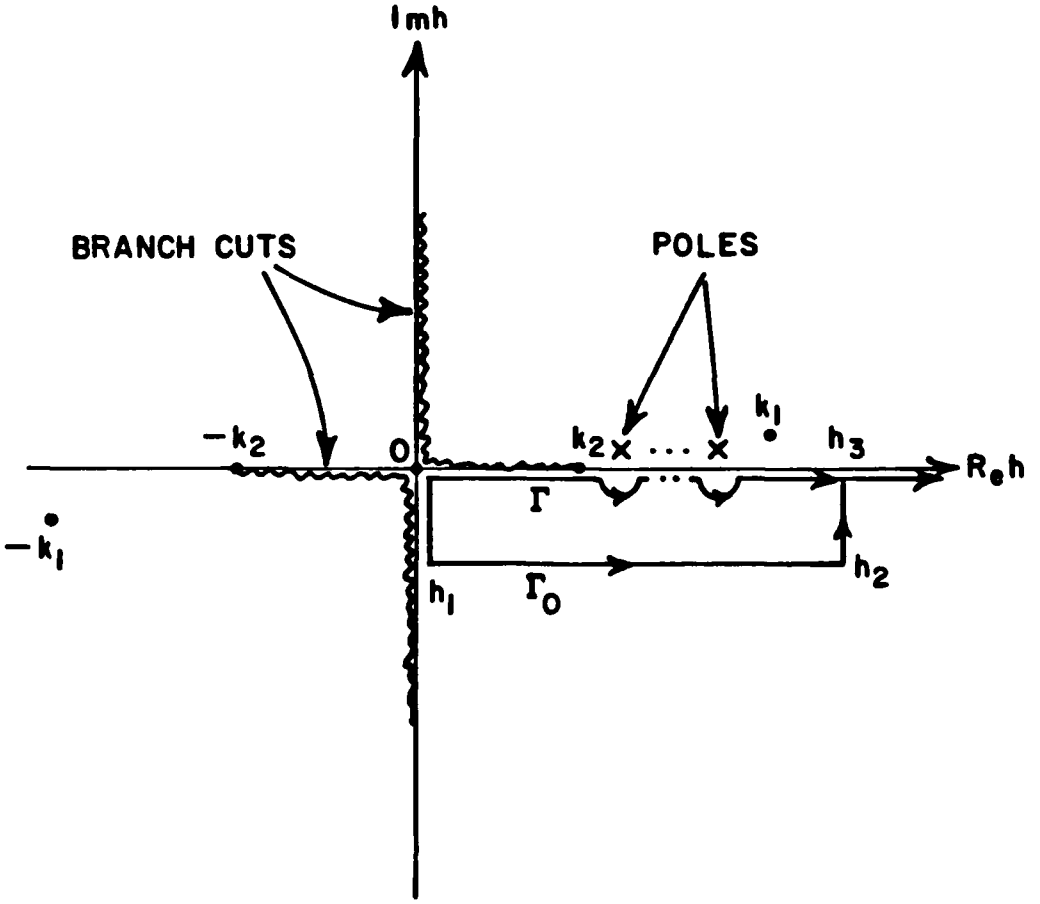

Figure 4.2. Proper contours of integration and branch cuts in the complex h-plane.

well, to use the deformed contour Γ_0 which starts from h=0 going down the negative imaginary axis to some point $h=h_1$ sufficiently away from the singularities. Next Γ_0 moves parallel to the real axis to some point $h=h_2$, with $\mathrm{Re}h_2>\mathrm{Re}k_1$, then travels vertically upward to meet the real axis at $h=h_3$. The final segment of Γ_0 extends from h_3 to $h=\infty$. The contour Γ_0 is also shown in Figure 4.2. It should be cautioned that one cannot let $\mathrm{Im}h_1$ become too negative since then the cosine functions in (4.106) (e.g., $\cos(hz_\ell)$ and $\cos(hz_{\ell c})$, $\ell=1,2$) become exponentially large. This will unfortunately cause numerical difficulty in accurately evaluating z_{12} which is typically very small.

d. The integral in (4.106) can be evaluated in three stages as symbolically written below:

$$z_{12} \simeq \int_0^{H_1} Q\, dh + \int_{H_1}^{H_2} Q\, dh + \int_{H_2}^{\infty} Q\, dh \quad , \tag{4.107}$$

where $H_2>H_1>\mathrm{Re}k_1$ and

$$Q(h) = A_{12} \sum_{n=0}^{N_{max}} \varepsilon_n W(n,h) \frac{\sin(n\phi_1)}{n} \frac{\sin(n\phi_2)}{n}$$

$$\cdot \cos(n\phi_{2c}) \cos(hz_{2c}) \tilde{Z}_1(h) \tilde{Z}_2(h) \quad . \tag{4.108}$$

Stage 1 refers to the integration from h=0 to $h=H_1$. The upper limit H_1 is chosen such that

$$\left|\sqrt{k_2^2 - H_1^2}\right| > N_{max} \text{ and } \left|\sqrt{k_2^2 - H_1^2} - N_{max}\right| > N_{max}^{1/3} \quad . \tag{4.109}$$

The integration is done numerically using Simpson's quadrature rule.

Stage 2 refers to the integration from $h=H_1$ to $h=H_2$. Because of condition (4.109), for all $h>H_1$, the function $W(n,h)$ can be greatly simplified by replacing the cylinder functions with their Debye asymptotic forms. Taking the leading term in (4.99) and substituting γ by $j\gamma$, one can deduce from (4.97) and (4.103) that

$$H_n^{(\frac{1}{2})}(\xi) \sim \sqrt{\frac{2}{\pi\xi\sin\gamma}}\, e^{\pm j[\xi(\sin\gamma-\gamma\cos\gamma)-\pi/4]} \quad , \tag{4.110}$$

and

$$H_n^{(\frac{1}{2})'}(\xi) = \frac{d}{d\xi} H_n^{(\frac{1}{2})}(\xi) \sim \pm\, j\sin\gamma H_n^{(\frac{1}{2})}(\xi) \quad , \tag{4.111}$$

where $\gamma(n,\xi)$ is defined by $\cos\gamma = n/\xi$. It readily follows that

$$\frac{H_n^{(1)}(\xi)}{H_n^{(2)}(\xi)} \sim e^{j2[\xi(\sin\gamma-\gamma\cos\gamma)-\pi/4]} \quad , \tag{4.112}$$

$$\frac{H_n^{(1)'}(\xi)}{H_n^{(2)'}(\xi)} \sim -\, e^{j2[\xi(\sin\gamma-\gamma\cos\gamma)-\pi/4]} \quad , \tag{4.113}$$

and

$$\gamma(n,\xi) = -j\ln\left[\frac{n}{\xi} + j\sqrt{1-\left(\frac{n}{\xi}\right)^2}\right] \quad . \tag{4.114}$$

Employing (4.112) - (4.114) will enable one to obtain

$$\frac{P_n}{S_n} \sim j\sin\gamma(n,\mu b)\,\frac{e^{\chi}+1}{e^{\chi}-1} \quad , \tag{4.115}$$

$$\frac{Q_n}{T_n} \sim j\sin\gamma(n,\mu b)\,\frac{e^{\chi}-1}{e^{\chi}+1} \quad , \tag{4.116}$$

where

$$\chi = j2\{\mu b[\sin\gamma(n,\mu b)-\gamma(n,\mu b)\cos\gamma(n,\mu b)] - \mu a[\sin\gamma(n,\mu a)-\gamma(n,\mu a)\cos\gamma(n,\mu a)]\} \quad . \tag{4.117}$$

It is now quite apparent that these asymptotic forms will reduce the complexity of $W(n,h)$ many folds.

Finally, Stage 3 refers to the integration from $h=H_2$ to $h=\infty$. H_2 can be chosen so that $\lambda \approx \mu \approx jh$ and $|\xi| >> n$, with $\xi=\mu a$, μb or λb. Consequently one sees that $\gamma(n,\xi)\approx\pi/2$, $\cos\gamma(n,\xi)\approx 0$, and $\sin\gamma(n,\xi)\approx 1$. One can further approximate that $P_n/S_n \approx -j$, $Q_n/T_n \approx -j$ and $r_n \approx j$. All these approximations greatly simplify $W(n,h)$ to

$$\tilde{W}(h) = \frac{j2h}{\pi b(1+\varepsilon_r)} \quad , \tag{4.118}$$

which is independent of n. In addition, noting that

$$\tilde{Z}_1(h) \simeq -\frac{\cos(hz_1)-\cos(\kappa_1 z_1)}{h^2} \quad , \tag{4.119}$$

$$\tilde{Z}_2(h) \simeq -\frac{\cos(hz_2)-\cos(\kappa_2 z_2)}{h^2} \quad , \tag{4.120}$$

and making use of trigonometric identities, one can write

$$\int_{H_2}^{\infty} Q(h)dh \simeq \frac{j2A_{12}}{\pi b(1+\varepsilon_r)} \sum_{n=0}^{N_{max}} \varepsilon_n \frac{\sin(n\phi_1)}{n} \frac{\sin(n\phi_2)}{n} \cos(n\phi_{2c}) \sum_{\ell=1}^{9} I_\ell \quad , \tag{4.121}$$

where

$$I_\ell = a_\ell \int_{H_2}^{\infty} \cos(b_\ell h) \frac{dh}{h^3} \quad , \ \ell=1,2,\ldots,9 \quad , \tag{4.122}$$

with

$$a_1 = \frac{1}{4} \ , \ b_1 = \left| |z_1-z_2| - z_{2c} \right| \quad , \tag{4.123}$$

$$a_2 = \frac{1}{4} \ , \ b_2 = \left| |z_1-z_2| + z_{2c} \right| \quad , \tag{4.124}$$

$$a_3 = \frac{1}{4} \ , \ b_3 = |z_1+z_2-z_{2c}| \quad , \tag{4.125}$$

$$a_4 = \frac{1}{4} \ , \ b_4 = z_1+z_2+z_{2c} \quad , \tag{4.126}$$

$$a_5 = -\frac{\cos(\kappa_1 z_1)}{2} \ , \ b_5 = |z_2-z_{2c}| \quad , \tag{4.127}$$

$$a_6 = -\frac{\cos(\kappa_1 z_1)}{2} \ , \ b_6 = z_2+z_{2c} \quad , \tag{4.128}$$

$$a_7 = -\frac{\cos(\kappa_2 z_2)}{2} \ , \ b_7 = |z_1-z_{2c}| \quad , \tag{4.129}$$

$$a_8 = -\frac{\cos(\kappa_2 z_2)}{2} \ , \ b_8 = z_1+z_{2c} \quad , \tag{4.130}$$

$$a_9 = \cos(\kappa_1 z_1)\cos(\kappa_2 z_2) \ , \ b_9 = z_{2c} \ . \tag{4.131}$$

Finally, employing an integration by parts, one can verify that, for $\ell=1,2,\ldots,9$,

$$\int_{H_2}^{\infty} \cos(b_\ell h)\,\frac{dh}{h^3} = \begin{cases} \dfrac{1}{2H_2^2} & , \ b_\ell = 0 \\ \dfrac{1}{2H_2}\left[\dfrac{\cos(b_\ell H_2)}{H_2} - b_\ell \sin(b_\ell H_2)\right] + \dfrac{H_2^2}{2}\,ci(b_\ell H_2), & b_\ell \neq 0 \end{cases} \tag{4.132}$$

where

$$ci(b_2H_2) \triangleq -\int_{b_2H_2}^{\infty} \frac{\cos t}{t}\, dt \qquad (4.133)$$

is known as the cosine integral.

For illustration purposes, two numerical examples of coupling between identical expansion modes are considered using the theory developed in this section.

Example 1: E-plane coupling

The geometry of this example consists of two identical modes, of length L = 0.15 m. and width W = 0.075 m., on a coated cylinder of radius a and dielectric coating of thickness t = 0.003175 m. with $\phi_{1c} = \phi_{2c} = 0$ and $z_{1c} = 0$. The separation, $S = z_{2c}$, between the modes varies in the z-direction only. The operating frequency is 633 MHz, with $\varepsilon_r = 2.56$ and $\tan\delta = 0.0015$.

In Table 4.1, results are given for the self impedance of a single expansion mode (z_{11}) on cylinders of various radii. It is evident that z_{11} converges to the infinite dielectric slab value as the cylinder becomes large. This is a good indication that the theory and analysis techniques presented here are valid. Table 4.1 also shows the convergence of the summing series (N_{max}), the contour of integration Γ_o (h_1 and h_3) and the limits of the three stages of integration (H_1 and H_2).

TABLE 4.1

SELF IMPEDANCE OF A SINGLE EXPANSION MODE

Radius a (λ_0)	Self Impedance z_{11} (volt-amp.)	N_{max}	h_1	h_3	H_1	H_2
0.25	0.145-j0.429	62	-j0.2	3.0	50.0	70.0
0.5	0.118-j0.422	121	-j0.1	3.0	50.0	70.0
1.0	0.104-j0.418	240	-j0.15	3.0	50.0	70.0
3.0	0.0957-j0.415	717	-j0.1	3.0	50.0	80.0
10.0	0.092-j0.419	1998	-j0.05	3.0	55.0	70.0
∞	0.092-j0.399	-	-	-	-	-

Note: λ_0 = free space wavelength = 0.474 (m).

Mutual impedance (z_{12}) of the expansion modes is plotted in Figure 4.3 as a function of separation between the modes for cylinders of radii $a = 0.25\lambda_0$, $0.5\lambda_0$, $1.\lambda_0$ and $10\lambda_0$, where λ_0 denotes the free space wavelength. It is seen that the coupling rapidly weakens for $S>0.3\lambda_0$. Generally this is in agreement with the planar dielectric slab case studied in Chapter II. It is interesting to observe that the degree of coupling between two expansion modes in the E-plane configuration varies slightly among cylinders of different radii. This leads one to conclude that the curvature of the cylindrical surface has little effect on the energy propagating in the z-direction as surface wave modes. The values of z_{12} are also listed in Table 4.2.

Example 2: H-plane coupling

This example repeats the data of Example 1 except that $z_{1c}=z_{2c}=0$, $\phi_{1c}=0$, and $S=b\phi_{2c}$ is the separation between the expansion modes which varies in the ϕ-direction only.

The results are plotted in Figure 4.4 and tabulated in Table 4.3. It is apparent that the coupling in the H-plane configuration gradually reduces as the radius of the cylinder increases. This can be explained by the fact that waves propagating circumferentially shed more energy into the surrounding space when the curvature is large. One may notice that, in the $a=0.25\lambda_0$ case, coupling is reinforced at $S=1\lambda_0$ which is close to the back side of the cylinder relative to expansion mode 1. This is due to the fact that waves which originate from mode 1 and

TABLE 4.2

MUTUAL IMPEDANCE BETWEEN TWO IDENTICAL EXPANSION MODES

IN THE E-PLANE

S (λ_o)	MUTUAL IMPEDANCE z_{12} (volt-amp.)			
	$a=0.25\lambda_o$	$a=0.5\lambda_o$	$a=1.0\lambda_o$	$a=10.0\lambda_o$
0.1	0.119-j7.528	0.095-j7.491	0.082-j7.472	-
0.25	0.068-j5.578	0.055-j5.555	0.048-j5.542	0.041-j5.523
0.32	0.0504-j.1981	0.04331-j.2028	0.03894-j.2037	-
0.4	0.023+j0.016	0.023+j0.007	0.022+j0.002	-
0.5	-0.005+j0.026	0.001+j.020	0.005+j0.015	0.006+j0.014
0.6	-0.021+j0.014	-0.013-j0.013	-0.009+j0.014	-
0.75	-0.020-j0.010	-0.016-j0.004	-0.014-j0.002	-0.011+j0.001
0.9	-0.002-j0.021	-0.004-j0.014	-0.004-j0.010	-
1.0	0.011-j0.016	0.005-j0.013	0.001-j0.009	0.0-j0.008

Note: λ_o = free space wavelength = 0.474 (m).

S = separation.

TABLE 4.3

MUTUAL IMPEDANCE BETWEEN TWO IDENTICAL EXPANSION MODES IN THE H-PLANE

S (λ_o)	MUTUAL IMPEDANCE z_{12} (volt-amp.)			
	$a=0.25\lambda_o$	$1=0.5\lambda_o$	$a=1.0\lambda_o$	$a=10.0\lambda_o$
0.1	0.1197-j0.4498	0.0991-j0.4519	0.08764-j0.4518	0.07961-j0.4512
0.25	0.06073-j0.05278	0.06021-j0.06751	0.05874-j0.07717	0.05693-j0.08243
0.32	0.03693-j0.00761	0.04289-j0.01818	0.04601-j0.02627	0.04538-j0.03098
0.4	0.01658+j0.007368	0.02515+j0.003735	0.02938+j0.000538	0.03318-j0.005387
0.5	0.002758+j0.007499	0.008558+j0.009884	0.01318+j0.01137	0.01925+j0.00874
0.6	-0.001596+j0.003122	-0.000127+j0.007564	0.002039+j0.01123	0.006643+j0.01124
0.75	-0.001627-j0.0006864	-0.003136+j0.001345	-0.00341+j0.00416	-0.003417+j0.008018
0.9	-0.001806-j0.0002059	-0.001278-j0.001153	-0.002807-j0.001194	-0.005704+j0.000997
1.0	-0.001728+j0.002626	-0.0000698-j0.000988	-0.000695-j0.00214	-0.004252-j0.001236

Note: λ_o = free space wavelength = 0.474 (m).
S = separation.

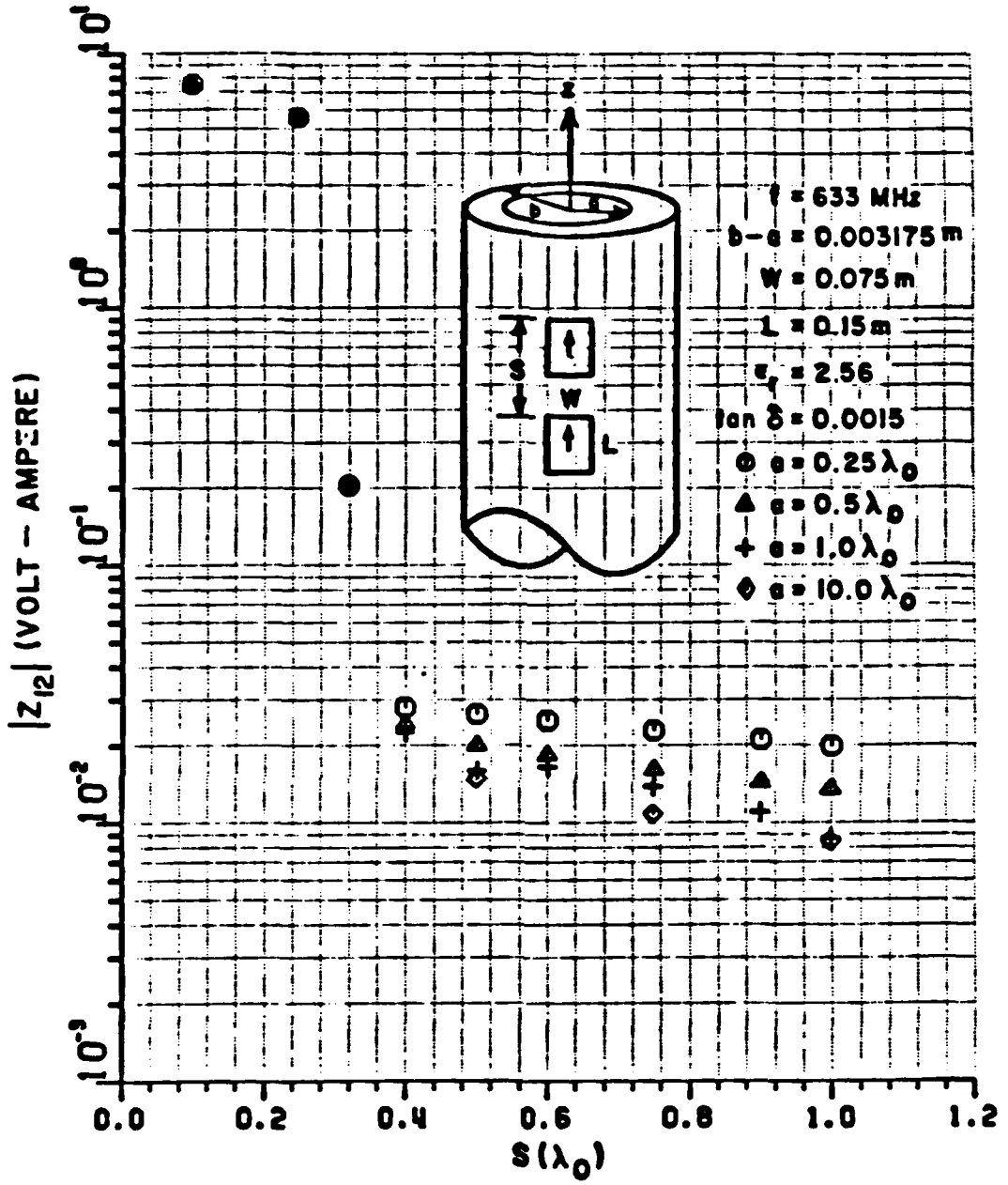

Figure 4.3. E-plane coupling for identical expansion modes on coated cylinders of radii a = $0.25\lambda_0$, $0.5\lambda_0$, $1.\lambda_0$ and $10.\lambda_0$ (λ_0 = 0.474 m.).

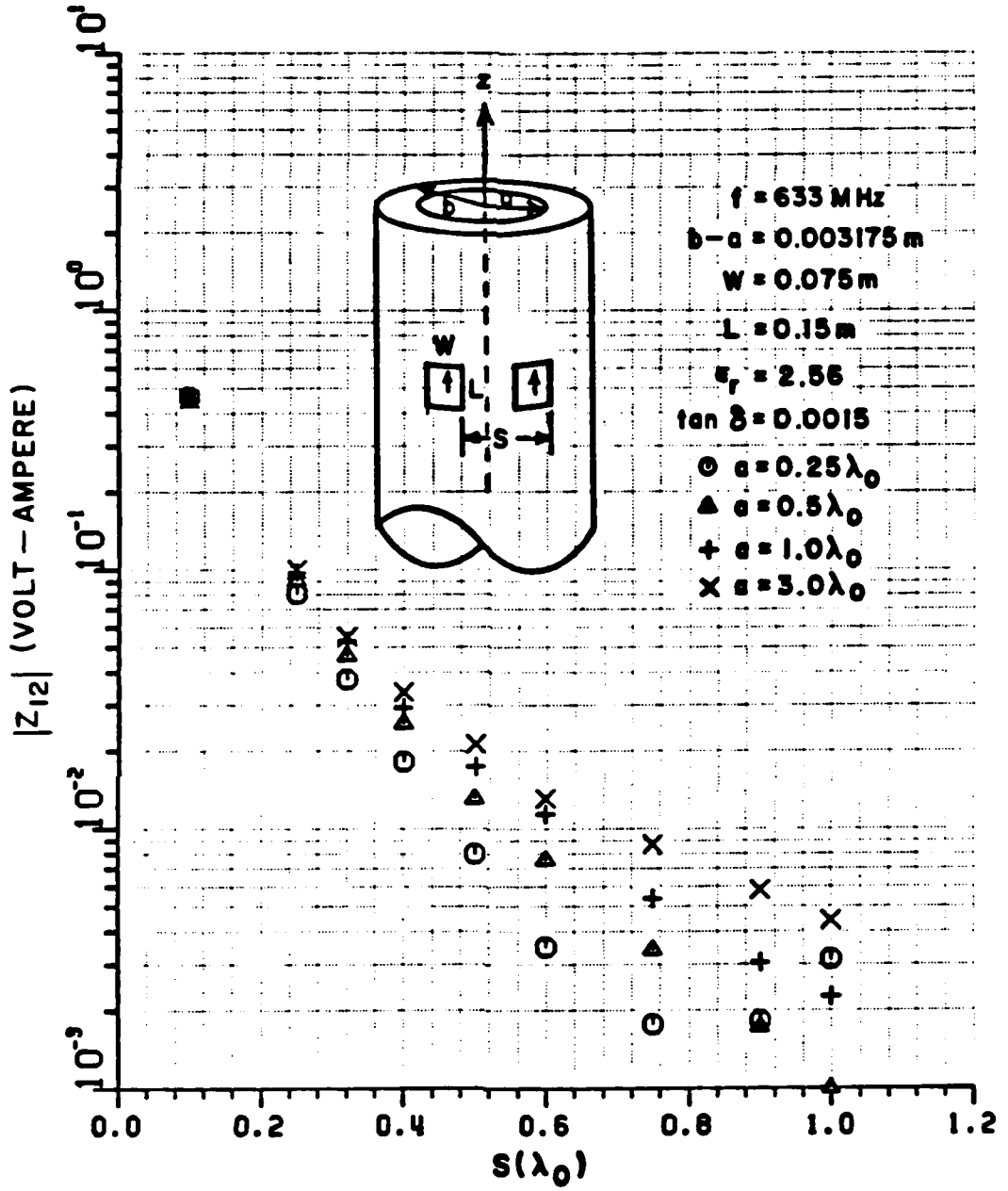

Figure 4.4. H-plane coupling for identical expansion modes on coated cylinders of radii a = $0.25\lambda_0$, $0.5\lambda_0$, $1.\lambda_0$ and $3.\lambda_0$ (λ_0 = 0.474 m.).

propagate circumferentially in opposite directions interact more strongly when the paths of propagation are short (as for the case of small cylinders), and weakly when the paths of propagation are long (as for the case of large cylinders) because of the loss of energy along the paths.

Figures 4.5 to 4.7 show that E-plane coupling is in general stronger than that of H-plane. This is also attributed to the shedding of energy away from the surface of the coated cylinder by the circumferentially propagating waves. Even though there is no curvature effect, it is interesting to recall that the H-plane coupling is also weaker than the E-plane coupling in the case of the planar structure.

E. FAR FIELD CALCULATION

If the current distribution $\bar{J}(\bar{r}') = \hat{\phi}' J_{\phi'}(\bar{r}') + \hat{z} J_{z'}(\bar{r}')$ is known for a microstrip antenna, then the field can be computed for an arbitrary $\bar{r} \in V_2$. In practice, it is of great interest to know the radiation pattern of the antenna. To this end, this section will derive a general expression via the method of steepest descent to facilitate the far field calculation.

By studying Equations (4.61) to (4.63), it becomes apparent that any electric field component, due to $\bar{J}$, can be expressed in the following form:

$$\sum_{n=0}^{\infty} \varepsilon_n \, T(\bar{r},n) \quad ,$$

where

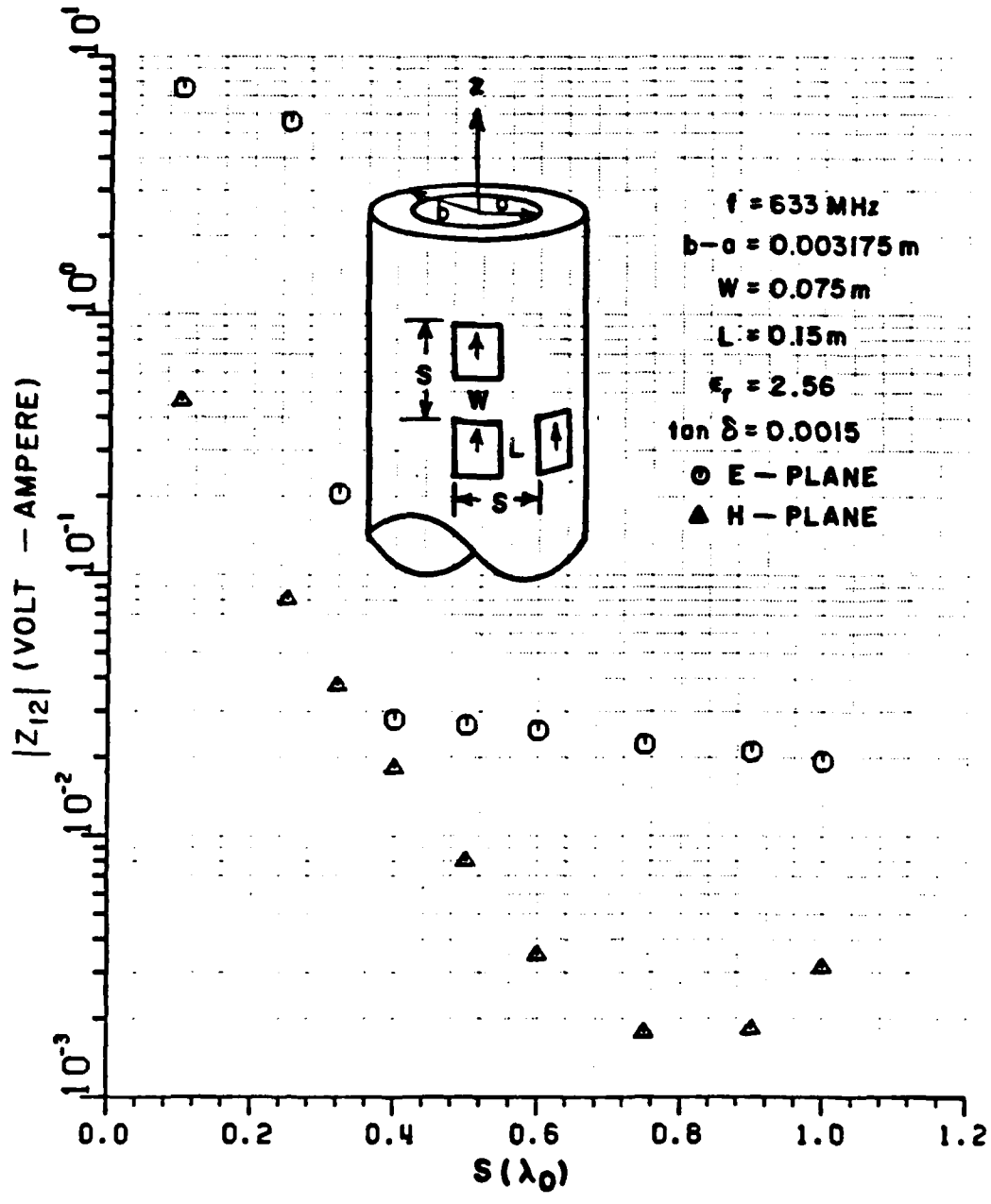

Figure 4.5. Coupling for identical expansion modes on a coated cylinder of radius a = $0.25\lambda_0$ (λ_0 = 0.474 m.).

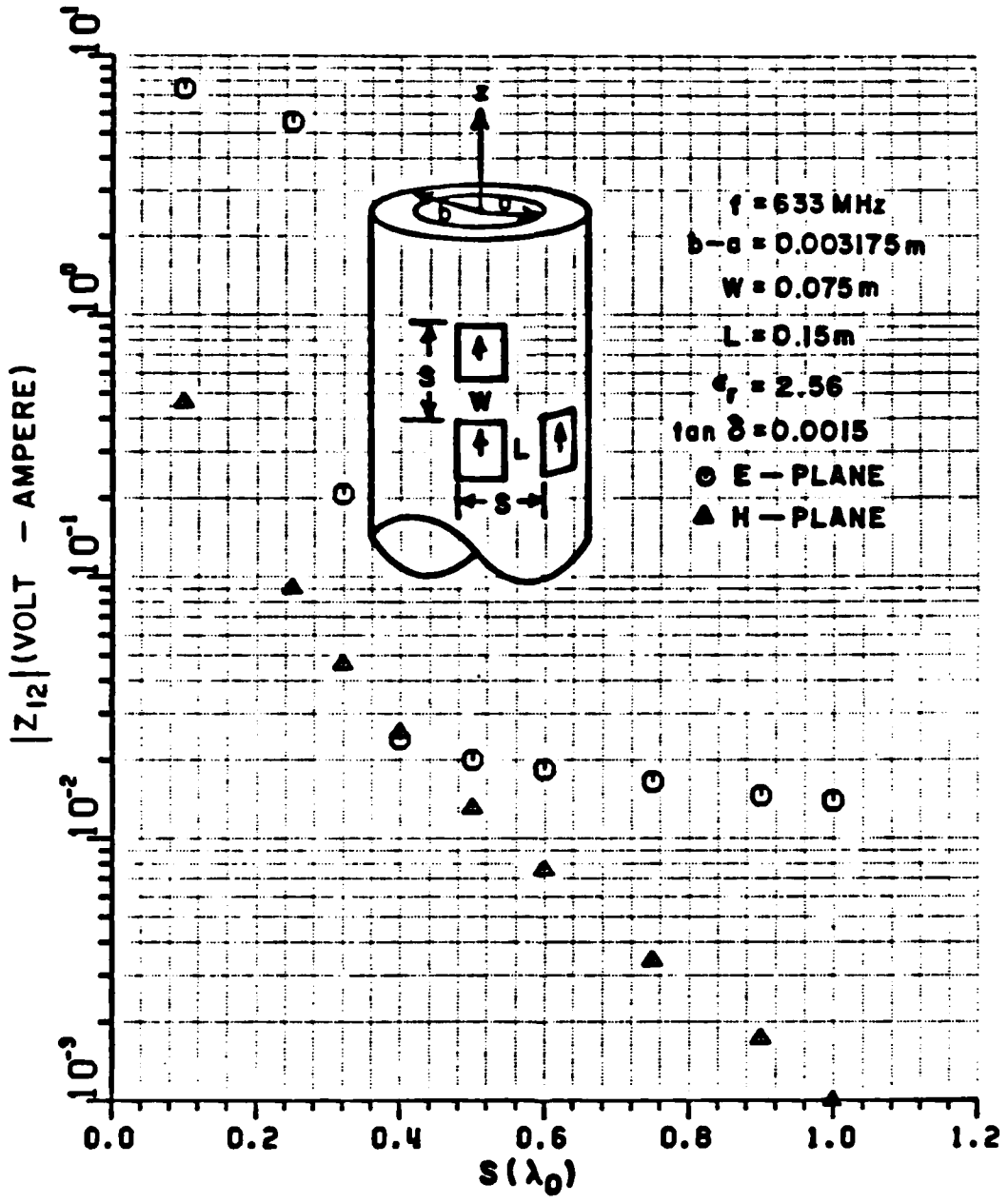

Figure 4.6. Coupling for identical expansion modes on a coated cylinder of radius a = $0.5\lambda_0$ (λ_0 = 0.474 m.).

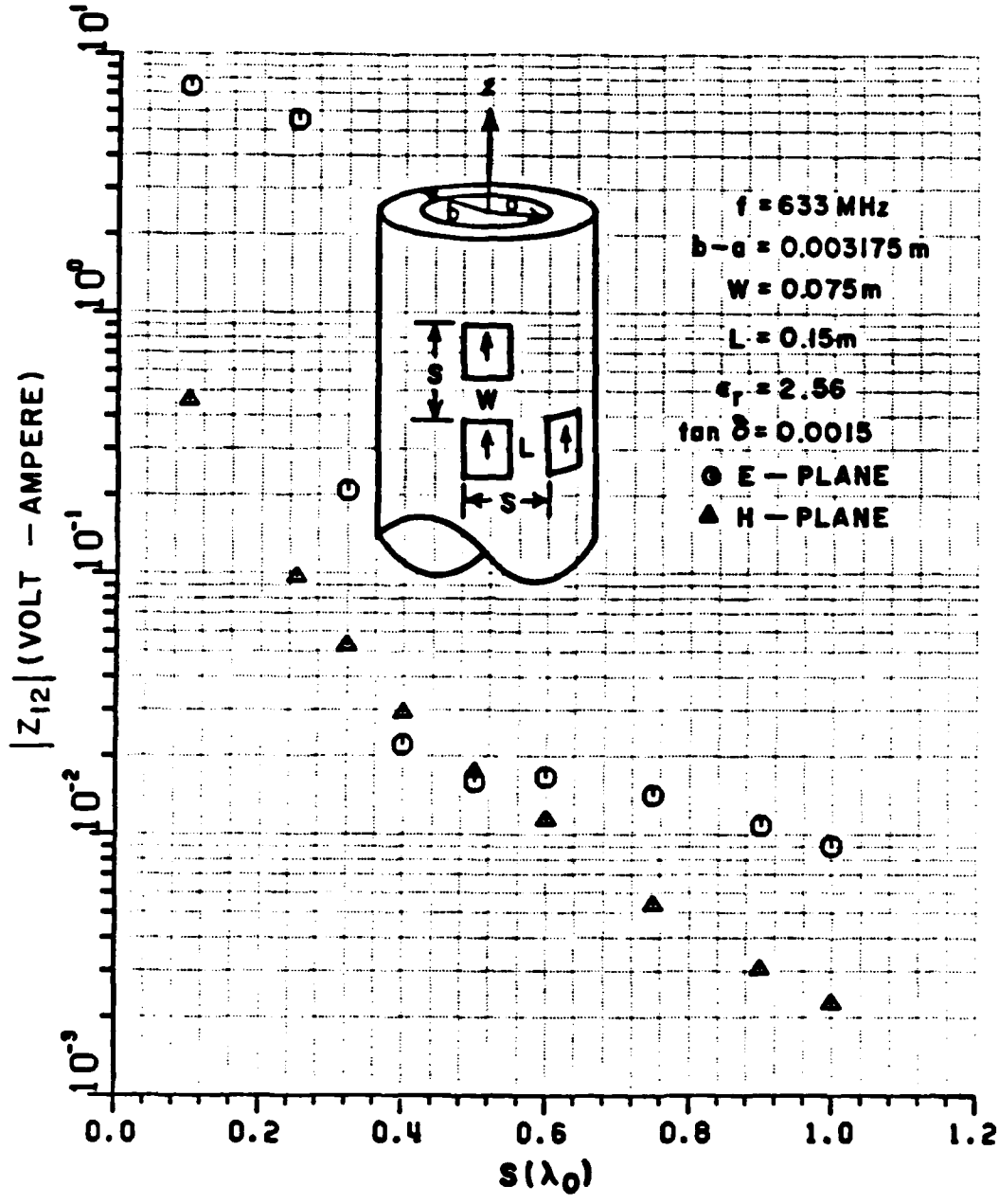

Figure 4.7. Coupling for identical expansion modes on a coated cylinder of radius a = 1.λ_0 (λ_0 = 0.474 m.).

$$T(\bar{r},n) = \int_{\Gamma} f(\phi,n,h) \begin{vmatrix} H_n^{(1)}(\lambda\rho) \\ H_n^{(1)'}(\lambda\rho) \end{vmatrix} e^{jhz}\, dh \quad , \tag{4.134}$$

$$f(\phi,n,h) = g(n,h) \int_S J_\alpha(\bar{r}') \begin{vmatrix} \cos \\ \sin \end{vmatrix} n(\phi-\phi') \; e^{-jhz'} bd\phi' dz' \quad , \tag{4.135}$$

$\alpha = \phi', z'$, S denotes the surface of the antenna, and g(n,h) involves the expansion coefficients of the Green's dyadic. Furthermore, $f(\phi,n,h)$ is an analytic function of the complex variable h along the path of integration Γ (Figure 4.8) with end points at infinity. The choice of Γ is discussed in Appendix G.

In the far zone, $|\lambda\rho| = |\rho\sqrt{k_2^2-h^2}\,| \to \infty$, one can employ the large argument approximations for the Hankel functions:

$$H_n^{(1)}(\lambda\rho) \sim \sqrt{\frac{2}{\pi\lambda\rho}}\; e^{j(\lambda\rho - n\pi/2 - \pi/4)} \quad , \tag{4.136}$$

and

$$H_n^{(1)'}(\lambda\rho) \sim j\sqrt{\frac{2}{\pi\lambda\rho}}\; e^{j(\lambda\rho - n\pi/2 - \pi/4)} \quad , \; n=0,1,2,\ldots \; . \tag{4.137}$$

Using these approximations in (4.134) reveals that it is sufficient to consider integral of the type:

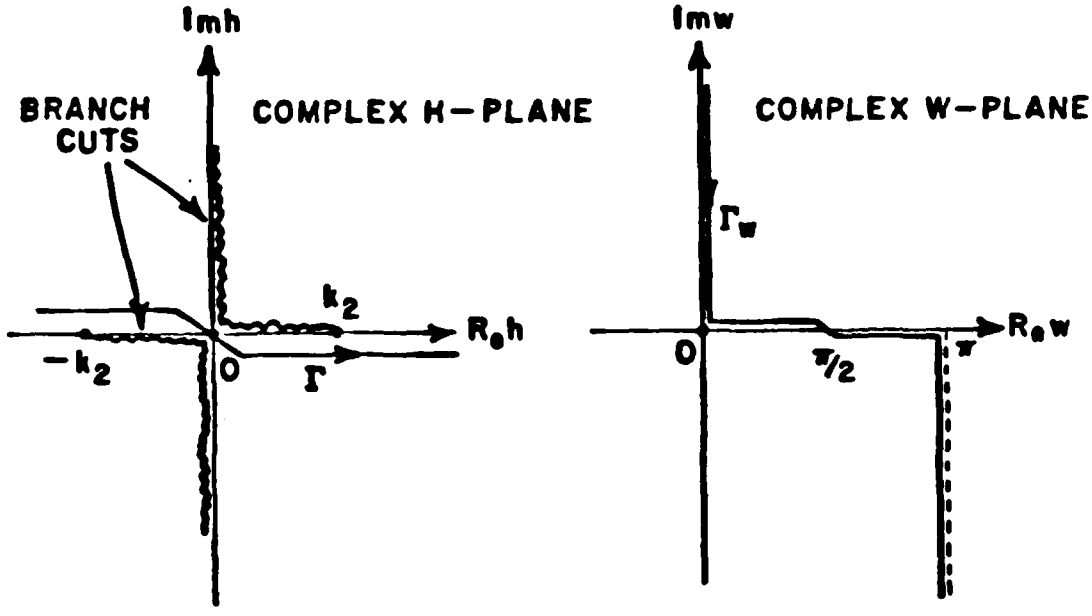

Figure 4.8. Contours of integration in the h-plane and the w-plane.

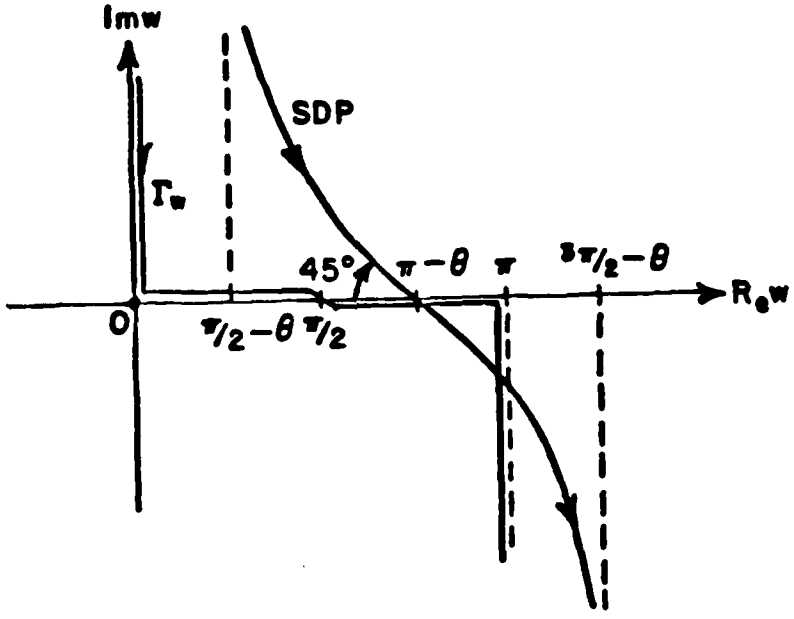

Figure 4.9. The steepest descent path.

$$T(\bar{r},n) = \int_{\Gamma} f(\phi,n,h) \sqrt{\frac{2}{\pi\lambda\rho}}\, e^{j(\lambda\rho - n\pi/2 - \pi/4)+jhz}\, dh \quad , \quad (4.138)$$

which can be evaluated asymptotically using the method of steepest descent as $|\lambda\rho| \to \infty$.

Introducing the transformation

$$h = -k_2 \cos w \quad (4.139)$$

and realizing that $z = r\cos\theta$, $\rho = r\sin\theta$, where r and θ are the usual spherical coordinates, one finds that

$$\rho \sqrt{k_2^2 - h^2} + hz = -k_2 r\cos(w+\theta) \quad . \quad (4.140)$$

Hence, (4.138) can be rewritten as

$$T(\bar{r},n) = \int_{\Gamma_w} F(\phi,n,w)\, e^{k_2 r q(w)}\, dw \quad , \; n=0,1,2,\ldots \; , \quad (4.141)$$

where the contour Γ in the h-plane is mapped onto the contour Γ_w in the w-plane as shown in Figure 4.8,

$$q(w) = -j\cos(w+\theta) \quad , \quad (4.142)$$

and

$$F(\phi,n,w) = e^{-j(n\pi/2 + \pi/4)} \sqrt{\frac{2k_2 \sin w}{\pi r \sin\theta}}\, f(\phi,n,-k_2\cos w) \quad . \quad (4.143)$$

The saddle point is given by solving

$$q'(w)\Big|_{w=w_s} = j\sin(w+\theta) = 0 \quad . \tag{4.144}$$

It is clear that $w_s = \pi-\theta$ is the appropriate saddle point. Observing that

$$q(w_s) = -j\cos(\pi-\theta+\theta) = j \tag{4.145}$$

and

$$q''(w_s) = j\cos(\pi-\theta+\theta) = -\,j \neq 0; \quad , \tag{4.146}$$

one realizes $\mathrm{Im}q(w) = 1$ along the steepest descent path (SDP), and w_s is a first-order saddle point since $q''(w_s)\neq 0$. Letting $w=w_r+jw_i$, one finds, along the SDP,

$$\mathrm{Im}q(w) = \mathrm{Im}\{-j\cos(w_r+\theta+jw_i)\} = -\cosh(w_i)\cos(w_r+\theta) = 1 \ . \tag{4.147}$$

As $w_i\to\pm\infty$, $\cosh(w_i)\to\infty$, thus $\cos(w_r+\theta)\to 0$ in order to satisfy (4.147). This suggests that the SDP is asymptotic to $w_r=\pi/2-\theta$ and $w_r=3\pi/2-\theta$. In addition, introducing the real variable β via the transformation

$$q(w) = q(w_s)-\beta^2 \quad , \tag{4.148}$$

leads to

$$\frac{dw}{d\beta}\bigg|_{\beta=0} = -\,\frac{2\beta}{q'(w)}\bigg|_{\beta=0} \quad . \tag{4.149}$$

Upon applying L'Hôpital's rule to the indeterminate form for $dw/d\beta$ in (4.149) when $\beta=0$ (i.e., $w=w_s$), one obtains

$$\left.\frac{dw}{d\beta}\right|_{\beta=0} = \sqrt{\frac{-2}{q''(w_s)}} = \sqrt{2}\, e^{-j\pi/4} \quad . \tag{4.150}$$

Equation (4.150) implies the SDP makes an angle of 45° with the real w-axis at $w=w_s$. The SDP is depicted in Figure 4.9.

Finally, a general expression for the first-order approximation of $T(\bar{r},n)$ is given by [28]:

$$T(\bar{r},n) \sim \sqrt{\frac{-2\pi}{k_2 r q''(w_s)}}\; F(\phi,n,w_s)\, e^{k_2 r q(w_s)} \quad , k_2 r \to \infty \quad . \tag{4.151}$$

Combining (4.136), (4.137), (4.138) and (4.151) yields

$$T(\bar{r},n) = \int_\Gamma f(\phi,n,h) \begin{bmatrix} H_n^{(1)}(\lambda\rho) \\ H_n^{(1)\prime}(\lambda\rho) \end{bmatrix} e^{jhz}\, dh$$

$$\sim \begin{bmatrix} 1 \\ j \end{bmatrix} 2e^{-j(n+1)\pi/2}\, f(\phi,n,\cos\theta)\, \frac{e^{jk_2 r}}{r} \quad , k_2 r \to \infty \quad . \tag{4.152}$$

This completes the fundamental portion of the far field calculation.

CHAPTER V

ASYMPTOTIC SOLUTIONS

A. INTRODUCTION

In the last chapter, all electric fields and impedances are exact eigenfunction solutions since they are derived by the method of Green's function which itself is expressed in terms of eigenmodes of the dielectric coated cylinder. These eigenfunction solutions are employed in Chapter IV to calculate the mutual coupling associated with microstrip arrays. In many situations, however, microstrip antennas may be used in the construction of phased arrays that are flush-mountable on large cylindrical objects such as an aircraft fuselage or space vehicles. The coupling between antenna elements plays a significant role in the design of these arrays. In such situations where the cylinder is large in terms of wavelength, it is best to use asymptotic high frequency methods, as opposed to an eigenfunction series solution, to analyze the coupling effect because the eigenfunction solution is poorly convergent. Moreover, the radiation mechanism is often obscured

in an eigenfunction solution. On the other hand, the asymptotic solutions are far less complicated from the viewpoint of computational effort and cost involved. More attractively, the asymptotic solutions may be interpreted in terms of ray-optics thereby revealing the radiation mechanism involved.

Asymptotic high frequency solutions usually result from asymptotic evaluations of the integral representations of Green's functions of the circumferentially-propagating type. Section B will discuss the alternative representations of the dyadic Green's function for the dielectric coated cylinder. It includes the integral representation of the circumferentially-propagating Green's function from which one can derive the residue series representation that provides nice ray-optical interpretation. Section C devotes to the derivation of alternative representations of the mutual impedance z_{12} between mode 1 and mode 2 considered in the numerical examples of Chapter IV. For simplicity, a two-dimensional (2-D) coupling problem involving two infinite conducting strips is formulated and analyzed asymptotically. A numerical example of the 2-D problem is treated in Section D. It serves to illustrate the validity and usefulness of asymptotic solutions.

B. ALTERNATIVE REPRESENTATIONS OF THE GREEN'S DYADIC

Integral transforms, such as the Laplace, Fourier, and Mellin transforms, can be found useful in many cases in converting relatively slowly converging series into much more rapidly converging ones. Upon

examining the series associated with the dyadic Green's function which converge slowly as the cylinder radius increases, it appears that the Poisson summation formula, which is based on the Fourier transform, can convert these poorly converging series into fast converging ones, at least in principle. One form of the Poisson summation formula can be stated as follows:

$$\sum_{n=-\infty}^{\infty} f(\alpha n) = \frac{1}{\alpha} \sum_{n=-\infty}^{\infty} F\left(\frac{2n\pi}{\alpha}\right) \quad , \tag{5.1}$$

where

$$F(\xi) = \int_{-\infty}^{\infty} f(\nu) e^{j\xi\nu} d\nu \quad , \tag{5.2}$$

and

$$f(\nu) = \frac{1}{2\pi} \int_{-\infty}^{\infty} F(\xi) e^{-j\xi\nu} d\xi \tag{5.3}$$

form a Fourier transform pair, and α is a scalar.

The utility of the Poisson summation formula in converting a slowly converging series into a rapidly converging one may be appreciated from the properties of the Fourier transforms. If $f(\nu)$ is a function which is concentrated near $\nu=0$, then $F(\xi)$ is spread out over the ξ-axis, or has an appreciable value for a large value of ξ; for instance, if $f(\nu)=\delta(\nu)$, then $F(\xi)=1$. Conversely, if $f(\nu)$ is spread out

along the ν-axis, then $F(\xi)$ is localized near $\xi=0$. A slowly converging series with a typical term $f(\alpha n)$ is then converted to a rapdily converging series with a typical term $F(2n\pi/\alpha)$, since F will be small for large values of n while $f(\alpha n)$ decreases slowly with increasing n.

From Equations (3-123), (3-125) and (3-126) one observes that every component of the Green's dyadic is composed of functions of the form

$$\frac{j}{8\pi} \int_{-\infty}^{\infty} S(\rho,\rho',\phi,\phi';h)e^{jh(z-z')}dh \quad ,$$

where

$$S(\rho,\rho',\phi,\phi';h) = \sum_{n=0}^{\infty} \epsilon_n \begin{bmatrix} g_e(\rho,\rho';n,h)\cos n(\phi-\phi') \\ g_o(\rho,\rho';n,h)\sin n(\phi-\phi') \end{bmatrix} \quad , \qquad (5.4)$$

with g_e and g_o being even and odd functions of n, respectively. Thus one only needs to consider S in looking for the alternative representations of the Green's dyadic.

The series S in (5.4) can be rearranged such that

$$S(\rho,\rho',\phi,\phi';h) = \sum_{n=-\infty}^{\infty} \begin{bmatrix} g_e(\rho,\rho';n,h) \\ -jg_o(\rho,\rho';n,h) \end{bmatrix} e^{jn(\phi-\phi')} \quad . \qquad (5.5)$$

In addition, employing the large order approximations of the cylinder functions:

$$J_\nu(z) \sim \frac{1}{2} \sqrt{\frac{2}{\pi\nu}} \left[\frac{ez}{2\nu}\right]^\nu , \tag{5.6}$$

$$H_\nu^{(1)}(z) \sim \mp j \sqrt{\frac{2}{\pi\nu}} \left[\frac{2\nu}{ez}\right]^\nu , \tag{5.7}$$

$$J_\nu'(z) \sim \frac{\nu}{z} J_\nu(z) , \tag{5.8}$$

$$H_\nu^{(1)\prime}(z) \sim -\frac{\nu}{z} H_\nu^{(1)}(z) , \tag{5.9}$$

with z, ν being complex numbers, one can easily verify that both g_e and g_o are square integrable over the interval $(-\infty,\infty)$, i.e.,

$$\int_{-\infty}^{\infty} \left[\begin{array}{c} |g_e(\rho,\rho';\nu,h)|^2 \\ |g_o(\rho,\rho';\nu,h)|^2 \end{array}\right] d\nu < \infty . \tag{5.10}$$

Clearly (5.10) also implies $|g_e|, |g_o| \to 0$ as $\nu \to \infty$. These properties of boundedness warrant the existence of the Fourier transforms of g_e and g_o. Hence the Poisson summation formula can be applied to the series in (5.5) to yield

$$\sum_{n=-\infty}^{\infty} \begin{bmatrix} g_e(\rho,\rho';n,h) \\ -jg_o(\rho,\rho';n,h) \end{bmatrix} e^{jn(\phi-\phi')}$$

$$= \sum_{n=-\infty}^{\infty} \int_{-\infty}^{\infty} \begin{bmatrix} g_e(\rho,\rho';\nu,h) \\ -jg_o(\rho,\rho';\nu,h) \end{bmatrix} e^{j\nu(\phi-\phi')} e^{j2n\pi\nu} d\nu$$

$$= \sum_{n=-\infty}^{\infty} \int_{-\infty}^{\infty} \begin{bmatrix} g_e(\rho,\rho';\nu,h) \\ -j\,\mathrm{sgn}(\phi-\phi')g_o(\rho,\rho';\nu,h) \end{bmatrix} e^{j\nu|\phi-\phi'| + j2n\pi\nu} d\nu \quad , \tag{5.11}$$

where

$$\mathrm{sgn}(x) = \begin{cases} 1 & , x > 0 \\ -1 & , x < 0 \end{cases} \quad . \tag{5.12}$$

Rearranging (5.11) will result in the following form:

$$\sum_{n=-\infty}^{\infty} \begin{bmatrix} g_e(\rho,\rho';n,h) \\ -jg_o(\rho,\rho';n,h) \end{bmatrix} e^{jn(\phi-\phi')}$$

$$= \sum_{n=0}^{\infty} \int_{-\infty}^{\infty} \begin{bmatrix} g_e(\rho,\rho';\nu,h) \\ -j\,\mathrm{sgn}(\phi-\phi')g_o(\rho,\rho';\nu,h) \end{bmatrix}$$

$$\begin{bmatrix} e^{j\nu(|\phi-\phi'|+2n\pi)} \pm e^{j\nu(2\pi-|\phi-\phi'|+2n\pi)} \end{bmatrix} d\nu. \tag{5.13}$$

The original representation which appears on the L.H.S. of (5.13) is associated with the "radially propagating" Green's function. Whereas the alternative representation which appears on the R.H.S. of (5.13) is found in the "circumferentially propagating" Green's function which is particularly suited to emphasize the ray-optic behavior of radiation in the shadow zone of the cylinder.

Since the integrand of (5.13) vanishes as $\nu \to \infty$ in the upper half plane, the contour of integration (along the real ν-axis) can be closed in this half plane to form a new (closed) contour C_ν, as shown in Figure 5.1(a), without affecting the value of the integral, or symbolically,

$$\sum_{n=0}^{\infty} \int_{-\infty}^{\infty} d\nu = \sum_{n=0}^{\infty} \int_{C_\nu} d\nu. \tag{5.14}$$

It is known that the simple poles of g_e or g_o form an ordered set $\{\nu_p : \mathrm{Re}\,\nu_p, \mathrm{Im}\,\nu_p > 0, p=1,2,3, \ldots\}$ in the first quadrant of the ν-plane. One can use Cauchy's theory to evaluate the R.H.S. of (5.14) to obtain the residue series:

$$\sum_{n=0}^{\infty} \int_{C_\nu} d\nu = j2\pi \sum_{n=0}^{\infty} \sum_{p=1}^{\infty} \begin{bmatrix} \mathrm{Res}[g_e(\rho,\rho';\nu_p,h)] \\ -j\,\mathrm{sgn}(\phi-\phi')\mathrm{Res}[g_o(\rho,\rho';\nu_p,h)] \end{bmatrix}$$

$$\cdot \begin{bmatrix} e^{j\nu_p(|\phi-\phi'|+2n\pi)} & \pm e^{j\nu_p(2\pi-|\phi-\phi'|+2n\pi)} \end{bmatrix} . \tag{5.15}$$

This residue series representation is important for analyzing the diffracted fields in the deep shadow region of the cylinder. Physically, each term in the series, corresponding to p=1,2,..., can be interpreted as a creeping wave mode that creeps around the cylinder n times, n=0,1,2,.... The exponential terms $e^{j\nu_p(|\phi-\phi'|+2n\pi)}$, and $e^{j\nu_p(2\pi|\phi-\phi'|+2n\pi)}$ (which corresponds to waves creeping around the cylinder in the direction opposite to that of the former) become exponentially decaying terms which attenuate faster as $|\phi-\phi'|$ become larger. Since $Im\nu_p$ increases with p, the higher order modes are attenuated very rapidly. So consequently one would probably need to retain only the first couple of terms. In addition, for large cylinders, the n=0 encirclement is sufficient because contributions from higher encirclements are negligible as the wave attenuates while creeping around the cylinder. The exponential decay of the creeping wave modes on the cylinder suggests that energy leaks away from the cylinder surface into the surrounding space.

Analytically, one may note that $Im\nu_p$, p=1,2,3..., is significantly greater than zero. Hence, contour C_ν can be deformed in such a way that, along the new contour $C_{\nu'}$(Figure 5.1(b)), the integration variable ν always has $Im\nu>>0$ thereby rapidly damping the encirclement terms with n>0. Consequently one can write

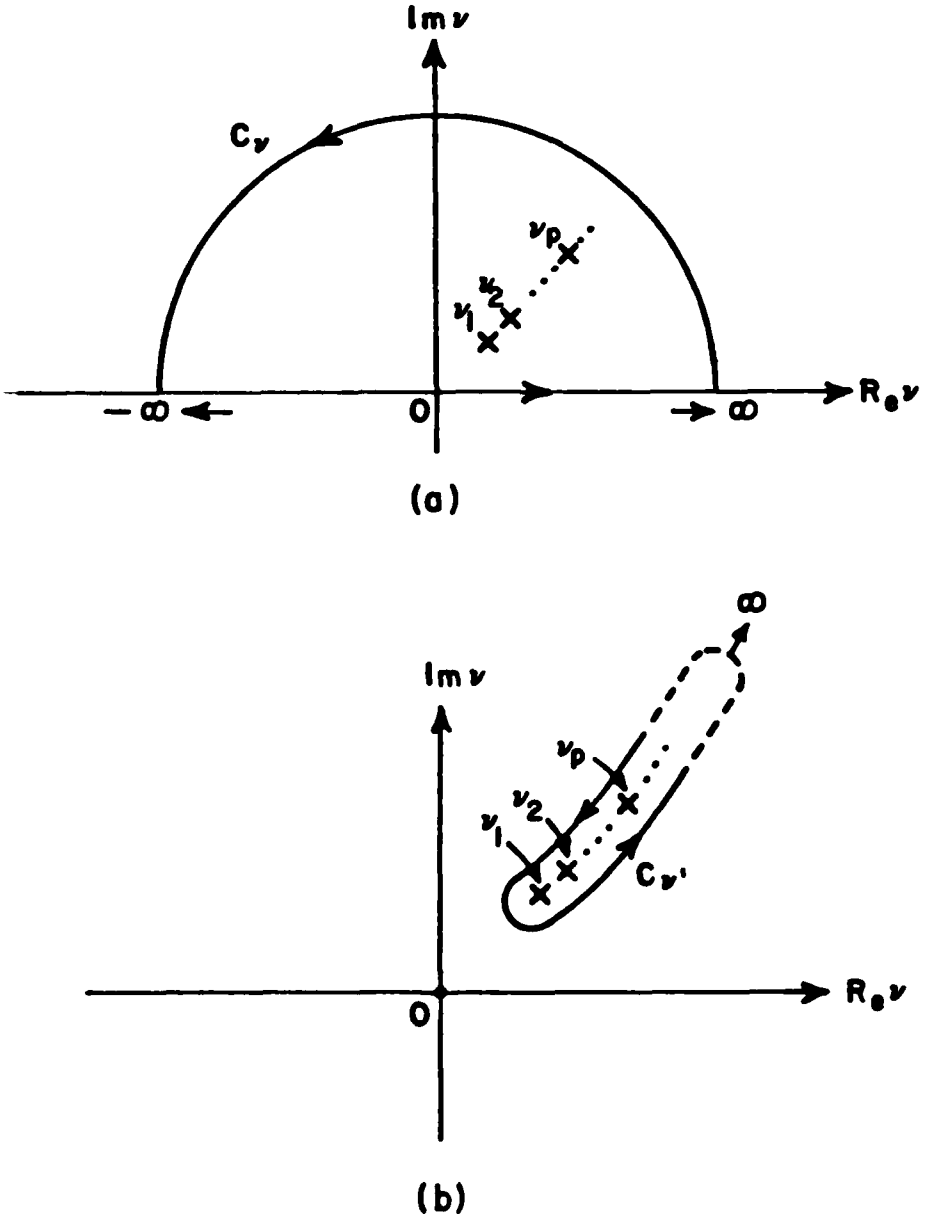

Figure 5.1. (a) Contour C_ν encloses the upper half ν-plane which contains the poles of g_e or g_o: $\nu_1, \nu_2, \ldots, \nu_p, \ldots$.
(b) The deformed contour $C_{\nu'}$ also encloses all the poles of g_e or g_o.

$$S(\rho,\rho',\phi,\phi';h) = \sum_{n=-\infty}^{\infty} \begin{bmatrix} g_e(\rho,\rho';n,h) \\ -jg_o(\rho,\rho';h,h) \end{bmatrix} e^{jn(\phi-\phi')}$$

$$\sim \int_{-\infty}^{\infty} \begin{bmatrix} g_e(\rho,\rho';\nu,h) \\ -j\,\mathrm{sgn}(\phi-\phi')g_o(\rho,\rho';\nu,h) \end{bmatrix} \begin{bmatrix} e^{j\nu|\phi-\phi'|} \pm e^{j\nu(2\pi-|\phi-\phi'|)} \end{bmatrix} d\nu$$

$$\sim j2\pi \sum_{p=1}^{\infty} \begin{bmatrix} \mathrm{Res}\,[g_e(\rho,\rho';\nu_p,h)] \\ -j\,\mathrm{sgn}(\phi-\phi')\mathrm{Res}[g_o(\rho,\rho';\nu_p,h)] \end{bmatrix}$$

$$\begin{bmatrix} e^{j\nu_p|\phi-\phi'|} \pm e^{j\nu_p(2\pi-\phi-\phi'|)} \end{bmatrix} \quad . \qquad (5.16)$$

The three representations of S in (5.16) are of different utility in evaluating S. The eigenmode solution, the first form, is exact and suitable for small cylinders numerically. The remaining two forms are valid for large cylinders. In particular, the integral representation can be used when $|\phi-\phi'|$ is small while the use of the residue series is most appropriate when $|\phi-\phi'|$ is large (in general, $|\phi-\phi'|>\frac{\lambda_o}{2b}$, λ_o is the free space wavelength).

C. ASYMPTOTIC EVALUATION OF z_{12}

As the radius of the coated cylinder increases, the asymptotic expansions of fields and impedances are deemed appropriate. The mutual impedance z_{12} between mode 1 and mode 2, both z-polarized as shown in Figure 4.1, obtained in Chapter IV is an eigenfunction solution which is not suitable for asymptotic expansion. It is desirable to derive an integral representation of z_{12} via the use of the Green's dyadic of the circumferentially-propagating type. Adopting the same notations used in Chapter IV, the z-component of the surface electric field due to mode 1 can be directly obtained from (4.63) as:

$$E^1_{1z}(b,\phi,z) = -\frac{\omega\mu_2}{8\pi k_2^2} \int_{S_1} ds' \int_{-\infty}^{\infty} dh \sum_{n=0}^{\infty} \varepsilon_n W(n,h)\cos n(\phi-\phi') J_{z1}(b,\phi',z')\, e^{jh(z-z')} \quad , \tag{5.17}$$

where $J_{1z}(b,\phi,z)$ and $W(n,h)$ are defined in (4.76) and (4.85), respectively, and

$$S_1 = \{\bar{r}=(b,\phi,z): -\phi_1 < \phi < \phi_1, -z_1 < z < z_1\} \quad . \tag{5.18}$$

By definition,

$$z_{12} = -\int_{S_2} E^1_{2z}(b,\phi,z) J_{2z}(b,\phi,z) ds \quad , \tag{5.19}$$

where $J_{2z}(b,\phi,z)$ is again defined in (4.76), and

$$S_2 = \{\bar{r} = (b,\phi,z) : \phi_{2c}-\phi_2<\phi<\phi_{2c}+\phi_2,\ z_{2c}-z_2<z<z_{2c}+z_2\} \quad . \tag{5.20}$$

Combining (5.17) - (5.20) one can explicitly write

$$z_{12} = \frac{\omega\mu_2}{8\pi k_2^2} \int_{z_{2c}-z_2}^{z_{2c}+z_2} dz \int_{\phi_{2c}-\phi_2}^{\phi_{2c}+\phi_2} bd\phi \int_{-z_1}^{z_1} dz' \int_{-\phi_1}^{\phi_1} bd\phi' \int_{-\infty}^{\infty} dh\ e^{jh(z-z')} \cdot$$

$$\cdot \sum_{n=0}^{\infty} \varepsilon_n W(n,h)\cos n(\phi-\phi') J_{1z}(b,\phi',z') J_{2z}(b,\phi,z) \quad . \tag{5.21}$$

Since $W(n,h)$ is an even function of n, it follows from (5.4) and (5.5) that

$$z_{12} = \frac{\omega\mu_2}{8\pi k_2^2} \int_{z_{2c}-z_2}^{z_{2c}+z_2} dz \int_{\phi_{2c}-\phi_2}^{\phi_{2c}+\phi_2} bd\phi \int_{-z_1}^{z_1} dz' \int_{-\phi_1}^{\phi_1} bd\phi' \int_{-\infty}^{\infty} dh\ e^{jh(z-z')} \cdot$$

$$\cdot \sum_{n=-\infty}^{\infty} W(n,h) e^{jn(\phi-\phi')} J_{1z}(b,\phi',z') J_{2z}(b,\phi,z) \quad . \tag{5.22}$$

Carrying out the integrations over the variables ϕ,ϕ',z and z' yields

$$z_{12} = \frac{A_{12}}{8} \int_{-\infty}^{\infty} dh\ \tilde{Z}_1(h)\tilde{Z}_2(h) \sum_{n=-\infty}^{\infty} \frac{W(n,h)}{n^2} \left[e^{jn(\phi_{2c}+\phi_2)} - e^{jn(\phi_{2c}-\phi_2)} \right] \cdot$$

$$\cdot \left[e^{-jn\phi_1} - e^{jn\phi_1} \right] \quad , \tag{5.23}$$

where $\tilde{Z}_\ell(h)$, $\ell=1,2$, and A_{12} are specified in (4.81) and (4.83), respectively. According to (5.13), (5.14) and (5.16), z_{12} in (5.23) can be written as follows:

$$z_{12} = \frac{A_{12}}{8} \int_{-\infty}^{\infty} dh\, \tilde{Z}_1(h)\tilde{Z}_2(h) \sum_{n=0}^{\infty} \int_{-\infty}^{\infty} W(\nu,h) \left[\Gamma_1[\nu) + \Gamma_2(\nu) - \Gamma_3(\nu) - \Gamma_4(\nu) \right] d\nu$$

$$= \frac{A_{12}}{8} \int_{-\infty}^{\infty} dh\, \tilde{Z}_1(h)\tilde{Z}_2(h) \sum_{n=0}^{\infty} \int_{C_\nu} W(\nu,h) \cdot \left[\Gamma_1[\nu) + \Gamma_2(\nu) - \Gamma_3(\nu) - \Gamma_4(\nu) \right] d\nu$$

$$\sim \frac{A_{12}}{8} \int_{-\infty}^{\infty} dh \tilde{Z}_1(h)\tilde{Z}_2(h) \int_{-\infty}^{\infty} W(\nu,h) \cdot \left[\Gamma_1[\nu) + \Gamma_2(\nu) - \Gamma_3(\nu) - \Gamma_4(\nu) \right] d\nu \quad , \qquad (5.24)$$

where

$$\Gamma_1(\nu) = e^{j\nu(|\phi_{2c}+\phi_2-\phi_1|+2n\pi)} + e^{j\nu(2\pi-|\phi_{2c}+\phi_2-\phi_1|+2n\pi)} \quad , \qquad (5.25)$$

$$\Gamma_2(\nu) = e^{j\nu(|\phi_{2c}-\phi_2+\phi_1|+2n\pi)} + e^{j\nu(2\pi-|\phi_{2c}-\phi_2+\phi_1|+2n\pi)} \quad , \qquad (5.26)$$

$$\Gamma_3(\nu) = e^{j\nu(|\phi_{2c}-\phi_2-\phi_1|+2n\pi)} + e^{j\nu(2\pi-|\phi_{2c}-\phi_2-\phi_1|+2n\pi)} \quad , \qquad (5.27)$$

$$\Gamma_4(\nu) = e^{j\nu(|\phi_{2c}+\phi_2+\phi_1|+2n\pi)} + e^{j\nu(2\pi-|\phi_{2c}+\phi_2+\phi_1|+2n\pi)} \quad , \qquad (5.28)$$

and C_ν is the contour enclosing all the poles of $W(\nu,h)$ in the upper half ν-plane. The closed contour integral in (5.24) can be readily evaluated by residue calculus to yield

$$z_{12} = \frac{j2\pi A_{12}}{8} \int_{-\infty}^{\infty} dh \tilde{Z}_1(h)\tilde{Z}_2(h) \sum_{n=0}^{\infty} \sum_{p=1}^{\infty} \text{Res } [W(\nu_p,h)] \cdot$$

$$\cdot \left[\Gamma_1(\nu_p) + \Gamma_2(\nu_p) - \Gamma_3(\nu_p) - \Gamma_4(\nu_p) \right]$$

$$\sim \frac{j2\pi A_{12}}{8} \int_{-\infty}^{\infty} dh \tilde{Z}_1(h)\tilde{Z}_2(h) \sum_{p=1}^{\infty} \text{Res } [W(\nu_p,h)] \cdot$$

$$\cdot \left[\Gamma_1(\nu_p) + \Gamma_2(\nu_p) - \Gamma_3(\nu_p) - \Gamma_4(\nu_p) \right] \quad . \quad (5.29)$$

As indicated in the last section, the alternative representations of z_{12} are derived on the basis that $W(\nu,h) \to 0$ as $\nu \to \infty$, and $W(\nu,h)$ is analytic on the upper half ν-plane except at the poles ν_p, $p=1,2,3,\ldots$. Also, the approximations in (5.24) and (5.29) are appropriate for large cylinders. It may be noted that the ray-optical interpretation of the residue series discussed in the last section still applies here.

As far as evaluating the residue series in (5.29) is concerned, only the first creeping wave mode will be sufficient for reasonable approximation due to rapid convergence of the series when the two modes are well separated (one or more free space wavelengths apart). As their separation reduces, the series is becoming poorly convergent and the

number of creeping wave modes will hence increase. Upon examining the complexity of $W(\nu,h)$ (equations (4.84) - (4.90) with ν replacing n), it appears that there is no known way to locate the poles of $W(\nu,h)$ analytically. One needs to resort to numerical techniques such as the Newton-Rhapson procedure to find these poles. Such task is by no means trivial. Thus, for small separations, it is more appropriate to evaluate the integral representation of z_{12} in (5.24).

To demonstrate the usefulness and power of the asymptotic solutions, it is best to consider the mutual coupling between two infinite, z-oriented conducting strips on the dielectric coated cylinder whose cross-section is shown in Figure 5.2. Strip ℓ, centered at $\phi=\phi_{\ell c}$, $\ell=1,2$, with $\phi_{1c}=0$, has constant and z-directed current $\bar{J}_\ell$, i.e.,

$$\bar{J}_\ell(\bar{r}) = \bar{J}_\ell(b,\phi,z) = \begin{cases} \hat{z}\,\dfrac{1}{2b\phi_\ell}, & |\phi-\phi_{\ell c}|<\phi_\ell,\ |z|<\infty,\ \ell=1,2 \\ 0, & \text{elsewhere} \end{cases} . \tag{5.30}$$

The mutual impedance z_{12} between strip 1 and strip 2 can be expressed as

$$z_{12} = -\int_{\phi_{2c}-\phi_2}^{\phi_{2c}+\phi_2} \bar{E}_2^1(\bar{r})\cdot\bar{J}_2(\bar{r})\,d\ell = -\int_{\phi_{2c}-\phi_2}^{\phi_{2c}+\phi_2} E_{2z}^1(\phi)\,\frac{1}{2b\phi_2}\,b\,d\phi \quad , \tag{5.31}$$

where $\bar{E}_2(\bar{r})$ denotes the electric field at the surface of the dielectric coated cylinder (or rigorously at $\rho=b^+$), and its z-component is given by

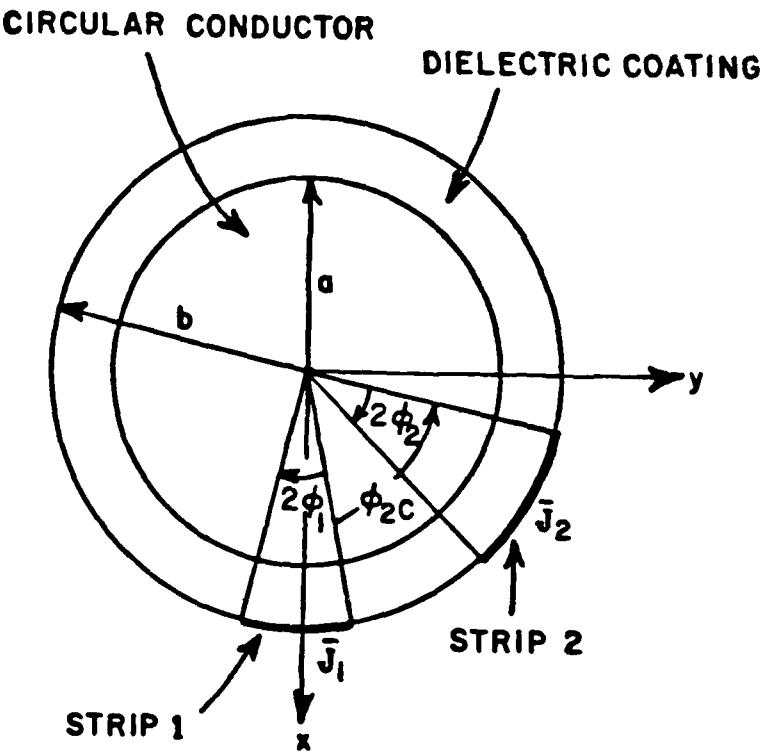

Figure 5.2. Cross-section of the dielectric coated cylinder with two infinite conducting strips.

$$E^1_{2z}(\phi) = -\frac{\omega\mu_2}{8\pi k_2^2} \int_{-\phi_1}^{\phi_1} b\,d\phi' \int_{-\infty}^{\infty} dz' \int_{-\infty}^{\infty} dh\; e^{jh(z-z')}$$

$$\sum_{n=0}^{\infty} \varepsilon_n W(n,h)\cos n(\phi-\phi') \frac{1}{2b\phi_1} \quad . \tag{5.32}$$

Making use of the results that

$$\int_{-\infty}^{\infty} e^{jh(z-z')}\, dz' = 2\pi e^{jhz}\delta(h) \quad , \tag{5.33}$$

and

$$\int_{-\infty}^{\infty} f(h)\delta(h)dh = f(o) \quad , \tag{5.34}$$

one can readily convert (5.32) to

$$E^1_{2z}(\phi) = -\frac{\omega\mu_2}{j8k_2^2\phi_1} \sum_{n=-\infty}^{\infty} \frac{W(n,o)}{n} \left[e^{jn\phi_1} - e^{-jn\phi_1} \right] e^{jn\phi} \quad . \tag{5.35}$$

Substituting (5.35) into (5.31) yields

$$z_{12} = \frac{\omega\mu_2}{16k_2^2\phi_1\phi_2} \sum_{n=-\infty}^{\infty} \frac{W(n,o)}{n^2} \left[e^{jn(\phi_{2c}-\phi_2+\phi_1)} + e^{jn(\phi_{2c}+\phi_2-\phi_1)} - e^{jn(\phi_{2c}-\phi_2-\phi_1)} - e^{jn(\phi_{2c}+\phi_2+\phi_1)} \right] \quad . \tag{5.36}$$

Next upon recalling identities (5.13)-(5.15) one will arrive at the following representations of z_{12}:

$$z_{12} = \frac{\omega\mu_2}{16k_2^2\phi_1\phi_2} \sum_{n=0}^{\infty} \int_{-\infty}^{\infty} \frac{W(\nu,o)}{\nu^2}$$

$$\left[\Gamma_1(\nu) + \Gamma_2(\nu) - \Gamma_3(\nu) - \Gamma_4(\nu) \right] d\nu$$

$$= \frac{j\pi\omega\mu_2}{8k_2^2\phi_1\phi_2} \sum_{n=0}^{\infty} \sum_{p=1}^{\infty} \text{Res} \left[W(\nu_p,o) \right]$$

$$\left[\frac{\Gamma_1(\nu_p) + \Gamma_2(\nu_p) - \Gamma_3(\nu_p) - \Gamma_4(\nu_p)}{\nu_p^2} \right] , \qquad (5.37)$$

where $\Gamma_\ell(\nu)$, $\ell=1,2,3,4$, are defined in (5.25)-(5.28) and ν_p, $p=1,2,\ldots$, are the poles of $W(\nu,o)$ in the upper half ν-plane.

As just explained earlier, for large cylinders, reasonable approximation can be attained by ignoring terms which correspond to creeping waves making $n>0$ encirclements around the coated cylinder, i.e.,

$$z_{12} \sim \frac{\omega\mu_2}{16k_2^2\phi_1\phi_2} \int_{-\infty}^{\infty} \frac{W(\nu,o)}{\nu^2}$$

$$\left[\Gamma_1(\nu) + \Gamma_2(\nu) - \Gamma_3(\nu) - \Gamma_4(\nu) \right] d\nu$$

$$\sim \frac{j\pi\omega\mu_2}{8k_2^2\phi_1\phi_2} \sum_{p=1}^{\infty} \text{Res} \left[W(\nu_p,o) \right]$$

$$\left[\frac{\Gamma_1(\nu_p) + \Gamma_2(\nu_p) - \Gamma_3(\nu_p) - \Gamma_4(\nu_p)}{\nu_p^2} \right] \quad . \tag{5.38}$$

Assuming $\mu_1=\mu_2$ and then recognizing that

$$\lambda = \sqrt{k_2^2 - h^2} = k_2 \quad , \quad \mu = \sqrt{k_1^2 - h^2} = \sqrt{\varepsilon_r}\, k_2 \quad \text{at } h = 0 \ , \tag{5.39}$$

expressions (4.86)-(4.90) reduce to the following simpler forms:

$$X_1(\nu,o) = k_2 \left[-\sqrt{\varepsilon_r}\, \frac{Q_\nu}{T_\nu}\bigg|_{h=0} + \varepsilon_r \Gamma_\nu \right] \quad , \tag{5.40}$$

$$X_2(\nu,o) = k_2 \left[-\sqrt{\varepsilon_r}\, \frac{P_\nu}{S_\nu}\bigg|_{h=0} + \Gamma_\nu \right] \quad , \tag{5.41}$$

$$X_3(\nu,o) = 0 \quad , \tag{5.42}$$

$$r_\nu = \frac{H'_\nu(k_2 b)}{H_\nu(k_2 b)} \quad , \tag{5.43}$$

$$\left.\frac{P_\nu}{S_\nu}\right|_{h=0} = \frac{J'_\nu(\sqrt{\varepsilon_r}k_2 b)\ H_\nu(\sqrt{\varepsilon_r}k_2 a) - J_\nu(\sqrt{\varepsilon_r}k_2 a)H'_\nu(\sqrt{\varepsilon_r}k_2 b)}{J_\nu(\sqrt{\varepsilon_r}k_2 b)\ H_\nu(\sqrt{\varepsilon_r}k_2 a) - J_\nu(\sqrt{\varepsilon_r}k_2 a)H_\nu(\sqrt{\varepsilon_r}k_2 b)} \quad , \tag{5.44}$$

and

$$\left.\frac{Q_\nu}{T_\nu}\right|_{h=0} = \frac{J'_\nu(\sqrt{\varepsilon_r}k_2 b)\ H'_\nu(\sqrt{\varepsilon_r}k_2 a) - J'_\nu(\sqrt{\varepsilon_r}k_2 a)H'_\nu(\sqrt{\varepsilon_r}k_2 b)}{J_\nu(\sqrt{\varepsilon_r}k_2 b)\ H'_\nu(\sqrt{\varepsilon_r}k_2 a) - J'_\nu(\sqrt{\varepsilon_r}k_2 a)H_\nu(\sqrt{\varepsilon_r}k_2 b)} \quad . \tag{5.45}$$

Then it follows from (4.85) that

$$W(\nu,o) = \frac{j2k_2}{\pi b}\ \frac{H_\nu(k_2 b)}{H'_\nu(k_2 b) + Z_\nu(o)H_\nu(k_2 b)} \quad , \tag{5.46}$$

where

$$Z_\nu(h) \triangleq -\sqrt{\varepsilon_r}\ \frac{P_\nu}{S_\nu} \quad . \tag{5.47}$$

Employing (5.46) in (5.38) gives

$$z_{12} \sim \frac{j\eta_2}{8\pi b\phi_1\phi_2} \int_{-\infty}^{\infty} \frac{H_\nu(k_2 b)}{H'_\nu(k_2 b)+Z_\nu(o)H_\nu(k_2 b)} \left[\frac{\Gamma_1(\nu)+\Gamma_2(\nu)-\Gamma_3(\nu)-\Gamma_4(\nu)}{\nu^2}\right] d\nu, \tag{5.48}$$

where $\eta_2 = \sqrt{\mu_2/\varepsilon_2}$ is the free space intrinsic impedance.

It has been pointed out that the manner in which z_{12} in (5.48) is being evaluated depends on the separation between the two strips. The quantity $b\phi_{2c}$ is a measure of separation between the strips. When $b\phi_{2c}$ is small (typically less than a quarter of free space wavelength), the integral representation of z_{12} is most suitable. When $b\phi_{2c}$ is large (typically greater than a free space wavelength), the residue series is an efficient representation of z_{12}. Each case is dealt with specifically in the following:

Case (a): $b\phi_{2c}$ is small.

The exponential terms of the form $e^{j\nu(2\pi-|\xi|)}$ in the functions $\Gamma_\ell(\nu)$, $\ell = 1,2,3,4$, can be dropped without sacrificing significant accuracy. Hence one can rewrite (5.48) as

$$z_{12} \sim \frac{j\eta_2}{\pi b \phi_1 \phi_2} \int_0^\infty \frac{H_\nu(k_2 b)}{H_\nu'(k_2 b)+Z_\nu(o)H_\nu(k_2 b)} \frac{\sin\nu\phi_1}{\nu} \frac{\sin\nu\phi_2}{\nu} \cos\nu\phi_{2c}\, d\nu \quad . \tag{5.49}$$

Letting $\alpha=\sqrt{\varepsilon_r}k_2 a$, $\beta = \sqrt{\varepsilon_r}k_2 b$, and $\gamma = k_2 b$, one may write

$$Q(\nu) \triangleq \frac{H_\nu(k_2 b)}{H_\nu'(k_2 b)+Z_\nu(o)H_\nu(k_2 b)}$$

$$= \frac{H_\nu^{(1)}(\alpha)H_\nu^{(2)}(\beta) - H_\nu^{(1)}(\beta)H_\nu^{(2)}(\alpha)}{-\sqrt{\varepsilon_r}\,[H_\nu^{(1)}(\alpha)H_\nu^{(2)}{}'(\beta) - H_\nu^{(1)}{}'(\beta)H_\nu^{(2)}(\alpha)] + (H_\nu^{(1)}{}'(\gamma)/H_\nu^{(1)}(\gamma))\,[H_\nu^{(1)}(\alpha)H_\nu^{(2)}(\beta) - H_\nu^{(1)}(\beta)H_\nu^{(2)}(\alpha)]} \quad . \tag{5.50}$$

Noting that $Q(\nu)$ is a slowly varying function, the contribution to the value of the integral of (5.49) due to large values of ν will be negligible because the remaining portion of the integrand, i.e., $\frac{\sin\nu\phi_1}{\nu}\ \frac{\sin\nu\phi_2}{\nu}\cos\nu\phi_{2c}$, is highly oscillatory (and diminishing) for large ν so that the positive and negative parts of the entire integrand tend to cancel each other. It is then clear that major contribution to the value of the integral arises from small values of ν only. In Appendix J, the Debye's asymptotic approximations of Hankel functions are employed to simplify $Q(\nu)$ yielding

$$z_{12} \sim \frac{j\eta_2}{\pi b\phi_1\phi_2} \int_0^\infty \left[\frac{-k_2 \sin F(\nu)}{\sqrt{\varepsilon_r k_2^2 - (\nu/a)^2}\cos F(\nu) - j\sqrt{k_2^2 - (\nu/a)^2}\sin F(\nu)} \right] \frac{\sin\nu\phi_1}{\nu}\ \frac{\sin\nu\phi_2}{\nu}\cos\nu\phi_{2c}\, d\nu \quad , \tag{5.51}$$

where

$$F(\nu) = \sqrt{\beta^2-\nu^2} - \sqrt{\alpha^2-\nu^2} + \nu(\cos^{-1}\nu/\alpha - \cos^{-1}\nu/\beta) \quad . \tag{5.52}$$

Introducing new variable $\zeta = \nu/a$ and using the thin substrate approximations that $b\phi_\ell \simeq a\phi_\ell$, $\ell=1,2$, $b\phi_{2c} \simeq a\phi_{2c}$, and $\frac{\nu}{b} \simeq \frac{\nu}{a}$, one can rewrite (5.51) as

$$z_{12} \sim \frac{k_2\eta_2}{\pi} \int_0^\infty \frac{\sin F(a\zeta)}{\sqrt{k_2^2 - \zeta^2}\,\sin F(a\zeta) + j\sqrt{\varepsilon_r k_2^2 - \zeta^2}\,\cos F(a\zeta)} \cdot \frac{\sin a\phi_1\zeta}{a\phi_1\zeta} \cdot \frac{\sin a\phi_2\zeta}{a\phi_2\zeta} \cos a\phi_{2c}\zeta \, d\zeta \quad . \tag{5.53}$$

Recognizing that

$$F(\nu) = b\sqrt{\varepsilon_r k_2^2 - (\nu/b)^2} - a\sqrt{\varepsilon_r k_2^2 - (\nu/a)^2} + \nu\left[\cos^{-1}\left[\frac{\nu}{\sqrt{\varepsilon_r}k_2 a}\right] - \cos^{-1}\left[\frac{\nu}{\sqrt{\varepsilon_r}k_2 b}\right]\right]$$

$$+ (b-a)\sqrt{\varepsilon_r k_2^2 - \zeta^2} = t\sqrt{k_1^2 - \zeta^2} \tag{5.54}$$

as $a \to \infty$ while keeping $t=(b-a)$, $a\phi_1$, $a\phi_2$ and $a\phi_{2c}$ constant, one obtains

$$\lim_{a\to\infty} z_{12} \sim \frac{k_2\eta_2}{\pi} \int_0^\infty \frac{\sin(t\sqrt{k_1^2-\zeta^2})}{\sqrt{k_2^2-\zeta^2}\sin(t\sqrt{k_1^2-\zeta^2}) + j\sqrt{k_1^2-\zeta^2}\cos(t\sqrt{k_1^2-\zeta^2})}$$

$$\cdot \frac{\sin(a\phi_1\zeta)}{a\phi_1\zeta} \frac{\sin(a\phi_2\zeta)}{a\phi_2\zeta} \cos(a\phi_{2c}\zeta)\, d\zeta \quad . \tag{5.55}$$

which is the mutual impedance between two infinite strips on a planar dielectric slab (grounded), with widths $2a\phi_1$, $2a\phi_2$, and $a\phi_{2c}$ distance apart, just as one might have expected. (5-55) is the final form used for computing z_{12} when $b\phi_{2c}$ is small.

Case (b): $b\phi_{2c}$ is large

As just commented, z_{12} in (5.48) is most appropriately represented as a residue series:

$$z_{12} \sim \frac{-\eta_2}{4b\phi_1\phi_2} \sum_{p=1}^{\infty} \left[\frac{H_\nu^{(1)}(\gamma)}{\frac{\partial}{\partial\nu}\left[H_\nu^{(1)'}(\gamma)+Z_\nu(o)H_\nu^{(1)}(\gamma)\right]} \left[\frac{\Gamma_1(\nu)+\Gamma_2(\nu)-\Gamma_3(\nu)-\Gamma_4(\nu)}{\nu^2} \right] \right]_{\nu=\nu_p} , \tag{5.56}$$

where $\gamma=k_2 b$, and ν_p, p=1,2,3, ..., are the roots of

$$H_\nu^{(1)'}(\gamma) + Z_\nu(o)H_\nu^{(1)}(\gamma) = 0 \quad . \tag{5.57}$$

In principle, the roots of (5.57) can be located by numerical techniques. However, the problem of finding even the first root would seem to be a formidable one. It is then most desirable to be able to approximate these roots analytically.

In applications, the thickness t of the dielectric coating is much less than the radius a of the cylinder. Thus it is reasonable to assume

$$|\mu b| >> 1, \; |\mu b - \mu a| = |\mu t| < 1, \tag{5.58}$$

where the second inequality means that the dielectric subtrate is electrically thin. Then, as shown in Appendix K, it is justifiable to write

$$Z_\nu(h) \simeq - \frac{\sqrt{\epsilon_r}}{\mu t} \quad , \tag{5.59}$$

which is independent of ν. In particular,

$$Z_\nu(o) \simeq - \frac{1}{k_2 t} \triangleq Z_s \quad . \tag{5.60}$$

So it is evident that the roots of (5.57) will be reasonably approximated by the roots of

$$Y_s H_\nu^{(1)'}(\gamma) + H_\nu^{(1)}(\gamma) = 0 \quad , \tag{5.61}$$

where

$$Y_s = 1/Z_s \tag{5.62}$$

is considerably less than 1 for thin substrates. Hence one would expect the roots of (5.61) are just slightly perturbed from the zeros of $H_\nu^{(1)}(\gamma)$. It is known that the zeros of $H_\nu^{(1)}(\gamma)$ or $H_\nu^{(1)'}(\gamma)$ when $\nu \approx \gamma$, $|\gamma|$ large, are given in first approximation by the zeros of the appropriate Airy function combinations or their derivatives. This is evident when one appeals to the Watson approximations [26]:

$$H_\nu^{(1)}(\gamma) \sim -\frac{jw_1(\sigma)}{m\sqrt{\pi}} \quad , \tag{5.63}$$

$$H_\nu^{(1)'}(\gamma) \sim \frac{jw_1'(\sigma)}{m^2\sqrt{\pi}} \quad , \tag{5.64}$$

where

$$m = \left(\frac{\gamma}{2}\right)^{1/3} = \left(\frac{k_2 b}{2}\right)^{1/3} \quad , \tag{5.65}$$

$$\sigma = \frac{\nu-\gamma}{m} = \frac{\nu-k_2 b}{m} \quad , \tag{5.66}$$

$$w_1(\sigma) = \sqrt{\pi}\,(B_i(\sigma) + jA_i(\sigma)) \quad , \tag{6.67}$$

with A_i and B_i denoting the Airy functions.

Substituting (5.63) and (5.64) into (5.61) leads to

$$\left(\frac{Y_s}{m}\right) w_1'(\sigma) - w_1(\sigma) = 0 \quad . \tag{5.68}$$

It is derived in Appendix L that the roots of (5.68), when (Y_s/m) is small, can be expanded into fast converging series given below:

$$\sigma_p(d) = t_p + d + \frac{t_p}{3} d^3 + \frac{1}{4} d^4 + \frac{t_p^2}{5} d^5 + \frac{7t_p}{18} d^6 + \left[\frac{t_p^3}{7} + \frac{5}{28}\right] d^7 + \ldots, \quad p = 1,2,3 \ldots \quad , \tag{5.69}$$

where

$$d = \frac{Y_s}{m} \quad , \quad \text{with } \left|\frac{Y_s}{m}\right| << 1 \quad , \tag{5.70}$$

$$t_p = \tau_p e^{j\pi/3} \quad , \tag{5.71}$$

and τ_p are the zeros of $A_i(-\tau)$. The values of τ_p are well tabulated in Logan [29], and only the first few are listed below:

$\tau_1 = 2.3381$

$\tau_2 = 4.0879$

$\tau_3 = 5.5206$

$\tau_4 = 6.7867$

$\tau_5 = 7.9441$

$\tau_6 = 9.0227$

$\tau_7 = 10.0402$.

It is clear from transformation (5.66) that the roots of (5.61) are related to the σ_p's as follows:

$$\nu_p = k_2 b + m \sigma_p \quad , \quad p = 1,2,3, \ldots \tag{5.72}$$

Next employing the Watson approximations (5.63) and (5.64) in $Q(\nu)$ defined in (5.50) yields

$$Q(\nu) \sim \frac{-jw_1(\sigma)/(m\sqrt{\pi})}{jw_1'(\sigma)/(m^2\sqrt{\pi}) - Z_s jw_1(\sigma)/(m\sqrt{\pi})}$$

$$\sim - \frac{w_1(\sigma)}{\frac{1}{m}\left[w_1'(\sigma) - \frac{1}{d} w_1(\sigma)\right]} \quad . \tag{5.73}$$

Since $w_1(\sigma)$ satisfies the Airy differential equation, i.e.,

$$w_1''(\sigma) - \sigma w_1(\sigma) = 0 \quad , \tag{5.74}$$

one can readily verify that

$$\frac{\partial}{\partial \nu} w_1'(\sigma) = w_1''(\sigma) \frac{\partial \sigma}{\partial \nu} = \frac{\sigma w_1(\sigma)}{m} \quad . \tag{5.75}$$

Using (5.75), and the fact that

$$w_1'(\sigma_p) = \frac{m}{Y_s} w_1(\sigma_p) = \frac{1}{d} w_1(\sigma_p) \quad , \; p = 1,2,3 \ldots \; , \tag{5.76}$$

one can compute

$$\frac{\partial}{\partial \nu}\left[\frac{1}{m}\left[w_1'(\sigma) - \frac{1}{d}\, w_1(\sigma)\right]\right]_{\nu=\nu_p \text{ or } \sigma=\sigma_p} = \frac{w_1(\sigma_p)}{m^2}\left[\sigma_p - \frac{1}{d^2}\right] . \quad (5.77)$$

It follows from (5.77) that

$$\text{Res}\left[Q(\nu_p)\right] = -\frac{1}{\frac{1}{m^2}\left[\sigma_p - \frac{1}{d^2}\right]} . \quad (5.78)$$

Making use of (5.78) in (5.48) results in the following residue series representation of z_{12}:

$$z_{12} \sim \frac{\eta_2}{4b\phi_1\phi_2} \sum_{p=1}^{\infty} \frac{1}{\left[\sigma_p - \frac{1}{d^2}\right]\left[\sigma_p + k_2 b/m\right]^2} \cdot \left\{\Gamma_1(\nu_p) + \Gamma_2(\nu_p) - \Gamma_3(\nu_p) - \Gamma_4(\nu_p)\right\} . \quad (5.79)$$

Expression (5.79) is the final form used for computing z_{12}.

Employing (5.46), (5.50) in (5.36), and making use of identities (5.4) and (5.5), one can easily obtain the eigenfunction expansion of the mutual impedance between the two infinite strips, i.e.,

$$z_{12} = \frac{j\eta_2}{2\pi b\phi_1\phi_2} \sum_{n=0}^{\infty} \varepsilon_n Q(n) \frac{\sin n\phi_1}{n} \frac{\sin n\phi_2}{n} \cos n\phi_{2c} . \quad (5.80)$$

Expression (5.80) will be used to check the results obtained by (5.55) or (5.79).

AD-A154 292 MUTUAL COUPLING ANALYSIS FOR CONFORMAL MICROSTRIP ANTENNAS(U) OHIO STATE UNIV COLUMBUS ELECTROSCIENCE LAB B W KWAN ET AL. DEC 84 712692-4 N00014-78-C-0049 3/3

UNCLASSIFIED F/G 9/5 NL

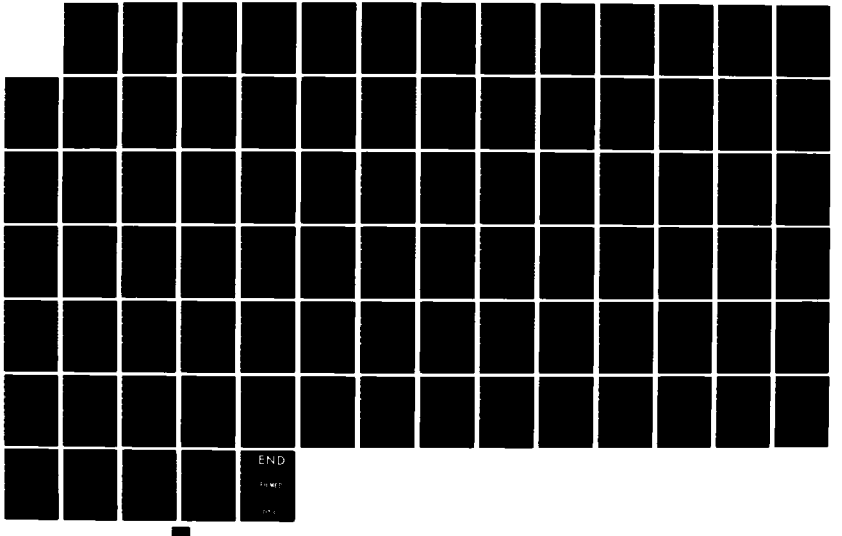

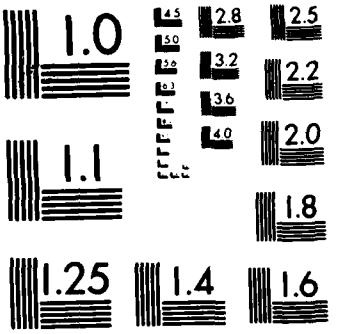

MICROCOPY RESOLUTION TEST CHART
NATIONAL BUREAU OF STANDARDS-1963-A

D. A NUMERICAL EXAMPLE

An example of mutual coupling between two infinite, z-oriented strips on a dielectric coated cylinder is presented to illustrate the effectiveness of asymptotic solutions. The antenna geometry and pertinent parameters under consideration are specified below:

current on each strip - uniform, z-directed

frequency - 300 (MHz)

λ_0 (free space wavelength) - 1. (m)

radius of conducting cylinder - 5. (m)

thickness of coating - 0.005 (m)

dielectric constant - 4.

loss tangent - 0.0001

width of each strip - 0.125 (m).

The mutual impedance z_{12} is a measure of coupling between the two strips. It is computed using two different asymptotic forms, which are the integral representation in (5.55) and the residue series in (5.79), and the exact eigenfunction expansion in (5.80) as well. The magnitude of z_{12} obtained using each representation is plotted against the separation S between the strips in Figure 5.3.

It is clear from Figure 5.3 that the coupling between strip 1 and strip 2 weakens as their separation increases. The integral representation agrees exceedingly well with the eigenfunction expansion

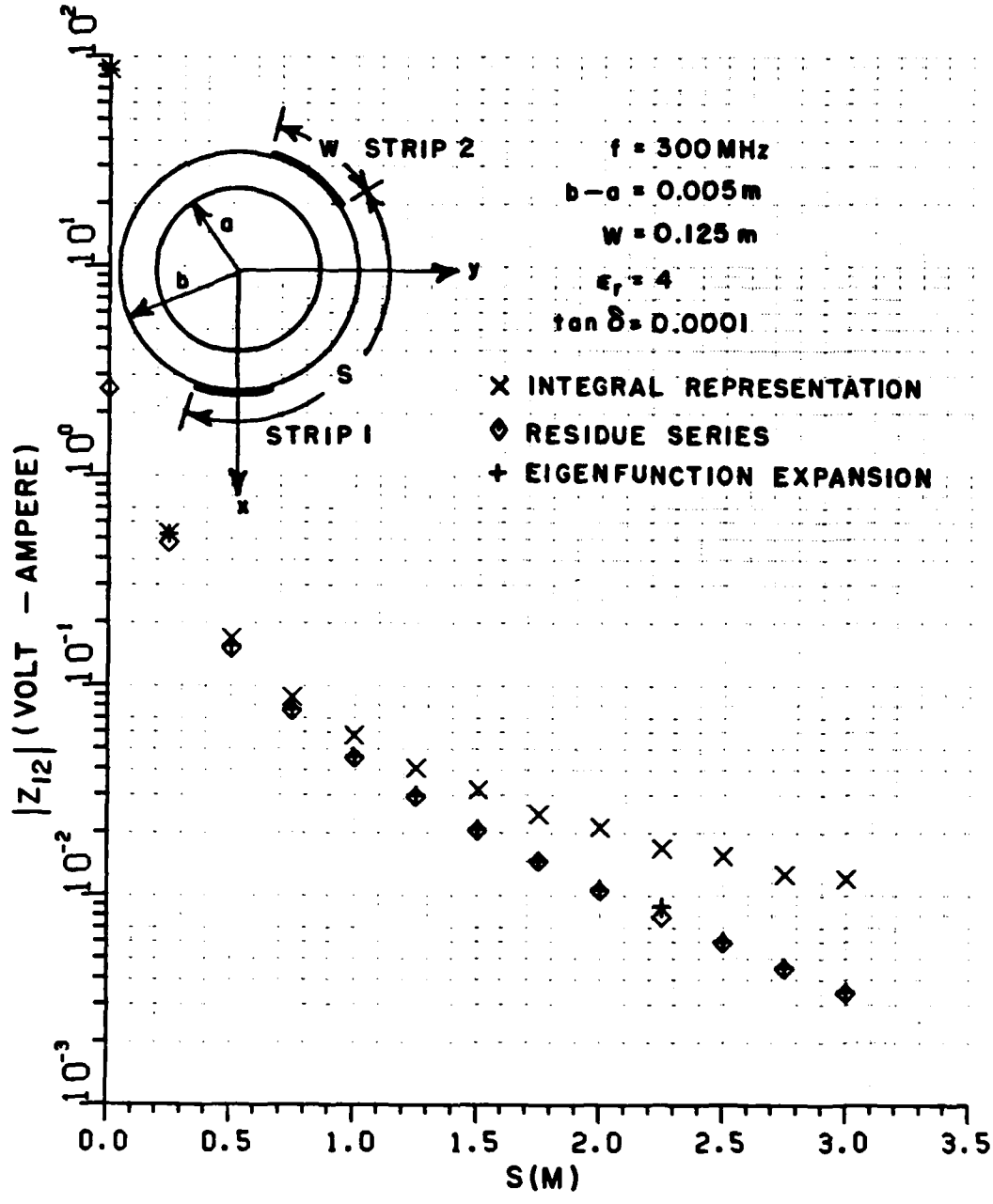

Figure 5.3. Comparison between integral representation, residue series and eigenfunction expansion of z_{12}.

for $S<0.25\lambda_0$, and they start drifting apart for $S>0.75\lambda_0$, with the former showing greater degree of coupling. This can be attributed to the fact that the integral representation stands for the coupling in the planar dielectric slab case in which no energy is shed into the surrounding space by the surface field while propagating along the air-dielectric interface, whereas in the case of the coated cylinder energy is continuously dissipated into the surrounding space while the surface field propagates around the curved surface of the cylinder. Hence coupling becomes gradually weaker as strip 2 moves deeper into the shadow region of strip 1. The residue series, on the other hand, shows excellent agreement with the eigenfunction expansion for $S>0.75\lambda_0$. The number of terms required in the series decreases as S increases. When $S=2\lambda_0$, for instance, 3 creeping wave modes are used, and only 1 creeping wave mode is needed when $S=3\lambda_0$. In the other extreme, a total of 56 modes are summed for $S<0.25\lambda_0$. It is quite apparent that a considerably large number of modes will be required to provide a good approximation of z_{12} when S=0. It may be noticed that the overlapping region for these two asymptotic representations is $0.25\lambda_0<S<0.75\lambda_0$.

CHAPTER VI

SUMMARY

Mutual coupling analysis is important in the design of antenna arrays with low sidelobes, or where other tight control of the radiation pattern is required. This work presents an analysis of the mutual coupling between conformal microstrip antennas for the following configurations:

1) rectangular microstrip patches printed on a grounded planar dielectric slab (the planar slab problem), and

2) rectangular microstrip patches printed on a dielectric coated cylinder (the coated cylinder problem).

It should be noted that the method of analysis proposed here can be applied to microstrip patches of arbitrary shape; although rectangular patches are treated for the sake of simplicity.

In analyzing the radiation or scattering from an array, one can formulate the problem as an integral equation in terms of the unknown currents flowing on the array elements. In the case of the microstrip array, this integral equation would contain in it's kernel the grounded

dielectric slab Green's function (planar slab problem) or the dielectric coated cylinder Green's function (coated cylinder problem). The moment method, which transforms the integral equation into a system of simultaneous equations, is the technique proposed to numerically solve this integral equation. In setting up the moment method solution, a crucial step is the calculation of the self and mutual impedances between the expansion and test modes. The central theme of this work is the efficient computation of these moment method quantities. A model has been provided to relate the moment method modal impedances to the port impedances of the microstrip antenna array under consideration.

For the planar slab problem, a moment method solution for microstrip antennas using the rigorous grounded dielectric slab Green's function has been presented. Piecewise sinusoids are chosen as expansion and test modes. Good agreement between calculated and measured values of mutual coupling has been shown. An expression for the far field radiation pattern has been derived via the method of stationary phase.

It has been demonstrated that the coated cylinder problem can be solved using two different approaches. The first approach utilizes the Green's function restricted to the case where the currents are tangential to and also situated at the surface of the dielectric coated cylinder. The fact that the source is being introduced only through the boundary conditions simplifies the calculation. This is similar to the method of solution for the planar slab problem. The second approach is

based on the dyadic Green's function for the dielectric coated cylinder. The use of the Green's dyadic enables one to solve a larger class of problems since the source can be arbitrary, and is not restricted to the surface of the coated cylinder. For this reason the Green's dyadic is employed in this mutual coupling analysis, with the idea that it may be extended to a more general configuration later.

The dyadic Green's function for the coated cylinder has been constructed using the principle of scattering superposition which requires the complete expansion of the free space dyadic Green's function. The structure of the free space Green's dyadic has been characterized for a general orthogonal curvilinear system. It is shown that the Green's dyadic can be cast in a form that consists of two solenoidal components, and an irrotational component which has the simple form of a dyadic delta function. This compact form permits one to obtain the eigenfunction expansion of the Green's dyadic most easily, since only the solenoidal vector wave functions are involved in the expansion. This expansion process is further facilitated by a new set of orthogonality conditions which do not involve the ρ coordinate.

Very general expressions for the elements of the impedance matrix and voltage vector (in the moment method solution) have been presented. Self and mutual impedances of an expansion mode on dielectric coated cylinders of various radii have been calculated. The results converge to that of the infinite planar slab case as the radius of cylinder increases, just as one expects. Mutual impedances, between two expansion modes, on coated cylinders of various radii have also been

computed. As expected, the magnitude of the mutual impedance decreases as the separation between the modes increases, or as the cylinder radius decreases. Expressions for the far field radiation pattern have been obtained using the steepest descent integration technique.

All of the above calculations for the coated cylinder problem are based upon eigenfunction expansions derived using the dyadic Green's function which is of the radially propagating type. These eigenfunction expansions are poorly convergent when the coated cylinder radius becomes electrically large. For large cylinders asymptotic high frequency solutions are preferable, because they are computationally more efficient, and can be interpreted in terms of ray-optics. An essential step in deriving asymptotic solutions for the coated cylinder problem has been the conversion of the radially propagating Green's dyadic into a circumferentially propagating type by using the Poisson summation formula. Thereby alternative expressions for the mutual impedance between two expansion modes have been obtained. These include the residue series which lends itself to ray-optical interpretation, and the integral representation which is in a form more suitable for asymptotic evaluation. A numerical example of coupling between two infinite conducting strips on a cylinder with thin dielectric coating has been presented. This example serves to illustrate the validity and power of asymptotic solutions.

This work presents an effective approach for analyzing coupling between conformal microstrip antennas by combining the Green's function theory and the moment method. Only a narrow aspect of the coupling problem has been considered. It is by no means complete. The following areas are recommended for future investigation:

1. Extending the aysmptotic solution of the mutual impedance between infinite strips to the case of finite length patches.

2. Rigorous modeling of source excitation (which requires the Green's function corresponding to source inside the dielectric).

3. Generation of data on microstrip antenna characteristics such as input impedance, radiation pattern and gain for practical design purposes.

APPENDIX A

DETERMINATION OF SPECTRAL FUNCTIONS

Expanding Equations (2.2) and (2.3) in rectangular coordinates and making use of (2.4) and (2.5) yields the following:

In region 1 (dielectric),

$$E_{x1}(\bar{r}) = -\frac{\partial}{\partial y}\psi_{e1} + \frac{1}{j\omega\varepsilon_1}\frac{\partial^2}{\partial x \partial z}\psi_{m1}$$

$$= \frac{j}{4\pi^2}\iint_{-\infty}^{\infty}\left\{k_y\tilde{\psi}_{e1} - \frac{j}{\omega\varepsilon_1}k_x k_{z1}\tilde{\psi}_{m1}\right\} e^{-j(k_x x + k_y y)} \sin k_{z1}(z+t)\,dk_x dk_y \,, \tag{A.1}$$

$$E_{y1}(\bar{r}) = \frac{\partial}{\partial x}\psi_{e1} + \frac{1}{j\omega\varepsilon_1}\frac{\partial^2}{\partial y \partial x}\psi_{m1}$$

$$= \frac{-j}{4\pi^2}\iint_{-\infty}^{\infty}\left\{k_x\tilde{\psi}_{e1} + \frac{j}{\omega\varepsilon_1}k_y k_{z1}\tilde{\psi}_{m1}\right\} e^{-j(k_x x + k_y y)} \sin k_{z1}(z+t)\,dk_x dk_y \,, \tag{A.2}$$

$$E_{z1}(\bar{r}) = \frac{1}{j\omega\epsilon_1}\left[\frac{\partial^2}{\partial z^2} + \epsilon_r k_o^2\right]\psi_{m1}$$

$$= \frac{-j}{4\pi^2}\int\int_{-\infty}^{\infty}\frac{[k_x^2 + k_y^2]}{\omega\epsilon_1}\ \tilde{\psi}_{m1}\, e^{-j(k_x x + k_y y)}\cos k_{z1}(z+t)\,dk_x dk_y\ , \tag{A.3}$$

$$H_{x1}(\bar{r}) = \frac{1}{j\omega\mu_o}\frac{\partial^2}{\partial x \partial z}\psi_{e1} + \frac{\partial}{\partial y}\psi_{m1}$$

$$= \frac{j}{4\pi^2}\int\int_{-\infty}^{\infty}\left[\frac{jk_x k_{z1}}{\omega\mu_0}\ \tilde{\psi}_{e1} - k_y\tilde{\psi}_{m1}\right]\cos k_{z1}(z+t)\, e^{-j(k_x x + k_y y)}\,dk_x dk_y\ . \tag{A.4}$$

$$H_{y1}(\bar{r}) = \frac{1}{j\omega\mu_o}\frac{\partial^2}{\partial y \partial z}\psi_{e1} - \frac{\partial}{\partial x}\psi_{m1}$$

$$= \frac{+j}{4\pi^2}\int\int_{-\infty}^{\infty}\left[\frac{jk_y k_{z1}}{\omega\mu_0}\ \tilde{\psi}_{e1} + k_x\tilde{\psi}_{m1}\right] e^{-j(k_x x + k_y y)}\cos k_{z1}(z+t)\,dk_x dk_y\ , \tag{A.5}$$

$$H_{z1}(\bar{r}) = \frac{1}{j\omega\mu_0}\left(\frac{\partial^2}{\partial z^2} + \epsilon_r k_o^2\right)\psi_{e1}$$

$$= \frac{-j}{4\pi^2}\int\int_{-\infty}^{\infty}\frac{1}{\omega\mu_0}(k_x^2 + k_y^2)\ \tilde{\psi}_{e1}\, e^{-j(k_x x + k_y y)}\sin k_{z1}(z+t)\,dk_x dk_y\ . \tag{A.6}$$

In region 2 (air),

$$E_{x2}(\bar{r}) = -\frac{\partial}{\partial y}\psi_{e2} + \frac{1}{j\omega\varepsilon_2}\frac{\partial^2}{\partial x \partial z}\psi_{m2}$$

$$= \frac{j}{4\pi^2}\int\int_{-\infty}^{\infty}\{k_y\tilde{\psi}_{e2} + \frac{k_x k_{z2}}{\omega\varepsilon_2}\tilde{\psi}_{m2}\}\, e^{-j(k_x x + k_y y + k_{z2} z)}\, dk_x dk_y \,, \tag{A.7}$$

$$E_{y2}(\bar{r}) = \frac{\partial}{\partial x}\psi_{e2} + \frac{1}{j\omega\varepsilon_2}\frac{\partial^2}{\partial y \partial z}\psi_{m2}$$

$$= \frac{-j}{4\pi^2}\int\int_{-\infty}^{\infty}\{k_x\tilde{\psi}_{e2} - \frac{k_y k_{z2}}{\omega\varepsilon_2}\tilde{\psi}_{m2}\}\, e^{-j(k_x x + k_y y + k_{z2} z)}\, dk_x dk_y \,, \tag{A.8}$$

$$E_{z2}(\bar{r}) = \frac{1}{j\omega\varepsilon_2}\left(\frac{\partial^2}{\partial z^2} + k_o^2\right)\psi_{e2}$$

$$= \frac{-j}{4\pi^2}\int\int_{-\infty}^{\infty}\frac{(k_x^2 + k_y^2)}{\omega\varepsilon_2}\tilde{\psi}_{e2}\, e^{-j(k_x x + k_y y + k_{z2} z)}\, dk_x dk_y \,, \tag{A.9}$$

$$H_{x2}(\bar{r}) = \frac{1}{j\omega\mu_o}\frac{\partial^2}{\partial x \partial z}\psi_{e2} + \frac{\partial}{\partial y}\psi_{m2}$$

$$= \frac{j}{4\pi^2}\int\int_{-\infty}^{\infty}\left[\frac{k_x k_{z2}}{\omega\mu_o}\tilde{\psi}_{e2} - k_y\tilde{\psi}_{m2}\right] e^{-j(k_x x + k_y y + k_{z2} z)}\, dk_x dk_y \,, \tag{A.10}$$

$$H_{y2}(\bar{r}) = \frac{1}{j\omega\mu_o} \frac{\partial^2}{\partial y \partial z} \psi_{e2} - \frac{\partial}{\partial x} \psi_{m2}$$

$$= \frac{j}{4\pi^2} \int\int_{-\infty}^{\infty} \left[\frac{k_y k_{z2}}{\omega\mu_0} \tilde{\psi}_{e2} + k_x \tilde{\psi}_{m2} \right] e^{-j(k_x x + k_y y + k_{z2} z)} dk_x dk_y \,, \tag{A.11}$$

$$H_{z2}(\bar{r}) = \frac{1}{j\omega\mu_0} \left(\frac{\partial^2}{\partial z^2} + k_o^2 \right) \psi_{e2}$$

$$= \frac{-j}{4\pi^2} \int\int_{-\infty}^{\infty} \frac{(k_x^2 + k_y^2)}{\omega\mu_0} \tilde{\psi}_{e2} e^{-j(k_x x + k_y y + k_{z2} z)} dk_x dk_y \,. \tag{A.12}$$

Enforcing the boundary conditions at z=0 (dielectric-air interface) specified by Equations (2.8) and (2.9) leads to

$$E_{x1} = E_{x2} \qquad \text{at} \quad z = 0 \tag{A.13}$$

$$E_{y1} = E_{y2} \qquad \text{at} \quad z = 0 \tag{A.14}$$

$$H_{x2} - H_{x1} = J_{sy} \qquad \text{at} \quad z = 0 \tag{A.15}$$

$$-H_{y2} + H_{y1} = J_{sx} \qquad \text{at} \quad z = 0 \,. \tag{A.16}$$

Use of Equations (A.13), (A.1) and (A.7) gives

$$k_y \tilde{\psi}_{e2} + \frac{k_x k_{z2}}{\omega\varepsilon_0} \tilde{\psi}_{m2} = \left[k_y \tilde{\psi}_{e1} - \frac{j}{\omega\varepsilon_0\varepsilon_r} k_x k_{z1} \tilde{\psi}_{m1}\right] \sin k_{z1} t \quad . \qquad (A.17)$$

Similarly, use of (A.14), (A.2) and (A.8) gives

$$k_x \tilde{\psi}_{e2} - \frac{k_y k_{z2}}{\omega\varepsilon_0} \tilde{\psi}_{m2} = \left[k_x \tilde{\psi}_{e1} + \frac{j}{\omega\varepsilon_0\varepsilon_r} k_x k_{z1} \tilde{\psi}_{m1}\right] \sin k_{z1} t \quad . \qquad (A.18)$$

Use of (A.15), (A.4), (A.10) and (2.10) gives

$$\left[\frac{k_x k_{z2}}{\omega\mu_0} \tilde{\psi}_{e2} - k_y \tilde{\psi}_{m2}\right] - \left[\frac{jk_x k_{z1}}{\omega\mu_0} \tilde{\psi}_{e1} - k_y \tilde{\psi}_{m1}\right] \cos k_{z1} t = -j\tilde{J}_{sy} \quad . \qquad (A.19)$$

Use of (A.16), (A.5), (A.11) and (2.10) gives

$$-\left[\frac{k_y k_{z2}}{\omega\mu_0} \tilde{\psi}_{e2} + k_x \tilde{\psi}_{m2}\right] + \left[\frac{jk_y k_{z1}}{\omega\mu_0} \tilde{\psi}_{e1} + k_x \tilde{\psi}_{m1}\right] \cos k_{z1} t = -j\tilde{J}_{sx} \quad . \qquad (A.20)$$

Adding (A.17) multiplied by k_y to (A.18) multiplied by k_x yields

$$(k_x^2 + k_y^2)\tilde{\psi}_{e2} = (k_x^2 + k_y^2)\tilde{\psi}_{e1} \sin k_{z1} t$$

$$\tilde{\psi}_{e2} = \sin k_{z1} t \, \tilde{\psi}_{e1} \quad . \qquad (A.21)$$

Adding (A.17) multiplied by k_x to (A.18) multiplied by $(-k_y)$ yields

$$\frac{(k_x^2 + k_y^2)\, k_{z2}}{\omega\varepsilon_0} \tilde{\psi}_{m2} = \frac{-jk_{z1}}{\omega\varepsilon_0\varepsilon_r} (k_x^2 + k_y^2)\, \tilde{\psi}_{m1} \sin k_{z1}t$$

$$\tilde{\psi}_{m2} = \frac{-jk_{z1}}{\varepsilon_r k_{z2}} \sin k_{z1}t\, \tilde{\psi}_{m1} \quad . \tag{A.22}$$

Adding (A.19) multiplied by k_x to (A.20) multiplied by $(-k_y)$ yields

$$\frac{k_{z2}}{\omega\mu_0} (k_x^2 + k_y^2)\tilde{\psi}_{e2} - j \frac{k_{z1}}{\omega\mu_0} (k_x^2 + k_y^2)\cos k_{z1}t\, \tilde{\psi}_{e1} = j[k_y\tilde{J}_{sx} - k_x\tilde{J}_{sy}]$$

$$\frac{(k_x^2 + k_y^2)}{\omega\mu_0} [k_{z1}\cos k_{z1}t\,\tilde{\psi}_{e1} + jk_{z2}\tilde{\psi}_{e2}] = k_x\tilde{J}_{sy} - k_y\tilde{J}_{sx} \quad . \tag{A.23}$$

Adding (A.19) multiplied by k_y to (A.20) multiplied by k_x yields

$$-(k_x^2 + k_y^2)\tilde{\psi}_{m2} + (k_x^2 + k_y^2)\tilde{\psi}_{m1}\cos k_{z1}t = -j[k_y\tilde{J}_{sy} + k_x\tilde{J}_{sx}]$$

$$(k_x^2 + k_y^2)[-\tilde{\psi}_{m2} + \tilde{\psi}_{m1}\cos k_{z1}t] = -j[k_y\tilde{J}_{sy} + k_x\tilde{J}_{sx}] \quad . \tag{A.24}$$

Using (A.21) in (A.23) leads to

$$\tilde{\psi}_{e1} = \frac{\omega\mu_0}{(k_x^2 + k_y^2)D_e} [k_x\tilde{J}_{sy} - k_y\tilde{J}_{sx}] \tag{A.25}$$

$$\tilde{\psi}_{e2} = \frac{\omega\mu_0 \sin k_{z1} t}{(k_x^2 + k_y^2) D_e} \left[k_x \tilde{J}_{sy} - k_y \tilde{J}_{sx}\right] \qquad \text{(A.26)}$$

where

$$D_e = k_{z1} \cos k z_1 t + j k_{z2} \sin k_{z1} t \quad . \qquad \text{(A.27)}$$

Using (A.22) in (A.24) leads to

$$\tilde{\psi}_{m1} = \frac{-j\varepsilon_r k_{z2}}{(k_x^2 + k_y^2) D_m} \left[k_x \tilde{J}_{sx} + k_y \tilde{J}_{sy}\right] \qquad \text{(A.28)}$$

$$\tilde{\psi}_{m2} = \frac{-k_{z1} \sin k_{z1} t}{(k_x^2 + k_y^2) D_m} \left[k_x \tilde{J}_{sx} + k_y \tilde{J}_{sy}\right] \qquad \text{(A.29)}$$

where

$$D_m = \varepsilon_r k_{z2} \cos k_{z1} t + j k_{z1} \sin k_{z1} t \quad . \qquad \text{(A.30)}$$

APPENDIX B

MUTUAL IMPEDANCE BETWEEN TWO EXPANSION (DIPOLE) MODES

In this appendix, the exact expressions for the mutual impedance between two surface expansion dipole modes on a lossy grounded dielectric slab are presented. The mutual impedance between an expansion dipole mode and an impressed source current, required in (2.46), will also be presented.

Figure B.1 shows two dipole modes of current densities $\bar{J}_m$ and $\bar{J}_n$, located on the surface of a grounded dielectric slab with parameters μ_o and $\varepsilon_r\varepsilon_o$. The ambient medium is free space with parameters μ_o and ε_o. Mode m is centered with respect to the (x,y) coordinate system. The center of mode n coincides with the origin of the (x',y') system which is displaced from the center of mode m by a position vector (x_o,y_o). The x'-axis is at an angle α with respect to the x-axis.

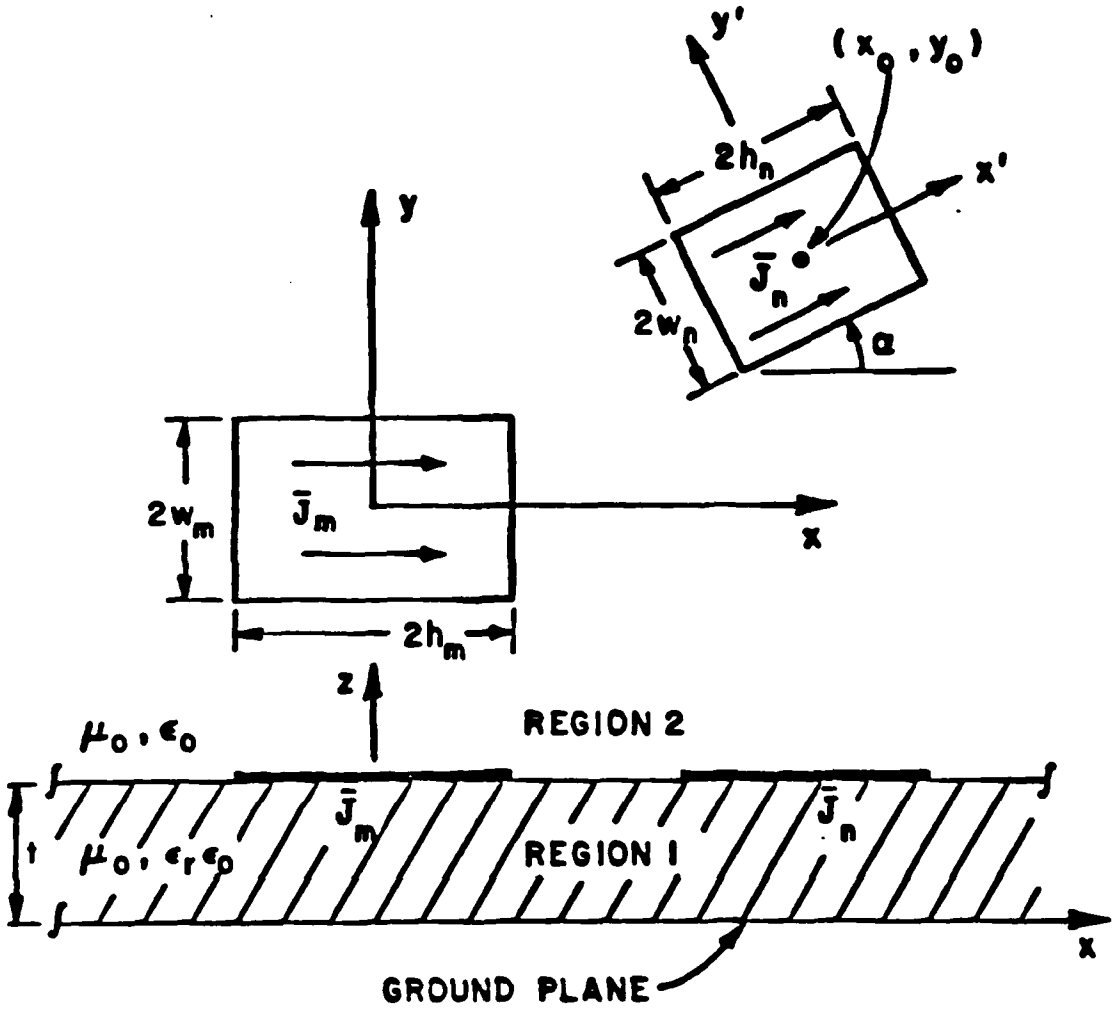

Figure B.1. Two expansion dipole modes on a grounded dielectric slab.

The mutual impedance between modes m and n is given by

$$z_{mn} = - \int_n \bar{E}_m(\bar{r}_o+\bar{r}') \cdot \bar{J}_n(\bar{r}')ds' \tag{B.1}$$

where the integration is over the surface of mode n in the z=0 plane; and

$$\bar{r}' = \hat{x}'x' + \hat{y}'y' = \hat{x}(x'\cos\alpha - y'\sin\alpha) + \hat{y}(x'\sin\alpha + y'\cos\alpha) \tag{B.2}$$

$$\bar{r}_o = \hat{x}x_o + \hat{y}y_o \quad . \tag{B.3}$$

Without loss of generality, it is assumed that

$$\bar{J}_m(\bar{r}) = \hat{x}J_{mx}(\bar{r}) + \hat{y}J_{my}(\bar{r}) \tag{B.4}$$

where $\bar{r} = \hat{x}x + \hat{y}y$ and

$$\bar{J}_n(\bar{r}') = \hat{x}'J_{nx'}(\bar{r}') + \hat{y}'J_{ny'}(\bar{r}') \quad . \tag{B.5}$$

It then follows from (2.17), (2.18), (2.24) and (2.26) that, at z=0,

$$E_{mx}(\bar{r}_o+\bar{r}') = \frac{j}{4\pi^2} \iint_{-\infty}^{\infty} [k_y \tilde{\psi}_{e2} + \frac{k_x k_{z2}}{\omega\epsilon_0} \tilde{\psi}_{m2}] e^{-j(k_x x_o + k_y y_o)}$$

$$\cdot e^{-j\phi(x',y',\alpha)} \, dk_x dk_y \tag{B.6}$$

$$E_{my}(\bar{r}_o+\bar{r}') = \frac{-j}{4\pi^2} \iint_{-\infty}^{\infty} [k_x \tilde{\psi}_{e2} - \frac{k_y k_{z2}}{\omega\varepsilon_0} \tilde{\psi}_{m2}] e^{-j(k_x x_o + k_y y_o)}$$

$$\cdot e^{-j\phi(x',y',\alpha)} \, dk_x dk_y \qquad (B.7)$$

where

$$k_{z2} = \sqrt{k_o^2 - k_x^2 - k_y^2} \quad , \; \mathrm{Im}k_{z2} < 0, \; \mathrm{Re}k_{z2} > 0 \quad , \qquad (B.8)$$

$$\phi(x',y',\alpha) = x'(k_x \cos\alpha + k_y \sin\alpha) + y'(-k_x \sin\alpha + k_y \cos\alpha) \quad , \qquad (B.9)$$

$$\tilde{\psi}_{e2} = \frac{\omega\mu_0 \sin k_{z1} t}{(k_x^2+k_y^2) D_e} [k_x \tilde{J}_{my} - k_y \tilde{J}_{mx}] \quad , \qquad (B.10)$$

$$\tilde{\psi}_{m2} = \frac{-k_{z1} \sin k_{z1} t}{(k_x^2+k_y^2) D_m} [k_x \tilde{J}_{my} + k_y \tilde{J}_{mx}] \quad , \qquad (B.11)$$

$$k_{z1} = \sqrt{\varepsilon_r k_o^2 - k_x^2 - k_y^2} \quad , \qquad (B.12)$$

$$D_e = k_{z1} \cos k_{z1} t + j k_{z2} \sin k_{z1} t \quad , \qquad (B.13)$$

$$D_m = \varepsilon_r k_{z2} \cos k_{z1} t + j k_{z1} \sin k_{z1} t \quad , \qquad (B.14)$$

$$\tilde{J}_{mx}(k_x,k_y) = \iint_{-\infty}^{\infty} J_{mx}(x,y) e^{j(k_x x + k_y y)} \, dxdy \quad , \qquad (B.15)$$

and

$$\tilde{J}_{my}(k_x,k_y) = \int_{-\infty}^{\infty}\int J_{my}(x,y)e^{j(k_x x+k_y y)}\,dxdy \quad . \tag{B.16}$$

Also one may note that the tangential component of $\bar{E}_m(\bar{r}_o+\bar{r}')$ on the surface of mode n is given by

$$\begin{aligned}\bar{E}_m^t(\bar{r}_o+\bar{r}') &= \hat{x}E_{mx}(\bar{r}_o+\bar{r}') + \hat{y}E_{my}(\bar{r}_o+\bar{r}') \\ &= \hat{x}'[E_{mx}(\bar{r}_o+\bar{r}')\cos\alpha + E_{my}(\bar{r}_o+\bar{r}')\sin\alpha] \\ &\quad + \hat{y}'[-E_{mx}(\bar{r}_o+\bar{r}')\sin\alpha + E_{my}(\bar{r}_o+\bar{r}')\cos\alpha] \quad .\end{aligned} \tag{B.17}$$

Combining (B.1), (B.5) and (B.17) yields

$$\begin{aligned}z_{mn} = -\int_{-h_n}^{h_n}\int_{-w_n}^{w_n} \{&[E_{mx}(\bar{r}_o+\bar{r}')\cos\alpha + E_{my}(\bar{r}_o+\bar{r}')\sin\alpha]J_{nx'}(x',y') \\ &+ [-E_{mx}(\bar{r}_o+\bar{r}')\sin\alpha + E_{my}(\bar{r}_o+\bar{r}')\cos\alpha]J_{ny'}(x',y')\}dy'dx' \quad .\end{aligned} \tag{B.18}$$

Next let

$$\begin{aligned}\tilde{J}_{nx'}(k_x,k_y,\alpha) &= \int_{-h_n}^{h_n}\int_{-w_n}^{w_n} J_{nx'}(x',y')e^{-j\phi(x',y',\alpha)}dy'dx' \\ &= \int_{-h_n}^{h_n}\int_{-w_n}^{w_n} J_{nx'}(x',y') \\ &\quad \cdot e^{-j[x'(k_x\cos\alpha+k_y\sin\alpha)+y'(-k_x\sin\alpha+k_y\cos\alpha)]}dy'dx'\end{aligned} \tag{B.19}$$

and

$$\tilde{J}_{ny'}(k_x,k_y,\alpha) = \int_{-h_n}^{h_n}\int_{-w_n}^{w_n} J_{ny'}(x',y')e^{-j\phi(x',y',\alpha)}dy'dx'$$

$$= \int_{-h_n}^{h_n}\int_{-w_n}^{w_n} J_{ny'}(x',y') \cdot e^{-j[x'(k_x\cos\alpha+k_y\sin\alpha)+y'(-k_x\sin\alpha+k_y\cos\alpha)]}dy'dx' \quad . \qquad (B.20)$$

Use of (B.6), (B.7), (B.19) and (B.20) in (B.18) leads to

$$z_{mn} = -\frac{j}{4\pi^2}\int_{-\infty}^{\infty}\int \left[\left[\left[(k_y\tilde{\psi}_{e2} + \frac{k_xk_{z2}}{\omega\varepsilon_0}\tilde{\psi}_{m2})\cos\alpha - (k_x\tilde{\psi}_{e2} - \frac{k_yk_{z2}}{\omega\varepsilon_0}\tilde{\psi}_{m2})\sin\alpha\right]\tilde{J}_{nx'}(k_x,k_y,\alpha)\right.\right.$$

$$\left.\left. - \left[(k_y\tilde{\psi}_{e2} + \frac{k_xk_{z2}}{\omega\varepsilon_0}\tilde{\psi}_{m2})\sin\alpha + (k_x\tilde{\psi}_{e2} - \frac{k_yk_{z2}}{\omega\varepsilon_0}\tilde{\psi}_{m2})\cos\alpha\right]\right.\right.$$

$$\left.\left. \cdot \tilde{J}_{ny'}(k_x,k_y,\alpha)\right]\right] e^{-j(k_xx_o + k_yy_o)}dk_xdk_y \quad . \qquad (B.21)$$

The mutual impedance between expansion dipole mode $\bar{E}_m$ and source current $\bar{J}_i$ can be computed according to (2.46)

$$V_m = \int_V \bar{E}_m(\bar{r}) \cdot \bar{J}_i(\bar{r})dv \quad . \qquad (B.22)$$

Since source $\bar{J}_i$ is modeled as a vertical filament of constant current inside the dielectric, it can be represented as

$$\bar{J}_i(\bar{r}) = \hat{z} I_i \delta(x-x_f)\delta(y-y_f) \quad , \; -\infty<x,y<\infty \; , \; -t<z<0 \tag{B.23}$$

where I_i is the magnitude of the feed current and (x_f,y_f) denotes the filament location in the x-y plane, with respect to the center of mode m.

Making use of (2.13), one can write

$$E_{mz}(\bar{r}) = \frac{-j}{4\pi^2} \iint_{-\infty}^{\infty} \frac{(k_x^2+k_y^2)}{\omega\varepsilon_0\varepsilon_r} \tilde{\psi}_{m1} \, e^{-j(k_x x+k_y y)} \cos k_{z1}(z+t) dk_x dk_y \; . \tag{B.24}$$

Inserting (B.23) and (B.24) into (B.22) and carrying out the volume integration gives

$$V_m = \frac{-jI_i}{4\pi^2} \iint_{-\infty}^{\infty} \frac{(k_x^2+k_y^2)}{\omega\varepsilon_0\varepsilon_r k_{z1}} \tilde{\psi}_{m1} \, e^{-j(k_x x_f+k_y y_f)} \sin k_{z1} t \, dk_x dk_y \; . \tag{B.25}$$

In both (B.24) and (B.25)

$$\tilde{\psi}_{m1} = - \frac{j\varepsilon_r k_{z2}}{(k_x^2+k_y^2)D_m} \left[k_x \tilde{J}_{mx} + k_y \tilde{J}_{my}\right] \; . \tag{B.26}$$

APPENDIX C

EVALUATION OF AN OSCILLATORY INTEGRAL BY THE STATIONARY PHASE METHOD

This appendix presents the derivation of the leading term of the asymptotic expansion of an oscillatory integral of the form

$$\bar{E}(\bar{r}) = \frac{1}{4\pi^2} \int_{-\infty}^{\infty}\int \bar{f}(k_x,k_y)\, e^{-j\bar{k}\cdot\bar{r}}\, dk_x dk_y \qquad (C.1)$$

where $\bar{r} = \hat{x}x+\hat{y}y+\hat{z}z$; $\bar{k} = \hat{x}k_x+\hat{y}k_y+\hat{z}k_z$ with $|\bar{k}| = k_o$; and $\bar{f}$ is a slowly varying vector function of k_x and k_y, and has no singularity near the stationary points of $\bar{k}\cdot\bar{r}$.

Equation (C.1) is a 2-D Fourier transform which can be evaluated asymptotically by the method of stationary phase. The method of stationary phase, simply stated, is based on the fact that, as $|\bar{r}| \to \infty$, the dominant contribution to the integral in (C.1) arises from the neighborhood of those values of k_x and k_y which make the phase $\bar{k}\cdot\bar{r}$ stationary, i.e., $\bar{k}\cdot\bar{r}$ does not change for first-order changes in k_x and

k_y. For those values of k_x and k_y that make the phase $\bar{k}\cdot\bar{r}$ vary rapidly, the integrand oscillates rapidly between equal positive and negative values, and the contribution to the value of the integral is small.

First it is noted that $k_z = \sqrt{k_o^2 - k_x^2 - k_y^2}$ and

$$\bar{k}\cdot\bar{r} = r\left[k_x \sin\theta\cos\phi + k_y \sin\theta\sin\phi + \sqrt{k_o^2 - k_x^2 - k_y^2}\,\cos\theta\right] \tag{C.2}$$

where θ and ϕ are the usual angle variables in spherical coordinates. The stationary phase points are determined by a solution of

$$\frac{\partial}{\partial k_x}\,\bar{k}\cdot\bar{r} = 0 \tag{C.3}$$

$$\frac{\partial}{\partial k_y}\,\bar{k}\cdot\bar{r} = 0 \quad . \tag{C.4}$$

Using (C.2) in (C.3) and (C.4) leads to

$$k_x = \frac{k_z \sin\theta\cos\phi}{\cos\theta} \tag{C.5}$$

$$k_y = \frac{k_z \sin\theta\sin\phi}{\cos\theta} \quad . \tag{C.6}$$

Since $k_x^2 + k_y^2 = k_o^2 - k_z^2$, it is seen that

$$k_z^2 \frac{\sin^2\theta}{\cos^2\theta} = k_o^2 - k_z^2$$

and hence

$$k_z = k_o \cos\theta \quad . \tag{C.7}$$

Substituting (C.7) into (C.5) and (C.6) yields the stationary values of k_x and k_y given below:

$$k_{xo} = k_o \sin\theta\cos\phi \tag{C.8}$$

$$k_{yo} = k_o \sin\theta\sin\phi \tag{C.9}$$

provided $\theta \neq \pi/2$. In the vicinity of the stationary phase point (k_{xo},k_{yo}) $\bar{k}\cdot\bar{r}$ can be approximated by the first few terms of its Taylor series, i.e.,

$$\bar{k}\cdot\bar{r} \simeq \bar{k}\cdot\bar{r}\Big|_{(k_{xo},k_{yo})} + \left[(k_x-k_{xo})\frac{\partial}{\partial k_x} + (k_y-k_{yo})\frac{\partial}{\partial k_y}\right]\bar{k}\cdot\bar{r}\Big|_{(k_{xo},k_{yo})}$$

$$+ \frac{1}{2}\left[(k_x-k_{xo})\frac{\partial}{\partial k_x} + (k_y-k_{yo})\frac{\partial}{\partial k_y}\right]^2 \bar{k}\cdot\bar{r}\Big|_{(k_{xo},k_{yo})} \quad . \tag{C.10}$$

(It should be noted that only the partial derivatives in (C.10) are evaluated at (k_{xo},k_{yo}).)

It can be shown that

$$\frac{\partial^2}{\partial k_x^2}\,\bar{k}\cdot\bar{r}\,\Big|_{(k_{xo},k_{yo})} = -\,r\cos\theta\,\left(\frac{1}{k_z}+\frac{k_x^2}{k_z^3}\right)\Big|_{(k_{xo},k_{yo})}$$

$$= -\,\frac{r}{k_0\cos^2\theta}\,(\cos^2\theta+\sin^2\theta\cos^2\phi)$$

$$\frac{\partial^2}{\partial k_y^2}\,\bar{k}\cdot\bar{r}\,\Big|_{(k_{xo},k_{yo})} = -\,r\cos\theta\,\left(\frac{1}{k_z}+\frac{k_y^2}{k_z^3}\right)\Big|_{(k_{xo},k_{yo})}$$

$$= -\,\frac{r}{k_0\cos^2\theta}\,(\cos^2\theta+\sin^2\theta\sin^2\phi)$$

$$\frac{\partial^2}{\partial k_x\partial k_y}\,\bar{k}\cdot\bar{r}\,\Big|_{(k_{xo},k_{yo})} = -\,r\cos\theta\,\frac{k_xk_y}{k_z^3}\Big|_{(k_{xo},k_{yo})}$$

$$= -\,\frac{r}{k_0\cos^2\theta}\,\sin^2\theta\sin\phi\cos\phi \qquad .$$

Consequently the phase can be written as

$$\bar{k}\cdot\bar{r} = k_0r - A(k_x-k_{xo})^2-B(k_y-k_{yo})^2-C(k_x-k_{xo})(k_y-k_{yo}) \qquad (C.11)$$

where

$$A = -\frac{1}{2}\frac{\partial^2}{\partial k_x^2}\,\bar{k}\cdot\bar{r}\,\Big|_{(k_{xo},k_{yo})} ,$$

$$B = -\frac{1}{2}\frac{\partial^2}{\partial k_y^2}\,\bar{k}\cdot\bar{r}\,\Big|_{(k_{xo},k_{yo})} ,$$

$$C = -\frac{\partial^2}{\partial k_x \partial k_y}\,\bar{k}\cdot\bar{r}\,\Big|_{(k_{xo},k_{yo})} .$$

In the neighborhood of the stationary phase point $\bar{f}(k_x,k_y)$ is slowly varying, so it may be replaced by $\bar{f}(k_{xo},k_{yo})$. Hence the asymptotic value of the integral for $\bar{E}(\bar{r})$ is given by

$$\bar{E}(\bar{r}) \sim \bar{f}(k_{xo},k_{yo})e^{-jk_o r}\,\frac{1}{4\pi^2}\iint_{R_o}$$

$$\cdot\, e^{j[A(k_x-k_{xo})^2+B(k_y-k_{yo})^2+C(k_x-k_{xo})(k_y-k_{yo})]}\,dk_x dk_y$$

where R_o is a small region centered on the stationary phase point from which comes the major contribution to the integral. As noted previously, for large r, the domain of integration may be extended over

the whole (k_x,k_y) plane without introducing significant error because of the rapid oscillation of the integrand for nonzero values of (k_x-k_{xo}) and (k_y-k_{yo}). Thus

$$\bar{E}(\bar{r}) \sim \bar{f}(k_{xo},k_{yo})e^{-jk_o r}\frac{1}{4\pi^2}\iint_{-\infty}^{\infty} \cdot e^{j[A(k_x-k_{xo})^2+B(k_y-k_{yo})^2+C(k_x-k_{xo})(k_y-k_{yo})]}\,dk_x dk_y \quad . \tag{C.12}$$

Next, applying a linear transformation T defined by

$$\begin{bmatrix} k_x \\ k_y \end{bmatrix} = T \begin{bmatrix} s \\ t \end{bmatrix} = \begin{bmatrix} s/\sqrt{A} + k_{xo} \\ t/\sqrt{B} + k_{yo} \end{bmatrix}$$

to (C.12) yields

$$\bar{E}(\bar{r}) \sim \bar{f}(k_{xo},k_{yo})e^{-jk_o r}\frac{1}{4\pi^2}\iint_{-\infty}^{\infty} e^{j[s^2+t^2+Cst/\sqrt{AB}]}\,|\det J_T|\,ds\,dt$$

$$\sim \bar{f}(k_{xo},k_{yo})e^{-jk_o r}\frac{1}{4\pi^2}\iint_{-\infty}^{\infty} e^{j[s^2+t^2+Cst/\sqrt{AB}]}\,\frac{ds\,dt}{\sqrt{AB}} \tag{C.13}$$

where

$$J_T = \begin{bmatrix} \frac{\partial k_x}{\partial s} & \frac{\partial k_x}{\partial t} \\ \frac{\partial k_y}{\partial s} & \frac{\partial k_y}{\partial t} \end{bmatrix} = \begin{bmatrix} \frac{1}{\sqrt{A}} & 0 \\ 0 & \frac{1}{\sqrt{B}} \end{bmatrix}$$ is the Jacobian matrix of T.

Completing the square for the s variable in (C.13) to obtain

$$\bar{E}(\bar{r}) \sim \bar{f}(k_{xo},k_{yo}) \frac{e^{-jk_o r}}{4\pi^2} \frac{1}{\sqrt{AB}} \int_{-\infty}^{\infty}\int e^{j[(s + \frac{Ct}{2\sqrt{AB}})^2 + t^2(1 - \frac{C^2}{4AB})]} \, dsdt \, .$$

(C.14)

Using the result

$$\int_{-\infty}^{\infty} e^{ja(u-u_o)^2} du = \sqrt{\frac{\pi}{a}} e^{j\pi/4}$$

in (C.14) gives

$$\bar{E}(\bar{r}) \sim \bar{f}(k_{xo},k_{yo}) \frac{e^{-jk_o r}}{4\pi^2} \cdot \frac{1}{\sqrt{AB}} \cdot \begin{bmatrix} \sqrt{\pi}\, e^{j\pi/4} \end{bmatrix} \begin{bmatrix} \sqrt{\frac{\pi}{1 - \frac{C^2}{4AB}}}\, e^{j\pi/4} \end{bmatrix}$$

$$\sim j\bar{f}(k_{xo},k_{yo}) \frac{e^{-jk_o r}}{2\pi} \frac{1}{\sqrt{4AB-C^2}} \quad . \qquad \text{(C.14)}$$

It may be observed that

$$\sqrt{4AB-C^2} = \left[4 \cdot \frac{r^2}{4k_o^2\cos^4\theta} (\cos^2\theta+\sin^2\theta\cos^2\phi)(\cos^2\theta+\sin^2\theta\sin^2\phi) - \frac{r^2}{k_o^2\cos^4\theta} \sin^4\theta\sin^2\phi\cos^2\phi \right]^{1/2}$$

$$= \frac{r}{k_o\cos^2\theta} \left[\cos^4\theta+\cos^2\theta\sin^2\theta(\sin^2\phi+\cos^2\phi)\right]^{1/2} = \frac{r}{k_o\cos\theta} \quad .$$

Therefore, the leading term in the asymptotic expansion of the integral in (C.1) is given by

$$\bar{E}(\bar{r}) \sim \frac{jk_o\cos\theta}{2\pi} \frac{e^{-jk_or}}{r} \bar{f}(k_{xo},k_{yo}) \quad . \qquad (C.15)$$

APPENDIX D

ORTHOGONALITY PROPERTIES OF CYLINDRICAL VECTOR EIGENMODES

Several orthogonality properties of the solenoidal vector eigenmodes or wave functions in cylindrical coordinates are stated and proved in the form of lemmas. For the sake of clarity, shortand notations are introduced first:

1. S_n designates a "+" or "-" sign, n=0,1,2,... (D.1)

2. $$\delta_{mn} = \begin{cases} 1 & m=n \\ 0 & m\neq n \end{cases} \quad , m,n = 0,1,2,.... \tag{D.2}$$

3. $$\varepsilon_n = \begin{cases} 1 & n=0 \\ 2 & n>1 \end{cases} \tag{D.3}$$

4. $$\lambda' = \sqrt{k_o^2 - h'^2} \quad , \mathrm{Im}\lambda' > 0, \ -\infty<h'<\infty$$

$$\lambda = \sqrt{k_o^2 - h^2} \quad , \mathrm{Im}\lambda > 0, \ -\infty<h<\infty \tag{D.4}$$

$$5.\quad A_{e_n}\,\Gamma_{e_m} = \begin{cases} A_{en}\Gamma_{en} + A_{on}\Gamma_{on} & , n>0 \\ A_{en}\Gamma_{en} & , n=0 \end{cases} \quad . \tag{D.5}$$

Lemma 1

$$\int_{-\infty}^{\infty} dh' \int_{-\infty}^{\infty} dz \int_{0}^{2\pi} \rho d\phi \; [A_{e_n} \hat{\rho} \times \nabla \times \bar{M}^{S_n}_{e_{n\lambda}}(h,\bar{r})] \cdot [\Gamma_{e_m} \bar{M}^{S_m}_{e_{m\lambda'}}(h',\bar{r})]$$

$$= \frac{4\pi^2}{\varepsilon_n} A_{e_n}\,\Gamma_{e_m}\,\rho\lambda^2\, Z_n^{S_n}(\lambda\rho)\,\frac{\partial}{\partial\rho}\, Z_m^{S_m}(\lambda\rho)\,\delta_{mn} \quad .$$

Proof:

Substituting (3.46) into the integrand furnishes

$$\text{L.H.S.} = \int_{-\infty}^{\infty} dh' \int_{-\infty}^{\infty} dz \int_{0}^{2\pi} \rho d\phi \; [A_{e_n}\{-\hat{\phi}(\lambda^2 Z_n^{S_n}(\lambda\rho)\begin{matrix}\cos\\ \sin\end{matrix} n\phi)\mp\hat{z}(*)\}]$$

$$\cdot\,[\Gamma_{e_m}\{\mp\hat{\rho}(*)-\hat{\phi}(\frac{\partial}{\partial\rho}\, Z_m^{S_m}(\lambda'\rho)\begin{matrix}\cos\\ \sin\end{matrix} m\phi)\}]e^{j(h+h')z}$$

$$= \int_{-\infty}^{\infty} dh' \int_{-\infty}^{\infty} dz \int_{0}^{2\pi} \rho d\phi\{[A_{e_n}\begin{matrix}\cos\\ \sin\end{matrix} n\phi][\Gamma_{e_m}\begin{matrix}\cos\\ \sin\end{matrix} m\phi]$$

$$\cdot\,\lambda^2 Z_n^{S_n}(\lambda\rho)\frac{\partial}{\partial\rho}\, Z_m^{S_m}(\lambda'\rho)\}e^{j(h+h')z} \quad .$$

One can observe that

$$\int_0^{2\pi} d\phi \, [A_{\substack{e_n \\ o}} \begin{matrix}\cos \\ \sin\end{matrix} n\phi][\Gamma_{\substack{e_m \\ o}} \begin{matrix}\cos \\ \sin\end{matrix} m\phi]$$

$$= \int_0^{2\pi} d\phi \, [A_{en}\Gamma_{em}\cos n\phi\cos m\phi + A_{en}\Gamma_{om}\cos n\phi\sin m\phi + A_{on}\Gamma_{em}\sin n\phi\cos m\phi$$

$$+ A_{on}\Gamma_{om}\sin n\phi\sin m\phi]$$

$$= \begin{cases} 2\pi A_{en}\Gamma_{en} & n=m=0 \\ \pi[A_{en}\Gamma_{en} + A_{on}\Gamma_{on}] & n=m\neq 0 \\ 0 & n\neq m \end{cases}$$

$$= \frac{2\pi}{\epsilon_n} A_{\substack{e_n \\ o}} \Gamma_{\substack{e_m \\ o}} \delta_{mn} \quad ,$$

and

$$\int_{-\infty}^{\infty} dz \, e^{j(h+h')z} = 2\pi\delta(h+h') \quad . \tag{D.6}$$

Thus,

$$\text{L.H.S.} = \int_{-\infty}^{\infty} dh' \left\{ \frac{4\pi^2}{\epsilon_n} A_{\substack{e_n \\ o}} \Gamma_{\substack{e_m \\ o}} \rho\lambda^2 Z_n^{\begin{matrix}S_n \\ \end{matrix}}(\lambda\rho) \frac{\partial}{\partial\rho} Z_m^{\begin{matrix}S_m \\ \end{matrix}}(\lambda'\rho)\delta_{mn} \right\} \delta(h+h')$$

$$= \frac{4\pi^2}{\epsilon_n} A_{\substack{e_n \\ o}} \Gamma_{\substack{e_m \\ o}} \rho\lambda^2 Z_n^{\begin{matrix}S_n \\ \end{matrix}}(\lambda\rho) \frac{\partial}{\partial\rho} Z_m^{\begin{matrix}S_m \\ \end{matrix}}(\lambda\rho)\delta_{mn} \quad .$$

Lemma 2.

$$\int_{-\infty}^{\infty} dh' \int_{-\infty}^{\infty} dz \int_{0}^{2\pi} \rho d\phi \; [A_{e_n} \hat{\rho} \times \nabla \times \overset{-S_n}{N}_{e_n\lambda}(h,\bar{r})] \cdot [\Gamma_{e_m} \overset{-S_m}{N}_{e_m\lambda'}(h',\bar{r})]$$

$$= - \frac{4\pi^2}{\epsilon_n} A_{e_n} \Gamma_{e_m} \rho\lambda^2 \frac{\partial}{\partial\rho} Z_n^{S_n}(\lambda\rho) \; Z_m^{S_m}(\lambda\rho) \; \delta_{mn} \quad .$$

Proof:

The proof is similar to that of Lemma 1 and will not be repeated here.

Lemma 3.

$$\int_{-\infty}^{\infty} dh' \int_{-\infty}^{\infty} dz \int_{0}^{2\pi} \rho d\phi \; [A_{e_n} \hat{\rho} \times \nabla \times \overset{-S_n}{M}_{e_n\lambda}(h,\bar{r})] \cdot [\Gamma_{e_m} \overset{-S_m}{N}_{e_m\lambda'}(h',\bar{r})] = 0 \quad .$$

Proof:

Substituting (3.46) and (3.47) in the integrand yields

$$\text{L.H.S.} = \int_{-\infty}^{\infty} dh' \int_{-\infty}^{\infty} dz \int_{0}^{2\pi} \rho d\phi \; \{A_{e_n}[-\hat{\phi} \lambda^2 Z_n^{S_n}(\lambda\rho)^{\cos}_{\sin} n\phi$$

$$\mp \hat{z} \frac{jhn}{\rho} Z_n^{S_n}(\lambda\rho)^{\sin}_{\cos} n\phi]\}$$

$$\cdot \{\Gamma_{e_m}[\hat{\rho}(*) \mp \hat{\phi} \frac{jh'm}{k_o\rho} Z_m^{S_m}(\lambda'\rho)^{\sin}_{\cos} m\phi + \hat{z} \frac{\lambda'^2}{k_o} Z_m^{S_m}(\lambda'\rho)^{\cos}_{\sin} m\phi \;]\}$$

$$\cdot e^{j(h+h')z} \quad .$$

Making use of (D.6) it is clear that integration on z produces the delta function $2\pi\delta(h+h')$. Hence,

$$\text{L.H.S.} = 2\pi \int_{-\infty}^{\infty} dh'\delta(h+h') \int_0^{2\pi} \rho d\phi \; \{[-A_{e_n} \begin{matrix}\cos\\ \sin\end{matrix} n\phi][\mp\Gamma_{e_m} \begin{matrix}\sin\\ \cos\end{matrix} m\phi]$$

$$\cdot \frac{j\lambda^2 h'm}{k_o\rho} \; Z_n^{S_n}(\lambda\rho)\; Z_m^{S_m}(\lambda'\rho)$$

$$+ [\mp A_{e_n} \begin{matrix}\sin\\ \cos\end{matrix} n\phi][\Gamma_{e_m} \begin{matrix}\cos\\ \sin\end{matrix} m\phi] \frac{j(\lambda')^2 hn}{k_o\rho} \; Z_n^{S_n}(\lambda\rho)\; Z_m^{S_m}(\lambda'\rho)\} \quad .$$

Clearly L.H.S. $\equiv$ 0 for n=m=0, and $n\neq m$. When $n=m\neq 0$,

$$\int_0^{2\pi} d\phi \; [-A_{e_n} \begin{matrix}\cos\\ \sin\end{matrix} n\phi][\mp\Gamma_{e_n} \begin{matrix}\sin\\ \cos\end{matrix} n\phi]$$

$$= \int_0^{2\pi} d\phi \; [A_{en}\Gamma_{en}\cos n\phi\sin n\phi - A_{en}\Gamma_{on}\cos n\phi\cos n\phi + A_{on}\Gamma_{en}\sin n\phi\sin n\phi$$

$$- A_{on}\Gamma_{on}\sin n\phi\cos n\phi] = \pi[-A_{en}\Gamma_{on} + A_{on}\Gamma_{en}] \quad .$$

Similarly, it can be verified that

$$\int_0^{2\pi} d\phi \; [\mp A_{e_n} \begin{matrix}\sin\\ \cos\end{matrix} n\phi][\Gamma_{e_n} \begin{matrix}\cos\\ \sin\end{matrix} n\phi] = \pi[-A_{en}\Gamma_{on} + A_{on}\Gamma_{en}] \quad .$$

$$\therefore \text{L.H.S.} = \begin{cases} 0 & n=m=0;\quad n\neq m \\ 2\pi^2(-A_{en}\Gamma_{on}+A_{on}\Gamma_{en}) \int_{-\infty}^{\infty} dh'\,\delta(h+h')\left[\frac{j\lambda^2 h'n}{k_0\rho} + \frac{j\lambda'^2 hn}{k_0\rho}\right] & \\ \quad \cdot Z_n^{Sn}(\lambda\rho)Z_n^{Sn}(\lambda'\rho) & n=m\neq 0 \end{cases}$$

$$= 0 \text{ for all } m,n \quad .$$

Lemma 4.

$$\int_{-\infty}^{\infty} dh' \int_{-\infty}^{\infty} dz \int_{0}^{2\pi} \rho d\phi \; [A_{e_n} \hat{\rho} \times \nabla \times \bar{N}^{Sn}_{e_{n\lambda}}(h,\bar{r})]\cdot[\Gamma_{e_m} \bar{M}^{Sm}_{e_{m\lambda'}}(h',\bar{r})] = 0 \quad .$$

Proof:

After substituting (3.46) and (3.47) in the integrand one will see

$$\text{L.H.S.} = \int_{-\infty}^{\infty} dh' \int_{-\infty}^{\infty} dz \int_{0}^{2\pi} \rho d\phi \; \{A_{e_n}[-\hat{z}(*)]\}\cdot\{\Gamma_{e_m}[\mp\hat{\rho}(*)-\hat{\phi}(*)]\} \equiv 0 \quad .$$

APPENDIX E

PROOF OF EQUATION (3.73)

The proof starts from Equations (3.69) and (3.71) which are relabelled here for easy reference:

$$\nabla x \nabla x \bar{\bar{G}}_{e1}(\bar{r},\bar{r}') - k_1^2 \bar{\bar{G}}_{e1}(\bar{r},\bar{r}') = 0 \quad , \tag{E.1}$$

$$\nabla x \nabla x \bar{\bar{G}}_{m1}(\bar{r},\bar{r}') - k_1^2 \bar{\bar{G}}_{m1}(\bar{r},\bar{r}') = 0 \quad , \tag{E.2}$$

where $\bar{r} \in V_1$, $\bar{r}' \in V_2$ and $k_1^2 = \omega^2 \mu_1 \varepsilon_1 = \omega^2 \mu_o \varepsilon_o \varepsilon_r$. Taking the curl of (E.1) and then subtracting it from (E.2) leads to the conclusion that

$$\bar{\bar{G}}_{m1}(\bar{r},\bar{r}') = \nabla x \bar{\bar{G}}_{e1}(\bar{r},\bar{r}') + \bar{\bar{\psi}}(\bar{r},\bar{r}') \tag{E.3}$$

where $\bar{\bar{\psi}}$ satisfies the same differential equation governing $\bar{\bar{G}}_{e1}$ and $\bar{\bar{G}}_{m1}$.

Next letting $\bar{E}_1$ and $\bar{H}_1$ be the electric and magnetic field in V_1, respectively, due to electric current source $\bar{J}$ in V_2 (with parameters μ_2 and ε_2), it can be shown that [19]

$$\bar{E}_1(\bar{r}) = j\omega\mu_2 \int_{V_2} \bar{\bar{G}}_{e1}(\bar{r},\bar{r}')\cdot\bar{J}(\bar{r}')dv' \quad . \tag{E.4}$$

From Maxwell's equations, it is clear that

$$\bar{H}_1(\bar{r}) = \frac{\nabla x\bar{E}_1(r)}{j\omega\mu_1} = \frac{\mu_2}{\mu_1} \int_{V_2} \nabla x\bar{\bar{G}}_{e1}(\bar{r},\bar{r}')\cdot\bar{J}(\bar{r}')dv' \quad . \tag{E.5}$$

However, in order to be consistent with the role of the magnetic Green's dyadic defined by (3.18), $\bar{\bar{G}}_{m1}$ must be sought such that

$$\bar{H}_1(\bar{r}) = \int_{V_2} \bar{\bar{G}}_{m1}(\bar{r},\bar{r}')\cdot\bar{J}(\bar{r}')dv' \quad . \tag{E.6}$$

Substituting (E.3) into (E.6) yields

$$\bar{H}_1(\bar{r}) = \int_{V_2} [\nabla x\bar{\bar{G}}_{e1}(\bar{r},\bar{r}')+\psi(r,r')]\cdot\bar{J}(\bar{r}')dv' \quad . \tag{E.7}$$

From (E.5) and (E.7) it is seen that

$$\bar{\bar{\psi}}(r,r') = \left(\frac{\mu_2}{\mu_1} - 1\right)\nabla x \bar{\bar{G}}_{e1}(r,r') \quad . \tag{E.8}$$

Using (E.8) in (E.3) gives

$$G_{m1}(\bar{r},\bar{r}') = \frac{\mu_2}{\mu_1}\nabla x \bar{\bar{G}}_{e1}(\bar{r},\bar{r}') \quad . \tag{E.9}$$

APPENDIX F

DETERMINATION OF THE EXPANSION COEFFICIENTS

The Green's dyadic $\bar{\bar{G}}_e$ for region $V=V_1 \cup V_2$ is represented as

$$\bar{\bar{G}}_e(\bar{r},\bar{r}') = U(\rho-b)\bar{\bar{G}}_{e2}(\bar{r},\bar{r}') + U(b-\rho)\bar{\bar{G}}_{e1}(\bar{r},\bar{r}')$$

$$= U(\rho-b)[\bar{\bar{G}}_0(\bar{r},\bar{r}') + \bar{\bar{G}}_{s2}(\bar{r},\bar{r}')] + U(b-\rho)\bar{\bar{G}}_{e1}(\bar{r},\bar{r}') \quad ,$$

$$\bar{r} \in V, \quad \bar{r}' \in V_2 \quad . \tag{F.1}$$

From (F.1), (3.87) and (3.88) it is clear that

$$\bar{\bar{G}}_e(\bar{r},\bar{r}')\Big|_{\rho=b^+<\rho'} = \bar{\bar{G}}_{e2}(\bar{r},\bar{r}')\Big|_{\rho=b^+<\rho'} = [\bar{\bar{g}}_0(\bar{r},\bar{r}') + \bar{\bar{G}}_{s2}(\bar{r},\bar{r}')]_{\rho=b^+<\rho'}$$

$$= \frac{j}{8\pi}\int_{-\infty}^{\infty} dh \sum_{n=0}^{\infty} \frac{\varepsilon_n}{\lambda^2} \{[\bar{M}^{-}_{o_{e}n\lambda}(h,\bar{r}) + A_{o_{e}n}\bar{M}^{+}_{o_{e}n\lambda}(h,\bar{r}) + B_{o_{e}n}\bar{N}^{+}_{e_{o}n\lambda}(h,\bar{r})]$$

$$\cdot \bar{M}^{+}_{o_{e}n\lambda}(-h,\bar{r}') + [\bar{N}^{-}_{o_{e}n\lambda}(h,\bar{r}) + C_{o_{e}n}\bar{N}^{+}_{o_{e}n\lambda}(h,\bar{r}) + D_{o_{e}n}\bar{M}^{+}_{e_{o}n\lambda}(h,\bar{r})]$$

$$\cdot \bar{N}^{+}_{e_{o}n\lambda}(-h,\bar{r}')\}_{\rho=b^+<\rho'} \quad . \tag{F.2}$$

Likewise, from (F.1) and (3.89) it is clear that

$$\bar{\bar{G}}_e(\bar{r},\bar{r}')\Big|_{\rho=b^- \text{ or } \rho=a} = \bar{\bar{G}}_{e1}(\bar{r},\bar{r}')\Big|_{\rho=b^- \text{ or } \rho=a}$$

$$= \frac{j}{8\pi}\int_{-\infty}^{\infty} dh \sum_{n=0}^{\infty} \frac{\varepsilon_n}{\lambda^2} \{[\alpha_{o}^{e}{}_{n}\bar{M}^{+}_{e}{}_{o}{}_{n\mu}(h,\bar{r}) + \beta_{e}^{o}{}_{n}\bar{N}^{+}_{o}{}_{e}{}_{n\mu}(h,\bar{r})$$

$$+ \gamma_{o}^{e}{}_{n}\bar{M}^{-}_{e}{}_{o}{}_{n\mu}(h,\bar{r}) + \tau_{e}^{o}{}_{n}\bar{N}^{-}_{o}{}_{e}{}_{n\mu}(h,r)]\,\bar{M}^{+}_{e}{}_{o}{}_{n\lambda}(-h,\bar{r}')$$

$$+ a_{o}^{e}{}_{n}\bar{N}^{+}_{e}{}_{o}{}_{n\mu}(h,\bar{r}) + b_{e}^{o}{}_{n}\bar{M}^{+}_{o}{}_{e}{}_{n\mu}(h,\bar{r}) + d_{o}^{e}{}_{n}\bar{N}^{-}_{e}{}_{o}{}_{n\mu}(h,\bar{r})$$

$$+ f_{e}^{o}{}_{n}\bar{M}^{-}_{o}{}_{e}{}_{n\mu}(h,\bar{r})]\bar{N}^{+}_{e}{}_{o}{}_{n\lambda}(-h,\bar{r}')\}_{\rho=b^- \text{ or } \rho=a} \quad . \qquad (F.3)$$

These 24 unknown coefficients ($A_{o}^{e}{}_{n}$, $B_{o}^{e}{}_{n}$, $C_{o}^{e}{}_{n}$, $D_{o}^{e}{}_{n}$, $\alpha_{o}^{e}{}_{n}$, $\beta_{o}^{e}{}_{n}$, $\gamma_{o}^{e}{}_{n}$, $\tau_{o}^{e}{}_{n}$, $a_{o}^{e}{}_{n}$, $b_{o}^{e}{}_{n}$, $d_{o}^{e}{}_{n}$ and $f_{o}^{e}{}_{n}$) are being determined from the 24 linear equations derived from the following set of boundary conditions (as defined by Equations (3.82) to (3.84)):

$$\hat{\rho} \times \bar{\bar{G}}_{e1}(\bar{r},\bar{r}')\Big|_{\rho=a} = 0 \qquad (F.4)$$

$$\hat{\rho} \times \bar{\bar{G}}_{e2}(\bar{r},\bar{r}')\Big|_{\rho=b^+} = \hat{\rho} \times \bar{\bar{G}}_{e1}(\bar{r},\bar{r}')\Big|_{\rho=b^-} \qquad (F.5)$$

$$\hat{\rho} \times \nabla \times \bar{\bar{G}}_{e2}(\bar{r},\bar{r}')\Big|_{\rho=b^+} = \hat{\rho} \times \frac{\mu_2}{\mu_1} \nabla \times \bar{\bar{G}}_{e1}(r,r')\Big|_{\rho=b^-} \quad . \tag{F.6}$$

Furthermore, it may be helpful to recall the explicit expressions of the $\bar{M}$ and $\bar{N}$ functions which are given below for the sake of convenience.

$$\bar{M}^{\pm}_{\substack{e\\o}n\lambda}(h,\bar{r}) = \left[\mp \hat{\rho} \frac{n}{\rho} Z_n^{\pm}(\lambda\rho) \begin{matrix}\sin\\\cos\end{matrix} n\phi - \hat{\phi} \frac{\partial}{\partial\rho} Z_n^{\pm}(\lambda\rho) \begin{matrix}\cos\\\sin\end{matrix} n\phi \right] e^{jhz} \tag{F.7}$$

$$\bar{N}^{\pm}_{\substack{e\\o}n\lambda}(h,\bar{r}) = \left[\hat{\rho} \frac{jh}{k} \frac{\partial}{\partial\rho} Z_n^{\pm}(\lambda\rho) \begin{matrix}\cos\\\sin\end{matrix} n\phi \mp \hat{\phi} \frac{jhn}{k\rho} Z_n^{\pm}(\lambda\rho) \begin{matrix}\sin\\\cos\end{matrix} n\phi \right.$$

$$\left. + \hat{z} \frac{\lambda^2}{k} Z_n^{\pm}(\lambda\rho) \begin{matrix}\cos\\\sin\end{matrix} n\phi \right] e^{jhz} \tag{F.8}$$

where $Z_n^+(\lambda\rho) = H_n^{(1)}(\lambda\rho)$, $Z_n^-(\lambda\rho) = J_n(\lambda\rho)$, and $\lambda = \sqrt{k^2-h^2}$, $\mathrm{Im}\lambda>0$. For simplicity, $H_n^{(1)}(\lambda\rho)$ will be denoted by $H_n(\lambda\rho)$, and $\frac{d}{d\xi} f(\xi)$ by $f'(\xi)$ throughout this appendix.

Substituting (F.3) into (F.4) produces, for n=0,1,2,...,

$$\hat{\rho} \times \left[\alpha_{\substack{e\\o}n} \bar{M}^{+}_{\substack{e\\o}n\mu}(h,\bar{r}) + \beta_{\substack{o\\e}n} \bar{N}^{+}_{\substack{o\\e}n\mu}(h,\bar{r}) + \gamma_{\substack{e\\o}n} \bar{M}^{-}_{\substack{e\\o}n\mu}(h,\bar{r}) + \tau_{\substack{o\\e}n} \bar{N}^{-}_{\substack{o\\e}n\mu}(h,r) \right]_{\rho=a} = 0 \tag{F.9}$$

$$\hat{\rho} \times \left[a_{\substack{e_n \\ o}} \bar{N}^{+}_{\substack{e_n \\ o}\mu}(h,\bar{r}) + b_{\substack{o_n \\ e}} \bar{M}^{+}_{\substack{o_n \\ e}\mu}(h,\bar{r}) + d_{\substack{e_n \\ o}} \bar{N}^{-}_{\substack{e_n \\ o}\mu}(h,\bar{r}) + f_{\substack{o_n \\ e}} \bar{M}^{-}_{\substack{o_n \\ e}\mu}(h,\bar{r}) \right]_{\rho=a} = 0$$

(F.10)

Using (F.7) and (F.8) in (F.9) and in (F.10) yields, respectively,

$$\hat{z}\left\{-\mu\left[\alpha_{\substack{e_n \\ o}} H_n'(\mu a) + \gamma_{\substack{e_n \\ o}} J_n'(\mu a)\right] \pm \frac{jnh}{k_1 a}\left[\beta_{\substack{o_n \\ e}} H_n(\mu a) + \tau_{\substack{o_n \\ e}} J_n(\mu a)\right]\right\}^{\cos}_{\sin} n\phi$$

$$\cdot e^{jhz} + \hat{\phi}\left\{-\frac{\mu^2}{k_1}\left[\beta_{\substack{o_n \\ e}} H_n(\mu a) + \tau_{\substack{o_n \\ e}} J_n(\mu a)\right]^{\sin}_{\cos} n\phi\, e^{jhz}\right\} = 0$$

(F.11)

and

$$\hat{z}\left\{-\mu\left[b_{\substack{o_n \\ e}} H_n'(\mu a) + f_{\substack{o_n \\ e}} J_n'(\mu a)\right] \mp \frac{jnh}{k_1 a}\left[a_{\substack{e_n \\ o}} H_n(\mu a) + d_{\substack{e_n \\ o}} J_n(\mu a)\right]\right\}^{\sin}_{\cos} n\phi$$

$$\cdot e^{jhz} + \hat{\phi}\left\{-\frac{\mu^2}{k_1}\left[a_{\substack{e_n \\ o}} H_n(\mu a) + d_{\substack{e_n \\ o}} J_n(\mu a)\right]^{\cos}_{\sin} n\phi\, e^{jhz}\right\} = 0 \,.$$

(F.12)

Next substituting (F.2) and (F.3) into (F.5) gives, for n=0,1,2,...,

$$\hat{\rho} \times \left[\bar{M}^{-}_{\substack{e_n \\ o}\lambda}(h,\bar{r}) + A_{\substack{e_n \\ o}} \bar{M}^{+}_{\substack{e_n \\ o}\lambda}(h,\bar{r}) + B_{\substack{o_n \\ e}} \bar{N}^{+}_{\substack{o_n \\ e}\lambda}(h,\bar{r})\right]_{\rho=b^+} =$$

$$\hat{\rho} \times \left[\alpha_{\substack{e_n \\ o}} \bar{M}^{+}_{\substack{e_n \\ o}\mu}(h,\bar{r}) + \beta_{\substack{o_n \\ e}} \bar{N}^{+}_{\substack{o_n \\ e}\mu}(h,\bar{r}) + \gamma_{\substack{e_n \\ o}} \bar{M}^{-}_{\substack{e_n \\ o}\mu}(h,\bar{r}) + \tau_{\substack{o_n \\ e}} \bar{N}^{-}_{\substack{o_n \\ e}\mu}(h,\bar{r})\right]_{\rho=b^-}$$

(F.13)

and

$$\hat{\rho} \times \left[\bar{N}^{-}_{e_{o}n\lambda}(h,\bar{r})+C_{e_{o}n}\bar{N}^{+}_{e_{o}n\lambda}(h,\bar{r})+D_{o_{e}n}\bar{M}^{+}_{o_{e}n\lambda}(h,\bar{r})\right]_{\rho=b^{+}} =$$

$$\hat{\rho} \times \left[a_{e_{o}n}\bar{N}^{+}_{e_{o}n\mu}(h,\bar{r})+b_{o_{e}n}\bar{M}^{+}_{o_{e}n\mu}(h,\bar{r})+d_{e_{o}n}\bar{N}^{-}_{e_{o}n\mu}(h,\bar{r})+f_{o_{e}n}\bar{M}^{-}_{o_{e}n\mu}(h,\bar{r})\right]_{\rho=b^{-}} . \tag{F.14}$$

Using (F.7) and (F.8) in (F.13) and in (F.14) yields, respectively,

$$\hat{z}\{-\lambda[J_n'(\lambda b)+A_{e_{o}n}H_n'(\lambda b)] \pm \frac{jnh}{k_2 b}[B_{o_{e}n}H_n(\lambda b)]\}^{\cos}_{\sin} n\phi$$

$$+ \hat{\phi}\{-\frac{\lambda^2}{k_2}B_{o_{e}n}H_n(\lambda b)^{\sin}_{\cos} n\phi\} = \hat{z}\{-\mu[\alpha_{e_{o}n}H_n'(\mu b)+\gamma_{e_{o}n}J_n'(\mu b)]$$

$$\pm \frac{jnh}{k_1 b}[\beta_{o_{e}n}H_n(\mu b)+\tau_{o_{e}n}J_n(\mu b)]\}^{\cos}_{\sin} n\phi + \hat{\phi}\{-\frac{\mu^2}{k_1}[\beta_{o_{e}n}H_n(\mu b)$$

$$+ \tau_{o_{e}n}J_n(\mu b)]^{\sin}_{\cos} n\phi\} \tag{F.15}$$

and

$$\hat{z}\{-D_{o_{e}n}\lambda H_n'(\lambda b) \mp \frac{jnh}{k_2 b}[J_n(\lambda b)+C_{e_{o}n}H_n(\lambda b)]\}^{\sin}_{\cos} n\phi$$

$$+ \hat{\phi}\{-[J_n(\lambda b)+C_{e_{o}n}H_n(\lambda b)]\frac{\lambda^2}{k_2}\}^{\cos}_{\sin} n\phi = \hat{z}\{-\mu[b_{o_{e}n}H_n'(\mu b)+f_{o_{e}n}J_n'(\mu b)] \mp \frac{jnh}{k_1 b}$$

$$\cdot [a_{e_{o}n}H_n(\mu b) + d_{e_{o}n}J_n(\mu b)]\}^{\sin}_{\cos} n\phi + \hat{\phi}\{-\frac{\mu^2}{k_1}[a_{e_{o}n}H_n(\mu b) + d_{e_{o}n}J_n(\mu b)]\}^{\cos}_{\sin} n\phi. \tag{F.16}$$

Finally, substituting (F.2) and (F.3) into (F.6) gives, for $n=0,1,2,\ldots,$

$$\hat{\rho} \times \frac{1}{\mu_2}\{\nabla\times\bar{M}^{-}_{e_{o}n\lambda}(h,\bar{r}) + A_{e_{o}n}\nabla\times\bar{M}^{+}_{e_{o}n\lambda}(h,\bar{r}) + B_{o_{e}n}\nabla\times\bar{N}^{+}_{o_{e}n\lambda}(h,\bar{r})\}_{\rho=b^{+}}$$

$$= \hat{\rho} \times \frac{1}{\mu_1}\{\alpha_{e_{o}n}\nabla\times\bar{M}^{+}_{e_{o}n\mu}(h,\bar{r}) + \beta_{o_{e}n}\nabla\times\bar{N}^{+}_{o_{e}n\mu}(h,\bar{r}) + \gamma_{e_{o}n}\nabla\times\bar{M}^{-}_{e_{o}n\mu}(h,\bar{r})$$

$$+ \tau_{o_{e}n}\nabla\times\bar{N}^{-}_{o_{e}n\mu}(h,\bar{r})\}_{\rho=b^{-}} . \tag{F.17}$$

and

$$\hat{\rho} \times \frac{1}{\mu_2}\{\nabla\times\bar{N}^{-}_{\substack{e\\o}n\lambda}(h,\bar{r}) + C_{\substack{o\\e}n}\nabla\times\bar{N}^{+}_{\substack{o\\e}n\lambda}(h,\bar{r}) + D_{\substack{e\\o}n}\nabla\times\bar{M}^{+}_{\substack{e\\o}n\lambda}(h,\bar{r})\}_{\rho=b^+}$$

$$= \hat{\rho} \times \frac{1}{\mu_1}\{a_{\substack{o\\e}n}\nabla\times\bar{N}^{+}_{\substack{o\\e}n\mu}(h,\bar{r}) + b_{\substack{e\\o}n}\nabla\times\bar{M}^{+}_{\substack{e\\o}n\mu}(h,\bar{r}) + d_{\substack{o\\e}n}\nabla\times\bar{N}^{-}_{\substack{o\\e}n\mu}(h,\bar{r})$$

$$+ f_{\substack{e\\o}n}\nabla\times\bar{M}^{-}_{\substack{e\\o}n\mu}(h,\bar{r})\}_{\rho=b^-} \quad . \tag{F.18}$$

Employing (F.7) and (F.8) in (F.17) results in

$$\hat{z}\,\frac{\mu_1}{\mu_2}\{-k_2\lambda B_{\substack{e\\o}n}H_n'(\lambda b) \mp \frac{jnh}{b}[J_n(\lambda b)+A_{\substack{o\\e}n}H_n(\lambda b)]\}^{\sin}_{\cos} n\phi$$

$$+ \hat{\phi}\,\frac{\mu_1}{\mu_2}\{-\lambda^2[J_n(\lambda b)+A_{\substack{o\\e}n}H_n(\lambda b)]\}^{\cos}_{\sin} n\phi = \hat{z}\{-k_1\mu[\beta_{\substack{o\\e}n}H_n'(\mu b)+\tau_{\substack{e\\o}n}J_n'(\mu b)]$$

$$\mp \frac{jnh}{b}[\alpha_{\substack{e\\o}n}H_n(\mu b)+\gamma_{\substack{o\\e}n}J_n(\mu b)]\}^{\sin}_{\cos} n\phi$$

$$+ \hat{\phi}\{-\mu^2[\alpha_{\substack{e\\o}n}H_n(\mu b)+\gamma_{\substack{o\\e}n}J_n(\mu b)]\}^{\cos}_{\sin} n\phi \tag{F.19}$$

and

$$\hat{z}\,\frac{\mu_1}{\mu_2}\{-k_2\lambda[J_n'(\lambda b)+C_{\substack{o\\e}n}H_n'(\lambda b)] \pm \frac{jnh}{b}D_{\substack{e\\o}n}H_n(\lambda b)\}^{\cos}_{\sin} n\phi$$

$$+ \hat{\phi}\,\frac{\mu_1}{\mu_2}\{-\lambda^2 D_{\substack{e\\o}n}H_n(\lambda b)\}^{\sin}_{\cos} n\phi = \hat{z}\{-k_1\mu[a_{\substack{o\\e}n}H_n'(\mu b)+d_{\substack{o\\e}n}J_n'(\mu b)]$$

$$\pm \frac{jnh}{b}[b_{\substack{e\\o}n}H_n(\mu b)+f_{\substack{e\\o}n}J_n(\mu b)]\}^{\cos}_{\sin} n\phi$$

$$+ \hat{\phi}\{-\mu^2[b_{\substack{e\\o}n}H_n(\mu b)+f_{\substack{e\\o}n}J_n(\mu b)]\}^{\sin}_{\cos} n\phi \quad . \tag{F.20}$$

For n=0,1,2,..., (F.11) must hold for all ϕ and z, thus one can conclude that

$$\beta_{e}^{o}{}_{n} H_n(\mu a) + \tau_{e}^{o}{}_{n} J_n(\mu a) = 0 \tag{F.21}$$

$$\alpha_{o}^{e}{}_{n} H_n'(\mu a) + \gamma_{o}^{e}{}_{n} J_n'(\mu a) = 0 \quad . \tag{F.22}$$

Using the same argument one can see from (F.15) that

$$\alpha_{o}^{e}{}_{n} \mu H_n'(\mu b) + \gamma_{o}^{e}{}_{n} \mu J_n'(\mu b) \mp \beta_{e}^{o}{}_{n} \frac{jnh}{k_1 b} H_n(\mu b) \mp \tau_{e}^{o}{}_{n} \frac{jnh}{k_1 b} J_n(\mu b)$$
$$- A_{o}^{e}{}_{n} \lambda H_n'(\lambda b) \pm B_{e}^{o}{}_{n} \frac{jnh}{k_2 b} H_n(\lambda b) = \lambda J_n'(\lambda b) \tag{F.23}$$

$$\beta_{e}^{o}{}_{n} \frac{\mu^2}{k_1} H_n(\mu b) + \tau_{e}^{o}{}_{n} \frac{\mu^2}{k_1} J_n(\mu b) - B_{e}^{o}{}_{n} \frac{\lambda^2}{k_2} H_n(\lambda b) = 0 \quad . \tag{F.24}$$

Similarly, (F.19) implies

$$\mp \alpha_{o}^{e}{}_{n} \frac{jnh}{b} H_n(\mu b) \mp \gamma_{o}^{e}{}_{n} \frac{jnh}{b} J_n(\mu b) - \beta_{e}^{o}{}_{n} k_1 \mu H_n'(\mu b) - \tau_{e}^{o}{}_{n} k_1 \mu J_n'(\mu b)$$
$$\pm A_{o}^{e}{}_{n} \frac{\mu_1}{\mu_2} \frac{jnh}{b} H_n(\lambda b) + B_{e}^{o}{}_{n} \frac{\mu_1}{\mu_2} k_2 \lambda H_n'(\lambda b) = \mp \frac{\mu_1}{\mu_2} \frac{jnh}{b} J_n(\lambda b) \quad , \tag{F.25}$$

$$\alpha_{o}^{e}{}_{n} \mu^2 H_n(\mu b) + \gamma_{o}^{e}{}_{n} \mu^2 J_n(\mu b) - A_{o}^{e}{}_{n} \frac{\mu_1}{\mu_2} \lambda^2 H_n(\lambda b) = \frac{\mu_1}{\mu_2} \lambda^2 J_n(\lambda b) \quad . \tag{F.26}$$

A second group of equations corresponding to (F.21) - (F.26) can be similarly obtained from (F.12), (F.16) and (F.20). For each $n=0,1,2,\ldots$, and for all ϕ, Equation (F.12) implies

$$a_{o}^{e_n} H_n(\mu a) + d_{o}^{e_n} J_n(\mu a) = 0 \tag{F.27}$$

$$b_{e}^{o_n} H_n'(\mu a) + f_{e}^{o_n} J_n'(\mu a) = 0 \quad . \tag{F.28}$$

Equation (F.16) implies

$$\mp a_{o}^{e_n} \frac{jnh}{k_1 b} H_n(\mu b) - b_{e}^{o_n} \mu H_n'(\mu b) \mp d_{o}^{e_n} \frac{jnh}{k_1 b} J_n(\mu b) - f_{e}^{o_n} \mu J_n'(\mu b)$$

$$\pm C_{o}^{e_n} \frac{jnh}{k_2 b} H_n(\lambda b) + D_{e}^{o_n} \lambda H_n'(\lambda b) = \mp \frac{jnh}{k_2 b} J_n(\lambda b) \quad , \tag{F.29}$$

$$a_{o}^{e_n} \frac{\mu^2}{k_1} H_n(\mu b) + d_{o}^{e_n} \frac{\mu^2}{k_1} J_n(\mu b) - C_{o}^{e_n} \frac{\lambda^2}{k_2} H_n(\lambda b) = \frac{\lambda^2}{k_2} J_n(\lambda b) \quad . \tag{F.30}$$

and (F.20) leads to

$$- a_{o}^{e_n} k_1 \mu H_n'(\mu b) \pm b_{e}^{o_n} \frac{jnh}{b} H_n(\mu b) - d_{o}^{e_n} k_1 \mu J_n'(\mu b) \pm f_{e}^{o_n} \frac{jnh}{b} J_n(\mu b)$$

$$+ C_{o}^{e_n} \frac{\mu_1}{\mu_2} k_2 \lambda H_n'(\lambda b) \mp D_{e}^{o_n} \frac{\mu_1}{\mu_2} \frac{jnh}{b} H_n(\lambda b) = - \frac{\mu_1}{\mu_2} k_2 \lambda J_n'(\lambda b) \tag{F.31}$$

$$b_{e}^{o}{}_{n}\mu^2 H_n(\mu b) + f_{e}^{o}{}_{n}\mu^2 J_n(\mu b) - D_{e}^{o}{}_{n}\frac{\mu_1}{\mu_2}\lambda^2 H_n(\lambda b) = 0 \quad . \tag{F.32}$$

From (F.21) and (F.22) it is obvious that

$$\beta_{e}^{o}{}_{n} = -\frac{J_n(\mu a)}{H_n(\mu a)}\ \tau_{e}^{o}{}_{n} \tag{F.33}$$

$$\alpha_{o}^{e}{}_{n} = -\frac{J_n'(\mu a)}{H_n'(\mu a)}\ \gamma_{o}^{e}{}_{n} \tag{F.34}$$

and from (F.24),

$$B_{e}^{o}{}_{n} = \frac{k_2}{k_1}\left(\frac{\mu}{\lambda}\right)^2 \frac{1}{H_n(\lambda b)}\left[\beta_{e}^{o}{}_{n}H_n(\mu b) + \tau_{e}^{o}{}_{n}J_n(\mu b)\right] \quad . \tag{F.35}$$

Equation (F.35) can be used in (F.23) to obtain

$$A_{o}^{e}{}_{n} = \frac{1}{H_n'(\lambda b)}\left\{-J_n'(\lambda b) + \frac{\mu}{\lambda}\left[\alpha_{o}^{e}{}_{n}H_n'(\mu b) + \gamma_{o}^{e}{}_{n}J_n'(\mu b)\right]\right.$$

$$\left. \pm \frac{jnh}{k_1 b}\frac{1}{\lambda}\left(\frac{\mu^2}{\lambda^2} - 1\right)\left[\beta_{e}^{o}{}_{n}H_n(\mu b) + \tau_{e}^{o}{}_{n}J_n(\mu b)\right]\right\} \quad . \tag{F.36}$$

Next one can obtain from (F.26) that

$$A_{o}^{e}{}_{n} = \frac{1}{H_n(\lambda b)}\left\{-J_n(\lambda b) + \frac{\mu_2}{\mu_1}\left(\frac{\mu}{\lambda}\right)^2\left[\alpha_{o}^{e}{}_{n}H_n(\mu b) + \gamma_{o}^{e}{}_{n}J_n(\mu b)\right]\right\}, \tag{F.37}$$

and

$$\frac{\mu_1}{\mu_2}\frac{jnh}{b}\left[A_{\substack{e_n\\o}}H_n(\lambda b) + J_n(\lambda b)\right] = \frac{jnh}{b}\left(\frac{\mu}{\lambda}\right)^2\left[\alpha_{\substack{e_n\\o}}H_n(\mu b) + \gamma_{\substack{e_n\\o}}J_n(\mu b)\right] . \tag{F.38}$$

One can also rearrange (F.25) such that

$$B_{\substack{o_n\\e}}\frac{\mu_1}{\mu_2}k_2\lambda H_n'(\lambda b) = \mp\frac{\mu_1}{\mu_2}\frac{jnh}{b}\left[A_{\substack{e_n\\o}}H_n(\lambda b) + J_n(\lambda b)\right] \pm \frac{jnh}{b}\left[\alpha_{\substack{e_n\\o}}H_n(\mu b)\right.$$

$$\left. + \gamma_{\substack{e_n\\o}}J_n(\mu b)\right] + k_1\mu\left[\beta_{\substack{o_n\\e}}H_n'(\mu b) + \tau_{\substack{o_n\\e}}J_n'(\mu b)\right] . \tag{F.39}$$

Combining (F.38) and (F.39) together leads to

$$B_{\substack{o_n\\e}} = \frac{1}{H_n'(\lambda b)}\cdot\frac{\mu_2}{\mu_1}\left\{\frac{k_1}{k_2}\frac{\mu}{\lambda}\left[\beta_{\substack{o_n\\e}}H_n'(\mu b) + \tau_{\substack{o_n\\e}}J_n'(\mu b)\right] \mp \frac{jnh}{k_2 b\lambda}\left(\frac{\mu^2}{\lambda^2} - 1\right)\right.$$

$$\left.\cdot\left[\alpha_{\substack{e_n\\o}}H_n(\mu b) + \gamma_{\substack{e_n\\o}}J_n(\mu b)\right]\right\} . \tag{F.40}$$

Equating (F.36) and (F.37), then using (F.33) and (F.34) yield

$$\frac{1}{H_n(\lambda b)}\left\{-J_n(\lambda b) + \frac{\mu_2}{\mu_1}\left(\frac{\mu}{\lambda}\right)^2\left[J_n(\mu b) - \frac{J_n'(\mu a)}{H_n'(\mu a)}H_n(\mu b)\right]\gamma_{\substack{e_n\\o}}\right\}$$

$$= \frac{1}{H_n'(\lambda b)}\left\{-J_n'(\lambda b) + \frac{\mu}{\lambda}\left[J_n'(\mu b) - \frac{J_n'(\mu a)}{H_n'(\mu a)}H_n'(\mu b)\right]\gamma_{\substack{e_n\\o}} \pm \frac{jnh}{k_1 b}\frac{1}{\lambda}\left(\frac{\mu^2}{\lambda^2} - 1\right)\right.$$

$$\left.\cdot\left[J_n(\mu b) - \frac{J_n(\mu a)}{H_n(\mu a)}H_n(\mu b)\right]\tau_{\substack{o_n\\e}}\right\}$$

which can further be rearranged to get

$$\frac{\mu}{\lambda}\,\gamma_{o}^{e}{}_{n}\left\{\frac{J_n'(\mu a)}{H_n'(\mu a)}H_n'(\mu b)H_n(\lambda b)-\frac{J_n'(\mu a)}{H_n'(\mu a)}H_n(\mu b)H_n'(\lambda b)\,\frac{\mu_2}{\mu_1}\,\frac{\mu}{\lambda}\right.$$

$$\left.+\frac{\mu_2}{\mu_1}\,\frac{\mu}{\lambda}\,J_n(\mu b)H_n'(\lambda b)-J_n'(\mu b)H_n(\lambda b)\right\}=J_n(\lambda b)H_n'(\lambda b)-J_n'(\lambda b)H_n(\lambda b)$$

$$\pm\frac{jnh}{k_1 b}\,\frac{1}{\lambda}\left[\left(\frac{\mu}{\lambda}\right)^2-1\right]\left[J_n(\mu b)-\frac{J_n(\mu a)}{H_n(\mu a)}H_n(\mu b)\right]H_n(\lambda b)\,\tau_{o}^{e}{}_{n}\quad . \qquad (F.41)$$

Making use of the observation that

$$J_n(\lambda b)H_n'(\lambda b)-J_n'(\lambda b)H_n(\lambda b)=\frac{j2}{\pi\lambda b}\quad ,$$

Equation (F.41) can be used to express $\gamma_{o}^{e}{}_{n}$ as follows:

$$\gamma_{o}^{e}{}_{n}=\frac{j2}{\pi\mu b}\,\frac{1}{X_o}\pm\frac{X_1}{X_o}\,\tau_{o}^{e}{}_{n} \qquad (F.42)$$

where

$$X_o=\left[\frac{\mu_2}{\mu_1}\,\frac{\mu}{\lambda}\,J_n(\mu b)H_n'(\lambda b)-J_n'(\mu b)H_n(\lambda b)\right]$$

$$-\frac{J_n'(\mu a)}{H_n'(\mu a)}\left[\frac{\mu_2}{\mu_1}\,\frac{\mu}{\lambda}\,H_n(\mu b)H_n'(\lambda b)-H_n'(\mu b)H_n(\lambda b)\right] \qquad (F.43)$$

$$X_1=\frac{jnh}{k_1 b}\,\frac{1}{\mu}\left[\left(\frac{\mu}{\lambda}\right)^2-1\right]\left[J_n(\mu b)-\frac{J_n(\mu a)}{H_n(\mu a)}H_n(\mu b)\right]H_n(\lambda b)\quad . \qquad (F.44)$$

Next equating (F.35) and (F.40) and rearranging gives

$$\frac{k_2^2}{k_1}\frac{\mu^2}{\lambda}\left[\beta_{e_{on}}H_n(\mu b)H_n'(\lambda b) + \tau_{e_{on}}J_n(\mu b)H_n'(\lambda b)\right]$$

$$= \frac{\mu_2}{\mu_1}\left\{\mu k_1\left[\beta_{e_{on}}H_n'(\mu b)H_n(\lambda b) + \tau_{e_{on}}J_n'(\mu b)H_n(\lambda b)\right]\right.$$

$$\left. \mp \frac{jnh}{b}\frac{k_1\mu}{k_1\mu}\left[\left(\frac{\mu}{\lambda}\right)^2 - 1\right]\left[\alpha_{e_{on}}H_n(\mu b)H_n(\lambda b) + \gamma_{e_{on}}J_n(\mu b)H_n(\lambda b)\right]\right\}, \qquad (F.45)$$

which can further be manipulated by using (F.33) and (F.34) to give

$$-\frac{J_n(\mu a)}{H_n(\mu a)}\left[\left(\frac{k_2}{k_1}\right)^2\frac{\mu}{\lambda}H_n(\mu b)H_n'(\lambda b) - \frac{\mu_2}{\mu_1}H_n'(\mu b)H_n(\lambda b)\right]\tau_{e_{on}}$$

$$+\left[\left(\frac{k_2}{k_1}\right)^2\frac{\mu}{\lambda}J_n(\mu b)H_n'(\lambda b) - \frac{\mu_2}{\mu_1}J_n'(\mu b)H_n(\lambda b)\right]\tau_{e_{on}}$$

$$= \mp\frac{\mu_2}{\mu_1}\frac{jnh}{k_1 b}\left[\left(\frac{\mu}{\lambda}\right)^2 - 1\right]\left[J_n(\mu b) - \frac{J_n'(\mu a)}{H_n'(\mu a)}H_n(\mu b)\right]H_n(\lambda b)\gamma_{e_{on}} \qquad (F.46)$$

or

$$(X_2 - X_3)\tau_{e_{on}} = \mp X_4\gamma_{e_{on}} \qquad (F.47)$$

where

$$X_2 = \left[\left(\frac{k_2}{k_1}\right)^2\frac{\mu}{\lambda}J_n(\mu b)H_n'(\lambda b) - \frac{\mu_2}{\mu_1}J_n'(\mu b)H_n(\lambda b)\right] \qquad (F.48)$$

$$X_3 = \frac{J_n(\mu a)}{H_n(\mu a)} \left[\left(\frac{k_2}{k_1}\right)^2 \frac{\mu}{\lambda} H_n(\mu b) H_n'(\lambda b) - \frac{\mu_2}{\mu_1} H_n'(\mu b) H_n(\lambda b) \right] \qquad \text{(F.49)}$$

$$X_4 = \frac{\mu_2}{\mu_1} \frac{jnh}{k_1 b} \frac{1}{\mu} \left[\left(\frac{\mu}{\lambda}\right)^2 - 1 \right] \left[J_n(\mu b) - \frac{J_n'(\mu a)}{H_n'(\mu a)} H_n(\mu b) \right] H_n(\lambda b) \; . \qquad \text{(F.50)}$$

Finally, using (F.42) in (F.47) yields

$$[X_2 - X_3] \tau_{e}^{o}{}_{n} = \mp X_4 \left[\frac{j2}{\pi b \mu} \frac{1}{X_0} \pm \frac{X_1}{X_0} \tau_{e}^{o}{}_{n} \right] \quad \text{or}$$

$$\tau_{e}^{o}{}_{n} = \mp \frac{j2}{\pi b \mu} \frac{X_4}{X_0} \; \frac{1}{\left[X_2 - X_3 + \frac{X_1 X_4}{X_0} \right]} \; . \qquad \text{(F.51)}$$

Up to this point, coefficients $\alpha_{o}^{e}{}_{n}$, $\beta_{o}^{e}{}_{n}$, $\gamma_{o}^{e}{}_{n}$, $\tau_{o}^{e}{}_{n}$, $A_{o}^{e}{}_{n}$ and $B_{o}^{e}{}_{n}$ have been determined. The remaining set of undertermined coefficients consists of $a_{o}^{e}{}_{n}$, $b_{o}^{e}{}_{n}$, $d_{o}^{e}{}_{n}$, $f_{o}^{e}{}_{n}$, $C_{o}^{e}{}_{n}$ and $D_{o}^{e}{}_{n}$ and will be found in a similar fashion as the previous set.

It is clear that (F.27) and (F.28) give

$$a_{o}^{e}{}_{n} = - \frac{J_n(\mu a)}{H_n(\mu a)} \; d_{o}^{e}{}_{n} \; , \qquad \text{(F.52)}$$

$$b_{e}^{o}{}_{n} = - \frac{J_n'(\mu a)}{H_n'(\mu a)} \; f_{e}^{o}{}_{n} \; . \qquad \text{(F.53)}$$

From (F.32), one will find

$$D_{e}^{o}{}_{n} = \frac{1}{H_n(\lambda b)} \frac{\mu_2}{\mu_1} \left(\frac{\mu}{\lambda}\right)^2 \left[b_{e}^{o}{}_{n} H_n(\mu b) + f_{e}^{o}{}_{n} J_n(\mu b)\right]$$

$$= \frac{1}{H_n(\lambda b)} \frac{\mu_2}{\mu_1} \left(\frac{\mu}{\lambda}\right)^2 \left[J_n(\mu b) - \frac{J_n'(\mu a)}{H_n'(\mu a)} H_n(\mu b)\right] f_{e}^{o}{}_{n} \qquad \text{(F.54)}$$

and from (F.29)

$$\mp \frac{jnh}{k_2 b} \left[J_n(\lambda b) + C_{o}^{e}{}_{n} H_n(\lambda b)\right] = \mp \frac{jnh}{k_1 b} \left[a_{o}^{e}{}_{n} H_n(\mu b) + d_{o}^{e}{}_{n} J_n(\mu b)\right]$$

$$- \mu\left[b_{e}^{o}{}_{n} H_n'(\mu b) + f_{e}^{o}{}_{n} J_n'(\mu b)\right] + D_{e}^{o}{}_{n} \lambda H_n'(\lambda b) \quad . \qquad \text{(F.55)}$$

But one gets from (F.30) that

$$\frac{jnh}{k_2 b} \left[J_n(\lambda b) + C_{o}^{e}{}_{n} H_n(\lambda b)\right] = \frac{jnh}{k_1 b} \left(\frac{\mu}{\lambda}\right)^2 \left[a_{o}^{e}{}_{n} H_n(\mu b) + d_{o}^{e}{}_{n} J_n(\mu b)\right] \quad .$$

(F.56)

Employing (F.56) in (F.55) results in

$$D_{e}^{o}{}_{n} = \frac{1}{H_n'(\lambda b)} \frac{\mu}{\lambda} \left\{\left[b_{e}^{o}{}_{n} H_n'(\mu b) + f_{e}^{o}{}_{n} J_n'(\mu b)\right]\right.$$

$$\left. \mp \frac{jnh}{k_1 b} \frac{1}{\mu} \left[\left(\frac{\mu}{\lambda}\right)^2 - 1\right]\left[a_{o}^{e}{}_{n} H_n(\mu b) + d_{o}^{e}{}_{n} J_n(\mu b)\right]\right\} \quad . \qquad \text{(F.57)}$$

Next, equating (F.54) and (F.57) and making use of (F.52) and (F.53) produce

$$\frac{1}{H_n(\lambda b)} \frac{\mu_2}{\mu_1} \left(\frac{\mu}{\lambda}\right)^2 \left[J_n(\mu b) - \frac{J_n'(\mu a)}{H_n'(\mu a)} H_n(\mu b)\right] f_{e_n^o}$$

$$= \frac{1}{H_n'(\lambda b)} \frac{\mu}{\lambda} \left\{\left[J_n'(\mu b) - \frac{J_n'(\mu a)}{H_n'(\mu a)} H_n'(\mu b)\right] f_{e_n^o}\right.$$

$$\left. \mp \frac{jnh}{k_1 b} \frac{1}{\mu} \left[\left(\frac{\mu}{\lambda}\right)^2 - 1\right]\left[J_n(\mu b) - \frac{J_n(\mu a)}{H_n(\mu a)} H_n(\mu b)\right] d_{e_n^o}\right\}$$

which can be rewritten as

$$f_{e_n^o} = \mp \frac{X_1}{X_0} d_{e_n^o} \quad . \tag{F.58}$$

One can readily deduce from (F.56) and (F.52) that

$$C_{e_n^o} = \frac{1}{H_n(\lambda b)} \left\{-J_n(\lambda b) + \frac{k_2}{k_1} \left(\frac{\mu}{\lambda}\right)^2 \left[J_n(\mu b) - \frac{J_n(\mu a)}{H_n(\mu a)} H_n(\mu b)\right] d_{e_n^o}\right\} . \tag{F.59}$$

Also, one can obtain from (F.31) that

$$C_{e_n^o} \frac{\mu_1}{\mu_2} k_2 \lambda H_n'(\lambda b) = \frac{\mu_1}{\mu_2} k_2 \lambda \left\{-J_n'(\lambda b) \pm \frac{jnh}{b} \frac{1}{k_2 \lambda} D_{e_n^o} H_n(\lambda b) + \frac{\mu_2}{\mu_1} \frac{k_1}{k_2} \frac{\mu}{\lambda}\right.$$

$$\left. \cdot \left[a_{e_n^o} H_n'(\mu b) + d_{e_n^o} J_n'(\mu b)\right] \mp \frac{\mu_2}{\mu_1} \frac{jnh}{k_2 b} \frac{1}{\lambda} \left[b_{e_n^o} H_n(\mu b) + f_{e_n^o} J_n(\mu b)\right]\right\} . \tag{F.60}$$

Making use of (F.52), (F.53) and (F.54) will reduce (F.60) to

$$C_{e_{o}n} = \frac{1}{H_n'(\lambda b)} \{-J_n'(\lambda b) \pm \frac{\mu_2}{\mu_1} \frac{jnh}{k_2 b} \frac{1}{\lambda} [(\frac{\mu}{\lambda})^2 - 1]$$

$$\cdot [J_n(\mu b) - \frac{J_n'(\mu a)}{H_n'(\mu a)} H_n(\mu b)] f_{e_{o}n} + \frac{\mu_2}{\mu_1} \frac{k_1 \mu}{k_2 \lambda}$$

$$\cdot [J_n'(\mu b) - \frac{J_n(\mu a)}{H_n(\mu a)} H_n'(\mu b)] d_{e_{o}n}\} \quad . \qquad \text{(F.61)}$$

Now if one equates (F.59) and (F.61), makes use of (F.58) and observes that $J_n(\lambda b)H_n'(\lambda b) - J_n'(\lambda b)H_n(\lambda b) = \frac{j2}{\pi \lambda b}$, he will find that

$$\frac{k_1}{k_2} \frac{\mu}{\lambda} \{X_2 - X_3 + \frac{X_1 X_4}{X_0}\} d_{e_{o}n} = \frac{j2}{\pi \lambda b}$$

or

$$d_{e_{o}n} = \frac{j2}{\pi b} (\frac{k_2}{k_1}) \frac{1}{\mu} \frac{1}{\left[X_2 - X_3 + \frac{X_1 X_4}{X_0}\right]} \quad . \qquad \text{(F.62)}$$

So far all coefficients have been determined. However, they can be simplified significantly. To facilitate the simplification process, it is convenient to define

$$p_n = - \frac{J_n(\mu a)}{H_n(\mu a)} \qquad \text{(F.63)}$$

$$q_n = -\frac{J_n'(\mu a)}{H_n'(\mu a)} \tag{F.64}$$

$$r_n = \frac{H_n'(\lambda a)}{H_n'(\lambda a)} \tag{F.65}$$

$$P_n = J_n'(\mu b) + p_n H_n'(\mu b) \tag{F.66}$$

$$Q_n = J_n'(\mu b) + q_n H_n'(\mu b) \tag{F.67}$$

$$S_n = J_n(\mu b) + p_n H_n(\mu b) \tag{F.68}$$

and

$$T_n = J_n(\mu b) + q_n H_n(\mu b) \quad . \tag{F.69}$$

Then it can be shown that

$$X_0 = [-Q_n + \frac{\mu_2}{\mu_1}\frac{\mu}{\lambda} r_n T_n]H_n(\lambda b) \tag{F.70}$$

$$X_1 = \frac{jnh}{k_1 b}\frac{1}{\mu}[(\frac{\mu}{\lambda})^2 - 1]H_n(\lambda b)S_n \tag{F.71}$$

$$X_2 = [-\frac{\mu_2}{\mu_1} J_n'(\mu b) + (\frac{k_2}{k_1})^2 \frac{\mu}{\lambda} r_n J_n(\mu b)]H_n(\lambda b) \tag{F.72}$$

$$X_3 = [\frac{\mu_2}{\mu_1} p_n H_n'(\mu b) - (\frac{k_2}{k_1})^2 \frac{\mu}{\lambda} r_n p_n H_n(\mu b)]H_n(\lambda b) \tag{F.73}$$

$$X_2 - X_3 = [-\frac{\mu_2}{\mu_1} P_n + (\frac{k_2}{k_1})^2 \frac{\mu}{\lambda} r_n S_n]H_n(\lambda b) \tag{F.74}$$

$$X_4 = \frac{jnh}{k_1 b}\frac{\mu_2}{\mu_1}[(\frac{\mu}{\lambda})^2 - 1]\frac{H_n(\lambda b)}{\mu} T_n \tag{F.75}$$

$$X_1X_4 = -\frac{\mu_2}{\mu_1}\left(\frac{nh}{k_1b}\right)^2 \frac{1}{\mu^2}\left[\left(\frac{\mu}{\lambda}\right)^2 - 1\right]^2 H_n^2(\lambda b) S_n T_n \qquad (F.76)$$

$$X_0(X_2-X_3) + X_1X_4 = \left[\frac{H_n(\lambda b)}{\mu}\right]^2 Y_n$$

$$Y_n = \left[-\mu Q_n + \frac{\mu_2}{\mu_1}\frac{\mu^2}{\lambda} r_n T_n\right]\cdot\left[-\frac{\mu_2}{\mu_1}\mu P_n + \left(\frac{k_2}{k_1}\right)^2 \frac{\mu^2}{\lambda} r_n S_n\right]$$

$$- \frac{\mu_2}{\mu_1}\left(\frac{nh}{k_1b}\right)^2 \left[\left(\frac{\mu}{\lambda}\right)^2 - 1\right]^2 S_n T_n \quad , \qquad (F.77)$$

$$\tau_{0_n}^{e} = \pm \frac{j2}{\pi b\mu} \frac{X_4}{(X_0(X_2-X_3)+X_1X_4)}$$

$$= \mp \frac{2nh}{\pi k_1 b^2}\left(\frac{\mu_2}{\mu_1}\right)\left[\left(\frac{\mu}{\lambda}\right)^2 - 1\right]\left[\frac{H_n(\lambda b)}{\mu^2}\right] \frac{T_n}{[H_n(\lambda b)/\mu]^2 Y_n} = \pm \tau_n \quad , \qquad (F.78)$$

$$\tau_n = \frac{2nh}{\pi k_1 b^2}\left(\frac{\mu_2}{\mu_1}\right)\left[1 - \left(\frac{\mu}{\lambda}\right)^2\right] \frac{T_n}{H_n(\lambda b) Y_n} \qquad (F.79)$$

$$\gamma_{0_n}^{e} = \frac{j2}{\pi b\mu} \frac{(X_2-X_3)}{(X_0(X_2-X_3)+X_1X_4)} = \frac{j2}{\pi b\mu}\left[-\frac{(X_2-X_3)}{[H_n(\lambda b)/\mu]^2 Y_n}-\right] = \gamma_n \quad , \qquad (F.80)$$

$$\gamma_n = \frac{j2}{\pi b}\left[-\frac{\mu_2}{\mu_1}\mu P_n + \left(\frac{k_2}{k_1}\right)^2 \frac{\mu^2}{\lambda} r_n S_n\right] \frac{1}{H_n(\lambda b)\gamma_n} \tag{F.81}$$

$$\alpha_{o}^{e_n} = q_n \gamma_n \tag{F.82}$$

$$\beta_{o}^{e_n} = \pm p_n \tau_n \tag{F.83}$$

$$A_{o}^{e_n} = A_n \tag{F.84}$$

$$A_n = -\frac{J_n(\lambda b)}{H_n(\lambda b)} + \left(\frac{\mu_2}{\mu_1}\right)\left(\frac{\mu}{\lambda}\right)^2 \frac{T_n}{H_n(\lambda b)} \gamma_n \tag{F.85}$$

$$B_{o}^{e_n} = \pm B_n \tag{F.86}$$

$$B_n = \left(\frac{k_2}{k_1}\right)\left(\frac{\mu}{\lambda}\right)^2 \frac{S_n \tau_n}{H_n(\lambda b)} \tag{F.87}$$

$$d_{o}^{e_n} = \frac{j2}{\pi b}\left(\frac{k_2}{k_1}\right)\frac{1}{\mu^2} \frac{\mu X_o}{[H_n(\lambda b)/\mu]^2 \gamma_n} = d_n \tag{F.88}$$

$$d_n = \frac{j2}{\pi b}\left(\frac{k_2}{k_1}\right)\frac{[-\mu Q_n + \left(\frac{\mu_2}{\mu_1}\right)\frac{\mu^2}{\lambda} r_n T_n]}{H_n(\lambda b)\ \gamma_n} \tag{F.89}$$

$$a_{o}^{e_n} = p_n d_n \tag{F.90}$$

$$f_{e_{o_n}} = \pm \frac{j2}{\pi b} \left(\frac{k_2}{k_1}\right) \frac{1}{\mu} \quad \frac{X_1}{(X_0(X_2-X_3)+X_1X_4)}$$

$$= \pm \frac{j2}{\pi b} \left(\frac{k_2}{k_1}\right) \frac{1}{\mu} \left[\left(\frac{jnh}{k_1 b}\right) \frac{1}{\mu} \left(\frac{\mu^2}{\lambda^2} - 1\right) H_n(\lambda b) S_n\right] \frac{1}{[H_n(\lambda b)/\mu]^2 \, Y_n}$$

$$= \pm \frac{2nh}{\pi b^2} \left(\frac{k_2}{k_1^2}\right) \left[1 - \left(\frac{\mu}{\lambda}\right)^2\right] \frac{S_n}{H_n(\lambda b) Y_n} = \pm f_n \quad , \qquad \text{(F.91)}$$

$$f_n = \frac{2nh}{\pi b^2} \left(\frac{k_2}{k_1^2}\right) \left[1 - \left(\frac{\mu}{\lambda}\right)^2\right] \frac{S_n}{H_n(\lambda b) Y_n} = \left(\frac{\mu_1}{\mu_2}\right) \left(\frac{k_2}{k_1}\right) \frac{S_n}{T_n} \tau_n \quad , \qquad \text{(F.92)}$$

$$b_{e_{o_n}} = \pm q_n f_n \quad , \qquad \text{(F.93)}$$

$$C_{e_{o_n}} = C_n \quad , \qquad \text{(F.94)}$$

$$C_n = - \frac{J_n(\lambda b)}{H_n(\lambda b)} + \left(\frac{k_2}{k_1}\right) \left(\frac{\mu}{\lambda}\right)^2 \frac{S_n d_n}{H_n(\lambda b)} \quad , \qquad \text{(F.95)}$$

and

$$D_{e_{o_n}} = \pm \left(\frac{\mu_1}{\mu_2}\right) \left(\frac{\mu}{\lambda}\right)^2 \frac{T_n f_n}{H_n(\lambda b)}$$

$$= \pm \left[\frac{\mu_1}{\mu_2} \left(\frac{\mu}{\lambda}\right)^2 \frac{T_n}{H_n(\lambda b)}\right] \cdot \left[\left(\frac{\mu_1}{\mu_2}\right) \left(\frac{k_2}{k_1}\right) \frac{S_n}{T_n} \tau_n\right]$$

$$= \pm \left(\frac{k_2}{k_1}\right) \left(\frac{\mu}{\lambda}\right)^2 \frac{S_n \tau_n}{H_n(\lambda b)} = B_{e_{o_n}} = \pm B_n \quad . \qquad \text{(F.96)}$$

APPENDIX G

ON THE FUNCTION $\sqrt{k^2-h^2}$

In solving electromagnetic problems that involve Fourier integrals, one will encounter a multi-valued function of the form

$$f(h) = \sqrt{k^2-h^2} \tag{G.1}$$

where $k = k'+jk''$ is the propagation constant and $h = h'+jh''$ is the integration variable going from $-\infty$ to ∞. In addition, one may notice that $k'>0$ and $k''>_<0$ for the $e^{\mp j\omega t}$ time variation. To ensure convergence of the integrals one often finds it necessary to enforce the condition that

$$\text{Im}f(h) >_< 0 \tag{G.2}$$

for the $e^{\mp j\omega t}$ time dependence. It turns out that condition (G.2) will define the path of integration.

Letting $f(h) = \tau' + j\tau''$, it is apparent that

$$f^2(h) = k^2 - h^2 = k'^2 - k''^2 - h'^2 + h''^2 + j2(k'k'' - h'h'') = \tau'^2 - \tau''^2 + j2\tau'\tau'' \quad . \tag{G.3}$$

Equating the imaginary parts of (G.3) gives

$$\tau'' = \frac{k'k'' - h'h''}{\tau'} \quad . \tag{G.4}$$

Next, equating the ral parts of (G.3) and then employing (G.4) yield

$$\tau'^2 - \left[\frac{k'k'' - h'h''}{\tau'} \right]^2 = k'^2 - k''^2 - h'^2 + h''^2 \quad , \tag{G.5}$$

which can be readily solved to obtain

$$\tau' = \left\{ \left[\left(\frac{k'^2 - k''^2 - h'^2 + h''^2}{2} \right)^2 + (k'k'' - h'h'')^2 \right]^{1/2} + \frac{k'^2 - k''^2 - h'^2 + h''^2}{2} \right\}^{1/2} \quad . \tag{G.6}$$

It is clear that τ' is always positive. Making use of this fact in conjunction with (G.4) leads to the conclusion that

1. for $\tau'' > 0$ on the path of integration ($e^{-j\omega t}$ time dependence), one can set $h''=0$ when $k''>0$, and $h' \gtrless 0$, $h'' \lessgtr 0$ when $k''=0$;

2. for $\tau''<0$ on the path of integration ($ej\omega t$ time dependence), one can set $h''=0$ when $k''<0$, and $h'>_{<}0$, $h''<_{>}0$ when $k''=0$.

Typical paths of integration, each denoted by Γ, on which $\tau''>0$ and $\tau''<0$ when $k''=0$ are shown, respectively, in Figures G.1 and G.2.

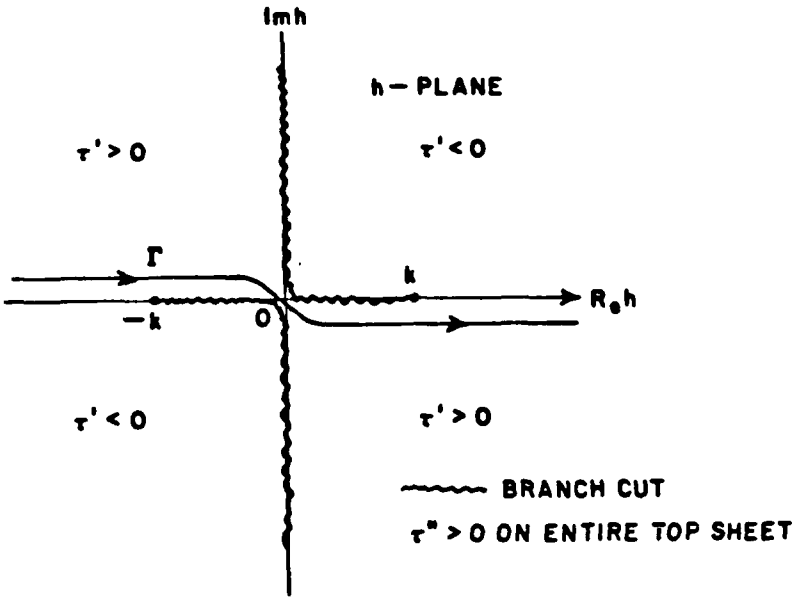

Figure G.1. Path of integration Γ in the h-plane and the analytic properties of $\sqrt{k^2-h^2}$ when k"=0 (for $e^{-j\omega t}$ time dependence).

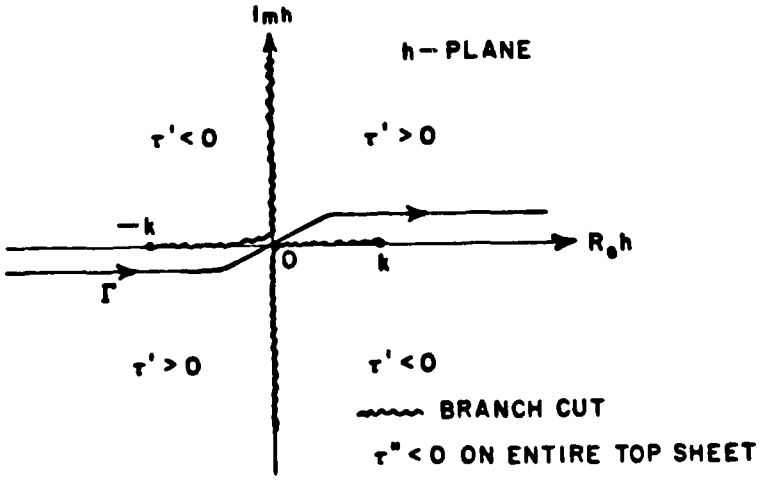

Figure G.2. Path of integration Γ in the h-plane and the analytic properties of $\sqrt{k^2-h^2}$ when k"=0 (for $e^{j\omega t}$ time dependence).

APPENDIX H

ON THE RATIOS P_n/S_n AND Q_n/T_n

From Equations (3.11) -(3.14) and (3.116)-(3.117), it is apparent that

$$\frac{P_n(\mu)}{S_n(\mu)} = \frac{J_n'(\mu b)H_n(\mu a)-J_n(\mu a)H_n'(\mu b)}{J_n(\mu b)H_n(\mu a)-J_n(\mu a)H_n(\mu b)} \quad , \tag{H.1}$$

and

$$\frac{Q_n(\mu)}{T_n(\mu)} = \frac{J_n'(\mu b)H_n'(\mu a)-J_n'(\mu a)H_n'(\mu b)}{J_n(\mu b)H_n'(\mu a)-J_n'(\mu a)H_n(\mu b)} \quad . \tag{H.2}$$

Since $H_n(\xi) = H_n^{(1)}(\xi) = J_n(\xi) + jY_n(\xi)$, where $Y_n(\xi)$ is the Neumann function of order n, one can rewrite (H.1) and (H.2) as follows:

$$\frac{P_n(\mu)}{S_n(\mu)} = \frac{J_n'(\mu b)Y_n(\mu a)-J_n(\mu a)Y_n'(\mu b)}{J_n(\mu b)Y_n(\mu a)-J_n(\mu a)Y_n(\mu b)} \quad , \tag{H.3}$$

and

$$\frac{O_n(\mu)}{T_n(\mu)} = \frac{J_n'(\mu b)Y_n'(\mu a)-J_n'(\mu a)Y_n'(\mu b)}{J_n(\mu b)Y_n'(\mu a)-J_n'(\mu a)Y_n(\mu b)} \quad . \tag{H.4}$$

By examining the ascending series for J_n and Y_n [26], one will note that

$$J_n(-z) = (-1)^n J_n(z) \quad , \tag{H.5}$$

and Y_n can be put in the form

$$Y_n(z) = \hat{Y}_n(z) + \frac{2}{\pi} \ln \frac{z}{2} J_n(z) \tag{H.6}$$

where $\hat{Y}(z)$ has the property that $\hat{Y}(-z) = (-1)^n \hat{Y}(z)$. Consequently,

$$Y_n(-z) = \hat{Y}(-z) + \frac{2}{\pi} \ln \left(\frac{-z}{2}\right) J_n(-z) = (-1)^n$$

$$\left[\hat{Y}_n(z) + \frac{2}{\pi} \ln \frac{z}{2} J_n(z) \pm j2J_n(z)\right] \quad . \tag{H.7}$$

Formally differentiating (H.5), (H.6) and (H.7) yields

$$J_n'(-z) = (-1)^{n-1} J_n'(z) \quad , \tag{H.8}$$

$$Y_n'(z) = \left[\hat{Y}_n'(z) + \frac{2}{\pi}\left[\frac{1}{z} J_n(z) + \ln \frac{z}{2} J_n'(z)\right]\right] \quad , \tag{H.9}$$

$$\hat{Y}_n'(-z) = (-1)^{n-1}\left[\hat{Y}_n'(z) + \frac{2}{\pi}\left[\frac{1}{z} J_n(z) + \ln \frac{z}{2} J_n'(z)\right] \pm j2J_n'(z)\right] .$$

It follows from (H.5)-(H.10) that

$$\frac{P_n(-\mu)}{S_n(-\mu)} = \Big[\{(-1)^{n-1} J_n'(\mu b)\} \{(-1)^n [\hat{Y}_n(\mu a) + \frac{2}{\pi} \ln \frac{\mu a}{2} J_n(\mu a) \pm j2J_n(\mu a)]\} - \{(-1)^n J_n(\mu a)\} \{(-1)^{n-1} [\hat{Y}_n'(\mu b) + \frac{2}{\pi} (\ln \frac{\mu b}{2} J_n'(\mu b) + \frac{1}{\mu b} J_n(\mu b)) \pm j2J_n'(\mu b)]\} \Big] \Big/ \Big[\{(-1)^n J_n(\mu b)\} \{(-1)^n [\hat{Y}_n(\mu a) + \frac{2}{\pi} \ln \frac{\mu a}{2} J_n(\mu a) \pm j2J_n(\mu a)]\} - \{(-1)^n J_n(\mu a)\} \cdot \{(-1)^n [\hat{Y}_n(\mu b) + \frac{2}{\pi} \ell_n \frac{\mu b}{2} J_n(\mu b) \pm j2J_n(\mu b)]\} \Big]$$

$$= \frac{(-1)^{2n-1} \{J_n'(\mu b) Y_n(\mu a) - J_n(\mu a) Y_n'(\mu b)\}}{(-1)^{2n} \{J_n(\mu b) Y_n(\mu a) - J_n(\mu a) Y_n(\mu b)\}} = - \frac{P_n(\mu)}{S_n(\mu)} \quad . \quad \text{(H.11)}$$

and

$$\frac{Q_n(-\mu)}{T_n(-\mu)} = \Big[\{(-1)^{n-1} J_n'(\mu b)\} \{(-1)^{n-1} [\hat{Y}_n'(\mu a) + \frac{2}{\pi} (\frac{1}{\mu a} J_n(\mu a) + \ln \frac{\mu a}{2} J_n'(\mu a)) \pm j2J_n'(\mu a)]\} - \{(-1)^{n-1} J_n'(\mu a)\} \cdot \{(-1)^{n-1} [\hat{Y}_n'(\mu b) + \frac{2}{\pi} (\frac{1}{\mu b} J_n(\mu b) + \ln \frac{\mu b}{2} J_n'(\mu b)) \pm j2J_n'(\mu b)]\} \Big] \Big/ \Big[\{(-1)^n J_n(\mu b)\} \{(-1)^{n-1} [\hat{Y}_n'(\mu a)$$

$$+ \frac{2}{\pi}\left(\frac{1}{\mu a} J_n(\mu a) + \ln \frac{\mu a}{2} J_n'(\mu a)\right) \pm j2J_n'(\mu a)]\}$$

$$- \{(-1)^{n-1} J_n'(\mu a)\} \cdot \{(-1)^n [\hat{Y}_n(\mu b) + \frac{2}{\pi} \ln \frac{\mu b}{2} J_n(\mu b)$$

$$\pm j2J_n(\mu b)]\}\Big]^{-}$$

$$= \frac{(-1)^{2(n-1)}\{J_n'(\mu b)Y_n'(\mu a) - J_n'(\mu a)Y_n'(\mu b)\}}{(-1)^{2n-1}\{J_n(\mu b)Y_n'(\mu a) - J_n'(\mu a)Y_n(\mu b)\}} = -\frac{Q_n(\mu)}{T_n(\mu)} \quad . \tag{H.12}$$

Thus from (H.11) and (H.12), it is seen that both P_n/S_n and Q_n/T_n are odd functions of μ.

APPENDIX I

CALCULATION OF CYLINDER FUNCTIONS: J_n, J_n', H_n, H_n'

It is well-known that all cylinder functions satisfy the following recurrence relations:

$$C_{n-1}(z) + C_{n+1}(z) = \frac{2n}{z} C_n(z) \quad , \tag{I.1}$$

$$C_{n-1}(z) - C_{n+1}(z) = 2C_n'(z) \quad , \tag{I.2}$$

where C denotes J, Y and $H \triangleq H^{(1)}$. Equation (I.1) indicates that any two known consecutuve members of a sequence $\{C_n(z)\}_o^N$ can be used to compute the entire sequence. Moreover, the corresponding sequence of derivatives $\{C_n'(z)\}_o^N$ can be subsequently computed via (I.2). Thus it is sufficient to consider how to evaluate the sequences $\{J_n(z)\}_o^N$ and $\{H_n(z)\}_o^N$ only.

From experience it is learned that the calculation of the sequence $\{J_n(z)\}_o^N$ is stable numerically only if the recurrence relations are applied downward, and unstable otherwise. In addition, only a finite sequence can be generated, i.e., $N < \infty$, because of the limited dynamic range of a digital computer.

One can verify that the sequence $\{\beta J_n(z)\}_0^N$ satisfies (I.1) and (I.2), where β is an arbitrary scalar. Next letting $\{\hat{J}_n(z)\}_0^{N+1}$ be such a sequence that

$$\hat{J}_{N+1}(z) = 0 \quad , \tag{I.3}$$

and

$$\hat{J}_N(z) = \alpha \quad , \tag{I.4}$$

where α is some vanishingly small number. The remainders of the sequence are calculated using the recurrence relation (I.1) downward. By setting $\{\hat{J}_n(z)\}_0^N = \{\beta J_n(z)\}_0^N$, one finds $J_n(z) = \hat{J}_n(z)/\beta$, n=0,1,...,N, and thus the sequence $\{J_n(z)\}_0^N$ will be determined as soon as β is known.

Noting $\beta = \hat{J}_n(z)/J_n(z)$, n=0,1,...,N, it is clear that $\beta=\hat{J}_0(z)/J_0(z)$ is most easily determined since $J_0(z)$ can be simply computed as follows:

1. When $|z| < 8$,

$$J_0(z) = \sum_{k=0}^{\infty} \frac{(-\frac{1}{4}z^2)^k}{(k!)^2} \quad , \tag{I.5}$$

where the series converges rapidly.

2. When $|z| > 8$,

$$J_0(z) = \frac{1}{\pi} \int_0^{\pi} e^{jz\cos\theta} d\theta \quad , \tag{I.6}$$

where the integral is evaluated by Simpson's quadrature.

Once the sequence $\{J_n(z)\}_0^N$ is generated, one can immediately move onto the calculation of the sequence $\{H_n(z)\}_0^N$ which is described below:

1. When $|z| < 8$, Lommel's formula [27, pp. 143] can be employed to evaluate $Y_0(z)$:

$$Y_0(z) = \frac{2}{\pi}\left[(\log\frac{z}{2} + \gamma)J_0(z) + \sum_{k=1}^{\infty}\frac{(z/2)^k J_k(z)}{k\cdot k!}\right] , \qquad (I.7)$$

where $\gamma = \lim_{m\to\infty}[1 + \frac{1}{2} + \frac{1}{3} + \ldots + \frac{1}{m} - \ln m] = .5772157$ is known as Euler's constant. Next it follows from the Wronskian,

$$W\{J_n(z),Y_n(z)\} = J_{n+1}(z)Y_n(z) - J_n(z)Y_{n+1}(z) = \frac{2}{\pi z},\ n=0,1,2,\ldots N-1, \qquad (I.8)$$

that the sequence $\{Y_n(z)\}_0^N$ is readily determined. Finally, making use of the relation $H_n(z) = J_n(z) + jY_n(z)$, the sequence $\{H_n(z)\}_0^N$ is obtained quite simply.

2. When $|z| > 8$, the sequence $\{H_n(z)\}_0^N$ is directly computed by first evaluating $H_0(z)$ via Hankel's asymptotic expansions [26]:

$$H_0(z) \sim \sqrt{\frac{2}{\pi z}}\,[P(z)+jQ(z)]\,e^{j(z-\pi/4)} , \qquad (I.9)$$

where

$$P(z) = 1 + \frac{1^2\cdot 3^2}{2!(8z)^2} + \frac{1^2\cdot 3^2\cdot 5^2\cdot 7^2}{4!(8z)^4} + \ldots , \qquad (I.10)$$

and

$$Q(z) = -\frac{1^2}{8z} + \frac{1^2 \cdot 3^2 \cdot 5^2}{3!(8z)^3} - \frac{1^2 \cdot 3^2 \cdot 5^2 \cdot 7^2 \cdot 9^2}{5!(8z)^5} + \cdots \quad , \tag{I.11}$$

then employing the Wronskian,

$$W\{J_n(z), H_n(z)\} = J_{n+1}(z)H_n(z) - J_n(z)H_{n+1}(z) = \frac{j2}{\pi z} \quad . \tag{I.12}$$

It must be mentioned that, as $\mathrm{Im}z \to \infty$, evaluating Jo(z) and Ho(z) according to (I.6) and (I.9), respectively, will encounter severe numerical problems commonly known as computer floating-point overflow and underflow. Such will prevent one to calculate the sequences $\{J_n(z)\}_o^N$ and $\{H_n(z)\}_o^N$ accurately. A simple but effective way to handle these problems is through the proper scaling of $J_o(z)$ and $H_o(z)$, and hence the resulting sequences. This means that $J_n(z)$ and $H_n(z)$ are being modified through multiplicative factors $\bar{e}^s$ and e^s, respectively, where s is some appropriate positive real number. Letting $\{\tilde{J}_n(z)\}_o^N$ and $\{\tilde{H}_n(z)\}_o^N$ be the scaled sequences corresponding to $\{J_n(z)\}_o^N = \{H_n(z)\}_o^N$, one can write

$$\{\tilde{J}_n(z)\}_o^N = \{e^{-s}J_n(z)\}_o^N = \{(\tilde{J}_o(z)/\hat{J}_o(z))\hat{J}_n(z)\}_o^N \quad , \tag{I.13}$$

and

$$\{\tilde{H}_n(z)\}_o^N = \{e^{s}H_n(z)\}_o^N \quad , \tag{I.14}$$

where

$$\tilde{J}_o(z) = e^{-s}J_o(z) = \frac{1}{\pi}\int_0^{\pi} e^{jz\cos\theta - s}d\theta \quad , \tag{I.15}$$

and $\tilde{H}_n(z)$ are computed sequentially according to the Wronskian,

$$W\{\tilde{J}_n(z),\ \tilde{H}_n(z)\} = \tilde{J}_{n+1}(z)\tilde{H}_n(z) - \tilde{J}_n(z)\tilde{H}_{n+1}(z) = \frac{j2}{\pi z},\ n=0,1,\ldots,N-1, \tag{I.16}$$

with

$$\tilde{H}_o(z) = e^{s}H_o(z) \sim \sqrt{\frac{2}{\pi z}}\ [P(z) + jQ(z)]\ e^{j(z-\pi/4)\ +\ s} \quad . \tag{I.17}$$

It is important to observe that the function W(n,h) in (4.83) is independent of the scaling factors $e^{\pm s}$. This is obvious if one realizes that (from Equations (4.88)-(4.92))

$$r_n = \frac{H_n'(\lambda b)}{H_n(\lambda b)} = \frac{\tilde{H}_n'(\lambda b)}{\tilde{H}_n(\lambda b)} \quad , \tag{I.18}$$

$$\frac{P_n}{S_n} = \frac{J_n'(\mu b)H_n(\mu a) - J_n(\mu a)H_n'(\mu b)}{J_n(\mu b)H_n(\mu a) - J_n(\mu a)H_n(\mu b)} = \frac{\tilde{J}_n'(\mu b)\tilde{H}_n(\mu a) - \tilde{J}_n(\mu a)\tilde{H}_n'(\mu b)}{\tilde{J}_n(\mu b)\tilde{H}_n(\mu a) - \tilde{J}_n(\mu a)\tilde{H}_n(\mu b)} \tag{I.19}$$

$$\frac{Q_n}{T_n} = \frac{J_n'(\mu b)H_n'(\mu a) - J_n'(\mu a)H_n'(\mu b)}{J_n(\mu b)H_n'(\mu a) - J_n'(\mu a)H_n(\mu b)} = \frac{\tilde{J}_n'(\mu b)\tilde{H}_n'(\mu a) - \tilde{J}_n'(\mu a)\tilde{H}_n'(\mu b)}{\tilde{J}_n(\mu b)\tilde{H}_n'(\mu a) - \tilde{J}_n'(\mu a)\tilde{H}_n(\mu b)} \tag{I.20}$$

APPENDIX J

ASYMPTOTIC FORM OF Q(ν)

In this appendix, an asymptotic form of Q(ν), defined by (5.50), based on the Debye approximations is derived. From (4.110) and (4.111), the Deybe approximations of $H_\nu^{(\frac{1}{2})}(\xi)$ and $H_\nu^{(\frac{1}{2})'}(\xi)$ can be written as:

$$H_\nu^{(\frac{1}{2})}(\xi) \sim \frac{2}{\pi} \frac{e^{\pm j(\sqrt{\xi^2-\nu^2} - \nu \cos^{-1}(\nu/\xi)-\pi/4)}}{(\xi^2-\nu^2)^{1/4}} , \qquad (J.1)$$

$$H_\nu^{(\frac{1}{2})'}(\xi) = \frac{\partial}{\partial \xi} H_\nu^{(\frac{1}{2})}(\xi) \sim \pm j \frac{\sqrt{\xi^2-\nu^2}}{\xi} H_\nu^{(\frac{1}{2})}(\xi) , \qquad (J.2)$$

where $|\xi|>|\nu|$, $|\xi-\nu|>|\nu^{1/3}|$, and ξ large. It follows that

$$\begin{vmatrix} H_\nu^{(1)}(\alpha) & H_\nu^{(2)}(\beta) \\ H_\nu^{(2)}(\alpha) & H_\nu^{(1)}(\beta) \end{vmatrix} \sim \frac{2}{\pi} \frac{e^{\mp jF(\nu)}}{(\alpha^2-\nu^2)^{1/4}(\beta^2-\nu^2)^{1/4}} , \qquad (J.3)$$

where

$$F(\nu) = \sqrt{\beta^2-\nu^2} - \sqrt{\alpha^2-\nu^2} + \nu(\cos^{-1}(\nu/\alpha) - \cos^{-1}(\nu/\beta)) \ . \qquad (J.4)$$

Also,

$$\frac{H_\nu^{(1)'}(\gamma)}{H_\nu^{(1)}(\gamma)} \sim j\frac{\sqrt{\gamma^2-\nu^2}}{\gamma} \ . \qquad (J.5)$$

Employing (J.3) and (J.5) in Q(ν) yields

$$Q(\nu) \sim \frac{e^{-jF(\nu)} - e^{jF(\nu)}}{j\sqrt{\varepsilon_r}\frac{\sqrt{\beta^2-\nu^2}}{\beta}\left[e^{-jF(\nu)} + e^{jF(\nu)}\right] + \frac{j\sqrt{\gamma^2-\nu^2}}{\gamma}\left[e^{-jF(\nu)} - e^{jF(\nu)}\right]} \ . \qquad (J.6)$$

Recalling that $\alpha = \sqrt{\varepsilon_r}\, k_2 a$, $\beta = \sqrt{\varepsilon_r}\, k_2 b$, and $\gamma = k_2 b$, one can deduce from (J.6) that

$$Q(\nu) \sim \frac{k_2\left\{e^{-jF(\nu)} - e^{jF(\nu)}\right\}}{j\left[\sqrt{\varepsilon_r k_2^2-(\nu/a)^2}\left[e^{-jF(\nu)} + e^{jF(\nu)}\right] + \sqrt{k_2^2-(\nu/a)^2}\left[e^{-jF(\nu)} - e^{jF(\nu)}\right]\right]} \qquad (J.7)$$

where it is assumed that a>>(b-a) such that (ν/b)≈(ν/a). It can be readily verified that (J.7) leads to

$$Q(\nu) \sim \frac{-k_2 \sin F(\nu)}{\sqrt{\varepsilon_r k_2^2-(\nu/a)^2}\cos F(\nu) - j\sqrt{k_2^2-(\nu/a)^2}\sin F(\nu)} \qquad (J.8)$$

which is used in (5.51).

APPENDIX K

THIN SUBSTRATE APPROXIMATION OF $Z_\nu(h)$

When a large cylinder of radius a is coated with an electrically thin substrate, one will have

$$|\mu b| = \left| b\sqrt{\varepsilon_r k_2^2 - h^2} \right| >> 1 \quad , \quad |\mu(b-a)| = |\mu t| < 1. \tag{K.1}$$

This permits one to approximate and hence simplify the complicated function $Z_\nu(h)$ defined in (5.47) as

$$Z_\nu(h) \triangleq -\sqrt{\varepsilon_r}\,\frac{P_\nu}{S_\nu} = -\sqrt{\varepsilon_r}\,\frac{H_\nu^{(1)}(\mu a)H_\nu^{(2)\prime}(\mu b) - H_\nu^{(2)}(\mu a)H_\nu^{(1)\prime}(\mu b)}{H_\nu^{(1)}(\mu a)H_\nu^{(2)}(\mu b) - H_\nu^{(2)}(\mu a)H_\nu^{(1)}(\mu b)} \,. \tag{K.2}$$

Denoting J_ν, $H_\nu^{(1)}$ or $H_\nu^{(2)}$ by C_ν, one can Taylor expand $C_\nu(\mu a)$ and $C_\nu'(\mu a)$ about μb by taking the first two leading terms as follows:

$$C_\nu(\mu a) \simeq C_\nu(\mu b) - \mu t C_\nu'(\mu b) \quad , \tag{K.3}$$

and

$$C_\nu'(\mu a) \approx C_\nu'(\mu b) - \mu t C_\nu''(\mu b) \quad . \tag{K.4}$$

Since C_ν satisfies the Bessel differential equation, one can write

$$C_\nu''(\mu b) = -\frac{1}{\mu b} C_\nu'(\mu b) - \left[1 - \left(\frac{\nu}{\mu b}\right)^2\right] C_\nu(\mu b) \quad . \tag{K.5}$$

Substituting (K.5) into (K.4) produces

$$C_\nu'(\mu a) \approx C_\nu'(\mu b)\left[1 + \frac{t}{b}\right] + \mu t\left[1 - \left(\frac{\nu}{\mu b}\right)^2\right] C_\nu(\mu b) \quad . \tag{K.6}$$

It may be pointed out that only (K.3), but not (K.5), is needed in approximating $Z_\nu(h)$. This is clear when one observes that

$$Z_\nu(h) \approx -\sqrt{\varepsilon_r}\; \frac{\begin{array}{l}[H_\nu^{(1)}(\mu b) - \mu t H_\nu^{(1)\prime}(\mu b)]H_\nu^{(2)\prime}(\mu b) - \\ - [H_\nu^{(2)}(\mu b) - \mu t H_\nu^{(2)\prime}(\mu b)]H_\nu^{(1)\prime}(\mu b)\end{array}}{\begin{array}{l}[H_\nu^{(1)}(\mu b) - \mu t H_\nu^{(1)\prime}(\mu b)]H_\nu^{(2)}(\mu b) - \\ - [H_\nu^{(2)}(\mu b) - \mu t H_\nu^{(2)\prime}(\mu b)]H_\nu^{(1)}(\mu b)\end{array}} \quad , \tag{K.7}$$

or

$$Z_\nu(h) \approx -\frac{\sqrt{\varepsilon_r}}{\mu t} \quad . \tag{K.8}$$

APPENDIX L

ROOTS OF $P(\sigma) = yw_1'(\sigma) - w_1(\sigma) = 0$

It is convenient to consider the roots of P as functions of y. Formally differentiating $P(\sigma) = 0$ with respect to y produces

$$w_1'(\sigma) + yw_1''(\sigma)\frac{d\sigma}{dy} - w_1'\frac{d\sigma}{dy} = 0 \quad . \tag{L.1}$$

Recalling that w_1 satisfies the Airy differential equation, one will note

$$w_1''(\sigma) = \sigma w_1(\sigma) \quad . \tag{L.2}$$

It is also clear from the equation $P(\sigma) = 0$ that

$$w_1(\sigma) = yw_1'(\sigma) \quad . \tag{L.3}$$

Employing (L.2) and (L.3) in (L.1) yields

$$w_1'(\sigma)\left\{1 + \left[y^2\sigma - 1\right]\frac{d\sigma}{dy}\right\} = 0 \quad . \tag{L.4}$$

One can easily derive from (L.4) the following non-linear differential equation which governs the roots of $P(\sigma) = 0$:

$$\frac{d\sigma}{dy} = \frac{1}{1-y^2\sigma} \quad . \tag{L.5}$$

It is readily observed that $y=0$ if only if $w_1(\sigma) = 0$. Since w_1 vanishes at

$$\sigma = t_p = e^{j\pi/3}\tau_p \qquad , \quad p = 1,2,3,\ldots, \tag{L.6}$$

where τ_p's are the zeros of $A_i(-\tau)$ (Airy function), one sees that

$$\sigma(0) = t_p \ , \ p = 1,2,3,\ldots \quad . \tag{L.7}$$

It is then natural to denote the solution of (L.5) corresponding to the intitial condition $\sigma(0) = t_p$ by $\sigma_p(y)$, $p = 1,2,3\ldots$.

Next letting $\sigma_p^{(n)} = \frac{d^n}{dy^n}\sigma_p(y)$, one can formally Taylor expand $\sigma_p^{(1)}(y)$ about $y=0$ as follows:

$$\sigma_p^{(1)}(y) = \sum_{n=0}^{\infty} \frac{\sigma_p^{(n+1)}(0)}{n!}\, y^n \quad . \tag{L.8}$$

For notational simplicity the symbol $\sigma^{(n)}$ will mean $\sigma_p^{(n)}$ in the following computations, unless specified otherwise. It is obvious from (L.5) that

$$\sigma^{(1)}(0) = 1 \ . \tag{L.9}$$

$$\sigma^{(2)}(y) = \frac{2y\sigma + y^2\sigma^{(1)}}{(1-y^2\sigma)^2} = [2y\sigma + y^2\sigma^{(1)}][\sigma^{(1)}]^2 \quad , \tag{L.10}$$

$$\sigma^{(2)}(0) = 0 \quad . \tag{L.11}$$

$$\sigma^{(3)}(y) = [2\sigma+2y\sigma^{(1)}+2y\sigma^{(1)}+y^2\sigma^{(2)}][\sigma^{(1)}]^2 + [2y\sigma+y^2\sigma^{(1)}][2\sigma^{(1)}\sigma^{(2)}]$$

$$= 2\sigma[\sigma^{(1)}]^2 + \{4y[\sigma^{(1)}]^3+4y\sigma\sigma^{(1)}\sigma^{(2)}\}+3y^2[\sigma^{(1)}]^2\sigma^{(2)} \quad , \tag{L.12}$$

$$\sigma^{(3)}(0) = 2\sigma(0)[1]^2 = 2t_p \quad . \tag{L.13}$$

$$\sigma^{(4)}(y) = 2[\sigma^{(1)}]^3+4\sigma\sigma^{(1)}\sigma^{(2)}+4\{[\sigma^{(1)}]^3+\sigma\sigma^{(1)}\sigma^{(2)}\}+4y\{3[\sigma^{(1)}]^2\sigma^{(2)}$$

$$+ [\sigma^{(1)}]^2\sigma^{(2)}+\sigma[\sigma^{(2)}]^2+\sigma\sigma^{(1)}\sigma^{(3)}\}+6y[\sigma^{(1)}]^2\sigma^{(2)}$$

$$+ 6y^2\sigma^{(1)}[\sigma^{(2)}]^2+3y^2[\sigma^{(1)}]^2\sigma^{(3)}$$

$$= 6[\sigma^{(1)}]^3+8\sigma\sigma^{(1)}\sigma^{(2)}+y\{22[\sigma^{(1)}]^2\sigma^{(2)}+4\sigma[\sigma^{(2)}]^2+4\sigma\sigma^{(1)}\sigma^{(3)}\}$$

$$+ y^2\{6\sigma^{(1)}[\sigma^{(2)}]^2+3[\sigma^{(1)}]^2\sigma^{(3)}\} \quad , \tag{L.14}$$

$$\sigma^{(4)}(0) = 6 \quad . \tag{L.15}$$

$$\sigma^{(5)}(y) = 18[\sigma^{(1)}]^2\sigma^{(2)}+8[\sigma^{(1)}]^2\sigma^{(2)}+8\sigma[\sigma^{(2)}]^2+8\sigma\sigma^{(1)}\sigma^{(3)}$$

$$+ \{22[\sigma^{(1)}]^2\sigma^{(2)}+4\sigma[\sigma^{(2)}]^2+4\sigma\sigma^{(1)}\sigma^{(3)}\}+y\{44\sigma^{(1)}[\sigma^{(2)}]^2$$

$$+ 22[\sigma^{(1)}]^2\sigma^{(3)}+4\sigma^{(1)}[\sigma^{(2)}]^2+8\sigma\sigma^{(2)}\sigma^{(3)}+4[\sigma^{(1)}]^2\sigma^{(3)}$$

$$+ 4\sigma\sigma^{(2)}\sigma^{(3)}+4\sigma\sigma^{(1)}\sigma^{(4)}\} + 2y\{6\sigma^{(1)}[\sigma^{(2)}]^2+3[\sigma^{(1)}]^2\sigma^{(3)}\}$$

$$+ y^2\{6[\sigma^{(2)}]^3 + 12\sigma^{(1)}\sigma^{(2)}\sigma^{(3)}+6\sigma^{(1)}\sigma^{(2)}\sigma^{(3)}+3[\sigma^{(1)}]^2\sigma^{(4)}\}$$

$$= 48[\sigma^{(1)}]^2\sigma^{(2)}+12\sigma[\sigma^{(2)}]^2+12\sigma\sigma^{(1)}\sigma^{(3)}+y\{60\sigma^{(1)}[\sigma^{(2)}]^2$$

$$+ 32[\sigma^{(1)}]^2\sigma^{(3)}+12\sigma\sigma^{(2)}\sigma^{(3)}+4\sigma\sigma^{(1)}\sigma^{(4)}\}+y^2\{3[\sigma^{(1)}]^2\sigma^{(4)}$$

$$+ 6[\sigma^{(2)}]^3+18\sigma^{(1)}\sigma^{(2)}\sigma^{(3)}\} \quad , \qquad \text{(L.16)}$$

$$\sigma^{(5)}(0) = 24t_p^2 \quad . \qquad \text{(L.17)}$$

$$\sigma^{(6)}(y) = 96\sigma^{(1)}[\sigma^{(2)}]^2+48[\sigma^{(1)}]^2\sigma^{(3)}+12\sigma^{(1)}[\sigma^{(2)}]^2+24\sigma\sigma^{(2)}\sigma^{(3)}$$

$$+ 12[\sigma^{(1)}]^2\sigma^{(3)}+12\sigma\sigma^{(2)}\sigma^{(3)}+12\sigma\sigma^{(1)}\sigma^{(4)}+\{60\sigma^{(1)}[\sigma^{(2)}]^2$$

$$+ 32[\sigma^{(1)}]^2\sigma^{(3)}+12\sigma\sigma^{(2)}\sigma^{(3)}+4\sigma\sigma^{(1)}\sigma^{(4)}\}+y\{60[\sigma^{(2)}]^3$$

$$+ 120\sigma^{(1)}\sigma^{(2)}\sigma^{(3)}+64\sigma^{(1)}\sigma^{(2)}\sigma^{(3)}+32[\sigma^{(1)}]^2\sigma^{(4)}+12[\sigma^{(3)}]^2\sigma$$

$$+ 12\sigma^{(1)}\sigma^{(2)}\sigma^{(3)}+12\sigma\sigma^{(2)}\sigma^{(4)}+4[\sigma^{(1)}]^2\sigma^{(4)}$$

$$+ 4\sigma\sigma^{(2)}\sigma^{(4)}+4\sigma\sigma^{(i)}\sigma^{(5)}\} + y\{6[\sigma^{(1)}]^2\sigma^{(4)}+12[\sigma^{(2)}]^3$$

$$+ 36\sigma^{(1)}\sigma^{(2)}\sigma^{(3)}\} + y^2\{...\}$$

$$= 168\sigma^{(1)}[\sigma^{(2)}]^2+92[\sigma^{(1)}]^2\sigma^{(3)}+16\sigma\sigma^{(1)}\sigma^{(4)}+48\sigma\sigma^{(2)}\sigma^{(3)}+y\{72[\sigma^{(2)}]^3$$

$$+ 232\sigma^{(1)}\sigma^{(2)}\sigma^{(3)}+12\sigma[\sigma^{(3)}]^2+16\sigma\sigma^{(2)}\sigma^{(4)}+4\sigma\sigma^{(1)}\sigma^{(5)}+42[\sigma^{(1)}]^2\sigma^{(4)}\}$$

$$+ y^2\{...\} \quad , \tag{L.18}$$

$$\sigma^{(6)}(0) = 280t_p \quad . \tag{L.19}$$

$$\sigma^{(7)}(y) = 168[\sigma^{(2)}]^3 + 336\sigma^{(1)}\sigma^{(2)}\sigma^{(3)} + 184\sigma^{(1)}\sigma^{(2)}\sigma^{(3)} + 92[\sigma^{(1)}]^2\sigma^{(4)}$$

$$+ 16[\sigma^{(1)}]^2\sigma^{(4)} + 16\sigma\sigma^{(2)}\sigma^{(4)} + 16\sigma\sigma^{(1)}\sigma^{(5)} + 48\sigma^{(1)}\sigma^{(2)}\sigma^{(3)}$$

$$+ 48\sigma[\sigma^{(3)}]^2 + 48\sigma\sigma^{(2)}\sigma^{(4)} + 72[\sigma^{(2)}]^3 + 232\sigma^{(1)}\sigma^{(2)}\sigma^{(3)} + 12\sigma[\sigma^{(3)}]^2$$

$$+ 16\sigma\sigma^{(2)}\sigma^{(4)} + 4\sigma\sigma^{(1)}\sigma^{(5)} + 42[\sigma^{(1)}]^2\sigma^{(4)} + y\{\ldots\} + y^2\{\ldots\} \ , \tag{L.20}$$

$$\sigma^{(7)}(0) = 900 + 720t_p \quad . \tag{L.21}$$

Substituting (L.9), (L.11), (L.13), (L.15), (L.17), (L.19) and (L.21) into (L.8), and recalling $\sigma^{(n)}(y) = \sigma_p^{(n)}(y)$, one obtains

$$\sigma_p^{(1)}(y) = 1 + t_p y^2 + y^3 + t_p^2 y^4 + \frac{7}{3} t_p y^5 + [t_p^3 + 5/4]\, y^6 + \ldots . \tag{L.22}$$

Integrating both sides of (L.21) over the interval [o,y], one finally arrives at

$$\sigma_p(y) = t_p + y + \frac{t_p}{3} y^3 + \frac{1}{4} y^4 + \frac{t_p^2}{5} y^5 + \frac{7t_p}{18} y^6$$

$$+ \left[\frac{t_p^3}{7} + \frac{5}{28} \right] y^7 \ , \ p = 1,2,3,\ldots \quad . \tag{L.23}$$

The Taylor series expansion (L.23) of the roots of $yw_1''(\sigma) - w_1(\sigma) = 0$ is most suitable when $|y| \ll 1$.

REFERENCES

[1] Deschamps, G.A., "Microstrip Microwave Antennas", presented at the 3rd USAF Symposium on Antennas, 1953.

[2] Gutton, H. and G. Baissinot, "Flat Aerial for Ultra High-frequencies", French Patent No. 703113, 1955.

[3] Howell, J.Q., "Microstrip Antennas", IEEE AP-S International Symp. Digest, 1972, pp. 177-180.

[4] Munson, R.E., "Conformal Microstrip Antennas and Microstrip Phased Arrays", IEEE Trans. on Antennas and Prop., Vol. AP-22, 1974, pp. 74-78.

[5] Bahl, I.J. and P. Bhartia, Microstrip Antennas, Artech House, Massachusetts, 1980.

[6] James, J.R., P.S. Hall and C. Wood, Microstrip Antenna Theory and Design, Peter Peregrinus, New York, 1981.

[7] IEEE Trans. Antennas Propagation, special issue on Microstrip Antennas and Arrays (D.C. Chang, editor), Vol. AP-29, No. 1, January 1981.

[8] Carver, K.R. and J.W. Mink, "Microstrip Antenna Technology", IEEE Trans. on Antennas and Prop., AP-29, pp. 2-24, January 1981.

[9] Mailloux, R.J., J.F. McIlvenna and N.P. Kernweis, "Microstrip Array Technology", IEEE Trans. on Antennas and Prop., AP-29, pp. 25-37, January 1981.

[10] Derneryd, A.G., "Linearly Polarized Microstrip Antennas", IEEE Trans. on Antennas and Prop., Vol. AP-24, pp. 846-851, November 1976.

[11] Lo, Y.T., D. Solomon and W.F. Richards, "Theory and Experiment on Microstrip Antennas", IEEE Trans. on Antennas and Prop., Vol. AP-27, pp. 137-145, March 1979.

[12] Newman, E.H. and P. Tulyathan, "Analysis of Microstrip Antennas Using Moment Methods", IEEE Trans. on Antennas and Prop., Vol. AP-29, pp. 47-53, January 1981.

[13] Alexopoulos, N.G., P.L.E. Uslenghi and N.K. Uzunoglu, "Microstrip Dipoles on Cylindrical Structures", Electromagnetics, Vol. 3, No. 3-4, pp. 311-326, July-December 1983.

[14] Alexopoulos, N.G. and I.E. Rana, "Mutual Impedance Computation Between Printed Dipoles", IEEE Trans. on Antennas and Prop., Vol. AP-29, No. 1, pp. 106-111, January 1981.

[15] Stratton, J.A., Electromagnetic Theory, McGraw-Hill, New York, 1941.

[16] Harrington, R.F., Time-Harmonic Electromagnetic Fields, McGraw-Hill, New York, 1961.

[17] Newman, E.H. and D.M. Pozar, "Electromagnetic Modeling of Composite Wire and Surface Geometries", IEEE Trans. on Antennas and Prop., Vol. AP-26, pp. 784-88, November 1978.

[18] Jedlicka, R.P., M.T. Poe and K.R. Carver, "Measured Mutual Coupling Between Microstrip Antennas", IEEE Trans. on Antennas and Prop., Vol. AP-29, pp. 147-49, January 1981.

[19] Tai, C.T., Dyadic Green's Functions in Electromagnetic Theory, Intext Educational Publishers, 1971.

[20] Tai, C.T., "Eigenfunction Expansion of Dyadic Green's Functions", Math. Note 28, Weapons Systems Laboratory, Kirtland Air Force Base, Albuquerque, New Mexico, 1973.

[21] Tai, C.T., "Singular Terms in the Eigenfunction Expansion of the Electric Dyadic Green's Functions", Technical Report, No. RL570, Rad. Lab., The University of Michigan, Ann Arbor, Michigan, March 1980.

[22] Collin, R.E., "On the Incompleteness of E and H Modes in Waveguides", Can. J. Phys., Vol. 51, pp. 1135-1140, June 1973.

[23] Rahmat-Samii, Y., "On the Question of Computation of the Dyadic Green's Function at the Source Region in Waveguides and Cavities", IEEE Trans. on Microwave Theory Tech., Vol. MTT-23, pp. 762-765, September 1975.

[24] Collin, R.E., "Eigenfunction Expansions and the Green's Dyadic", 37 pages of notes presented as part of Ohio State University's Department of Electrical Engineering Collo. Ser., February 26, 1981.

[25] Pathak, P.H., "On the Eigenfunction Expansion of Electromagnetic Dyadic Green's Functions", submitted to the IEEE Trans. on Antennas and Propagation.

[26] Abramowitz, M. and I.A. Stegun, Handbook for Mathematical Functions, Dover Publications, Inc., New York.

[27] Watson, G.N., A Treatise on the Theory of Bessel Functions, Second Edition, Cambridge University Press, 1966.

[28] Felsen, L.B. and N. Marcuvitz, Radiation and Scattering of Waves, Prentice-Hall, Inc., New Jersey, 1973.

[29] Logan, N.A., "Numerical Investigation of Electromagnetic Scattering and Diffraction by Convex Objects", Missiles and Space Division, Lockheed Aircraft Corporation, Final Report, December 1965.

[30] De Assis Fonseca, S.B. and A.J. Giarola, "Analysis of Microstrip Wraparound Antennas Using Dyadic Green's Function", IEEE Trans. on Antennas and Prop., Vol. AP-31, pp. 248-253, March 1983.

END

FILMED

7-85

DTIC